# *In-situ* Bioremediation and Molecular Microbiological Monitoring of Ammonia Contaminated Groundwater

Evelyn Joyce

Ph.D.
2022

South East Technological University

# *In-situ* Bioremediation and Molecular Microbiological Monitoring of Ammonia Contaminated Groundwater

Evelyn Joyce

## Supervisors:

Dr. Nabla Kennedy
Dr. Lee Coffey
Dr. David Ryan

Submitted in fulfilment of the requirements of the degree of Doctor of Philosophy
South East Technological University

Submitted September 2022

## Acknowledgements

For my Mother and Father.

Abstract

# *In-situ* Bioremediation and Molecular Microbiological Monitoring of Ammonia Contaminated Groundwater

Evelyn Joyce

To reduce ammonia contamination in groundwater, two Permeable Reactive Barriers (PRBs) were installed in a closed landfill site in Ennis, Co. Clare to act as a sustainable *in-situ* bioremediation solution. The PRBs were designed to reduce ammonia ($NH_4$-N) contamination in the groundwater by cycling ammonia through the nitrogen cycle to dinitrogen gas thereby reducing contamination of the receiving surface water bodies. The PRBs were designed to promote the first (aerobic) stage of the nitrogen cycle in PRB1, i.e., nitrification and the second (anaerobic) stage of the nitrogen cycle in PRB2 i.e., denitrification. Monitoring wells were installed upstream of the PRBs, within the PRBs, between the PRBs and downstream of the PRBs, resulting in five monitoring wells.

These five monitoring wells (S1- S5) were monitored onsite for pH, DO, temperature, and electrical conductivity. Water samples were analysed to determine concentrations of ammoniacal nitrogen, nitrite, nitrate, and total organic carbon. eDNA was extracted from water collected from the monitoring wells and analysed to determine abundance of nitrogen cycling functional genes (i.e., bacterial, and archaeal *amoA* as well as *nirK, nirS* and *nosZ*). eDNA from both PRBs at six monthly intervals was used to investigate the microbial communities present. The results showed that PRB1 significantly reduced the $NH_4$-N contamination in the groundwater and that PRB2 significantly reduced the concentrations of the resulting nitrification by-products nitrite ($NO_2$) and nitrate ($NO_3$) thereby signalling bioremediation. Concentrations of target contaminant, $NH_4$-N, were significantly lower in downstream monitoring S5 compared to all other monitoring wells. The molecular analysis confirmed that nitrogen cycling microbes were present on the site and suggested that the PRBs were functioning as a bioremediation solution for ammonia contamination.

## Declaration

I hereby certify that this material, which I now submit for assessment on the programme of study leading to the award of PhD, is entirely my own work and has not been taken from the work of others, save and to the extent that such work has be cited and acknowledged within the text of my work.

Signed: *Evelyn Joyce*

ID No.: 02398664

Date: June 06th 2022

## Table of Contents

## List of Figures

# List of Tables

## List of Abreviations

AOA: Ammonia Oxidising Archaea

AOB: Ammonia Oxidising Bacteria

AOM: Ammonia Oxidising Microbes

Clare Co. Co: Clare County Council

DEM: Denitrifier Enrichment Medium

DO: Dissolved Oxygen

EC: Electrical Conductivity

EPA: Environmental Protection Agency

GCN: Gene Copy Number

NEM: Nitrifier Enrichment Medium

NGS: Next Generations Sequencing

$NH_4$-N: Ammoniacal Nitrogen

NOB: Nitrite Oxidising Bacteria

$NO_2$: Nitrite

$NO_3$: Nitrate

NTC: Non-Template Control

ORC: Oxygen Releasing Compound

PAH: Polycyclic Aromatic Hydrocarbons

PCB:  Polychlorinated Biphenyls

PRB: Permeable Reactive Barrier

SAC: Special Area of Conservation

SPA: Special Protection Area

TOC: Total Organic Carbon

ZOI: Zone of Influence

# General Introduction

Groundwater pollution is an issue in Ireland and around the globe. In the past it was caused by carelessness and a lack of understanding while nowadays our groundwater resources are becoming increasingly strained by anthropogenic processes. This study identified a problem (ammonia contamination of shallow groundwater) and set about providing a viable and sustainable solution (bioremediation through the use of permeable reactive barriers).

To address ammonia contamination of groundwater and receiving surface waters at a closed landfill site in Ennis, Co. Clare a full-scale bioremediation site was designed and installed in June 2015 and was monitored monthly for two years. The bioremediation site comprised of two permeable reactive barriers (PRBs) that were designed to be sustainable and economically viable and once in place, the site was monitored monthly for relevant field parameters (i.e., pH, dissolved oxygen (DO), temperature, and electrical conductivity) and chemical parameters (i.e., ammoniacal nitrogen, nitrite, nitrate, and total organic carbon) over a two-year period. Water samples were also collected so that eDNA could be extracted and nitrogen cycling microbes could be monitored quarterly by quantifying nitrogen cycling functional genes. Amplicon sequencing was carried out on eDNA samples collected from the PRBs at six monthly intervals to characterise the microbial communities and to chronicle changes in community composition over time.

Chapter I introduces the nitrogen cycle, the issues of ammonia contamination, the concept of bioremediation and the factors influencing the design of the PRBs and the bioremediation site. The molecular methods that were used to monitor microbial nitrogen cycling are discussed. It also outlines case studies where similar applications of bioremediation have been used so that knowledge for the study strategy could be gleaned from previous experiments.

Chapter II describes the results of a desk-based study that was conducted to fully assess the geology, hydrogeology, and groundwater vulnerability of the study site. Previous reports and site investigations of the landfill were examined, and relevant findings are summarised. With this information in mind the design and installation of the bioremediation site with two PRBs and associated monitoring wells are outlined. The field and chemical results over the 24-month period are discussed with regard to the efficacy of the PRBs.

Chapter III focuses on the functional gene analysis that was performed on eDNA extracted from the groundwater collected from the five monitoring wells on a quarterly basis. This involved

functional gene analysis on genes associated with nitrification (i.e., bacteria and archaeal *amoA*) and denitrification (i.e., *nirK, nirS* and *nosZ)*, analysed using qPCR. These results were used to examine correlations between functional gene presence or absence and field and chemical parameters to ascertain whether microbial bioremediation of ammonia was taking place.

The final chapter, Chapter IV, focuses on the next generation sequencing that was applied to eDNA that was extracted from the PRBS at six monthly intervals. These results were used to examine the microbial communities that were present in the PRBs and to chronicle any changes in community composition over the 24 months.

To our knowledge these were the first set of full-scale *in-situ* sequential PRBs designed to bioremediate ammonia from groundwater, and it is hoped that the knowledge generated from this body of work can be used to inform bioremediation strategies for contaminated sites in future.

# Chapter I: Literature Review of Ammonia Bioremediation from Polluted Groundwater

## 1.1 Introduction

The global nitrogen cycle is one of the most important nutrient cycles on the planet with large natural flows of nitrogen from the atmosphere into terrestrial and marine ecosystems (Fowler et al., 2013; Hayatsu et al., 2008; Vitousek, et al., 2013; Leininger et al., 2006; Prosser & Nicol, 2008; Jickells et al., 2013). Despite this, it is still not fully understood due to the complexity of the relationships between all driving forces. Irish scientist Robert Boyle first suggested air was composed of tiny molecules or "corpuscles" in 1660 (Morris et al., 2009). John Evelyn, in 1675, identified an aquatic equivalent when he concluded that rainwater contained beneficial material that he named "celestial nitre" (Radojevic & Harrison, 1992). Daniel Rutherford, a Scottish scientist, isolated elemental nitrogen in 1772, though it remained formally unnamed until 1790 when French scientist Jean Antoine Chaptal bestowed the name "nitogéne" combining French and Greek words meaning sodium carbonate and "to bring forth" (Morris et al., 2009). Sixteen years prior to this, Priestly (1774), described in his book "Experiments and observations on different kinds of air", experiments that led him to discover ammonia. A century later and riding on the back of the industrial revolution, the importance of nitrate was realised in order to feed the booming human population, leading directly to the War of the Pacific (1879 – 1883). Chile, Peru and Bolivia waged war for the control of a 220 mile long deposit of guano, with UK-backed Chile claiming victory and the UK claiming 70% of the Chilean nitrate industry (Morris et al., 2009). In 1909, in a bid to avoid ammonia wars, German scientist Fritz Haber synthesised ammonia from nitrogen and hydrogen gas and, in 1913, Carl Bosch employed Haber's ammonia synthesis on a large scale (Galloway et al., 2013), leading to the "Haber – Bosch" process and the global industrial production of ammonia for use in explosives and fertilisers; this process outstripped natural nitrogen fixation in the 1970s (Galloway et al., 2003). Smil (2001) described the industrialisation of ammonia production as being of greater fundamental importance than the invention of the airplane, nuclear energy, spaceflight, or television and believed that the explosive expansion of the human population would never have been possible without the industrial synthesis of ammonia. While scientific advancement led to a heightened understanding, development and exploitation of the nitrogen cycle, societal concern grew from the negative effects on humans and ecosystems

associated with excess reactive nitrogen in the environment. Human activities have dramatically accelerated the global fixation and movement of reactive nitrogen, with rapidly increasing rates of fossil fuel combustion and use of synthetic fertilisers (Niu et al., 2016; Vitousek et al., 1997) causing eutrophication in many US and EU lakes to be noted as early as 1947 (De Jong, 2007). Further adverse effects of the exploitation and excessive use of nitrogen have been identified and documented such as coastal eutrophication in 1913 (Smil, 2001); nine coastal dead zones being described in the 1960s (Selman et al., 2008); in 1968, the link between inter country $NO_x$ emissions and freshwater acidification (Grennfelt et al., 2020); the role of nitrogen oxides in ozone depletion (Crutzen, 1970); in 1972, the link between nitric acid and acid rain (Gorham, 1998); the contribution of $N_2O$ to the greenhouse effect in 1985 (Farman et al., 1985); and in 2011, 540 coastal dead zones were identified on a global level (Galloway et al., 2003) .

## 1.2 The Nitrogen Cycle

Despite many of the pathways in the microbial nitrogen cycle being described over a century ago, additional fundamental pathways continue to be discovered. These findings indicate that there is still a lot to learn regarding the microbial nitrogen cycle, the organisms responsible for it and their interactions in natural and human environments (Ward & Jensen, 2014). The following figure, Figure 1.1, modified from Kuypers et al. (2018), shows that the nitrogen-transforming processes have vastly different fluxes and do not form one balanced nitrogen cycle as is often depicted.
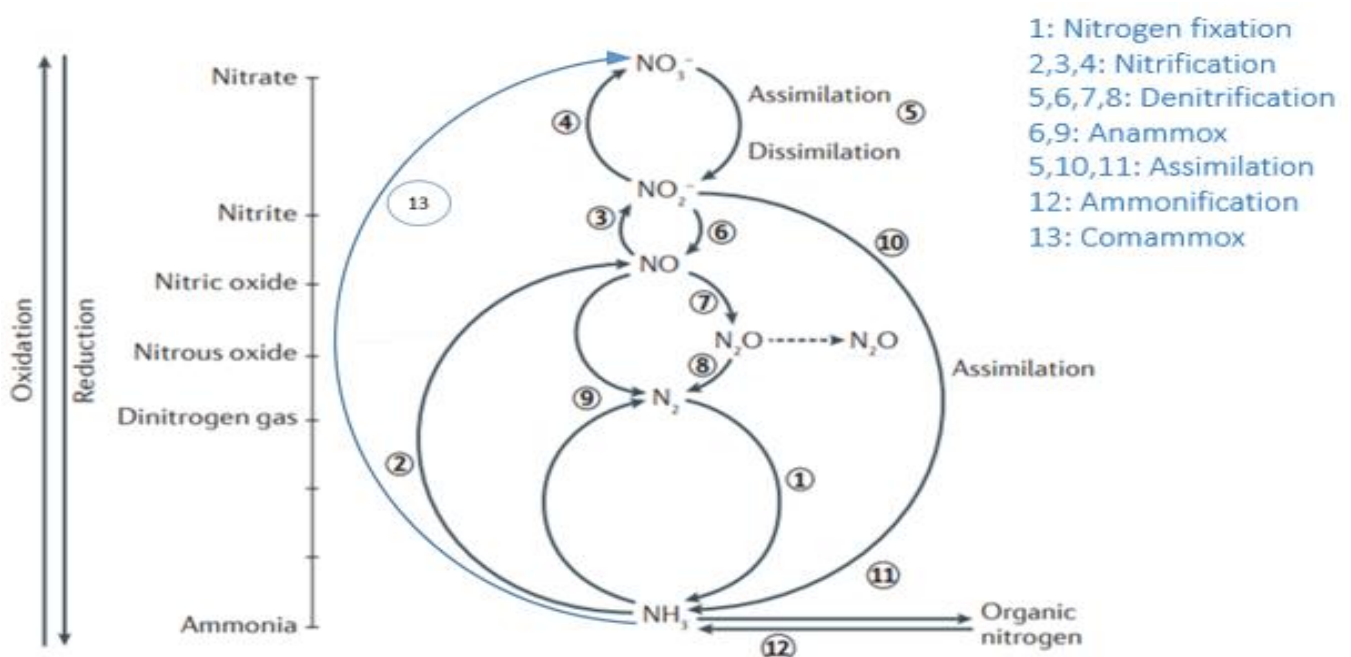


Figure 1. 1: Nitrogen transforming processes involved in the nitrogen cycle, Kuyper's et al. (2018), amended to include the comammox process

Reactive nitrogen fixed by natural processes or through anthropogenic activity is processed chemically in the atmosphere and largely by microbial and plant biochemistry in terrestrial and marine environments (Fowler et al., 2013). The nitrogen fixation process is the conversion of molecular, unreactive, dinitrogen gas ($N_2$) to nitrogen combined with other elements, such as oxygen and hydrogen, into reactive forms that can readily undergo chemical reactions (Strock, 2008). The largest reservoir of freely available nitrogen is in the form of atmospheric dinitrogen gas that is only available to microorganisms that carry the nitrogenase metalloenzyme (widespread in bacteria and archaea) and thus can fix dinitrogen into ammonia (Kuypers et al., 2018). The subsequent process of converting ammonia to nitrite and then to nitrate is known as nitrification.

## 1.2.1 Nitrification

In most environments, nitrification is carried out by diverse assemblages of ammonia-oxidizing and nitrite-oxidizing microorganisms (Kuypers & Marchant, 2018). Nitrification is (apart from comammox, described in Section 1.2.2 below), a two-step process, the first being the microbial oxidation of ammonia to nitrite by ammonia oxidising bacteria (AOB) and/ or archaea (AOA), and subsequently, the conversion of nitrite to nitrate is carried out by nitrite oxidising bacteria (Siripong & Rittmann, 2007).  The initial step of nitrification ($NH_3 \rightarrow NO_2$) is catalysed by bacteria belonging to the beta- and gamma-*Pseudomonadota* (formerly *Proteobacteria*) groups, and by archaea that are members of the *Thaumarchaeota* (Bouskill et al., 2012), by oxidising ammonia to hydroxylamine using the enzyme ammonia monooxygenase (AMO) (Kuypers et al., 2018). It was originally thought that ammonia oxidisers were almost exclusively bacteria, but it is now known that archaea play an important role in oxidising ammonia (Pester et al., 2002). A study conducted by Francis et al. (2005), first found the archaeal *amoA* gene in coastal and marine waters. Subsequent studies lead to the understanding that AOA play a significant role (Leininger et al., 2006; Prosser & Nicol, 2008; Smith & Osborn, 2009; Kelly et al., 2011; Limpiyakorn, et al., 2011; Meinhardt et al., 2015) in the nitrogen cycle, although studies conducted by Di et al. (2009) and Li et al. (2015) maintained that the significance of archaea as ammonia oxidisers is over rated. The reason bacteria were originally thought to be the main contributors in the oxidation of ammonia was due to the fact that they responded to culturing in the laboratory. Mere isolation of organisms from an environment does not demonstrate their activity, and the fact that there are more bacterial than archaeal ammonia oxidisers in culture may be irrelevant (Prosser & Nicol, 2008).

Relating microbial diversity and function to ecological processes remains a central question in the study of soil microbial ecology which can be addressed through the use of functional gene analysis and DNA microarrays (Kelly, 2003).

The second major step (NO$_2 \rightarrow$ NO$_3$) is carried out by nitrite oxidising bacteria that belong to five genera (*Nitrobacter*, *Nitrospira*, *Nitrococcus*, *Nitrospina* and *Nitrotoga*) using the enzyme nitrite oxidoreductase (*NXR*) (Bouskill et al., 2012).

### 1.2.2   Comammox

Costa et al. (2006) postulated that a complete ammonia oxidiser existed that could convert ammonia directly to nitrate rather than through nitrite and coined the phrase "comammox", meaning complete ammonia oxidation, as illustrated below in Figure 1.2 (Santoro, 2016).
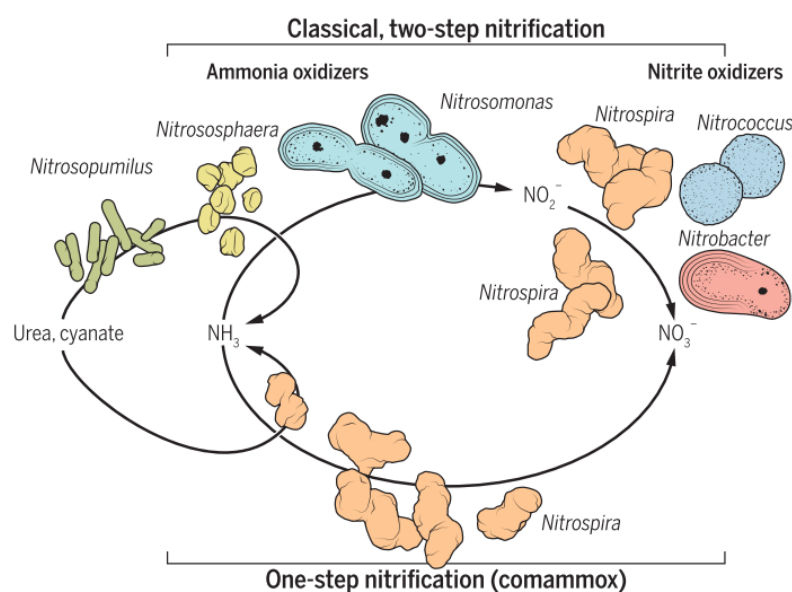


Figure 1. 2: Recent studies have uncovered nitrifiers that are capable of complete nitrification i.e., comammox Santoro (2016)

Costa et al. (2006) went on to describe methods that might isolate such complete ammonia oxidisers: enrichments (batch, chemostat and biofilm) and dilution culture. Van Kessel et al. (2015) obtained a stable enrichment culture from a bioreactor that was inoculated and supplied with low concentration of ammonium, nitrite, and nitrate under hypoxic conditions. DNA was extracted and sequenced from this culture resulting in two high-quality draft genomes of two *Nitrospira* species. Both genomes contained the full AMO and hydroxylamine dehydrogenase (HAO) genes for ammonia oxidation and also the nitrite oxioreductase (*NXR*) subunits necessary for nitrite oxidation in *Nitrospira*, indicating that the *Nitrospira* species has the genetic potential to perform comammox. Further investigation led to the conclusion that complete ammonia oxidation is

possible in a single organism, and two *Nitrospira* species capable of catalysing this process were identified. Following this, it was further concluded that a whole group of ammonia oxidising bacteria had been overlooked, which disproved the long-held assumption that nitrification is always catalysed by two distinct functional groups. Daims et al. (2015) also carried out enrichment cultures and through substrate analysis determined that some of the microbes present in the culture must be capable of complete ammonia oxidation. Subsequent sequencing led to a *Nitrospira* species being identified and the highly enriched strain was provisionally classified as "*Candidatus* Nitrospira *inoptina", inoptina* meaning "unexpected, surprising".

### 1.2.3   Denitrification

Denitrification is central to the nitrogen cycle and involves the reduction of nitrate via a chain of microbial reduction reactions to nitrogen gas (Knowles, 1982). It is the anaerobic respiration of nitrite to nitric oxide ($NO_2 \rightarrow NO$) and nitrous oxide to dinitrogen ($N_2O \rightarrow N_2$) (Stein & Klotz, 2016), steps 5 to 8 in Figure 1.1 above. Denitrifying organisms (members of the genera *Pseudomonas, Paracoccus* and *Bacillus*) tend to be ubiquitous in surface water, soil, and groundwater (Beauchamp et al*., 1989*). They are mostly facultative anaerobic heterotrophs i.e. they obtain both their energy and carbon from the oxidation of organic compounds, however, some denitrifying bacteria are autotrophs, obtaining their energy from the oxidation of inorganic species (Rivett et al., 2008). This dissimilatory process, in which nitrate is used as an oxidant in anaerobic respiration, usually involves heterotrophs such as *Pseudomonas denitrificans* (Prescott et al*.,* 2002). It has also been found that a wide variety of bacteria can carry out aerobic denitrification and are distributed across diverse environments (Hayatsu et al*.,* 2008; Ji et al., 2015).

### 1.2.4   Anammox

Anaerobic ammonium oxidation (anammox), steps 6 and 9 in Figure, 1.1 above, is carried out by microorganisms that can oxidise ammonium anaerobically using nitrite and ammonium to form dinitrogen gas (Wiszniowski et al., 2006; Stein & Klotz, 2016).  The first evidence for anaerobic ammonium oxidation to $N_2$ gas was obtained from anoxic (denitrifying) bioreactors of wastewater treatment plants (WWTPs) (Mulder et al., 1995). Much is now known about these processes and many of the microorganisms involved, yet our understanding of the nitrogen cycle has been upended twice in the past few years, first by the discovery of anammox in natural systems (e.g. bacterium Nitrosomonas eutropha (Prescott et al., 2002), and more recently by the discovery of anaerobic ammonia oxidation within the domain Archaea (Francis et al., 2007). Anammox bacteria

have not yet been successfully cultured but have been estimated to perform up to 50% of global nitrification (Fuerst & Sagulenko, 2011; Chen et al., 2019). This anaerobic process is a novel, promising, low-cost alternative to conventional denitrification systems (van de Graaf et al. 1996; Jetten et al., 2002; Ward, 2011).

## 1.3 Ammonia

Naturally, ammonia is formed by the decomposition of organic matter and is a product of nitrogen fixation carried out by microbial processes and plant biochemistry in terrestrial and marine ecosystems. As described above, the Haber-Bosch method of ammonia production was what led to an explosion of ammonia concentrations in atmospheric, terrestrial, and marine environments. In 2018, 175 million tonnes of ammonia was produced globally by industry (USGS, 2020). The immense industrial acceleration of the nitrogen cycle and industrial use of artificial nitrogen fertilizers worldwide has enabled humankind to greatly increase food production, but it has also led to a host of environmental problems, ranging from eutrophication of terrestrial and aquatic systems to global acidification (Gruber & Galloway, 2008). Ammonia as a contaminant is problematic and persistent in nature and it is becoming increasingly important to find a viable and sustainable solution (Jickells et al., 2013). Ammonia significantly contributes to eutrophication due to the oxygen consumption in receiving waters from the oxidisation of ammonia (Karrman & Jonsson, 2001). It is toxic to aquatic life (Wurts, 2003) and is a known cause of fish kills though the most common ammonia-related problems experienced by fish are affected growth, gill condition, organ weights and haematocrit (Milne et al., 2000). In an article published by *Science* magazine, Stokstad (2014) stated that ammonia, when combined with other air pollutants, can cause asthma, bronchitis, and heart attacks. The article went on to say that, in economic terms, the cost of ammonia health-wise ($36 bn) outweighs the net value resulting from ammonia use i.e., exported food ($23.5 bn).

### 1.3.1   Sources and Regulations

The UK's Department for Environment, Food and Rural Affairs estimated in 2002 that 70 - 80% of nitrate found in English surface and ground waters was derived from agriculture (DEFRA, 2006). The Irish Environmental Protection Agency (EPA) estimates that agriculture is the source of 99% of ammonia emissions in Ireland, with the remaining percent due to transport and industry (Kelleghan et al., 2020). Loads of total nitrogen from Irish rivers to the marine environment have increased by 26% between 2012 and 2014 (Trodd & O'Boyle, 2020). The same study went on to

say that 24% of the groundwater sites tested had high nitrate concentrations, i.e., >25 mg L$^{-1}$. While ammonia is a major constituent of many contaminated groundwaters, its movement through aquifers is complex and poorly documented (Böhlke et al., 2006).

Natural levels of ammonia in groundwater and surface water are usually below 0.2 mg L$^{-1}$ while anaerobic groundwater may contain up to 3 mg L$^{-1}$ (WHO, 2003). The presence of ammonia in groundwater poses health and environmental concerns and is strictly regulated by local authorities and the EPA (EPA, 2021). The EPA provided a guideline value of 0.15 mg L$^{-1}$ for ammonia concentrations in groundwater in their interim report, Towards Setting Guideline Values for the Protection of Groundwater in Ireland (EPA, 2003). Ammonia concentrations should not exceed 0.175 mg L$^{-1}$ in groundwater according to the European Communities Objectives (Groundwater) Regulations 2010 (S.I. No. 9 of 2010). In surface water, ammonia concentrations should be below 0.14 mg L$^{-1}$ as per European Communities Objectives (Surface Waters) Regulations 2009 (S.I. No. 272 of 2009).

Ammoniacal nitrogen ($NH_3$-N) is the measure commonly used for testing the concentration of ammonium ions in water or waste liquids and for quantifying values in waste treatment. It is measured in mg L$^{-1}$.

### 1.3.2 Ammonia in Landfill Leachate

Landfilling of municipal waste is an important issue in Ireland and in the rest of the world. As population growth and consumption increase so does waste production. While there is a growing emphasis on recycling and composting and incineration is encouraged, $10 - 20\%$ of incinerator residue must ultimately be landfilled (Wisznowski et al., 2006). Landfill leachate is generated by precipitation infiltrating and percolating down through a landfill body. Groundwater and surface water surrounding landfills are threatened due to this infiltration of rainwater resulting in extensive amounts of landfill leachate, generally enriched in organic matter, ammonium, and metals (Nooten & Diels, 2008). Because the quality and quantity change over time in the same landfill, leachate is considered one of the categories of wastewater with the greatest impact on the environment (Abiriga et al., 2021). Focusing on the most common type of landfill that receives a mixture of municipal, commercial, and mixed industrial waste, landfill leachate may be characterised as a water-based solution of four groups of pollutants: dissolved organic matter (e.g. acids, alcohol), inorganic macro components (e.g., ammonium, potassium), heavy metals (e.g., lead, cadmium) and xenobiotic organic compounds (e.g., pesticides) (Kjeldsen et al., 1994).

Modern landfills in Ireland are engineered in such a way that all generated leachate is collected, treated, either on or off site, and prevented from infiltrating the groundwater or from entering surface water bodies in the locality. In 2013, there was approximately 1.1 million tonnes of landfill leachate collected from municipal solid waste landfills (Brennan et al., 2016). The most common treatment practice in Ireland is to discharge leachate to sewers (51%) or removal by tanker for treatment in WWTPs (48%) with less than 1% being treated on-site (Morris et al., 2018). In the Republic of Ireland, non-compliance with $NH_4$-N emission limits values at some WWTPs have been attributed to leachate loading and, in many instances, leachate acceptance has been discontinued In WWTPs (Brennan et al., 2016). However, historic landfill sites were previously established without any engineering and in locations that were unsuitable, e.g., flood plains and riverbanks based on a "dilute and disperse" method. Due to the more stringent regulations being applied to landfill facilities the number of landfills in Ireland has reduced from two hundred in the mid-nineties to six in current operation (EPA, 2015). Often, shallow reservoirs or groundwater adjacent to these sources became contaminated with ammonia (Rivett et al., 2008). Ammonia also constitutes a problem since it is a nutrient that is toxic to aquatic life and expected to be present in high concentrations in leachates (>100 mg L$^{-1}$) for decades (Christensen et al., 2001). Concentrations in landfill leachate have been estimated by Christensen et al. (2001), to range between 50 mg L$^{-1}$ and 2,200 mg L$^{-1}$ and most of the nitrogen found in landfill leachate is in the form of ammoniacal nitrogen due to the anaerobic conditions prevailing in landfills (Wakida & Lerner, 2005). Brennen et al., (2017) recorded $NH_4$-N concentrations of up to 378 mg L$^{-1}$ in leachate being treated at an Irish WWTP. Figure 1.3, below, was produced from Kulikowska & Klimiuk (2008), and illustrates the ammoniacal nitrogen ($NH_4$-N) concentrations in leachate sampled from a municipal waste landfill in Poland over a four year period (2004 – 2007). Ammoniacal nitrogen concentrations increased from 98 mg L$^{-1}$ in month 23 to 364 mg L$^{-1}$ in month 73 of the study.
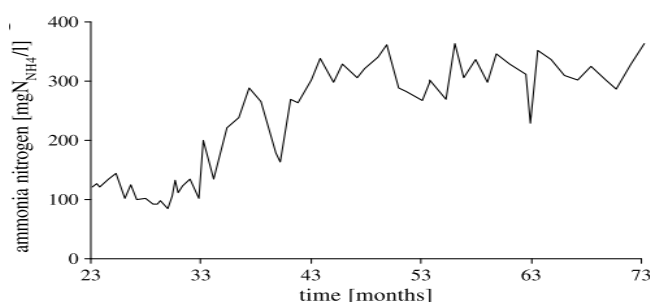


Figure 1. 3: $NH_4$-N concentrations in municipal landfill leachate from Wyseika, Poland, from 2004 to 2007 Kulikowska & Kilmuik, (2008)

According to Ehrig (1989), the release of soluble nitrogen from municipal solid waste into leachate continues over a long period in comparison with soluble organics. Ammoniacal nitrogen is present in leachate from young landfills owing to the deamination of amino acids during destruction of organic compounds (Tatsi & Zouboulis, 2002) and is persistent in leachate and found in high concentrations in samples collected from older landfills. Hydrolysis and fermentation of the nitrogenous fractions of biodegradable substrate lead to high ammonia concentrations in older landfills (Carley & Mavinic, 1991). There is a lack of data available regarding the longevity of ammonia concentrations issuing from Irish landfills. In a study of 50 German landfills, ammonia concentrations did not show a significant decrease even 30 years after landfill closure (Krumpelbeck & Ehrig, 1999). This study focus is on groundwater that is contaminated by ammonia from a closed landfill site in the West of Ireland as described in Chapter 2, Section 2.2.1.

### 1.3.3 Treatment

In response to EU legislation, the EPA in Ireland introduced a technical amendment to waste licences in 2013 so that the problems arising from unsuitably located, un-engineered landfills could be retrospectively addressed. The amendment stated that: "Within eighteen months of the date of this technical amendment, the licensee shall carry out a risk screening and where necessary a technical assessment in accordance with the Guidance on the Authorisation of Discharges to Groundwater, published by the EPA. A report on the outcome of the screening and where relevant the recommendations of the technical assessment in relation to the setting of groundwater compliance points and values, shall be included in the next Annual Environmental Report (AER)." As a result of this amendment, local authorities and other private owners were required to have any relevant landfill risk-assessed to establish whether their landfill was causing pollution to groundwater. The most common problem was caused by historic landfills that were not appropriately situated or engineered, resulting in ammonia plumes beneath the landfill that migrate over time and enter local surface water receptors. The amendment further stipulated that: "Any actions required to demonstrate compliance with the European Communities Environmental Objectives (Groundwater) Regulations 2010, as amended shall be agreed by the Agency and implemented before 22nd December 2015." In cases where landfills were causing pollution to groundwater, the licensee was required to supply to the EPA a schedule of appropriate works that would be implemented to reduce and stop pollution to groundwater. This technical

amendment placed an even higher emphasis on finding a sustainable solution to reducing ammonia pollution in groundwater.

New applications and sustainable methods for the removal of ammonia from groundwater are necessary if we are to meet the increasingly stringent EU discharge regulation standards (Jetten et al., 2002) and the cost of compliance is already significant (Knapp, 2005). Most of the remediation approaches to date have involved pumping groundwater (Majone et al., 2015) and either using the groundwater as fertiliser, removing the nitrate by physical means (e.g., reverse osmosis, ion exchange, or electro-dialysis), or simply disposing of the contaminated water (Garrett & Hudson, 2005). Studies by the US EPA found that commonly used pump-and-treat (P&T) technologies (pump the water and treat it at the surface) rarely restored sites that had contaminated groundwater to background conditions (Thiruvenkatachari et al., 2008). Other conventional leachate treatment methods, such as air stripping, coagulation, flocculation and settling, are often costly in terms of initial investment in plant equipment, energy input and frequent use of additional chemicals (Wiszniowski et al., 2006). In The Netherlands, it has been estimated that remediation of its 4,000 old landfills will cost about 10 billion euro (Röling et al., 2000a). Rivet et al. (2008), stated that the cost of compliance was already significant in the UK alone. The cost of nitrate treatment to ensure potable water supplies were below 50 mg L$^{-1}$ amounted to £16 million per annum during 1992–1997 (Dalton & Brand-Hardy, 2003) and was predicted to rise to £58 million per annum by 2010 as low-nitrate water for blending became scarcer (DEFRA, 2006). A report by the UK's House of Commons (HC, 2018) described nitrate pollution as "The UK's Nitrate Time Bomb", and the British Geological Survey (BGS) warned that it might take 60 years or more for historic applications of nitrate to peak in groundwater. The report quoted their minister as stating, "For years we are still going to be suffering the consequences of overuse of synthetic fertilisers". A cost-effective, sustainable, and *in-situ* treatment solution is bioremediation technology. Bioremediation is the utilisation of natural biological activity to destroy or render harmless various contaminants (Vidali, 2001) and will be discussed in Section 1.5.

## 1.4 Molecular Methods

It has been estimated that less than 1% of all bacterial cells in soil can be cultured in the current types of microbiological media (Amann et al., 1995; Felske et al., 1999) and even as far back as 1985, it was generally accepted that culture-dependent surveys suffer from the "great plate count

anomaly" (Staley & Konopka, 1985). "The great plate count anomaly" was coined by Staley & Konopka (1985) to describe the difference in orders of magnitude between the numbers of cells from natural environments that form colonies on agar media and the numbers that can be quantified through microscopy. These indications of the uncultured nature of the vast diversity of life in the soil have stimulated development of culture-independent study of microbial communities (Torsvik & Øvreås, 2002). The development of culture-independent techniques which bypass the need for isolation and laboratory cultivation of individual species has fundamentally changed studies in environmental microbiology (Suenaga, 2012). This technological progress has repeatedly demonstrated that the phylogenetic identities and metabolic capabilities of microbes within any environmental sample are far more diverse than we had imagined (Bier et al., 2015). These advances have significantly improved the process of efficacy determination and implementation of microbial bioremediation strategies (Desai et al., 2010) or as per Galvão et al. (2005) molecular techniques allow researchers to peer directly into contaminated sites, so that information about environmentally relevant actions can be gathered, irrespective of whether the microbial community can be cultured. Understanding links between molecular analyses, physiological studies and measurements of nitrogen cycling processes requires a knowledge of the significance of ammonia oxidiser species and functional diversity for global cycling of nitrogen (Prosser & Embley, 2002).

### 1.4.1   eDNA Sampling and Extraction

For downstream molecular analysis to function optimally, obtaining DNA of high quality is paramount for ensuring confidence in all subsequent steps. In aquatic environments eDNA is collected using filter membranes made from various materials (e.g., cellulose nitrate, nylon) and pore sizes (e.g., 0.1 μm, 0.2 μm and 0.4 μm) that the sample water is pumped through. Membrane filtration through 0.22 μm pore size is continuously considered and commercially traded as a sterile filtering procedure (Wang et al., 2007).

The aim of nucleic acid extraction method is to isolate DNA of suitable integrity, purity and of sufficient quantity for diagnostic applications by qPCR (Terry & Parks, 2002). DNA extraction techniques can be broadly divided into three categories; organic extraction (phenol–chloroform method); nonorganic method (salting out and proteinase K treatment); and adsorption method (silica–gel membrane) (Nupta, 2019). The cetyltrimethylammonium bromide (CTAB) method is an organic extraction method that has been used widely for DNA extraction (Demeke & Henkins,

2010). It is effective for a wide range of matrices though it uses hazardous chemicals and is time consuming (International Organization for Standardization, 2005). Most commercially available kits and published protocols utilise the non-organic method by using detergent, to disrupt the cell wall, as an initial step for extracting DNA followed by a proteinase K enzyme treatment to remove any contaminants. Some commercial kits use the adsorption method by binding DNA to silica-based matrices or magnetic beads, followed on by elution, to avoid exposure to organic solvents such as chloroform (Demeke & Jenkins, 2010). Commercial DNA kits are less time consuming to use and involve less hazardous chemicals but are costly. Smith et al., (2005) compared the costs of various DNA extraction methods (for the extraction of DNA from potatoes) and found that the costs (Canadian dollars) per sample varied between $0.50 for CTAB and $3.70 and $5.90 for commercial kits, Wizard magnetic DNA purification system (Promega) and DNA isolation kit for cells and tissues (Roche I), respectively.

### 1.4.2   Functional Genes

Physiological traits, such as denitrification, are not limited to specific microbial taxa and are studied independent of culture through the relevant functional genes (Heylen et al., 2006) and the favoured approach to hunting for niche specialisation of certain archaea and bacteria is to determine the presence/ absence, abundance and relative abundance of respective functional genes (Prosser & Nicol, 2012). Function-based approaches focus on distribution and abundance of organisms based on their metabolism (e.g., chemolithic autotrophs) via quantifying functional genes (Colloff et al., 2008), e.g., those that code for enzymes involved in nutrient cycling like ammonium monooxygenase (*amoA*) and nitrate reductase (*nirS/ nirK*) (Nocker et al., 2007). The analysis of the abundance and community structure of functional genes involved in the biogeochemical cycling of nitrogen offers an approach to directly link microbial groups to site characteristics and ecosystem processes (Kennedy & Egger, 2010; Levy-Booth et al., 2014). Figure 1.4 below shows the key functional genes involved in nitrogen cycling.
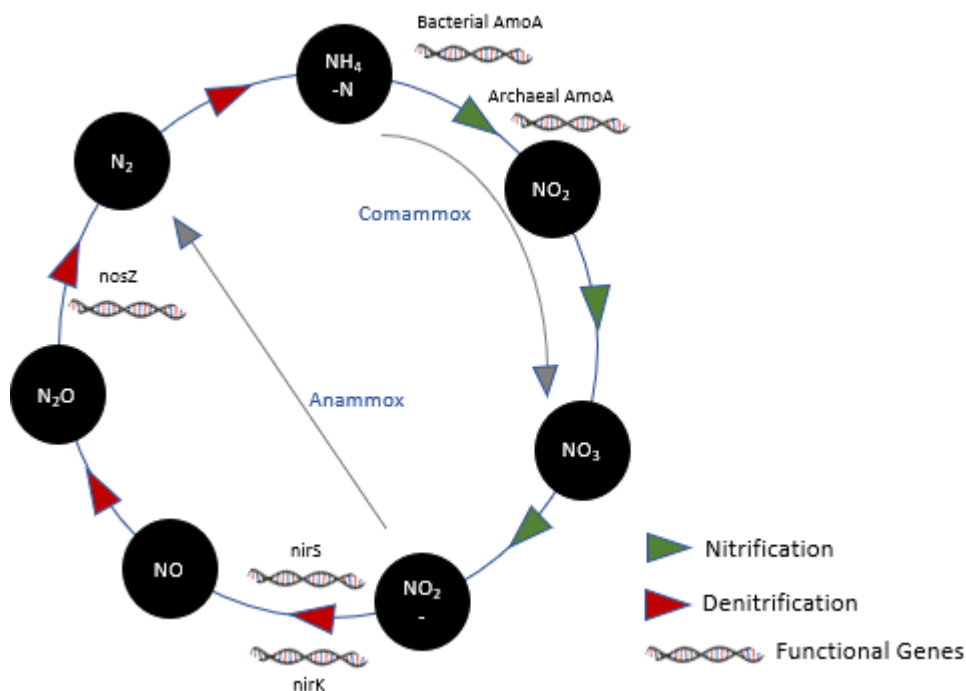
Figure 1. 4: The nitrogen cycle with key functional genes involved in nitrification and denitrification (archaeal and bacterial *amoA*, *nirK, nirS, nosZ*).

Key nitrogen cycling functional genes, their function within the nitrogen cycle and examples of microbes that contain them are outlined in Table 1.1 below.

Table 1. 1: Key nitrogen cycling functional genes, the reactions they are responsible for, and examples of microbes that contain them.

| Functional Gene | Reaction | Example Organism |
|---|---|---|
| Bacterial *amoA* | $NH_4$-N $\rightarrow$ $NO_2$ | *Nitrosomonas* sp., *Nitrosospira* sp. |
| Archaeal *amoA* | | *Nitrosopumilus maritimus* |
| *nirK* | $NO_2 \rightarrow NO$ | *Blastobacter denitrificans, Pseudomonas denitrificans, Pseudomonas stutzeri* |
| *nirS* | | *Alcaligenes denitrificans, Pseudomonas aeruginosa* |
| *nosZ* | $N_2O \rightarrow N_2$ | *Alcaligenes denitrificans* |

The *amoA* functional gene is found in archaea and bacteria that are responsible for the conversion of ammonia ($NH_3$) to nitrite ($NO_2$) by the nitrification process, by first oxidising $NH_3$ to hydroxylamine ($NH_2OH$) using the enzyme ammonia monooxygenase (*amoA*), and has proven to be an effective molecular marker for ammonia oxidising microorganisms (Reed et al., 2010). Casciotti & Ward (2001) stated that classical denitrifying bacteria have a series of enzymes: nitrate reductase, nitrite reductase, nitric oxide reductase, and nitrous oxide reductase, which allow them to utilise nitrate ($NO_3$), nitrite ($NO_2$), nitric oxide (NO), and nitrous oxide ($N_2O$), respectively, in

anaerobic respiration. The reduction of $NO_2$ to $NO$ is central to denitrification and is catalysed by two different types of nitrite reductase enzymes (*Nir*); either a cytochrome cd1 enzyme encoded by *nirS* or a Cu-containing enzyme encoded by *nirK* (Throback et al., 2004). $N_2O$ reduction is the final step in the denitrification pathway catalysed by nitrous oxide reductase (*nosZ*) enzyme and coded for by the *nosZ* functional gene (Scala & Kerkhof, 1998).

Since Woese and Fox (1997), ribosomal RNA genes have been used as standard phylogenetic markers in molecular taxonomic studies, including the pioneering studies on the tree of life. 16S rRNA in prokaryotes has been the phylogenetic marker of choice from an early stage and has been used extensively to date (Woese, 1987). The 16S rRNA functional gene is ubiquitous in all bacteria and archaea. It is composed of conserved and variable regions which allow primers to be designed to target all bacteria and archaea, but also contains variable regions in which differences in the sequence of bases allow for determination of various species (Kim & Chun, 2014). Markers such as the 16S rRNA gene (16S) of bacteria and archaea are frequently used to characterise the taxonomic composition and phylogenetic diversity of environmental samples (Langille et al., 2013). The 16S gene is one of the most studied and characterised genes with well-developed phylogenetic trees and taxonomic information readily available in a variety of databases (Kim et al., 2014).

### 1.4.3 Conventional PCR

By using polymerase chain reaction (PCR), essentially any nucleic acid sequence (e.g., a functional gene) present in a complex sample can be amplified in a cyclical process to generate a large number of identical copies that can be readily analysed (Kubista et al., 2006). PCR is a nucleic acid based technique and produces millions of copies of a target area of a gene, an entire gene, or a cluster of genes (Malik et al., 2008) and thus relies greatly on the sufficient extraction and purification of DNA. PCR is the *in vitro* imitation of natural DNA replication, which can then be repeated on a large scale (Paiva-Cavalcanti et al., 2010). PCR-based techniques are now almost universally used. The advantage of PCR is that with the selection of appropriate primer combinations, genes of specific groups of organisms within the community can be selectively amplified for downstream analysis such as amplicon sequencing.

### 1.4.4 Quantitative PCR

The need to quantify microbial populations is a pressing one in many areas of microbial ecology (Okano et al., 2004). Heid et al. (1996) developed a novel "real time" quantitative PCR method

that measures PCR product through a dual-labelled fluorogenic probe (i.e., TaqMan Probe) or an intercalating nucleic acid staining dye (i.e., SYBR Green) which monitors amplification in real-time rather than at the end like conventional PCR. Real-time PCR (or qPCR) approaches are now widely applied in microbial ecology to quantify the abundance and expression of taxonomic and functional gene markers within the environment (Smith & Osborn, 2009). Unlike other quantitative PCR methods, real-time PCR does not require post-PCR sample handling, which results in faster and higher throughout assays and reduces potential PCR product carry-over contamination (Heid et al., 1996). Only one target gene per reaction can be measured which makes qPCR expensive and it uses a large quantity of DNA (Zhang et al., 2021). Digital PCR monitors fluorescence only during the exponential phase and is considered as the most precise PCR technique compared to qPCR and end-point PCR and less affected by inhibition (Whale et al., 2012) though it is more time consuming as it requires a significant amount of manual input (Sreejith et al., 2018). Using gBlocks gene fragments as synthetic templates for qPCR improves accuracy of qPCR and allows for detection of wild type DNA (Conte et al., 2018).

Even though fairly conserved primers can be designed for some functional genes of interest (e.g., *amoA, nirS, nirK*), the success of amplification is habitat/ecosystem dependent, most likely due to variations in the quality of extracted DNA, community complexity, sequence divergence, and target gene abundance (Zhou et al., 2015).

### 1.4.5 Amplicon Sequencing

Molecular methods are being used to link microorganisms to key processes, which has led to a major shift in the understanding of nitrogen cycling in the past decade (Levy-Booth et al., 2014). amplicon sequencing of DNA extracted from environmental sources has transformed the field of microbial ecology by increasing the speed and the throughput of DNA sequencing by orders of magnitude (Zhou et al., 2015). Creating a census of microbial communities at contaminated sites has enabled insights into specific microbial groups that are sensitive or most affected, resilient and predominant, or actively involved in bioremediation (Desai et al., 2010).

#### 1.4.5.1 Amplicon Sequencing Technologies

Effective high-throughput sequencing technologies for analysing microbial community structure and functions are critical for advancing bioremediation. Next generation sequencing (NGS) produces a massively parallel analysis from multiple samples where small sections of DNA are ligated with adaptors for random reads during DNA amplification, providing large volumes of

information within a short space of time (Zhang et al., 2011). Sequencing and phylogenetic analysis of 16S rRNA genes provides the foundation for modern study of microbial communities (Zhou et al.,2015). PCR-based 16S rRNA cloning analysis has driven the explosion of information about community memberships and vastly expanded the known diversity of microbial life (Pace, 1997). Several amplicon sequencing platforms have been developed and are widely used, including the Illumina (e.g., HiSeq, MiSeq), Roche 454 GS FLX, SOLiD 5500 series, and Ion Torrent/Ion Proton platforms (Zhou et al., 2015). The 454 GS Junior (Roche), MiSeq (Illumina) and Ion Torrent PGM (Life Technologies) are laser-printer sized and offer modest set-up and running costs (Loman et al., 2012).

## 1.5    Bioremediation

Composition of microbial communities can be indicative of (potential for) intrinsic bioremediation in landfill leachate polluted aquifers (Röling et al., 2000a). On-site or "*in-situ*" bioremediation creates subsurface environmental conditions, typically through reduction oxidation manipulation, which induces the degradation of chemicals (i.e., the target chemical) via microbial-catalysed biochemical reactions (USPEA, 1999; Faris & Vlassopoulos, 2002) and is more cost effective than the "pump and treat" *ex-situ* treatment as discussed in Section 1.1.3. Passive *in-situ* groundwater remediation using Permeable Reactive Barriers (PRBs), as discussed in Section 1.5.1 below, is a relatively new and innovative technology, with a high potential to significantly reduce the cost of treating contaminated shallow aquifers and therefore contribute to the preservation of groundwater resources (Roehl et al., 2005). In order to apply the most effective *in-situ* groundwater bioremediation technique, a knowledge of the site background, history of contamination and contaminant characteristics is required (USEPA, 1999). The biological method of nitrification/ denitrification is probably the most effective and cheapest process to eliminate nitrogen from leachate (Wiszniowski et al., 2006). To facilitate in-situ bioremediation of ammonia (that is, to facilitate both nitrifying and denitrifying bacteria) it must be ensured that the correct parameters are present (e.g., DO (DO), pH levels etc.).

### 1.5.1    Permeable Reactive Barriers

To date, one of the most promising bioremediation technologies is the use of PRBs filled with reactive materials to intercept and decontaminate plumes of pollution in the subsurface (Mountjoy et al., 2003; Patterson et al., 2004; Thiruvenkatachari et al., 2008). A PRB consisting of permanent, semi-permanent or replaceable reactive media placed in the subsurface intercepting

the flow of a plume of contaminated groundwater, which must move through it as it flows, typically under its natural gradient, creates a passive treatment system (Thiruvenkatachari et al., 2008). The US EPA (USEPA, 1999) defines PRBs as an emplacement of reactive media in the subsurface designed to intercept a contaminated plume, provide a flow path through the reactive media, and transform the contaminant(s) into environmentally acceptable forms to attain remediation concentration goals down-gradient of the barrier. Taking advantage of the biocompatibility and high efficiency of nitrifying and denitrifying bacteria is increasingly used in the treatment of water (Qiu et al., 2012). *In-situ* bioremediation of ammonia utilises the processes of the nitrogen cycle in order to convert the toxic ammonia to dinitrogen ($N_2$) and nitrous oxide ($N_2O$) (Figure 1.2) (Kuypers et al., 2018).

There are two main types of permeable reactive barriers: the continuous reactive barrier and the "funnel and gate" type (Starr & Cherry, 1994). The continuous reactive barrier enables a flow through its full cross section and its configuration is characterised by a single reactive zone installed across the contaminant plume (Roehl et al., 2005). Continuous reactive barriers are preferable when an inexpensive reactive material is used, while funnel and gate type barriers are more appropriate when expensive reactive material is used, as the impermeable funnel directs the contaminated plume towards the reactive material in the barrier, both illustrated below in Figure 1.5.
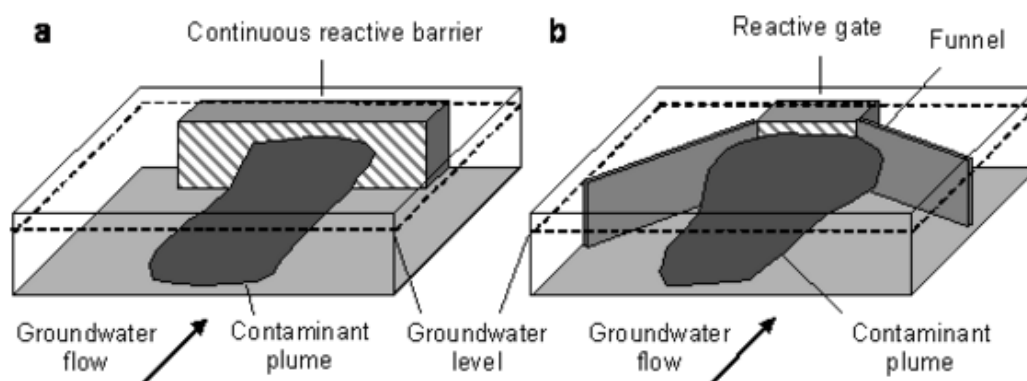


Figure 1. 5: Two types of permeable reactive barrier: a) Continuous reactive barrier, b) Funnel and gate http://biomine.brgm.fr (2016).

The selection of the material to be used in the PRBs depends on the nature of the contaminant in question and the remediation approach involved. The materials (chemical and/or biological reagents or catalysts) are chosen to react with the contaminants to render them harmless by the time they pass out the other side of the PRB (Golab et al., 2006).

The factors to be considered when choosing the reactive material for a PRB are reactivity, stability, availability and cost, hydraulic performance, environmental compatibility and safety (Gavaskar, 1999). It is desirable to have low residence time and a correspondingly high reaction rate in order to keep the barrier thickness to within acceptable limits. The reactive material should be expected to remain active over a long period of time as replacing reactive material within the barrier would be very disruptive and difficult (Richardson & Nicklow, 2002). Stability under fluctuating temperatures, pH, pressure, and other antagonistic parameters is also required. Permeability of the reactive material depends on its particle size distribution and must be greater or equal to that of the surrounding soil to provide optimum permeability so appropriate particle size must be determined. Selection of the particle size of the reactive medium should consider the trade-off between reactivity and hydraulic conductivity. Generally, higher reactivity requires lower particle size (higher total surface area), whereas higher hydraulic conductivity requires larger particle size (Gavaskar et al., 2000). Large amounts of reactive material may be required, so low cost and logistical availability is desirable, and there should be no risk to workers' health due to handling of the reactive material.

In the case of ammonia remediation, the PRBs that are most suitable are sequential microbial barriers. Elimination of nitrogen in wastewater needs both denitrifiers and nitrifiers (Zou et al., 2014) and as such requires sequential PRBs, providing suitable conditions to promote nitrification in the initial PRB and denitrification in the following PRB. The number of bacteria in leachate-contaminated aquifers is relatively high compared with the number of bacteria usually found in pristine aquifers (Christensen et al., 1994). This means that altering environmental parameters in order to promote microbial activity should suffice rather than the introduction of specific nitrogen cyclers. Success of *ex-situ* or *in-situ* bioremediation relies heavily on the relative abundance, structure, catabolic versatility and biotic/abiotic interactions of the microbial communities (aerobic/ anaerobic) that are indigenously present, amended or stimulated at contaminated sites (Desai et al., 2010) and their role is critical to the removal of ammonia that is toxic to organisms and ecosystems even at low concentrations (Pollard, 2006).

## 1.5.2   Case Studies

Addy et al. (2016) reviewed 26 published studies that researched using denitrifying bioreactors for nitrate removal. The review found that at least a six hour retention time was needed for effective nitrate removal and also noted that bioreactor beds and laboratory columns were more effective

than PRBs at removing nitrate (also noted by Schipper et al. (2010)). The available literature on sequential nitrification- denitrification systems is reviewed below.

Robertson & Cherry (1995) were the first to suggest denitrification of septic-system nitrate through the use of reactive porous media barriers. These barriers were designed so that there was capacity for nitrification to occur to the influent $NH_4$-N before reaching the denitrification cell, thereby becoming the first example of an *in-situ* passive sequential barrier system to treat $NH_4$-N, though the focus was on the subsequent nitrate treatment. The study found that though the design of the PRB was useful for diffusing $O_2$, it was ineffective at removing nitrate due to the lack of a carbon source. Following on from this study, Robertson et al. (2007) carried out further investigations where it was found that the denitrification process consumed 1% of the carbon source per year and in 2008, Robertson & Vogan found that after 15 years the PRB medium was still performing nitrate denitrification at 50% capacity.

In 1998, following the discovery of the annamox process (Mulder et al., 1995), Kuai & Verstraete investigated its role in the bioremediation of ammonia from high nitrogen wastewater in an oxygen-limited autotrophic nitrification-denitrification (OLAND) system. The study concluded that while the treatment capacity was low, it had potential.

Jun et al. (2009), designed two lab scale rectors for studying the feasibility of PRBs to remediate groundwater contaminated by leachate. The columns were filled with zero valent iron (ZVI) and oxygen releasing compound (ORC). Mixed media proved more effective at contaminant removal with removal rates of $NH_4$-N reaching 97.4%. While there were some issues with pore space filling due to precipitation and biofouling it was concluded that a sequenced PRB system would be effective in treating landfill leachate contaminated groundwater.

Another Belgian study, conducted by Van-Nooten et al. (2010) sought to design a multifunctional PRB to treat contaminants in landfill leachate including ammonium. A column study was set up using varying grades of sand as substrate and diluted inoculum originating from an aerated nitrification compartment of the landfill wastewater treatment system. It was found that when using a combination of nitrification and denitrification, ammonium removal rates exceeded 98%. The study concluded that field implications would mean that nitrification and denitrification compartments be 1.3 m and 0.7 m thick, respectively. It also suggested that oxygen be supplied to the first compartment and carbon to the second.

A laboratory scale sequential nitrification- denitrification system was explored by Kong et al. (2015). This study incorporated the use of ORC and found that the $O_2$ concentrations increased 10-fold from 2 mg L$^{-1}$ to greater than 20 mg L$^{-1}$. NH$_4$-N concentrations were successfully reduced from 10 mg N L$^{-1}$ through a combination of adsorption and microbial degradation, with 70% of the NH$_4$-N removal being attributed to microbial nitrification after 54 operating days. Another column filled with spongy iron and pine bark saw NO$_3$ concentrations reduce from 14 mg N L$^{-1}$ to less than 5 mg N L$^{-1}$.

In 2012, a pilot scale zeolite PRB (Li et al., 2014) was designed to remove ammonia from groundwater through sequential nitrification, adsorption, and denitrification. The PRB (6 m long, 3 m wide, 3 m high) was composed of three layers, sand (0.5 – 1.0 m); ORC and sand (1.0 – 1.3 m); and zeolite (1.3 – 2.5 m). The initial sand layer was to act as a sieve for suspended solids. ORC was added to the second layer to enhance bacterial nitrification by releasing oxygen to the groundwater. The final layer was designed to ensure NH$_4$-N removal through adsorption and to provide an anaerobic environment to allow for the reproduction of denitrifying bacteria. The study found that >90% of NH$_4$-N was removed over a wide range of influent concentrations, with adsorption, nitrification (after 10 months of operation) and denitrification all contributing to the *in-situ* remediation of nitrogen species.

Huang et al. (2015) sought to design a fully passive PRB with ORC and clinoptilolite. Clinoptilolite is a natural zeolite that has proven to be effective at removing ammonia from groundwater through ion exchange (Du et al., 2005). This column set up involved three columns to simulate PRBs. PRB 1 was packed with just clinoptilolite as a control; PRB2 was packed with ORC and clinoptilolite (the intended full-scale design) and the third PRB was packed with less ORC, ceramicite (as supporting material) and clinoptilolite. This column study did not include inoculum, instead relying on the correct environmental/ laboratory conditions to support the growth of N-cycling microorganisms. Nearly complete NH$_4$-N removal (>99%) occurred in all three PRBs though the study concluded that in PRB 1, the NH$_4$-N removal was due to ion exchange rather than biological process as in PRB2 and PRB3, where there was an oxygen supply. This study led to a full scale *in-situ* PRB being installed in Shenyang, China in 2012.

Hou et al. (2014), installed China's first field-scale PRB in 2012, designed to remediate ammonium nitrogen from a contaminated river that infiltrates a groundwater aquifer that serves as a municipal drinking water supply. A zeolite filled PRB was constructed to protect a groundwater

abstraction well. It was constructed in a U-shape, 15 m long x 1 m wide x 40 m deep, fed by gravity. This study demonstrated ammonium concentrations in the groundwater decreasing from 2- 10 mg L$^{-1}$ to <0.5 ml L $^{-1}$. This was concluded to be as a result of sorption and ion exchange and after one year of continuous operation there was no evidence of microbial ammonia oxidation.  These case studies were used to inform the design of a bioremediation site with the aim of reducing ammonia contamination in shallow groundwater using PRBs.

## 1.6 Bioremediation Study

The premise of the study was to utilise an existing site where ammonia contamination of groundwater was an issue and employ bioremediation technology. As previously discussed, the nitrogen cycle, in the (aerobic) nitrification phase oxidises ammonia to nitrate and in the (anaerobic) denitrification phase then reduces nitrate to dinitrogen, an odourless and colourless gas, through intermediary steps. With this in mind, the site was designed to facilitate and encourage these two processes, nitrification, and denitrification in two separate, sequential PRBs. The first PRB was designed to encourage nitrification, the second denitrification. A summary of the parameters required for both PRBs is provided below in Figure 1.6. To satisfy the sustainability and economic viability the reactive materials to promote the requirements of each PRB would be locally sourced and tested, outlined in Chapter 2, Section 2.3.1.

### 1.6.1 Permeable Reactive Barrier 1

The design for the first PRB was to construct it with material that allows aeration, elevated pH, and bacterial adherence, as these are the environmental conditions that allow nitrifying bacteria and archaea to thrive. The optimum environmental parameters described by Wiszniowski et al. (2006) that would facilitate aerobic bioremediation are an optimum pH of 7.5, a minimum DO concentration of 1.0 mg L$^{-1}$ and a temperature ranging between 5 and 40°C. Although pH is a major factor influencing the growth and activity of all microorganisms, high levels of nitrification activity and nitrifier growth were observed in biofilm and suspended-biomass reactors at pH values as low as 4.3 and 3.8, respectively. Ward et al., (2011) and Li et al. (2014) found that pH values of 6.4 to 7.9 had little effect on the nitrification and denitrification process. In an on-site pilot study carried out by Jokela et al. (2002), a level of nitrification of leachate (NH$_4$-N between 160 and 270 mg N L$^{-1}$, COD between 1300 and 1600 mg L$^{-1}$) above 90% was achieved in a crushed brick biofilter with a loading rate of 50 mg L$^{-1}$ NH$_4$-N per day, even at temperatures as low as 5 - 10°C. This implied that good nitrification rates could be achieved in an *in-situ* bioremediation site under Irish conditions

where groundwater temperatures could be as low as 5°C. Surface attachment provides an additional mechanism for community establishment (Ward, 2011) and attachment reduces the likelihood of removal of cells by bulk flow of groundwater. Soil nitrifiers must respond to changing conditions, and evolution and community structure may be driven by the ability to survive unfavourable conditions and respond rapidly when conditions improve. There is evidence that ammonia oxidizers are more strongly attached to soil particles than heterotrophs (Ward, 2011), which PRB2 was designed to accommodate.

## 1.6.2 Permeable Reactive Barrier 2

Section 1.2.3 outlined that the conditions preferable for denitrifying bacteria are low level of DO, a neutral to low pH and an available carbon source, and that these specific environmental criteria must be met to enable denitrifying bacteria activity. The necessary parameters outlined by Gibert et al. (2008) also include a physical support for suitable bacterial attachment.

A study was carried out by Robertson & Cherry (1995), on the use of PRBs to remove nitrate from septic systems. This study used waste cellulose solids (i.e., sawdust and leaf compost) as the reactive material and found that the barriers were successful in attenuating 60% - 100% of input nitrate levels up to 125 ml $N^{-1}$ over their first year of operation. They also concluded that the barriers contained sufficient carbon mass to allow denitrification to occur for decades without the need for carbon replenishment, and potentially for up to 200 years! A readily available source of carbon is important in subsurface environments, as the lack of readily available organic carbon has often been reported as the most common limitation to denitrification (Bedessem et al., 1994).

Gibert et al. (2008) suggested an appropriate pH to range between 5.5 and 8.0, though incomplete reduction can occur at a pH value below 6 resulting in the accumulation of the undesirable nitrate ion (Wiszniowski et al., 2006). Temperature ranges for optimum denitrifying conditions should be between 25°C and 35°C (Gilbert et al., 2008). However, this is unrealistic for *in-situ* bioremediation in temperate climates such as Ireland. Reducing temperatures (i.e. from 20°C to 10°C) in a study carried out by Ilies & Mavinic (2001) on nitrification and denitrification rates of ammonia in landfill leachate showed that nitrification rates remained constant until reaching temperatures of 10°C while denitrification rates became inhibited when reaching a temperature of 17°C. Wiszniowski et al. (2006) suggested that denitrification will occur successfully with temperatures ranging between 5°C and 60°C.

Low levels of oxygen are required for anaerobic denitrification of ammonia to take place according to Gibert et al. (2008). Consequently, recommended DO levels should be kept below the value of 0.5 mg $L^{-1}$ $O_2$ (Wiszniowski et al., 2006). However, Gómez et al. (2002) found that denitrification was almost constant with a DO concentration of up to 4.5 mg $L^{-1}$ $O_2$ and Zou et al. (2014) found that an aerobic denitrifying consortium could achieve a specific denitrifying rate of 32.93 mg N under DO of 1.0 - 1.5 mg $L^{-1}$ at 10 °C.

### 1.6.3 Oxygen Releasing Compound

As described above in Section 1.4., oxygenation of the groundwater is an important element in the design of a PRB for nitrifying bacteria. Therefore, in order to ensure enough $O_2$ for optimum nitrifier growth, various oxygenation methods were investigated. To overcome low available oxygen, oxygen-releasing compounds (ORC) including calcium peroxide and magnesium peroxide present a potential choice because it can combine with water to form oxygen gas (Huang et al., 2015; Liu et al., 2006, Dong et al., 2009). ORC Advanced™ (Regenesis) is an engineered, oxygen release compound designed specifically for enhanced, *in situ* aerobic bioremediation of contamination plumes in groundwater and saturated soils. Upon contact with groundwater, this calcium oxy-hydroxide based material becomes hydrated producing a controlled-release of molecular oxygen (17% by weight) for periods of up to 12 months on a single application. Oxygen produced by ORC Advanced™ accelerates aerobic biodegradation processes up to 100 times faster than natural degradation rates (Van-Nooten et al., 2010). Twenty-five kg of ORC Advanced™ was sourced costing €491.
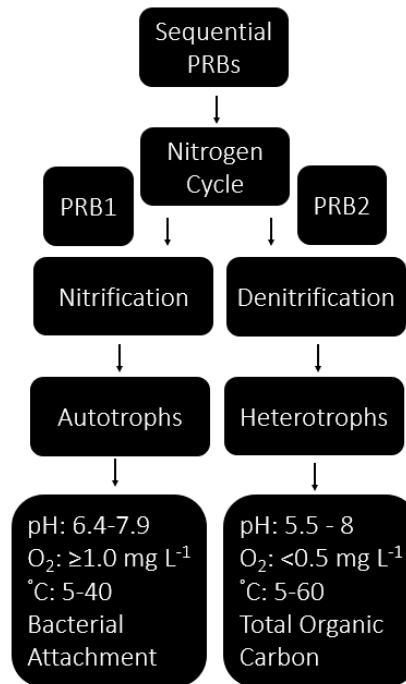
Figure 1. 6: Flow chart showing decision concepts and parameters required for PRB1 and PRB2

### 1.6.4 Project Aim

The aim of this project was to investigate the issue surrounding groundwater pollution, specifically in this case, the pollution of groundwater by ammonia, a prevalent issue in Ireland and around the globe. Following an investigation of remediation solutions, it was decided that bioremediation was the most aspirational and appropriate. The objectives of this bioremediation solution were that it needed to be financially and environmentally sustainable, *in-situ* and if effective could be easily applied to other sites with similar issues.

In response to more stringent EU laws and resulting EPA regulations, this experiment aimed to combine microbial processes and remediation to reduce ammonia contamination in shallow groundwater at a closed landfill site. Bioremediation technologies are becoming a more sought-after technique for on-site remediation due to their sustainability and cost effectiveness compared with the heavy work load and expense of pump and treat technologies (Majone et al., 2015). The bioremediation technology (i.e., PRBs) trialled on-site for this project was reliant on processes involved in the nitrogen cycle, specifically nitrification and denitrification. Two PRBs were designed and constructed to perform nitrogen cycling: the initial PRB providing suitable conditions for nitrification (the microbial conversion of ammonia to nitrate), the second providing suitable conditions for denitrification (whereby nitrate is microbially reduced to nitrous oxide and

dinitrogen gases). Field monitoring and chemical analysis were carried out monthly for the two-year study period and the results are presented and discussed in Chapter 2.

To effectively understand and explore this bioremediation technology, molecular analysis also took place. Functional gene analysis was performed quarterly across the bioremediation site, discussed in Chapter 3. Microbial community analysis was also employed to supplement the other investigations, discussed in Chapter 4.

The overall aim of this study was to investigate a known problem and provide a viable solution. It was hoped that this investigation into potential bioremediation solutions could be used, at best, as a remediation solution for ammonia contamination of shallow groundwater and at worst be used to further understand and explore bioremediation solutions.

In summary the main hypothesis to be tested was: PRBs can provide an environmentally and economically sustainable solution to ammonia contamination in shallow groundwater.

# Chapter II. Chemical Analysis of Bioremediation of Ammonia from Shallow Groundwater at Doora Landfill.

## 2.1 Introduction

Groundwater pollution by ammonia is an issue around the globe. In Ireland, it is a particular issue in inappropriately engineered landfill sites that are often located closed to surface water receptors (Chan, 2009). Waste legislation introduced in 2013 meant that landfill licence holders had to retrospectively address pollution incidences caused by badly engineered and inappropriately located landfills. *In-situ* techniques and microbial action are being increasingly viewed as a cost-effective approach to groundwater bioremediation. Regarding ammonia, this involves harnessing the naturally existing processes involved in the nitrogen cycle and encouraging the microbes that catalyse these processes to convert ammonia ultimately (through intermediary steps) to dinitrogen. To date, one of the most promising bioremediation technologies is the use of Permeable Reactive Barriers (PRBs) filled with reactive materials to intercept and decontaminate plumes of pollution in the subsurface (Thiruvenkatachari et al., 2008; Mountjoy et al., 2003; Patterson et al., 2004). The materials (chemical and/or biological reagents or catalysts) are chosen to react with the contaminants to render them harmless by the time they pass out the other side of the PRB (Golab et al*.,* 2006). The factors to be considered when choosing the reactive material for a PRB are reactivity, stability, availability, cost, hydraulic performance, environmental compatibility and safety (Gavaskar, 1999).

An exciting opportunity arose when Clare County Council, the licence holders of a landfill with a legacy of pollution issues, allowed a bioremediation strategy to be investigated as an *in-situ* solution to ammonia contamination of the shallow groundwater beneath their landfill. The aspiration of the bioremediation strategy was to biologically remediate the ammonia contamination in the groundwater to within acceptable limits before it reached the surface water receptors.

This chapter outlines the site investigation that took place to fully inform the bioremediation strategy. A desk-based study was conducted to assess the local geology, hydrogeology, and topography. The design of the permeable reactive barriers and construction of the bioremediation site is discussed, as are the field and chemical parameters used to monitor bioremediation success. The aspirations of this bioremediation solution were that it needed to be financially and

environmentally sustainable, *in-situ* and if effective could be easily applied to other sites with similar issues.

### 2.2.1 Background Information

There are 447 landfills in Ireland, 344 of which are closed sites (Chan, 2009). One of these is a closed landfill, Doora, in Co. Clare that is unlined and bounded to the north and west by surface water, both of which are designated under the EU Habitats Directive as part of the Lower River Shannon Special Areas of Conservation (SAC). "Dilute and disperse" was the principle that the landfill was designed under, hence its proximity to surface water bodies. This site had reported issues of high ammonia contamination in the shallow groundwater and as such provided the ideal conditions for this bioremediation study. In 1998, the operators of Doora Landfill, Clare County Council, agreed to pay £350,000 to 14 residences after an action was taken to the High Court where the environmental impact of Doora Landfill was the core issue (Irish Times, 1998).

Characterising hydrogeological conditions and contaminant profile to determine whether PRB installation is applicable at this site was the initial step in PRB design  (ITRC, 1999). Doora Landfill is a non-hazardous, municipal waste landfill located in a semi-rural area approximately 1.6 kilometres east of Ennis town, Co. Clare. It opened in 1956 and a waste licence (Reg. No. W0031-01) was issued to Clare County Council by the Environmental Protection Agency on May 24th, 2001, for the operation, closure, and after-care of the facility. The application for this facility was not received until 27/02/1998 (prescribed date 01/10/1997) and as a result did not comply with Section 39 of the Waste Management Act 1996 (meaning that it operated landfill activity without a valid licence). Landfilling commenced in the southwestern area of the site adjacent to Quin Road and progressed gradually toward the northeast of the site. The landfill and its ancillaries occupy an area of 29.8 hectares with 18.7 hectares used for landfilling. In accordance with condition 5.1.2 of the waste licence, no waste was accepted at the landfill for deposition after June 30th, 2001, and in accordance with condition 4.18.1 no waste was accepted for transfer after June 30th, 2002. Although many old landfills are now closed, the cessation of landfill operations does not stop chemical release into the environment (Röling et al., 2001). The site has been developed into a public park amenity area with walking tracks and a GAA playing field and is bounded to the south by the R469 road, to the north by the Gaurus River and farmland, to the east by farmland and to the west by the Fergus River. As an unlined site it was operated on the principle of dilution and dispersion of the leachate generated. Leachate abstraction and collection began at the site in 2008

but was suspended for much of 2009 as remediation works were taking place. In November 2009, leachate tankering from site to the wastewater treatment plant recommenced. The site topography is gently sloped and rises to 10.5 m above sea level at the centre of the northeast section of the site from 3.449 m OD at monitoring well BR2 (located within the bioremediation site) in the southwest area of the site. The site overview map is provided in Figure 2.1 below.
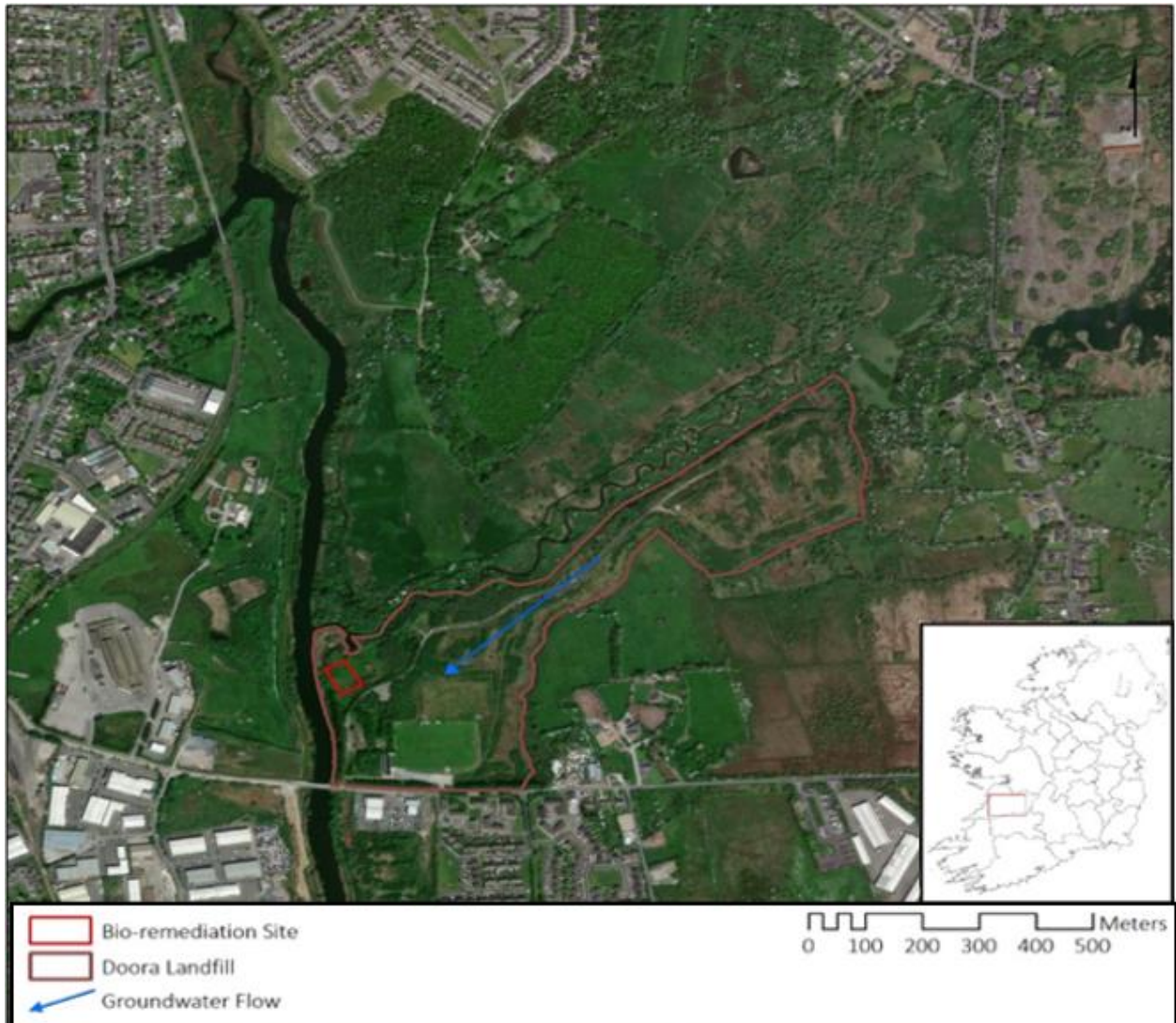


Figure 2. 1: Doora Landfill overview showing the extent of the landfill, the location of the bioremediation site and the map showing its location in a national context.

### 2.2.1.1 Geology

The geological map for the site area (GSI Sheet 17, 1:100k) indicated that the site is underlain mainly by pale grey clean skeletal limestone of the Burren Formation. The Geological Survey of Ireland (GSI) reports numerous karst features, and many sinking streams in the region (GSI, 2016) which is indicative of a highly karstified limestone. GSI reports that while karstification is ubiquitous in the area, karst features are probably limited to around 10 m below ground level (i.e.,

in the upper weathered limestone). An investigation carried out by Fehily Timoney & Co. as part of Doora Landfill Waste Licence Application (WLA) in 1998 (FTC, 1998), documents a weathered limestone overlying the competent limestone in all of their deep boreholes. A review of the GSI information and maps indicated that the onsite overburden material comprises discrete areas of estuarine sediments (silt/ clay), limestone till and made ground. FTC (1998) found that the bedrock is overlain by approximately 10 m of overburden. In ascending order, this overburden consists of silty sandy gravel (till), clay, marl, and peat. The till is continuous across the site while the clays, marls and peats are absent in the centre of the site. In the centre of the site, the limestone nearly rises to the ground level, and is overlain by the till, which is continuous to the ground surface. FTC (1998) also notes that during the initial stages of development, peat was partially removed from areas in the western part of the site and this stripped area was infilled with waste.

### 2.2.1.2 Aquifer Type

In Ireland, aquifer potential is divided into three broad categories: Regionally Important, Locally Important, and Poor. Based on the GSI Guidelines on Aquifer Classification and Vulnerability, the bedrock aquifer beneath the Doora Landfill site is considered to be a regionally important karst aquifer. The GSI aquifer classification map for the landfill area is provided in Figure 2.2 below, courtesy of SNC Environment (2014).
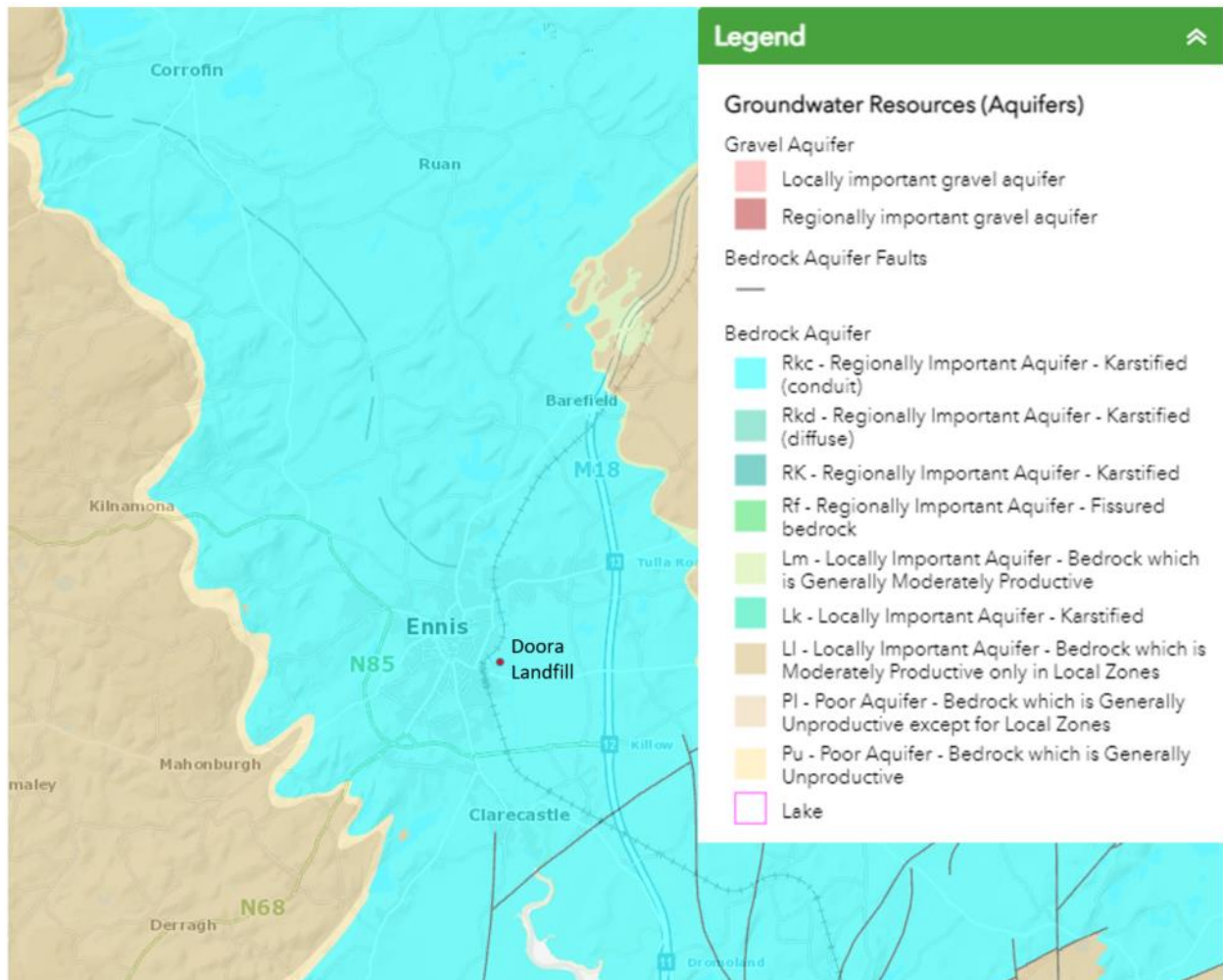
Figure 2. 2: GSI aquifer classification map showing Doora Landfill to be in an area where the aquifer is described as regionally important

Regionally important bedrock aquifers are characterised by high abstraction rates or 'excellent yields' (i.e., greater than 400 m$^3$ d$^{-1}$). The site is located within a karstified area where the vulnerability is high. In regionally important aquifers the horizontal flow system is not considered to be limited. Accordingly, horizontal pathways to pollutant migration are expected at the landfill.

### 2.2.1.3 Groundwater Vulnerability

The GSI classifies groundwater vulnerability into four general categories: Extreme, High, Moderate, and Low (GSI, 2016). The classification system is further divided into bedrock and sand/gravel aquifers. This classification system is based on the permeability and thickness of the soil overlying the aquifer. In principle, thicker layers of fine-grained soils overlying an aquifer would generally provide more protection to the aquifer and such a setting would tend towards a low vulnerability rating. Outcropping bedrock aquifers would tend towards an extreme vulnerability rating. The GSI identifies Doora landfill site as both a high and moderate vulnerability aquifer,

implying that surface pollutants would move quickly and in relatively high quantities from the ground surface into the underlying aquifer. The north-eastern section of the landfill is classed as moderately vulnerable except for a strip along the north-eastern boundary that is classed as high vulnerability. The south-western and central sections of the Doora Landfill site are classed as high vulnerability. A copy of the GSI aquifer vulnerability map is provided in Figure 2.3 below.
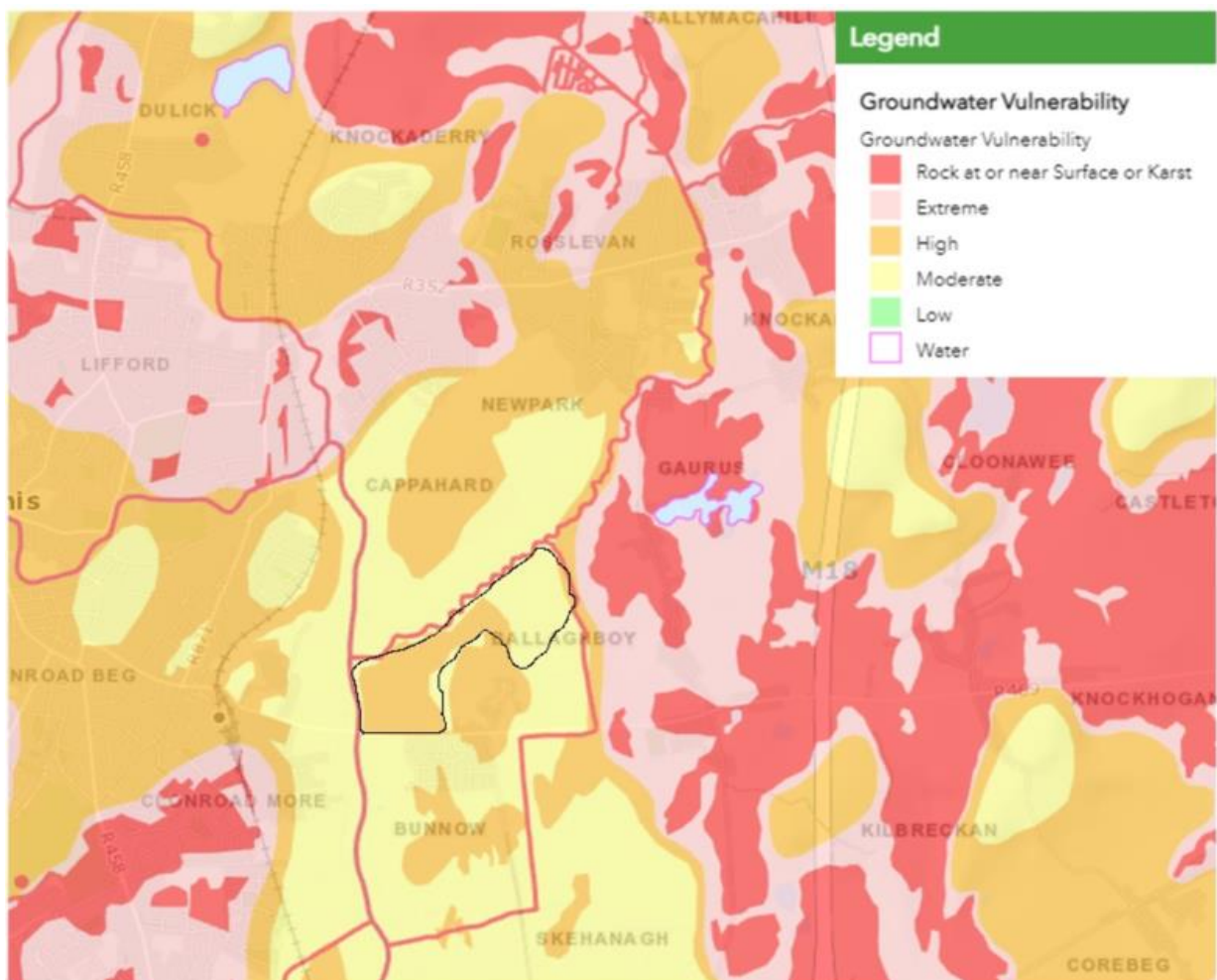


Figure 2. 3: GSI Aquifer Vulnerability Map showing Doora Landfill (outlined in black) to be in an area of moderate to high vulnerability

During the preparation of the Environmental Impact Statement (EIS) accompanying the Waste Licence Application (WLA), Fehily Timoney & Co. (FTC, 1998) identified five groundwater abstraction wells located in Ennis. These wells were installed in 1964 and it is not known whether they are still in use. A second GSI search for groundwater abstraction wells between Doora and Clarecastle did not indicate any wells within 3 km downgradient of the landfill. Two private wells were noted approximately 1 km southeast of the site. Other groundwater abstraction wells

located near the Doora Landfill site are the council well (not used for public supply) and a private well used for agricultural purposes located 500 m downgradient of site.

To help protect groundwater abstractions, the GSI and the EPA define Source Protection Areas (SPA) around known wells. The SPAs are created to provide a buffer around groundwater sources (e.g., regional, group or individual drinking water sources and industrial abstraction sources) and limit the types of developments and activities completed within or immediately surrounding the zone of contribution (ZOC) of any groundwater source to ensure that groundwater quality is maintained. The ZOC is divided into two areas:

1. Inner Protection Area (SI) – the SI is designed to protect groundwater quality from immediate impacts from human activities. The SI area in non-karst areas is delineated based on a 100-day time of travel for groundwater (and/or associated contaminants) from the source defined from the groundwater velocity and hydrogeological gradient or from a fixed radius distance of 300 m from the source.

2. Outer Protection Area (SO) - The SO covers the whole catchment area of a groundwater source and is defined by the GSI as "the area needed to support an abstraction from long-term groundwater recharge (i.e., the proportion of effective rainfall that infiltrates to the water table)". A conservative factor can be used to calculate the SO where the maximum daily abstraction rate is increased (usually by 50%) to allow for possible future increased abstraction rates and for extension of ZOC in dry weather periods. A flow direction variation has also been included by the GSI (i.e., ±10-20°) when estimating ZOC area to take account of the heterogeneity of Irish aquifers and possible errors in estimating groundwater flow direction. An arbitrary radius distance approach from source of approximately 1000 m can also be used in the absence of technical hydrogeological data. The GSI have mapped groundwater abstraction wells and their SPAs in the vicinity of the Doora Landfill site. The closest Source Protection Area to the Doora Landfill is located northeast of Ennis town approximately 2.7 km upgradient from the landfill. Based on the results of a review of the EPA's Envision database and mapping resources, the groundwater body in and around the Doora Landfill was characterised as follows:

- The groundwater body Water Framework Directive (WFD) status for monitoring completed on between 2007 and 2012 was considered "Good".
- The Fergus River was classified as "Poor" and the Gaurus River was classified as "Moderate".

- The regional groundwater body around the Ennis area had an EPA WFD Risk Score that classified it as "at risk of not achieving good status", indicating that various sources in the region may be contributing inputs to the groundwater body that may be impacting groundwater quality.

### 2.2.1.4 Site Hydrogeology

The estimated effective rainfall for the site is 776 mm year$^{-1}$ with a recharge coefficient of 20% resulting in an estimated groundwater recharge of 175 mm year$^{-1}$ for the northern section of the site and 155 mm year$^{-1}$ for the southern section of the site (GSI, 2016). The landfilled area at Doora is estimated at 9.8 ha in the south of the site and 8.9 ha in the north. Based on these estimates, approximately 230,000 m$^3$ of precipitation falls on the site (22 ha) annually. Of this volume, approximately 15,500 m$^3$ per year infiltrates into the groundwater system in the northern section of the site and 15,100 m$^3$ infiltrates into the groundwater system in the southern section of the site. It is estimated that approximately 138,000 m$^3$ discharges as overland flow (through bog and surface drainage), and the balance of 61,400 m$^3$ leaves the site through the combined effect of evaporation and plant transpiration. These general estimates assume natural conditions, and do not account for engineered drainage systems or alterations to the land. The Doora Landfill site is located on the floodplain of the Fergus and Gaurus Rivers, which is an area of regional groundwater discharge. The Gaurus River is a relatively small tributary to the Fergus River and flows southwards along the northern and western boundary of the site from the northeast corner to the southwest corner where it joins the Fergus River. The Fergus River flows along the western boundary of the landfill site for approximately 345 m after it is joined by the Gaurus River.

The site is also drained by a network of manmade drains, mainly via a surface water drain that runs parallel to the Gaurus River on the northwestern boundary of the site before discharging into the Gaurus. Several smaller surface water drains also flow into this drain before entering the Gaurus River. The location of the Fergus and Gaurus Rivers are provided on the site layout plan provided in Figure 2.1.

Since karstification is ubiquitous throughout the region, most of the groundwater moves through an epikarstic layer in the limestone that may only be a few metres thick (weathered surface of limestone). The epikarstic layer would comprise interconnected solutionally-enlarged conduits that allow rapid groundwater flows. In the Fergus Valley, groundwater speeds of up to 240 m hr$^{-1}$ have been observed in the epikarst (GSI, 2016). Below the epikarst zone, groundwater flow is likely restricted to fewer karst conduits and fractures/bedding planes. Restrictions on groundwater flow likely increases with depth, until competent limestone is reached, where flow is limited primarily

to fracture flow (e.g., bedding planes). Previous site investigations (FTC, 1998) have suggested a strong hydraulic connectivity between the Fergus River and the bedrock aquifer underlying the site, which is illustrated by the varying groundwater levels in the groundwater wells in response to the tidal cycle. FTC (1998) estimated the hydraulic conductivity of the weathered limestone underlying the site to be $2 \times 10^{-5}$ m s$^{-1}$ (based on a single packer test result). Groundwater flow in the overburden material is believed to be controlled by the sand and gravel till, which would act as a preferential flow path. The hydraulic conductivity of the till underlying the site was estimated at $2 \times 10^{-5}$ m s$^{-1}$ (FTC, 1998) based on a single rising head test. The hydraulic conductivity of the till and weathered limestone are equal (albeit by limited testing), which suggests they have a strong hydraulic connection. Although the flow through the peat, marl and clay is expected to be significantly lower, a hydraulic connection with the underlying till and weathered limestone would be expected (e.g., infiltration of surface water is expected). It is noted that FTC (1998) indicated that waste fill is located below the water table and adjacent to the River Fergus on the west end of the site. Groundwater flow direction was found to be flowing in a south to southwest direction, towards the Gaurus and the Fergus Rivers (FTC, 1998). The hydraulic gradient in the overburden was calculated to be 0.125 and the bedrock gradient was calculated to be 0.0105. Note that hydraulic gradient is in units of m d$^{-1}$ and is usually expressed without units.

### 2.2.1.5 Surface Water

Doora Landfill site is oriented in a southwest to northeast direction and is located within the floodplain of the Gaurus and Fergus Rivers. The lower area of the site is bordered to the west by the Fergus River and to the north by the lower section of the Gaurus River, a tributary of the Fergus. The central and upper sections of the landfill are bordered to the northwest by a man-made surface water drain located at the toe of the landfill body and then the Gaurus River approximately 20 m beyond. The site topography is generally flat at the lower areas with an increased slope to the north (main landfill body). The northern section of the landfill slopes to the north, south, east, and west and surface water drains exist to the north, east and west. Surface water runoff to the south is directed to an underground drainage system and is ultimately discharged to the Fergus River approximately 30 m upstream from Doora Bridge on the Quin Road. The location of the landfill and the surface water bodies are provided in Figure 2.1.

## 2.2.1.6 Receptor Assessment Summary

The groundwater vulnerability beneath the site is classified as high. The landfill is not located within a GSI published source protection zone though there are two private wells and one agricultural well between 1 km and 0.5 km down hydraulic gradient of the site.

## 2.2.1.7 NATURA 2000

NATURA 2000 are sites that have been designated under the EU Habitats Directive (Special Areas of Conservation (SACs)) and the EU Birds Directive (Special Protection Areas (SPAs)). These sites are afforded greater environmental protection under EU law to protect the integrity of their habitat and status. There are a number of NATURA 2000 sites located throughout County Clare though only a few occur within 5 km of Doora Landfill. Doora Landfill is located approximately 3 km upstream of the River Shannon and River Fergus Estuaries Special Protection Area (SPA) (Site Code 004077) and approximately 3 km downstream of the Ballyallia Lough SPA (Site Code 004041). It is located approximately 2 km downstream of the Ballyallia Lough SAC (Site Code 000014) and is fringed by the Lower River Shannon SAC (Site Code 002165) on its western and northern boundaries (i.e., the Gaurus and Fergus Rivers). The NATURA 2000 site deemed to be potentially affected by the Doora Landfill is the Lower River Shannon SAC. The SAC is 120 km long and Doora Landfill is located within 5 km of its most northerly point (see Figure 2.4 below).

Figure 2. 4: Aerial photograph showing Doora Landfill and the proximity of the Lower R. Shannon SAC (Biodiversity Ireland, 2016).

The site is selected for EU Habitats Directives Annex I habitats alluvial wet woodlands and lagoons. Other Annex I habitats include floating river vegetation, *Molinia* meadows, estuaries, tidal mudflats, Atlantic salt meadows, Mediterranean salt meadows, *Salicornia* mudflats, sandbanks, perennial vegetation of stony banks, sea cliffs, reefs and large shallow inlets and bays. Annex II

species for which the SAC is selected for are Bottle-nosed Dolphin, Sea Lamprey, River Lamprey, Brook Lamprey, Twaite Shad, Freshwater Pearl Mussel, Atlantic Salmon, and Otter. The Bottle-nosed dolphin is found in the lower reaches of the SAC and is not associated with the Fergus River or the Doora Landfill. None of the fish species of interest have been noted to spawn in the upper reaches of the Fergus River and the pollution sensitive Freshwater Pearl Mussel has been noted in the Cloon River with no records of it occurring in the Fergus River. The SAC features of interest most relevant to Doora Landfill are mudflats and sandflats not covered at low tide and otter as evidence of both have been noted at the landfill site. A Red Data species occurring along the Fergus Estuary is the Golden Dock (*Rumex maritimus*) though it has never been noted at the landfill site.

## 2.2 Materials and Methods

### 2.2.1 Site Assessment

Due to the problematic nature and many issues surrounding Doora, Clare County Council commissioned a number of site assessments which are presented in Table 2.1 below.

Table 2. 1: Site assessments carried out at Doora Landfill

| Year | Assessment title | Company |
|------|------------------|---------|
| 1992 | Doora Landfill Site Ground Investigation | Fehily Timoney & Co |
| 1998 | Investigation at Doora Landfill Site | Irish Geotechnical Services |
| 1998 | Section C.6 of Waste Licence Application Document | Fehily Timoney & Co |
| 1998 | Hydrogeological Cross Sections, Doora Landfill | Fehily Timoney & Co. |
| 2004 | Submission on Trial Hole Investigations | Fehily Timoney & Co. |
| 2013 | Doora Landfill Porewater Sampling Programme | SNC- Environment |
| 2014 | Doora Landfill Hydrogeological Report | SNC- Environment |

These reviews, reports and assessments were used to better understand the site and allowed a location for the bioremediation site to be chosen e.g., groundwater flow rate and direction of flow. In order to design the PRBs and to determine their precise location and orientation, a review of site geology, hydrogeology and background information was undertaken.

### 2.2.2 PRB Design and Construction

Initially, Clare County Council needed to be approached to ascertain whether they were interested in allowing this bioremediation project to go ahead at their landfill site. Considering the landfill's

poor record and the new legislation introduced by the EU and subsequently by the EPA, Clare Co. Co. were agreeable to investigate a potentially inexpensive and sustainable treatment system to be trialled at their site. Due to the invasive nature of the PRBs and the disturbance caused at the closed landfill by the PRB installation, permission was required from the EPA by Clare County Council. As outlined in Chapter 1, the purpose of the PRBs was to provide suitable environments for nitrogen cycling bacteria: nitrifiers in PRB1 and denitrifiers in PRB2. The following table, Table 2.2, summarises the optimum conditions (Wiszniowski et al., 2006) required in both PRBs as discussed in Section 1.6.

Table 2. 2: Summary of optimum conditions for nitrifying and denitrifying bacteria in PRB1 and PRB2, respectively.

| Parameter | PRB1 | PRB2 |
|---|---|---|
| pH | 6.4 - 7.9 | 5.5 - 8.0 |
| $O_2$ | $\geq 1.0$ mg $L^{-1}$ | $<0.5$ mg $L^{-1}$ |
| °C | 5 - 40 | 5 - 60 |

Before optimisation of reactive materials and laboratory experiments could commence, the parameters to be measured needed to be determined. pH, DO, temperature and electrical conductivity would be measured on site. Laboratory analysis on groundwater collected from the bioremediation site would be carried out to determine concentrations of ammoniacal nitrogen, nitrite, nitrate, and total organic carbon. Downstream molecular analysis would be carried out on the eDNA extracted from the site to give an insight into the microbial communities and processed on the site.

### 2.2.2.1 Field Parameters

The field parameters monitored monthly on-site were pH (pH units), DO (mg $L^{-1}$), electrical conductivity ($\mu$S $cm^{-1}$) and temperature (°C). Groundwater samples from the site were collected by lowering dedicated tubing into the wells and using foot valves to pump the water to the surface where it could be collected and monitored. DO was measured monthly on-site using a handheld MW600 DO Meter & MA840 Polargraphic probe (Milwaukee Instruments). On-site monthly monitoring of pH took place using a handheld 0.6" LCD Accurate pH Tester Meter. Electrical conductivity was measured on-site using the AZ-8361 Pen Conductivity TDS meter and temperature was measured using the AZ-8361 Pen Conductivity TDS meter.

*2.2.2.2 Chemical Analysis*

On-site monitoring commenced with PRB installation (June 2015) for a period of 24 months. Clare County Council are required to carry out monthly analysis on samples collected from their on-site monitoring wells and surrounding surface water bodies. Groundwater samples from the bioremediation monitoring wells were collected in tandem and sent for analysis along with to Jones Environmental Forensics in the UK, so that chemical results from the bioremediation site would be directly comparable with results from the landfill monitoring wells and also the surrounding surface waters. Samples were collected using Waterra piping and footvalves in designated collection bottles. These were then sent at 4°C under the appropriate chain of custody to Jones Environmental where analysis took place the following day. Jones Environmental is a fully accredited UK based laboratory and has been carrying out chemical analysis on groundwater, surface water and leachate samples from the Doora Landfill site since 2012. They carry out their anions and ammonium analysis using an Aquakem Photometric Analyser. The ions were determined by turbidity and these ions included ammonium, nitrate, and nitrite. See Table 2.3 below for the limits of detection (LOD) and accreditations for ammonium, nitrate, and nitrite.

Table 2. 3: Jones Environmental Limit of Detection (LOD) and accreditation for ion concentrations

|  |  | ISO 17025 Accreditation Applicable for; | | |
|---|---|---|---|---|
|  | LOD (mg $L^{-1}$) | Waters | Leachates | Soils |
| Ammonium | 0.03 | ✓ | ✓ | ✓ |
| Nitrate | 0.2 | ✓ | ✓ | ✗ |
| Nitrite | 0.02 | ✓ | ✓ | ✗ |

In order to carry out analysis of total organic carbon in water samples Jones Environmental used a TOC Analyser that is a fully automated non-dispersive infrared (NDIR) gas analyser. The method detection limit for this procedure was 2 mg $L^{-1}$ and has full ISO 17025 accreditation for analysis on surface water, ground water and leachate. Total organic carbon was calculated by subtracting the known quantity of inorganic carbon from the measurement of total carbon. Measurement of total carbon was determined by a sample being injected into a combustion tube converting the carbon compounds into $CO_2$, which was then sent through a halogen scrubber into the NDIR where the $CO_2$ was detected. Inorganic carbon was determined by acidifying the sample with hydrochloric acid, which converted the inorganic carbon to $CO_2$, which was then measured using the NDIR.

*2.2.2.3 Reactive Material Optimisation*

To establish appropriate reactive materials to use for the PRBs on-site, bench scale laboratory tests were carried out. As described earlier two sequential microbial PRBs were to be introduced into the bioremediation site. To encourage the growth of nitrifiers, a PRB with increased pH and DO levels and containing a substratum that allows bacterial adherence was desirable for PRB 1. Ideal PRB 2 conditions included lower pH and DO concentrations while containing a carbon rich substrate for the heterotrophic denitrifiers. As such, bench tests were carried out to test the appropriateness of different reactive materials for both PRBs. Materials located locally to the landfill were tested to give an indication of their appropriateness for use as reactive materials in the PRBs. Various grades of limestone (i.e., 20 mm, 40mm and mixed grade) were sourced from a local quarry and mulch (composed of garden waste) was sourced from Inagh landfill in County Clare. These tests were not replicated as robust analysis and monitoring of the reactive materials would take place onsite over a 24-month period.

2.2.2.3.1 Bench Test 1- Reactive Materials

To simulate the construction of PRB1, 500 ml of water was collected from downstream (already established) monitoring well S5 and 690 g of crushed cement (<550 mm in diameter) was added. To simulate PRB2, 500 ml of water collected from S5 was used with 150 g of mulch. In addition, 500 ml of site water was collected and monitored without any additions. pH, DO air temperature and water temperature was monitored in the three samples over a three-week period at two different temperatures: 4°C and 19°C. This bench test was carried out in order to test potential reactive materials for the permeable reactive barriers. Limestone was tested for PRB 1 as a potential reactive material and its effect on pH and DO concentrations in landfill groundwater under two different temperatures over a three-week period.

2.2.2.3.2 Bench Test 2 - Limestone Grades

On conferring with the Senior Executive Engineer from Clare County Council, he advised that a local quarry would supply limestone for the reactive material of PRB 1 and had different grades to choose from. To check whether different grades of limestone had different effects on the pH and DO a bench test was carried out using groundwater from the landfill and three different grade types: 20 mm (limestone with a diameter no greater than 20 mm), 40 mm, and mixed limestone (a variety of sizes and including a high volume of dust). Three litre containers were used. To the first container 1.2 kg of 20 mm stone was added and landfill water (600 ml) was added to the one

litre mark. To the second container 1.2 kg of 40 mm stone was added with 750 ml landfill water and 1.2 kg of mixed stone was added to the third with 520 ml water to fill to the litre mark. The study lasted 21 days.

### 2.2.2.3.3 Bench Test 3 - Magnesium Peroxide

Considering passive aeration in PRB 1 might not raise the DO to the appropriate levels, active oxygenation options were assessed. A bench test was carried out to monitor the DO concentrations with the addition of magnesium peroxide complex (Aldrich, Germany) over 5 days. Groundwater from the landfill was collected and the equivalent of 10 kg, 20 kg and 100 kg of the complex was added to 10 $m^3$ water (i.e., 0.05 g, 0.1 g, and 0.5 g, respectively to 50 ml water). A control sample where no magnesium peroxide was added was also monitored for DO concentrations.

### 2.2.2.3.4 Bench Test - Oxygen Releasing Compound

Another bench test was carried out on active oxygenation, this time with an oxygen releasing compound (ORC) (as described in Section 1.4.4), routinely sold as a remediation agent from Regenesis$^{Tm}$ that they claim remains active for one year. This study was carried out over nine days at room temperature and as with the magnesium peroxide, groundwater was collected from the landfill site and the equivalent of 10 kg, 20 kg, and 100 kg per 10 $m^3$ volume of water was added (i.e., 0.05 g ORC/ 50 ml; 0.1 g/ 50 ml and 0.5 mg /50 ml, respectively). No ORC was added to the control sample.

### *2.2.2.4 Column Experiments*

In order to provide small-scale versions of conditions in the field, column experiments were conducted in the lab. A set of four columns were constructed with the top half representing PRB 1 and the lower half representing PRB 2. The columns were made using 4" pipes with tapped containers to act as reservoirs so that water could be easily collected for analysis, Figure 2.5 below.
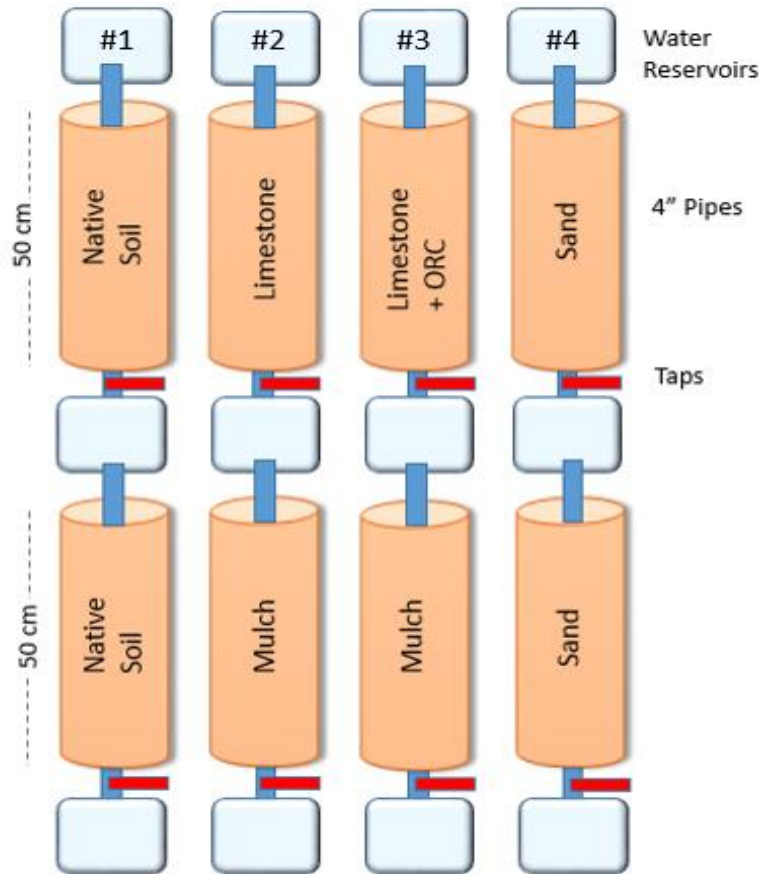
Figure 2. 5: Column design replicating on-site permeable reactive barriers using 4" diameter pipes intersected by tap reservoirs. Native soil was collected from the site, while potential materials were used for the remainder. Sterile sand acted as the control.

Contaminated groundwater was collected from Doora landfill for use in the column experiment. The first set of columns contained only native landfill cap material (soil mixed with waste material) collected from the site so to represent on-site conditions before any alteration was made. The second set of columns was designed to replicate the initial design; the first column filled with local limestone (40 mm), the same as the reactive material to be in PRB 1, while the second column contained locally sourced mulch, the same as to be used in PRB 2 on-site. The third set of columns contained limestone with the addition of ORC (2.24 g) in the first part, the same as the planned on-site conditions and mulch in the second part. The fourth set contained sterile sand in both the column representing PRB 1 and PRB 2. The sand was autoclaved (121°C x 15 PSI x 15 min) to ensure that there would be no established microbial community. Water reservoirs were placed at the beginning of each column set so that initial measurements could be taken. A reservoir was also placed in the middle of each column set so analysis could be carried out after the landfill water passed through the column representing PRB 1 and again at the end of the sets of columns so that analysis could be carried out on the groundwater sample at the end of the experiment. The

groundwater was measured after two-day retention time per column for field parameters (pH, DO, temperature and electrical conductivity) and chemical parameters ($NO_2$, $NO_3$, $NH_4$-N, and total organic carbon). These tests were not replicated as robust analysis and monitoring of the reactive materials would take place onsite over a 24-month period.

### 2.2.3 PRB Installation

Once the reactive material of the PRBs were chosen, attention turned to the exact location and orientation of the PRBs. Upgradient GW wells were highly contaminated and SW3 (the surface water sampling and monitoring point downstream of the bioremediation site) showed high concentrations of $NH_4$-N. Considering the GW flow work that FTC carried out, this study aimed to intercept the contamination plume before it reached surface water receptors. For the PRBs to intercept the groundwater plume they needed to be installed perpendicular to the direction of the groundwater flow. A site investigation carried out by Fehily, Timoney & Co. in 1998 assessed the groundwater flow direction using falling-head tests. Once groundwater flow was established, the orientation and exact location of the PRBs could be chosen. A planned site visit was conducted on March 25th, 2015, with the Senior Executive Engineer of Clare County Council and final plans were made.

Two sequential PRBS (with incorporated monitoring wells (S2 and S4)) were installed within the landfill site on June 10th, 2015. Five metres up-gradient, a monitoring well (S1) was installed, 4 m deep, in order to completely intercept the water table. Another monitoring well (S3) was installed between the PRBs. Finally, an on-site monitoring well (OB2/ S5) was incorporated into the bioremediation site acting as downstream monitoring well. As this well was already established, historical analytical data was available for it. Figure 2.6 below shows the layout of the bioremediation site.

Figure 2. 6: Aerial photograph showing the layout of the bioremediation site including the PRBs 1 and 2, and monitoring wells S1 to S5.

PRB 1 was designed to encourage growth of nitrifying microbes (i.e., to raise pH and DO and to allow for microbe adherence) while PRB was designed to lower pH, DO, and provide a carbon source as illustrated in Figure 2.7 below.
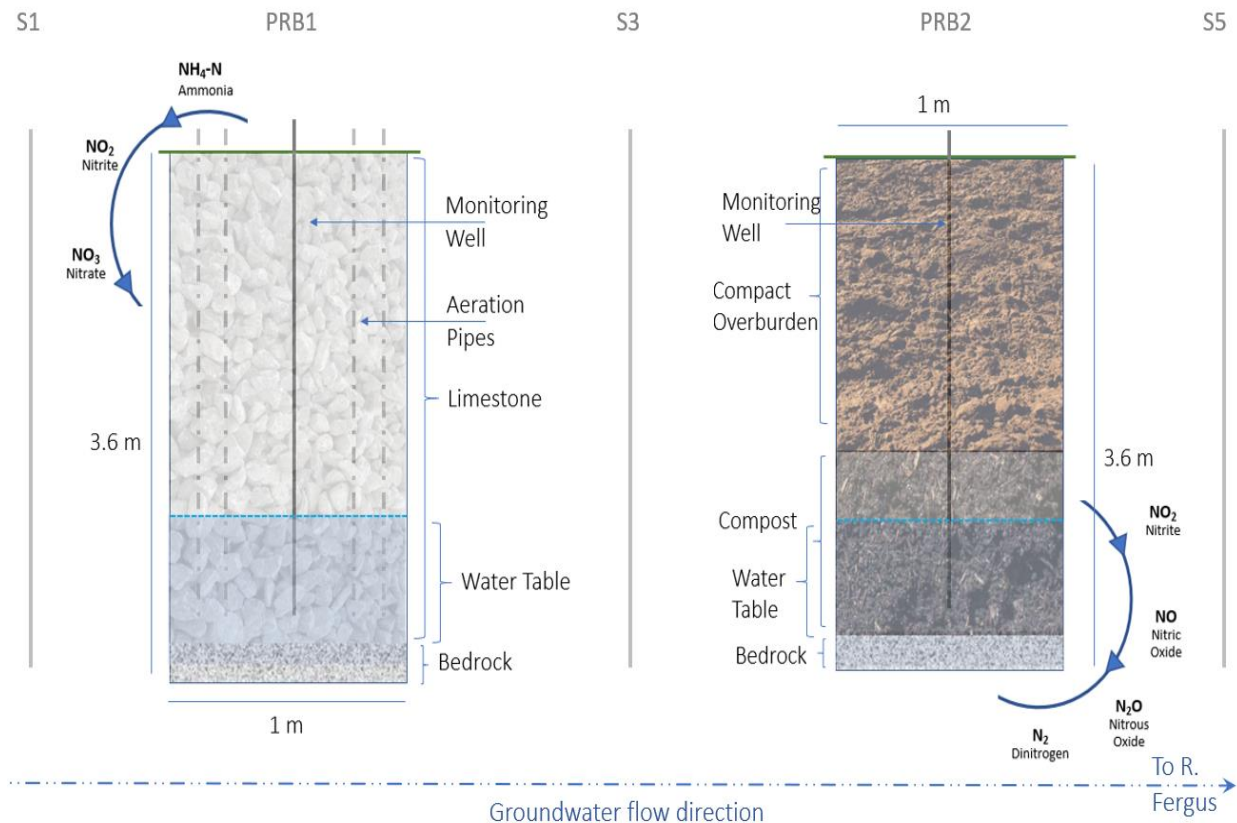
Figure 2. 7: Permeable reactive barrier design showing reactive material used and the expected bioremediation pathways in each PRB.

### 2.2.2.1 Permeable Reactive Barrier 1

Limestone from a local quarry was selected and tested in the laboratory using bench and column tests. PRB 1 was constructed to be 3.6 m deep, 10 m long and 1 m wide coming to a total volume of 36,000 $m^3$, therefore requiring 36 tonnes of limestone to fill. The entire PRB was filled with coarse limestone >40 mm in diameter to allow for larger pore space and therefore allowing passive oxygenation to take place. 108 m of 4" PVC perforated pipes were also installed in bundles of three (in 4 m lengths) along the length of the PRB, see Figure 2.8. A central aeration pipe was designated to also double as a monitoring well within the PRB.

Five meters up-gradient of PRB 1 a monitoring well was installed (S1) so that monitoring of the groundwater could occur before reaching the PRBs. An excavator installed a 4" PVC pipe 3.6 m deep, filled around the base with coarse stone to hold the well in place and to allow for some filtration of material loosened by the disturbance. The soil/ waste mixture extracted was then replaced around the monitoring well to ground level. A 5 m monitoring well (S3) of the same design was installed 5 m downstream of PRB 1 so as to be halfway between PRB 1 and PRB 2. The designs of PRB 1 and PRB 2 are displayed above in Figure 2.8.

47

### 2.2.2.2    Permeable Reactive Barrier 2

PRB 2 was also constructed to be 3.6 m deep, 10 m long and 1 m wide (total volume of 36,000 $m^3$). Mulch from another landfill operated by Clare Co. Co. was chosen and tested to be the fill material. This was chosen for its ability to reduce pH levels and 4 tonnes were added to PRB 2 until above the groundwater level and then the soil/ waste material that was excavated was back filled and compacted into PRB 2 to reduce oxygen infiltration (Figure 2.7 above). A photograph showing the construction of the PRBs can be seen below, Figure 2.8.



Figure 2. 8: Photograph showing construction and materials of PRB 1 (on right) and PRB 2 (on left) on June 10th, 2015.

Figure 2.8 above shows PRB 1 construction with aeration pipes and limestone. Also shown here is the construction of PRB 2 where the overburden (with high waste quantity) has been removed and the mulch has been placed next to the trench prior to infilling. Finally, an already established overburden well (OB2/S5) located 10 m down-gradient from PRB2 was incorporated into the bioremediation site to act as the final monitoring point. Since this well had $NH_4$-N concentration data since 2012 it was hoped that any fluctuating $NH_4$-N concentrations could be compared with historic data.

### 2.2.3 Statistical Analysis

Statistical analysis (XLSTAT Ver. 2021.4.1) was used to ascertain whether the PRBs significantly altered the concentrations of the field and chemical parameter concentrations in the bioremediation. Where parameter data were normal (Shapiro-Wilk Test) and homoscedastic

(Levene's Test) (i.e., pH, temperature, and electrical conductivity), One-Way ANOVA was used followed by a post hoc Tukey's HSD test for mean comparisons to determine seasonal and spatial relationships. Where parameter data were neither of these (and/or less than MDL) (i.e., DO, $NH_4$-N, $NO_2$, $NO_3$ TOC), the Kruskal-Wallis test as per Helsel et al. (2005) was used followed by a Bonferroni correction of $\alpha = 0.005$, and the Dunn's test applied post hoc. Pearson's correlations tests were performed in Microsoft Excel, with the p- values extrapolated and the Bonferroni correction applied.

## 2.3 Results

Figures 2.9 – 2.15, below, illustrate the results of the bench tests as described in Section 2.2.2.3. Column experiments are described in Section 2.2.2.4 and the results are illustrated below in Figures 2.16 – 2.18. Figures 2.19 – 2.36 outline the results for the field parameters and chemical analysis of the groundwater collected from the bioremediation site over a two-year period (June 2015 to May 2017). The results below are presented in a way so as to make them comparable with the molecular results that will be discussed in Chapters 3 and 4. The complete monthly field and chemical results are tabulated in Appendix A. Distance (m) describes the distance of the PRB and/or monitoring well from the surface water receptor (S5 being closest).

### 2.3.1 Bench Tests

As described in Section 2.2.2.3, four bench tests were carried out to determine suitable material for PRB infill. Results of Bench Test 1, the effect of limestone on pH and dissolved concentrations at 4°C and 19°C, are shown below in Figure 2.9. As can be seen, there was not a large difference between the two temperature sets. Increases in pH (initial pH, 6.34) were noted at the beginning of the experiment once the limestone was added to the landfill groundwater at both 4°C and 19°C, and it remained elevated for the remainder of the experiment with a final pH of 11.54 (19°C) and 12.24 (4°C) on day 21. DO concentrations showed an initial increase in the groundwater after addition of limestone at 19°C from 4.2 mg L$^{-1}$ to 7.2 mg L$^{-1}$ on day 2 but decreased gradually over the remainder of the experiment to 4.0 mg L$^{-1}$ on day 21 of the experiment. DO concentrations at 4°C reached 7.2 mg L$^{-1}$ on day 13 of the bench test and gradually decreased to 6.5 mg L$^{-1}$ on day 21. From this experiment it was seen that limestone had potential to be the reactive material for PRB 1. Although it elevated the pH too much, it was thought that this could be remedied by using a lower dose, and it had the desired effect of increasing the DO concentrations. However, since

the oxygen concentrations decreased over time, it was suspected that active oxygenation might be necessary for PRB 1 at the field site to raise DO.
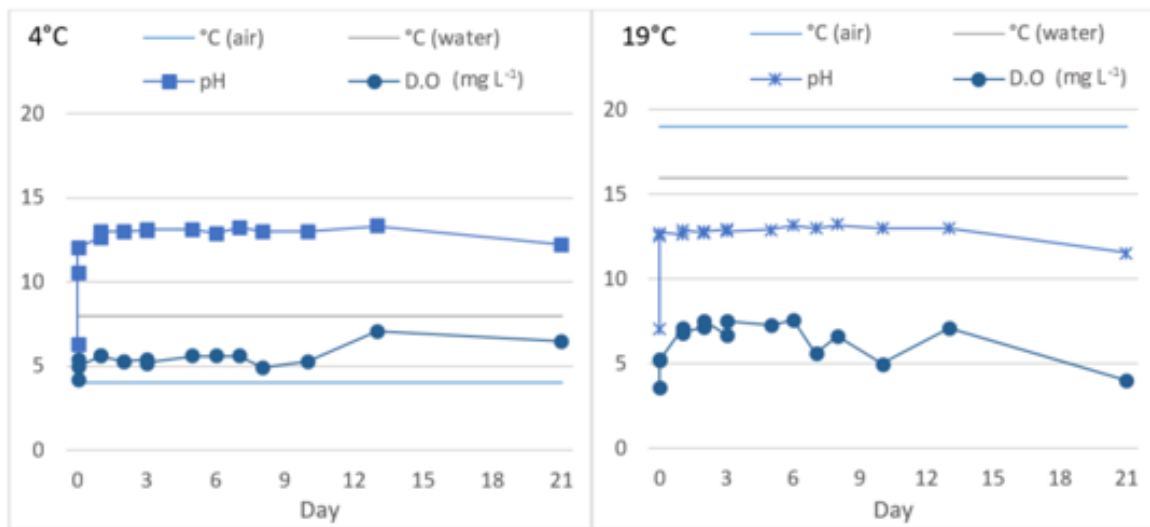


Figure 2. 9: Bench Test PRB1- Effect of limestone on pH and DO concentrations in landfill groundwater at different temperatures (4°C & 19°C).

Mulch was the reactive material assessed for use in PRB 2, selected in order to reduce the pH and DO levels. The effects that this reactive material had on pH and DO can be seen in Figure 2.10 below. In PRB 2 mulch bench test, the pH did not vary greatly throughout the study. The initial pH of 6.84 in PRB 2 at 19°C fell slightly to 6.82. In PRB 2 at 4°C, pH rose slightly from 6.34 at the beginning of the study to 7.25 at Day 21. DO concentrations in PRB 2 at 19°C fell steadily from an initial concentration of 3.2 mg L$^{-1}$ to 2.1 mg L$^{-1}$ on Day 21. Similar reductions in DO concentrations were noted in PRB 2 at 4°C, where concentrations fell steadily from an initial concentration of 4.2 mg L$^{-1}$ to 1.5 mg L$^{-1}$ at the end of the study. These values showed that mulch was a suitable reactive material for PRB 2, lowering the DO. While there was a slight increase in pH, it was still within the suitable range for the growth of nitrate reducing bacteria.
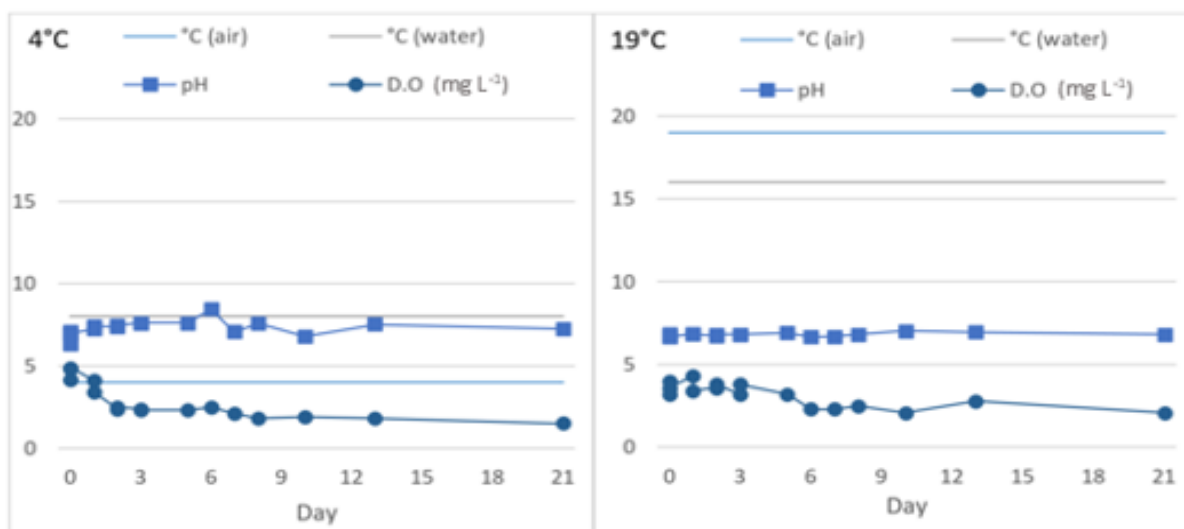
Figure 2. 10: PRB2 Bench test- effect of mulch on pH and DO concentrations in landfill groundwater at different temperatures (4°C & 19°C).

The following graph, Figure 2.11 shows the pH and DO in the control sample where there was no reactive material added to the landfill groundwater. There was a gradual increase in both pH and DO concentrations noted in the control sample, with the pH rising to 8.23 from 6.54. DO concentrations rose from 4.2 to 5.1 mg L$^{-1}$ and remained elevated until the end of the experiment with a DO concentration of 6.4 mg L$^{-1}$. This increase in DO concentrations was thought to be due to the landfill sample being exposed to air. All further bench tests were carried out at room temperature.
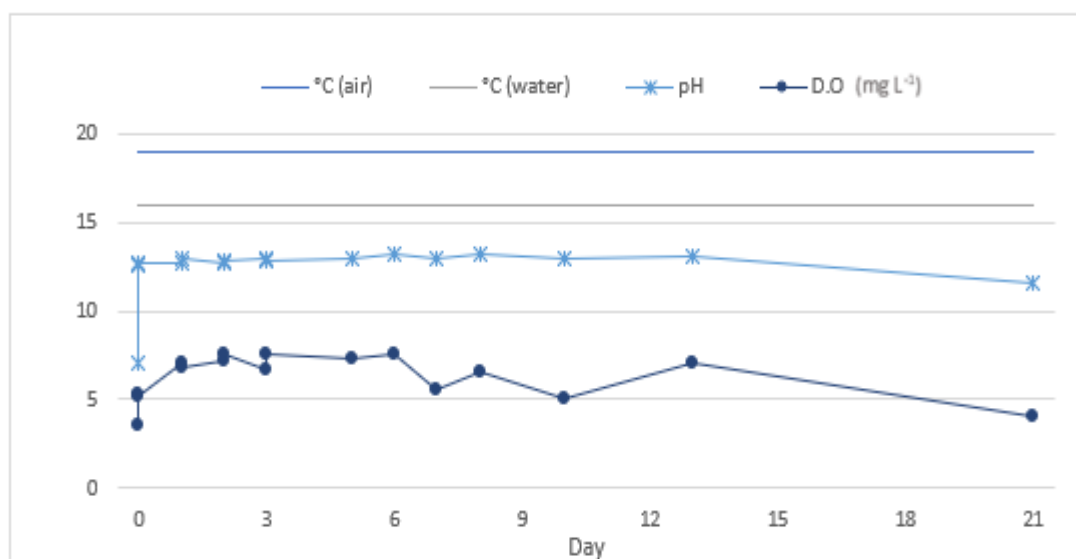


Figure 2. 11: Control Bench test- pH and DO concentrations in landfill groundwater with no reactive material at 19°C

The results of Bench Test 2 showing the effect of limestone grades on pH and DO concentrations in contaminated groundwater are shown below in Figures 2.12 and 2.13. The results showed that

51

there was little difference in pH and DO concentrations between the different limestone grades. There was a slight increase in pH and a decrease in DO in all three samples.
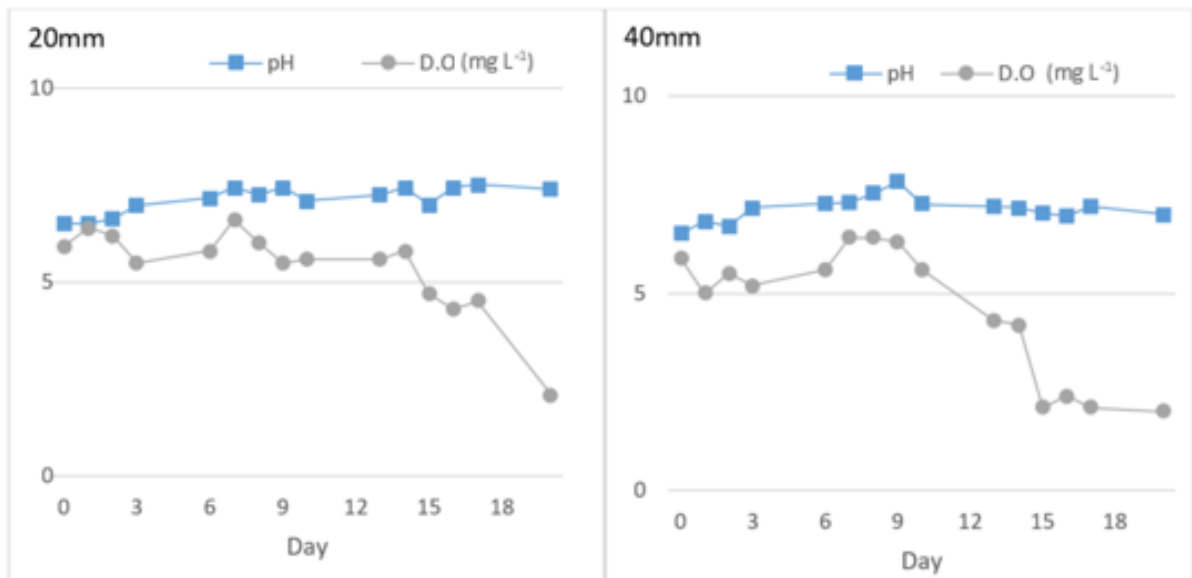


Figure 2. 12: Effect of 20 mm and 40 mm limestone on pH and DO concentrations in landfill groundwater
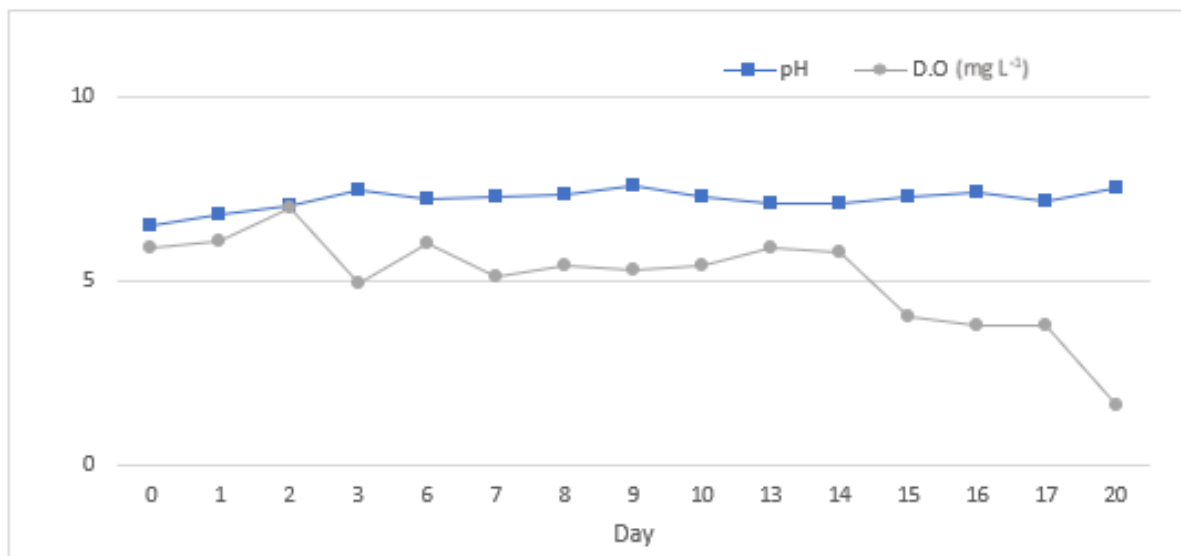


Figure 2. 13: Effect of limestone mix on pH and DO concentrations in landfill groundwater

The results of Bench Test 3, the efficacy of magnesium peroxide at raising pH and DO in contaminated groundwater are presented below in Figure 2.14. The results showed that there was an initial increase in concentrations of pH and DO in all samples tested. The 100 kg samples resulted in a more pronounced increase in pH and DO but in all samples the DO concentrations decreased after an initial increase after Day 3. The final DO concentrations ranged between 4.3

mg L$^{-1}$ (control) and 4.9 mg L$^{-1}$ (20 kg sample). This called into question the efficacy of magnesium peroxide over time.
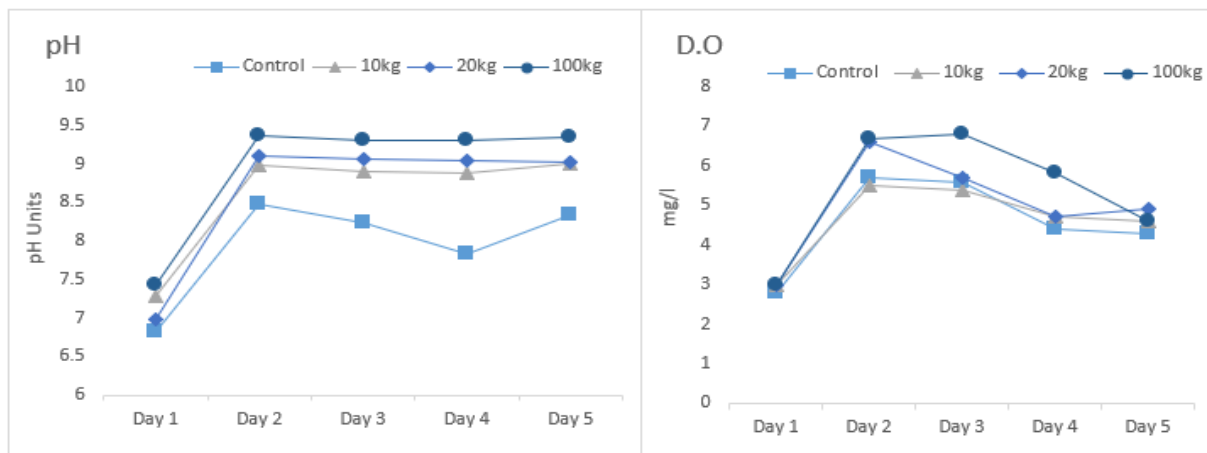


Figure 2. 14: Effect of magnesium peroxide on pH and DO concentrations in landfill groundwater

Results of Bench Test 4 showing the effect of oxygen releasing compound on pH and DO concentrations in contaminated groundwater are shown below in Figure 2.15. DO concentrations fell from an initial concentration of 5.6 mg L$^{-1}$ to 4.7 mg L$^{-1}$ (Control) and to 5.1 mg L$^{-1}$ (10 kg). Concentrations in the 20 kg and 100 kg samples showed an overall increase in DO at the end of the study (6.8 mg L$^{-1}$ and 10 mg L$^{-1}$, respectively). The ORC also caused an increase in pH levels rising to 8.8 (20 kg) and 9.8 (100 kg).
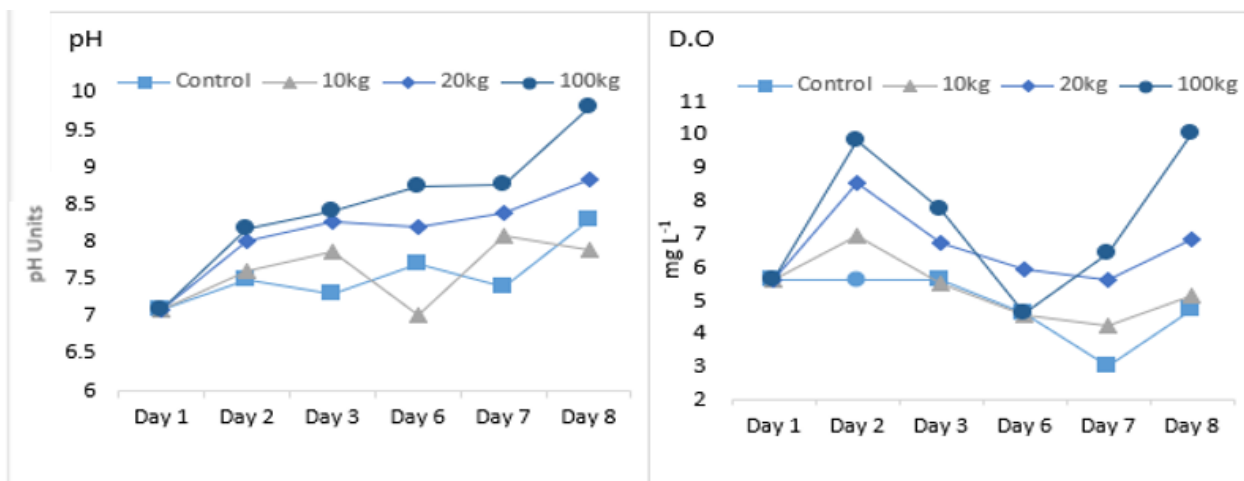


Figure 2. 15: pH and DO concentrations in landfill groundwater augmented by oxygen releasing compound

These bench tests enabled materials to be agreed with the Senior Executive Engineer at Clare County Council. PRB 1 would consist of limestone from the local quarry and perforated pipes for passive aeration and if necessary 20 kg of ORC would be added to assist in the oxygenation of the

PRB. PRB2 would consist of mulch from another Clare County Council landfill and would be back filled with compacted overburden (as described Section 2.2.2).

## 2.3.2 Column Experiments

As described in Section 2.2.2.4, column studies were carried out to simulate the on-site PRBs in the lab. The initial concentrations of field and laboratory parameters were measured, and the values are illustrated in the top reservoir of the following figure, Figure 2.16. It should be noted that there was no replication during the column experiments, so the results are not statistically significant. It was expected that DO concentrations would increase after retention in the initial column. DO rose from 0.76 mg $L^{-1}$ to 7.8 mg $L^{-1}$ in the column set # 4 which contained sand only. DO concentrations in the on-site conditions (column set #3) rose from 0.76 mg $L^{-1}$ to 5.23 mg $L^{-1}$. This was the smallest increase in DO concentration of all the column sets, but it still represented a DO concentration high enough to allow ammonia oxidising bacteria and archaea to grow (Wiszinowski et al., 2006). Concentrations of DO decreased after the second stage across the four sets of columns as intended. The biggest reduction occurred in column set #1, native cap material (soil and waste), with the smallest reduction occurring in column set #3. Considering that the measurements were taken in the reservoir after each column, aeration is likely to have occurred which would potentially not give a true reflection of in-column conditions.

pH fluctuated as expected in most columns with values rising after flowing through the first column and decreasing after the second column in columns #2 and #3. This was also the case in column set #4, sand, though not as pronounced. In contrast, pH rose after the first column in set #1, native cap soil, and remained unchanged after the second column.
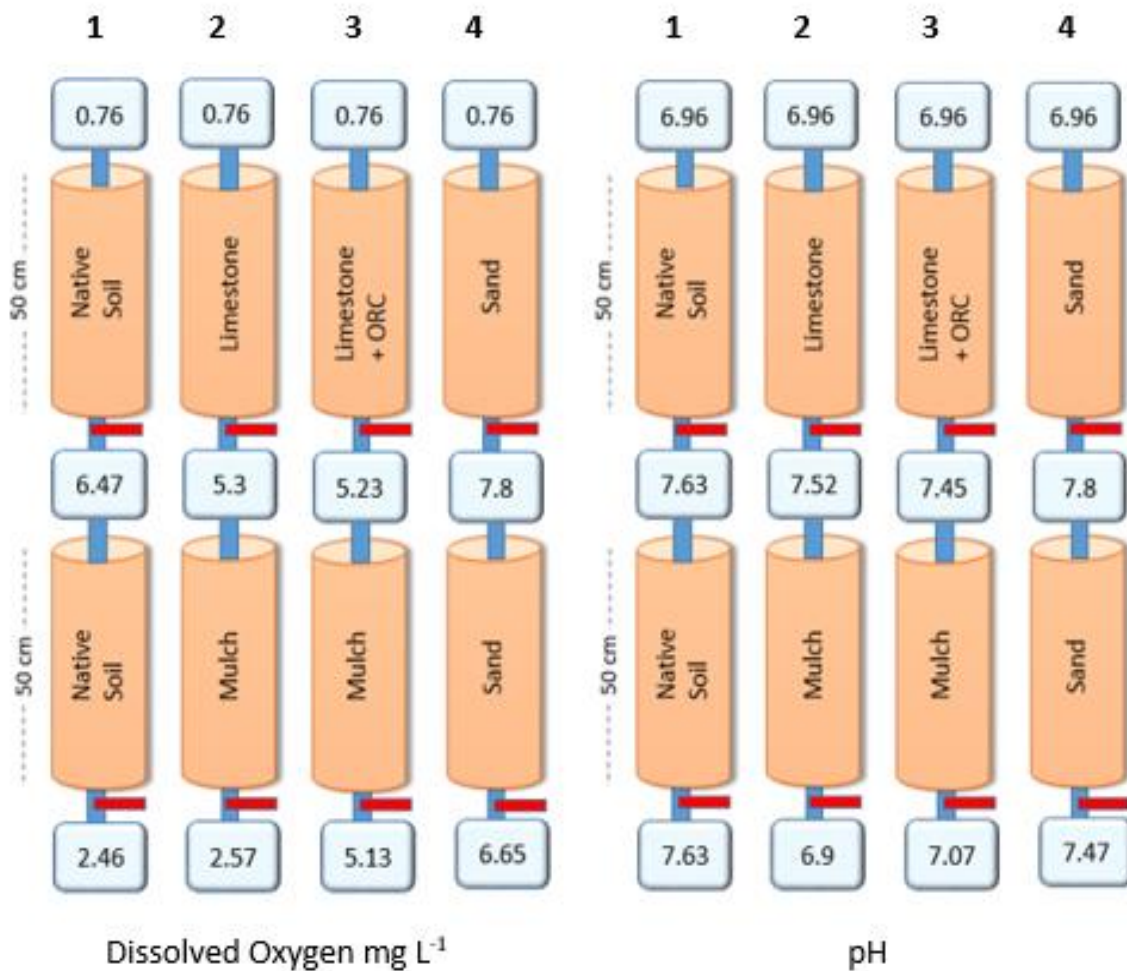
Figure 2. 16: DO (mg L$^{-1}$), left and pH (right) concentrations during column experiment

The ammoniacal nitrogen concentrations were the most important parameter in this study as the experiments aimed to reduce this parameter in the contaminated groundwater plume. Reductions of NH$_4$-N occurred in all column-sets as can be seen from Figure 2.17, below.
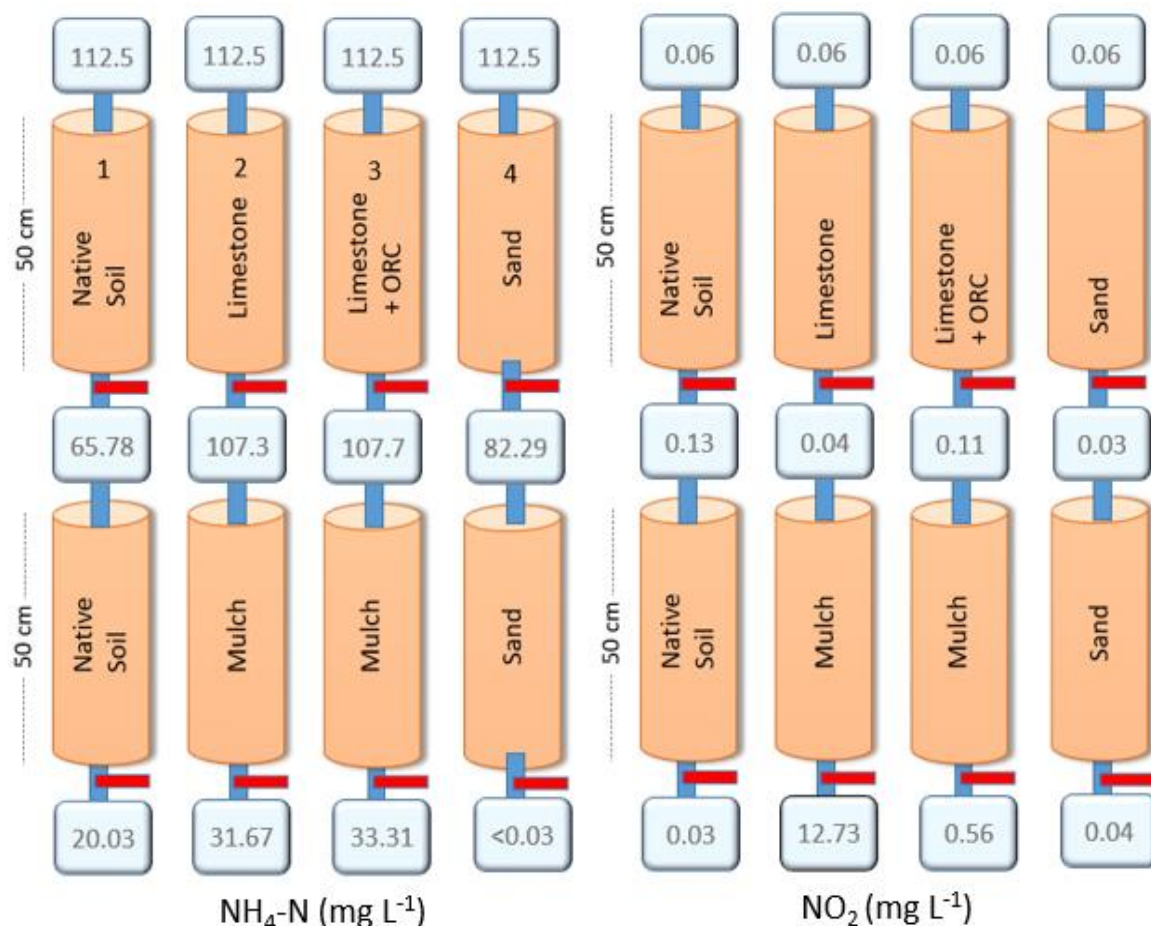
Figure 2. 17: Ammoniacal nitrogen and nitrite concentrations during column experiment

The best performance in the removal of ammoniacal nitrogen came from column set #4, sand. Concentrations were reduced from an initial concentration of 112.5 mg $L^{-1}$ to 82.29 mg $L^{-1}$ after the first column and to below the method detection limit (MDL) of 0.03 mg $L^{-1}$ after the second column. This successful reduction in $NH_4$-N in column set #4 was most likely due to physical filtration/ adsorbance rather than bioremediation (Hou et al., 2014). Column set #2 (initial bioremediation site conditions) performed better than column set #3 (same as set #2 but with the addition of ORC). Column set # 1, native soil also showed reduction, outperforming sets #2 and #3.

Regarding $NO_2$ concentrations, column sets #1 and #4 showed the greatest reductions in $NO_2$ concentrations, from an initial concentration of 0.06 mg $L^{-1}$ to 0.03 mg $L^{-1}$ and 0.04 mg $L^{-1}$, respectively. Column set #2 saw an initial reduction after the first column to 0.04 mg $L^{-1}$ but an increase after the second column to 12.73 mg $L^{-1}$. Column set # 3 saw a slight increase in $NO_2$ concentrations to 0.11 mg $L^{-1}$ after the first column and to 0.56 mg $L^{-1}$ after the second set. Considering the reactive material in the second part of both column sets #2 and #3, there was a

large difference in $NO_2$ concentrations. Again, this could be due to the heterogeneity of the mulch used. Also, since nitrite is easily oxidised to nitrate it does not persist in the environment, so the higher concentration of nitrite is most likely due to the fresh nature of the mulch used and the brevity of the column experiment. The nitrate and total organic carbon concentrations are outlined in Figure 2.18 below. Column sets #1 and #4 performed best again, showing reduced $NO_3$ concentrations from 0.5 mg $L^{-1}$ to 0.5 mg $L^{-1}$ and 1.3 mg $L^{-1}$, respectively. Column sets #2 and #3 saw large increases in $NO_3$, rising to levels of 218.3 mg $L^{-1}$ and 331.3 mg $L^{-1}$, respectively. Again, this is likely due to the mulch. There was no big increase in total organic carbon concentrations after the first set of columns in all of the column sets. The biggest increase occurred in column set # 2, rising from an initial concentration of 41 mg $L^{-1}$ to 45 mg $L^{-1}$ after the first column and to 127 mg $L^{-1}$ after the second column. Column set #3 also saw an increase in TOC concentrations at the end of the experiment, remaining at 41 mg $L^{-1}$ after the first column and rising to 77 mg $L^{-1}$ after the second column. Column set #1 saw an overall reduction to 33 mg $L^{-1}$, while column set #4 saw a reduction to 16 mg $L^{-1}$, at the end of the experiment.
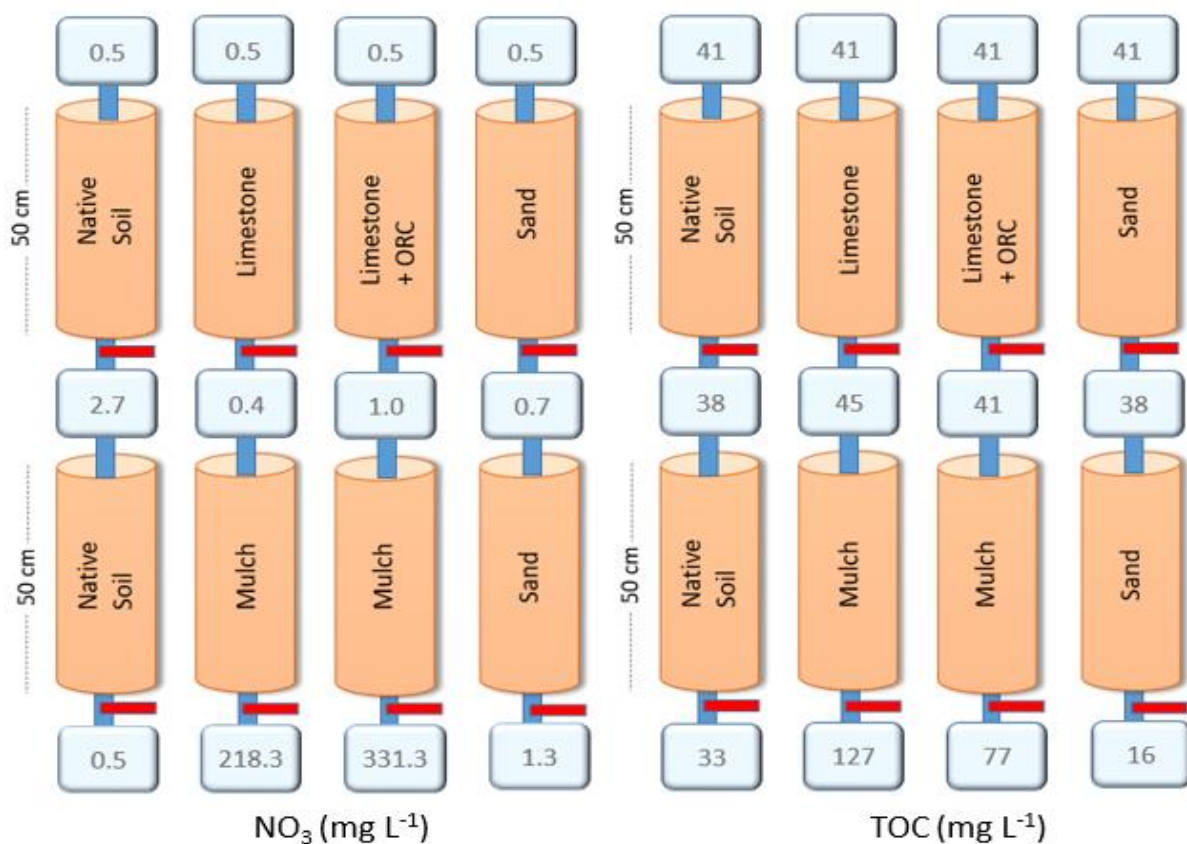


Figure 2. 18: Nitrate and total organic carbon concentrations during column experiment

Despite column sets #2 and #3 not showing the most efficient removal of NH$_4$-N, it was decided that the PRBs would be designed using limestone and aeration pipes in PRB1, and that local mulch would be used in PRB2. The removal of NH$_4$-N from column set #4 was not due to microbial activity as the sand had been sterilised and it is unlikely that sufficient microbial activity would occur until nitrogen cycling microbes had become established (Kim et al., 2013). The premise of the PRBs was to remediate NH$_4$-N biologically and it was thought that column sets 2 and 3 did not contain established communities of N-cyclers and that ammonia bioremediation could have occurred in the experiment if ran for longer. Kim et al. (2013) described nitrifiers as slow growers and Li et al. (2014) suggested that nitrification in a PRB will begin to occur after approximately 10 months of operation. Time constrains meant that the column experiments could not be run for this this length of time before constructing the PRBs.

### 2.3.3 Field Parameters

Field parameters, pH, DO, temperature, and electrical conductivity were measured monthly on site. Statistical analysis was carried out as per Section 2.2.3. Below, Figure 2.19 shows the pH levels in the bioremediation site in relation to the distance from the local surface water receptor at 6 monthly intervals for the duration of the project. The pH results show that over time pH increased, from 6.6 in PRB 1 when it was installed in June 2015 to 7.3 a year later in June 2016, to 8.12 at the end of the experiment in May 2017. There was also an increase in PRB2, though less pronounced, from 6.6 in June 2015 to 7.3 in June 2016 to 7.8 in May 2017.
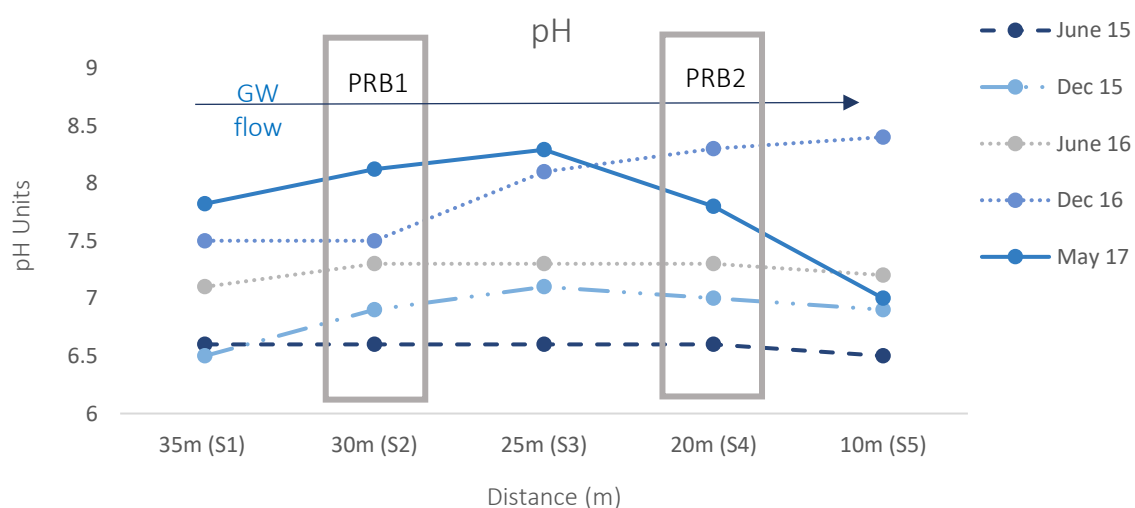


Figure 2. 19: pH concentrations in sampling wells (S1-S5) of bioremediation site at six monthly intervals from June 2015 - May 2017

Figure 2.20 below shows pH concentrations in all sampling wells over the 24-month study. The pH results across the site ranged from 6.4 in S5, September 2015 to 8.4 in S5, 2016. The average pH in PRB1 over the two-year sampling period was 7.09, and 7.15 in PRB2. The median in both PRBs was 7.0. Statistical analysis (one-way ANOVA, $\alpha = 0.05$) showed that there was a significant difference ($p<0.05$) in the pH concentrations between months in the study period (F=8.44, F crit=1.64) but not between wells (F=1.40, F crit= 2.45).
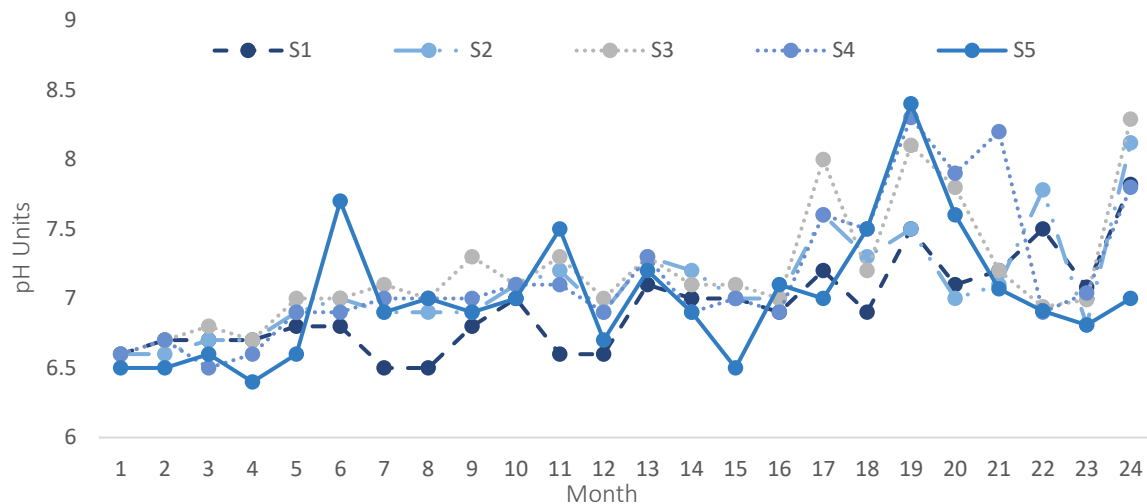


Figure 2. 20: pH levels in all sampling wells (S1-S5) from June 2015 – May 2017.

DO concentrations are illustrated below in Figures 2.21 and 2.22. To boost DO concentrations in PRB1, 20 kg of Regenesis$^{Tm}$ Oxygen Releasing Compound (ORC) was added in November 2015 (month 6) as DO concentrations were 1.3 mg L$^{-1}$ in October 2015. Concentrations in December 2015 rose to 5.0 mg L$^{-1}$ in PRB1 and across the bioremediation site, from 4.9 mg L$^{-1}$ upstream in S1, to 4.1 mg L$^{-1}$ in PRB2 and 3.6 mg L$^{-1}$ in S5. This would suggest that the groundwater flow was slow enough to allow for the effects of the ORC to be influential upstream In S1. The average DO concentration in PRB1 was 2.14 mg L$^{-1}$ and 2.00 mg L$^{-1}$ in PRB2, and the median value for each PRB was 2.03 mg L$^{-1}$ and 1.88 mg L$^{-1}$, respectively. Statistical analysis (Kruskal-Wallis test) showed that there was no significant difference ($p<0.005$) in DO concentrations between wells (H= 3.61, p= 0.46), but that there was a significant difference between sampling times in the study (H = 83.73, p < 0.001).
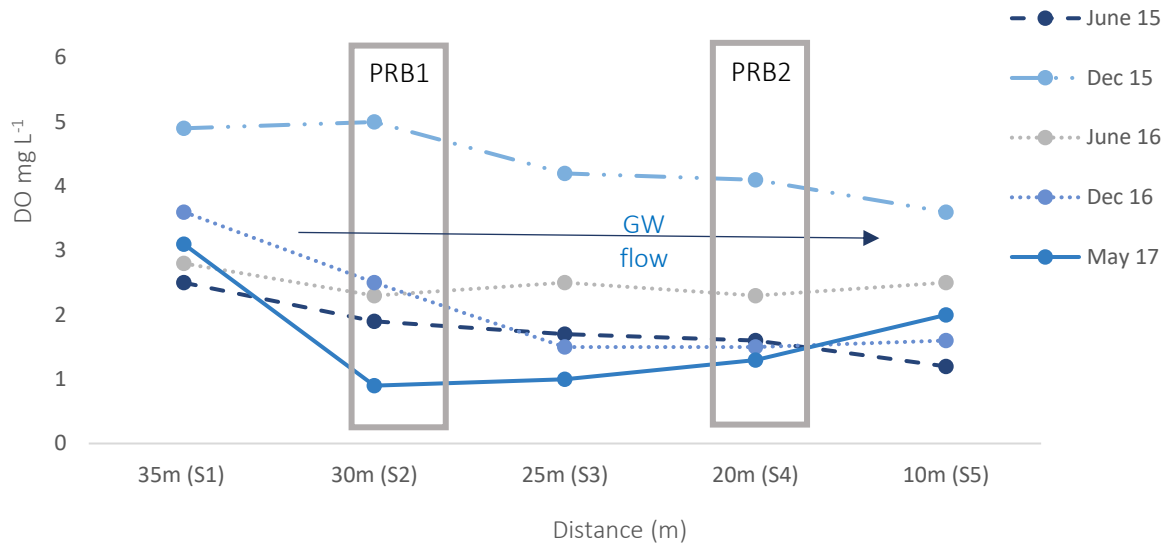
Figure 2. 21: Dissolved oxygen concentrations in sampling wells of bioremediation site from June 2015 - May 2017.
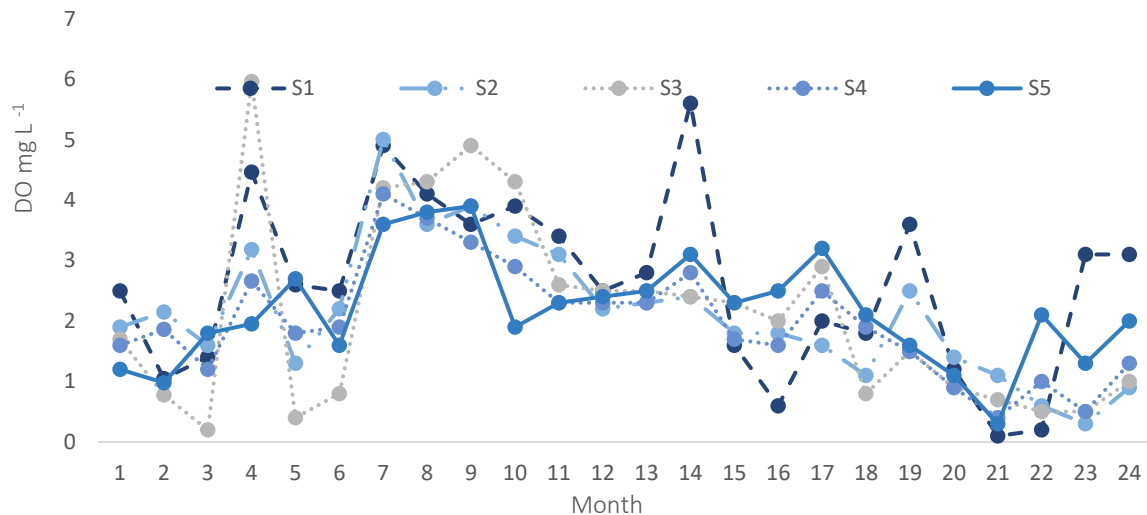


Figure 2. 22: Dissolved oxygen concentrations in sampling wells (S1-S5) on bioremediation site from June 2015 - May 2017

Below are the temperature results presented in Figures 2.23 and 2.24. The lowest temperature recorded (7.9°C) was in water collected from PRB2 in February 2016. The highest temperature recorded (18.1°C) was in water collected from S1 in July 2016. Figure 2.24 shows temperature concentrations in all sampling wells over the 24-month study. The temperature range across the bioremediation site was suitable for nitrifiers and denitrifiers as discussed in Section 2.2.2. The average temperatures in PRB1 and PRB2 were 13.09°C and 12.42°C, respectively, while the median values were 12.65°C and 12.55°C. Statistical analysis (one way ANOVA, $\alpha = 0.05$) showed a significant difference ($p<0.05$) between sampling times (F= 18.50, F crit = 1.65) but not between wells (F= 1.45, F crit = 2.45). This is understandable as temperature is seasonably dependent.
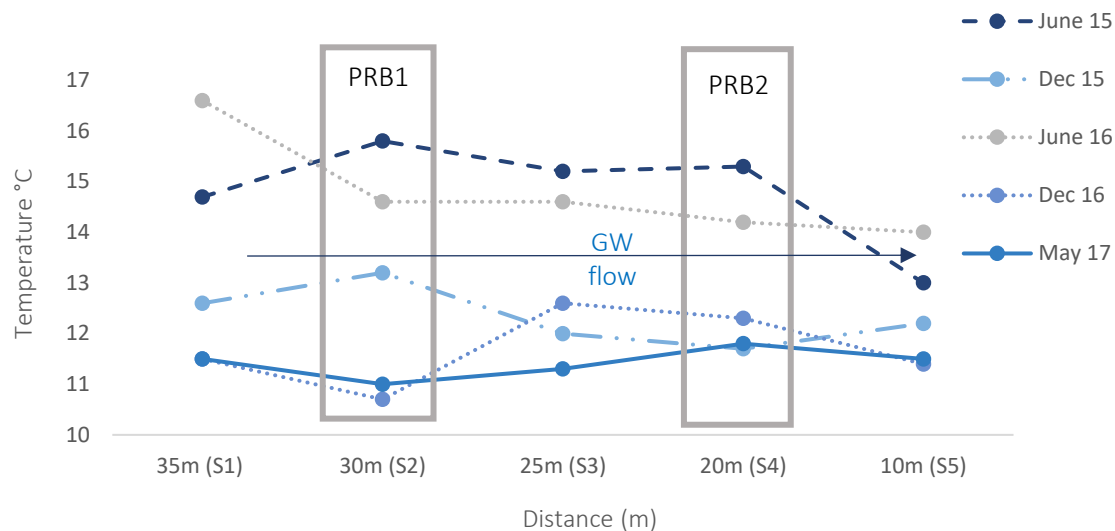
Figure 2. 23: Temperature recorded in sampling wells (S1- S5) on bioremediation site from June 2015 - May 2017.
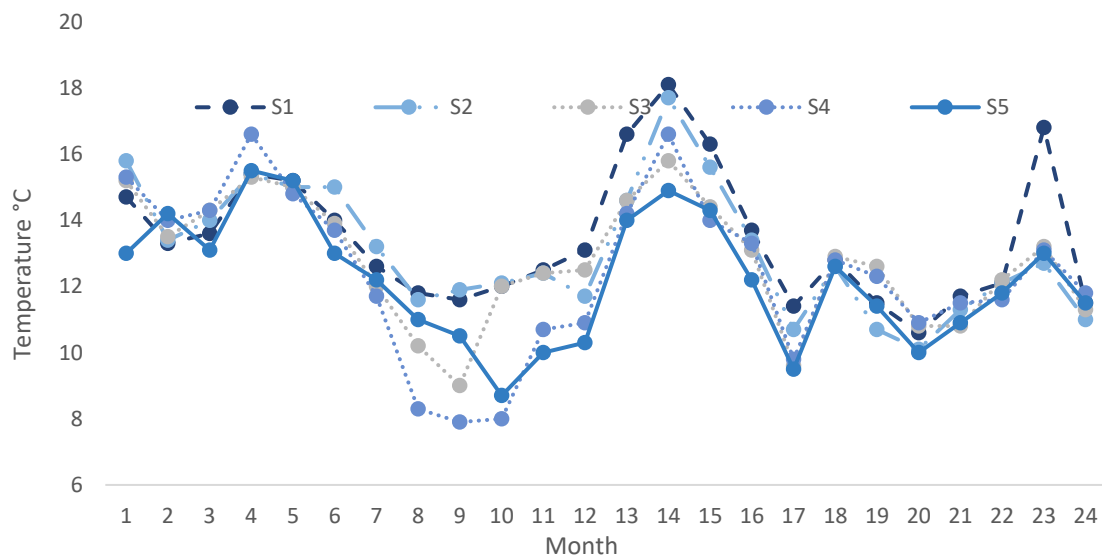


Figure 2. 24: Temperature recorded in all sampling wells (S1-S5) on bioremediation site from June 2015 - May 2017.

The electrical conductivity results are presented in Figures 2.25 and 2.26 below. The highest electrical conductivity value was recorded in water collected from S1 in May 2017 (2720 $\mu$S cm$^{-1}$). The lowest result (520 $\mu$S cm$^{-1}$) was noted in S5 in February 2016 and electrical conductivity was significantly lower in S5 than in the other monitoring wells throughout the study (Tukey's, p < 0.002). The highest average noted in all five sampling points was in PRB2 (1633 $\mu$S cm$^{-1}$) with an average electrical conductivity of 1445 $\mu$S cm$^{-1}$ recorded in PRB2. The lowest average was noted in S5 (968.5 $\mu$S cm$^{-1}$).  A significant difference (one way ANOVA, $\alpha$ = 0.05) in electrical conductivity was noted between sampling times (F= 4.30, F crit = 1.64) and between wells (F= 14.36, F crit = 2.45).
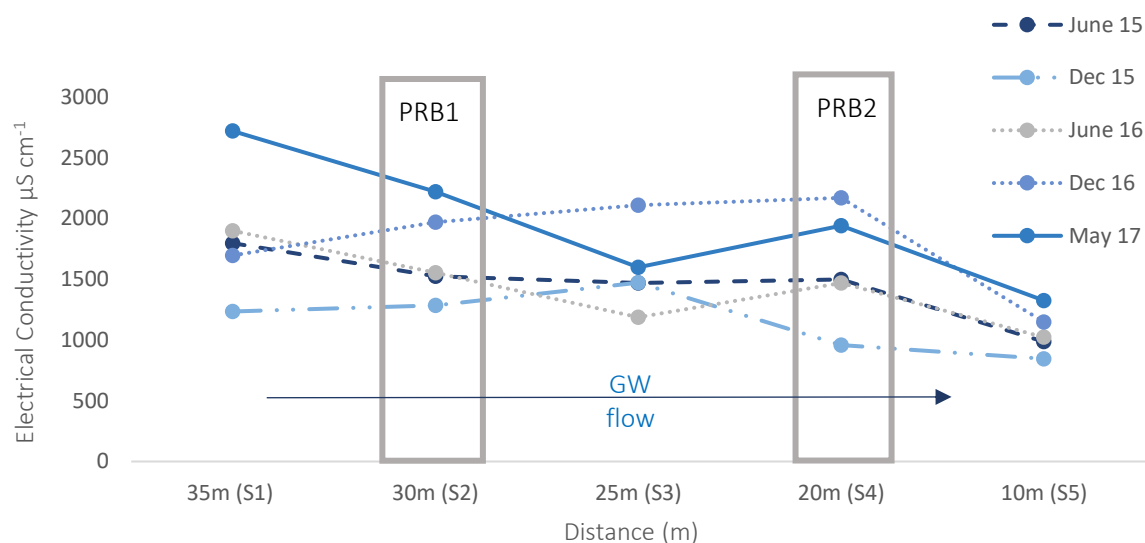
Figure 2. 25: Electrical conductivity levels in sampling wells (S1-S5) on bioremediation site from June 2015 - May 2017.
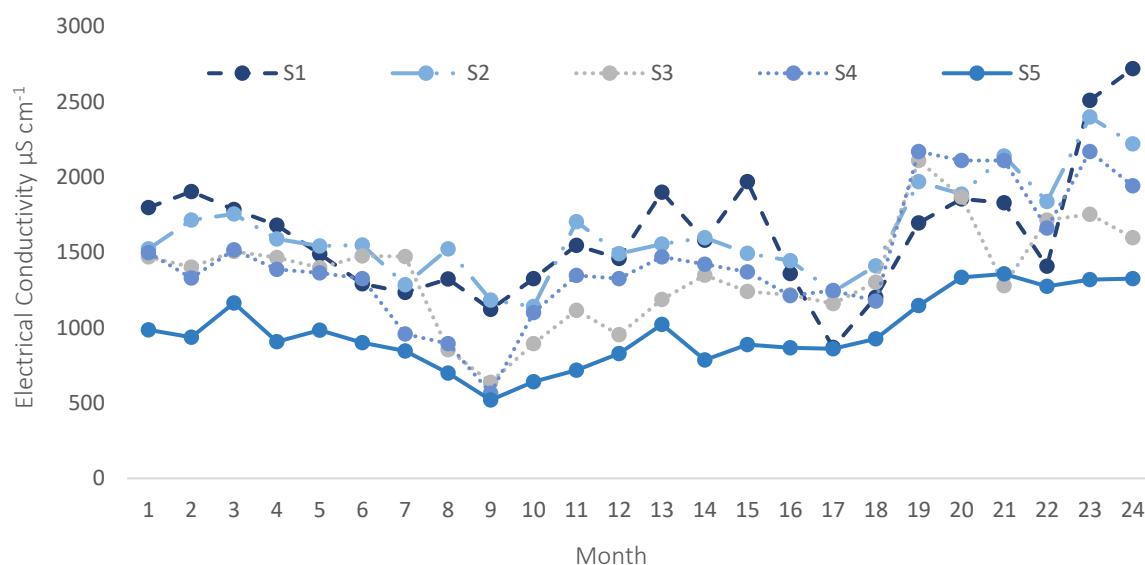


Figure 2. 26: Electrical conductivity recorded in all sampling wells (S1-S5) on bioremediation site from June 2015 - May 2017

## 2.3.4 Chemical Results

Concentrations of ammoniacal nitrogen, nitrite, nitrate, and total organic carbon were measured and monthly results are shown in Figures 2.27 – 2.28 below. Concentrations of ammoniacal nitrogen decreased across the bioremediation site from an average of 113.26 mg $L^{-1}$ in S1 to an average of 7.97 mg $L^{-1}$ in S5 (Figure 2.27). Figure 2.28 below shows $NH_4$-N concentrations in all sampling wells over the 24-month study. Concentrations ranged from a low of 1.68 mg $L^{-1}$ in S5 (February 2016), to a high of 192.12 mg $L^{-1}$ in S1 (June 2016). The average concentration of $NH_4$-

N in PRB1 was 103.68 mg $L^{-1}$ and 83.26 mg $L^{-1}$ in PRB2. Statistical analysis (Kruskal-Wallis test) showed that there was a significant difference between wells (H= 68.22, p = 5.39 x $10^{-14}$) and no significant difference due to sampling time (H = 31.90, p = 0.10). While there was only a modest correlation noted between $NH_4$-N and electrical conductivity (outlined in Section 2.3.5 below), Mohammad-Pajooh et al. (2017) noticed a strong correlation between both parameters, and both concentrations of $NH_4$-N and electrical conductivity were significantly lower (p <0.005) in downstream well S5 when compared with the other monitoring wells. At month 11, $NH_4$-N concentrations begin to decrease in water sampled from PRB1 and continued in a general downward trend until the end of the study (highlighted red in Figure 2.28). There was a significantly lower concentration of $NH_4$-N in downstream monitoring well S5 and a significantly lower concentration in monitoring well S3 than there was in upstream monitoring well S1 (Dunn's test, p < 0.005). This would suggest that PRB1 (S2) was enabling a reduction in $NH_4$-N concentrations, possibly through bioremediation (i.e., through nitrification in PRB1 where $NH_4$-N is being oxidised to $NO_2$ and $NO_3$).
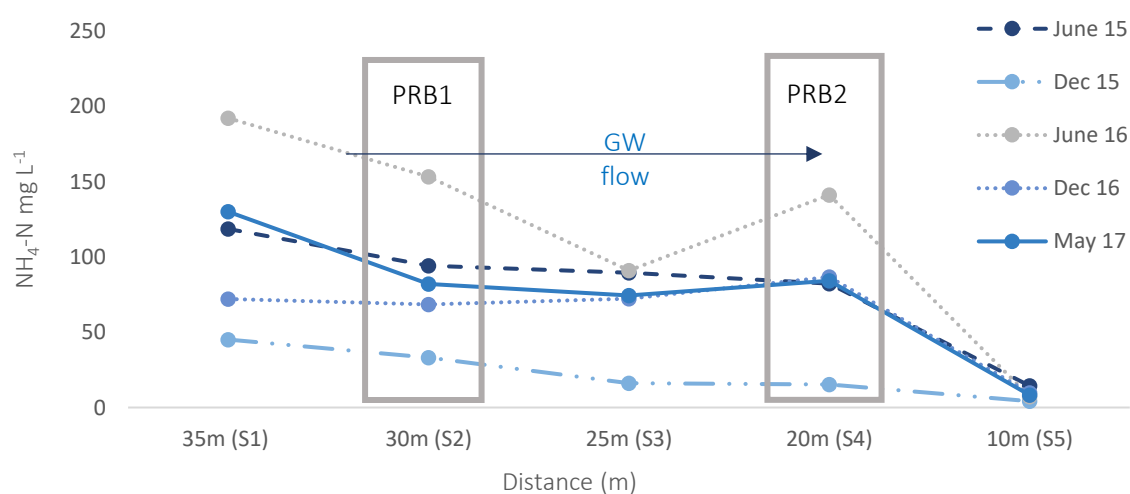


Figure 2. 27: Ammoniacal nitrogen concentrations in sampling wells (S1-S5) on bioremediation site from June 2015 - May 2017.
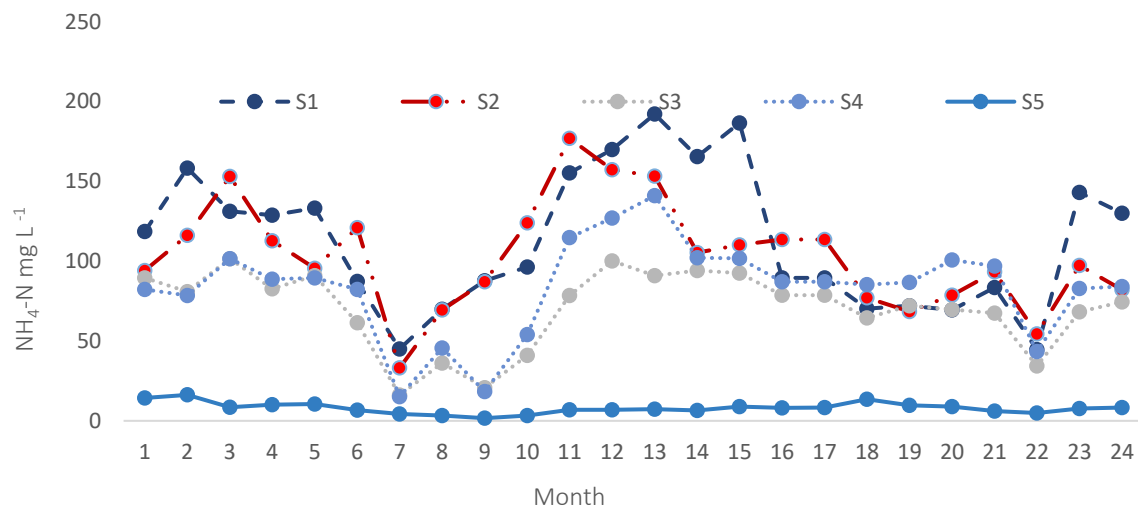
Figure 2. 28: Ammoniacal nitrogen concentrations in sampling wells (S1-S5) on bioremediation site from June 2015 - May 2017 with concentrations in PRB1 outlined in red.

The nitrite results are presented below in Figures 2.29 – 2.30. Of the 120 sampling events, only 30 had results that were greater than the MDL (0.02 mg $L^{-1}$), ranging from 0.04 mg $L^{-1}$ (S4, June 2014) to 1.83 mg $L^{-1}$ (S1, September 2015). This was not surprising as nitrite is easily transformed to nitrate and does not persist for long periods of time in the environment. Figure 2.29 below shows $NO_2$ concentrations in all sampling wells over the 24-month study. No detectable levels of nitrite were recorded in S5 for the 24-month sampling period. Statistical analysis (Kruskal-Wallis test) showed that there was a significant difference between wells (H= 11.11, p = 2.54 x $10^{-2}$), but no significant difference between sampling times over the 24-month period (H = 12.06, p = 0.97). Concentrations in monitoring wells S4 (PRB2) and S5 were significantly lower than in S1 and S3 (Dunn's test, p <0.005) and $NO_2$ concentrations in S3 were significantly higher than in S2 (PRB1). Significantly higher concentrations of $NO_2$ downstream of S2 (PRB1) could be an indication of the first step of nitrification, ammonia oxidation, occurring in PRB1 where $NO_2$ is a product.
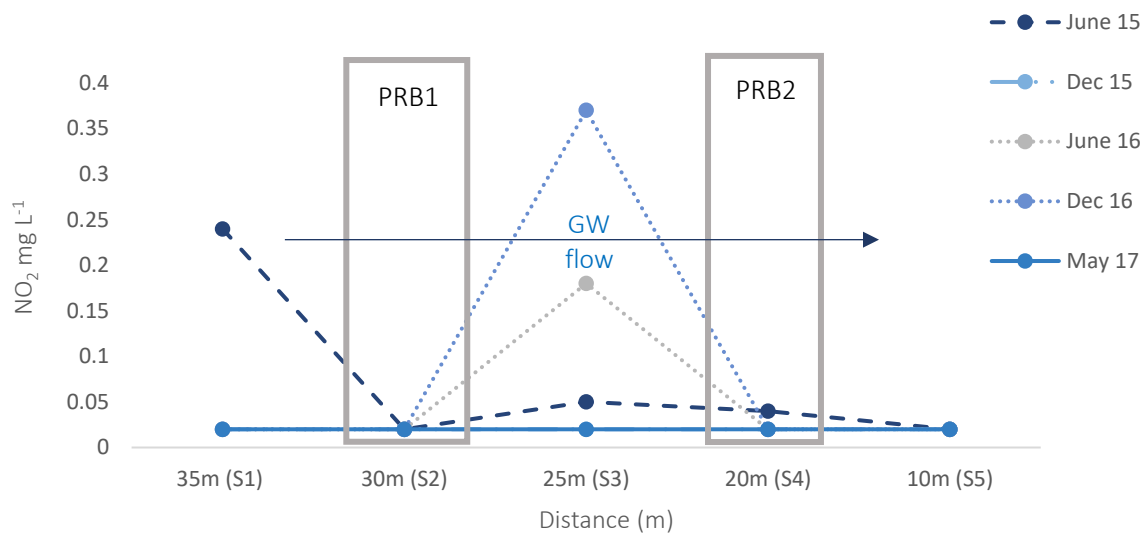
Figure 2. 29: Nitrite concentrations in sampling wells (S1-S5) on bioremediation site from June 2015 - May 2017.
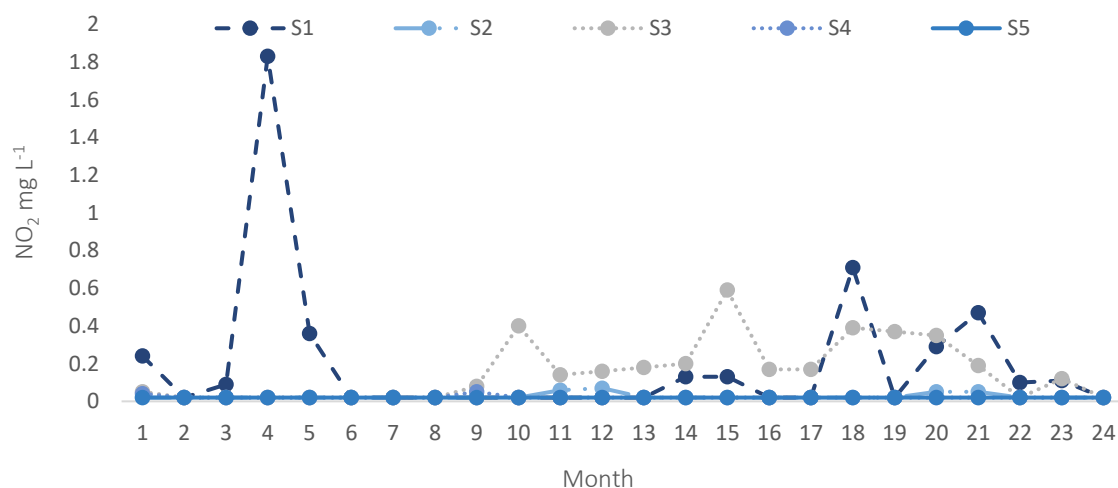


Figure 2. 30: Nitrite concentrations in sampling wells (S1-S5) on bioremediation site from June 2015 - May 2017.

Concentrations of nitrate are presented below in Figures 2.31 and 2.32. Concentrations of nitrate decreased across the bioremediation site, from an average of 1.9 mg $L^{-1}$ in S1, to an average of 0.30 mg $L^{-1}$ in S5. Figure 2.32 below shows $NO_3$ concentrations in all sampling wells over the 24-month study. A notable spike of 19.8 mg $L^{-1}$ was recorded in September 2015 in upstream monitoring well S1. Figure 2.32 shows the concentrations of $NO_3$ in S3 (highlighted in red) throughout the 24-month period showing elevated concentrations after month 10. As Li et al. (2014) suggest, nitrification in a PRB will begin to occur after approximately 10 months of operation, which would explain the increased $NO_3$ concentrations in the bioremediation site

beginning from month 10 in the monitoring well (S3) downstream from PRB1. This coincided with a downward trend in NH$_4$-N concentrations in PRB1 from month 11 as discussed above. Concentrations of nitrate remained low downstream in PRB2, potentially indicating denitrification. Statistical analysis (Kruskal-Wallis test) showed that there was a significant difference between wells (H= 23.18, p = 1.16 x 10$^{-4}$) and also between sampling months (H= 40.21, p = 8.65 x 10$^{-5}$). Concentrations in downstream monitoring well S5 were significantly lower than in monitoring well S3 (Dunn's test, p <0.005). The increase in NO$_3$ in the monitoring well downstream from PRB1 at month 10 (as found by Li et al., 2014) coinciding with NH$_4$-N reductions in PRB1 and the significantly (p <0.005) lower concentrations of NO$_3$ all pointed towards nitrogen cycling (nitrification in PRB1 and denitrification in PRB2).
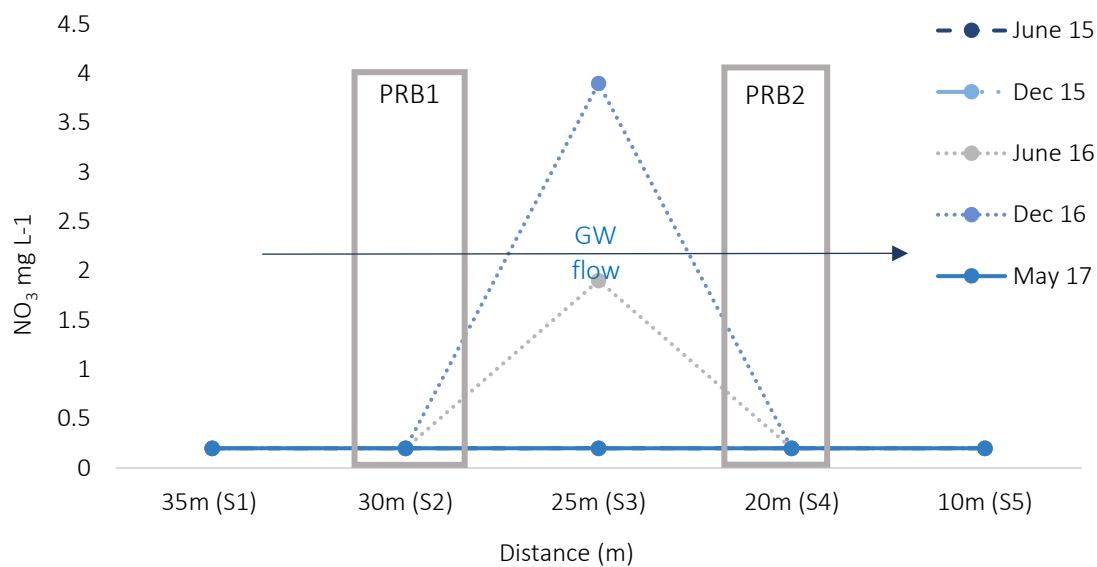


Figure 2. 31: Nitrate concentrations in sampling wells (S1-S5) on bioremediation site from June 2015 - May 2017.
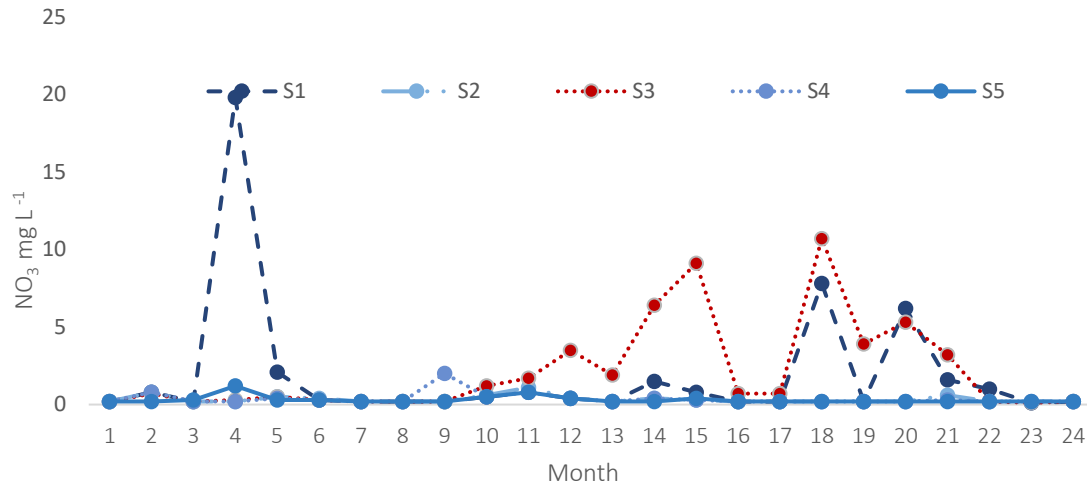
Figure 2. 32: Nitrate concentrations in sampling wells (S1-S5) on bioremediation site from June 2015 - May 2017 with $NO_3$ concentrations highlighted in red.

The total organic carbon results are presented below in Figures 2.33 and 2.34. The average concentration and median value for total organic carbon was 19.38 mg $L^{-1}$ and 14.50 mg $L^{-1}$ respectively, in PRB1, and 18.54 mg $L^{-1}$ and 13 mg $L^{-1}$ respectively, in PRB2. Concentrations of total organic carbon ranged from the MDL of 2 mg $L^{-1}$ to 74 mg $L^{-1}$ in S2 in May 2016. Statistical analysis (Kruskal-Wallis test) showed that there was no significant difference between wells (H= 7.46, p = 0.11), but there were significant differences in concentrations at different sampling times over the 24-month study (H = 63.65, p = 1.12 x $10^{-5}$). The significant difference over time did not relate to seasonal variability.
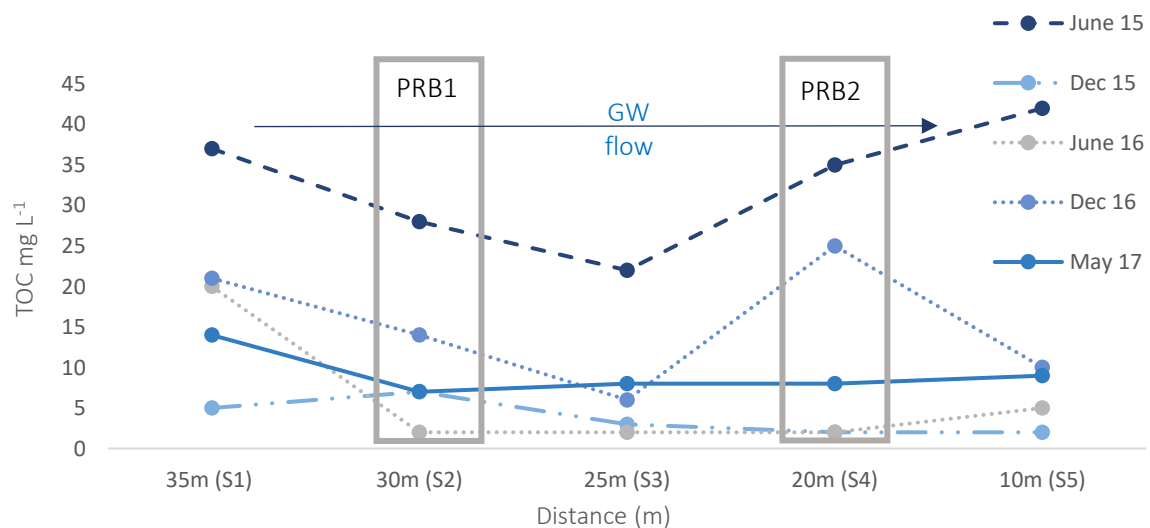


Figure 2. 33: Total organic carbon concentrations in sampling wells (S1-S5) on bioremediation site from June 2015 - May 2017.
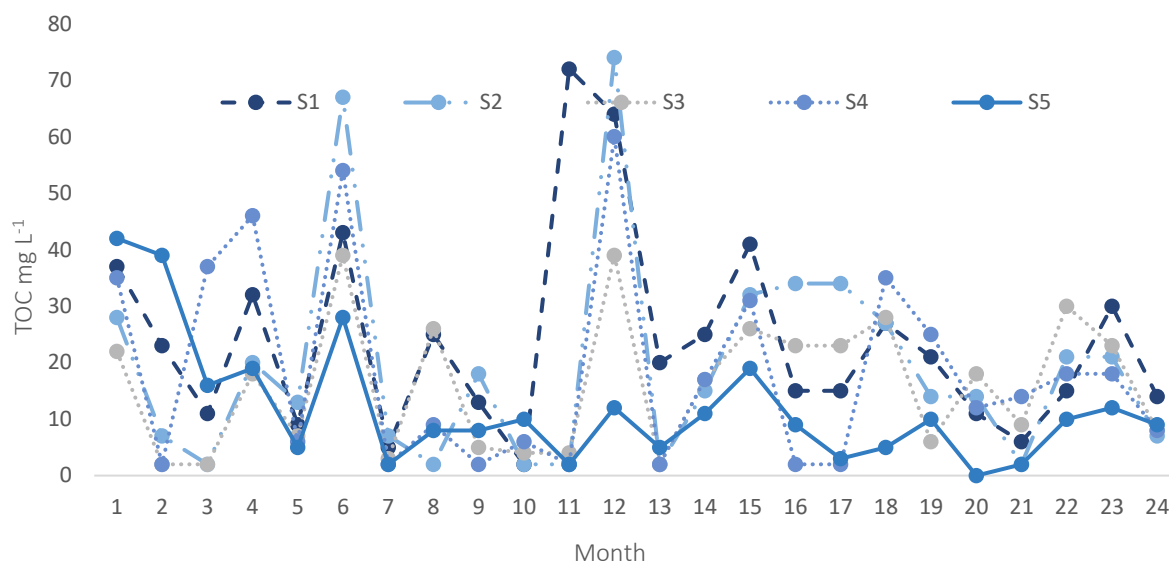
Figure 2. 34: Total organic carbon concentrations in sampling wells (S1-S5) on bioremediation site from June 2015 - May 2017.

## 2.3.5 Correlations

To further understand the results and the interactions between the parameters tested and the relationship between the wells, correlations tests (Pearson's) were carried out. The p- values were extrapolated in Microsoft Excel and the Bonferroni correction was applied. Table 2.4 below outlines the correlation coefficients of all parameters in each well. The cells are highlighted according to whether they are of statistical significance (yellow illustrates a p value of < 0.05, green illustrates a Bonferroni corrected p value of < 0.003). The negative numbers denote negative correlations while positive numbers describe a positive correlation.

Table 2. 4: Correlation coefficients between all eight parameters tested in each sampling well with p values < 0.05 highlighted in yellow and Bonferroni corrected p values Bonferroni highlighted in green.

| S1 | pH | DO | Temp | EC | NH4-N | NO2 | NO3 |
|---|---|---|---|---|---|---|---|
| DO | -0.25 | | | | | | |
| Temp | -0.20 | 0.26 | | | | | |
| EC | 0.41 | -0.08 | 0.28 | | | | |
| NH4-N | -0.13 | 0.12 | 0.68 | 0.47 | | | |
| NO2 | -0.13 | 0.10 | 0.19 | 0.02 | -0.02 | | |
| NO3 | -0.12 | 0.14 | 0.11 | -0.01 | -0.04 | 0.96 | |
| TOC | -0.36 | 0.12 | 0.25 | 0.04 | 0.48 | 0.02 | 0.05 |
| **S2/ PRB1** | pH | DO | Temp | EC | NH4-N | NO2 | NO3 |
| DO | -0.31 | | | | | | |
| Temp | -0.41 | 0.08 | | | | | |
| EC | 0.23 | -0.61 | -0.22 | | | | |
| NH4-N | -0.21 | -0.04 | 0.23 | -0.10 | | | |
| NO2 | -0.06 | -0.03 | -0.36 | 0.17 | 0.40 | | |
| NO3 | -0.14 | 0.13 | 0.03 | 0.01 | 0.49 | 0.47 | |
| TOC | -0.08 | -0.17 | 0.11 | -0.21 | 0.17 | 0.21 | -0.18 |
| **S3** | pH | DO | Temp | EC | NH4-N | NO2 | NO3 |
| DO | -0.08 | | | | | | |
| Temp | -0.53 | -0.20 | | | | | |
| EC | 0.24 | -0.56 | 0.29 | | | | |
| NH4-N | -0.06 | -0.38 | 0.62 | 0.19 | | | |
| NO2 | 0.30 | -0.01 | -0.02 | 0.01 | 0.14 | | |
| NO3 | 0.16 | -0.17 | 0.15 | 0.05 | 0.25 | 0.80 | |
| TOC | -0.18 | -0.11 | 0.04 | -0.01 | 0.07 | 0.08 | 0.24 |
| **S4/ PRB2** | pH | DO | Temp | EC | NH4-N | NO2 | NO3 |
| DO | -0.32 | | | | | | |
| Temp | -0.34 | -0.28 | | | | | |
| EC | 0.54 | -0.82 | 0.27 | | | | |
| NH4-N | 0.14 | -0.44 | 0.45 | 0.44 | | | |
| NO2 | -0.19 | 0.20 | -0.19 | -0.37 | -0.40 | | |
| NO3 | -0.16 | 0.32 | -0.38 | -0.49 | -0.35 | 0.70 | |
| TOC | -0.24 | -0.19 | 0.37 | 0.13 | 0.30 | -0.06 | -0.27 |
| **S5** | pH | DO | Temp | EC | NH4-N | NO2 | NO3 |
| DO | -0.11 | | | | | | |
| Temp | -0.40 | -0.06 | | | | | |
| EC | 0.13 | -0.67 | 0.11 | | | | |
| NH4-N | -0.12 | -0.52 | 0.48 | 0.29 | | | |
| NO2 | 0.00 | 0.00 | 0.00 | 0.00 | 0.00 | | |
| NO3 | -0.20 | -0.04 | 0.14 | -0.27 | 0.02 | 0.00 | |
| TOC | -0.37 | -0.37 | 0.43 | -0.06 | 0.55 | 0.00 | 0.06 |

Table 2. 5: Strength of Correlation

| 0.00 - 0.19 | A very weak correlation |
|-------------|-------------------------|
| 0.20 -0.39 | A weak correlation |
| 0.40 - 0.69 | A modest correlation |
| 0.70 - 0.89 | A strong correlation |
| 0.90 - 1.00 | A very strong correlation |

Significantly ($p < 0.05$) very strong and strong positive correlations were noted between $NO_2$ and $NO_3$ in wells S1, S3 and S4 showing correlation coefficients of 0.96, 0.80 and 0.70, respectively. This was expected as $NO_2$ and $NO_3$ exist as consecutive steps in the nitrogen cycle

The only other parameters to show a significant relationship were electrical conductivity and DO displaying a strong negative correlation (-0.82) also noticed by Külköylüoğlu et al., (2007) in shallow water. Increased electrical conductivity is indicative of increased salinity which reduces water's ability to absorb oxygen. This correlation is illustrated in the scattergram, Figure 2.35 below.
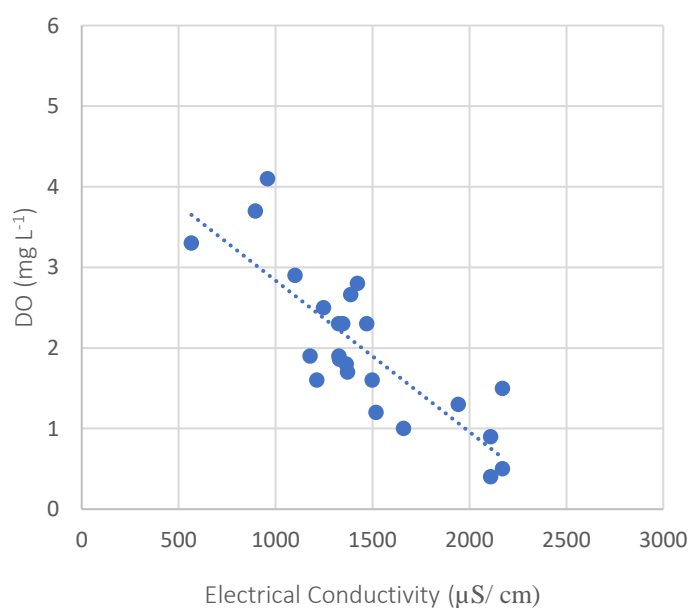


Figure 2. 35: Scattergram showing negative correlation (-0.82) between electrical conductivity and DO in PRB2

## 2.3.6 Historical data

To understand further the ammoniacal nitrogen concentrations in the bioremediation site, historical $NH_4$-N data for OB2 (S5) were obtained and are presented below in Figure 2.36.
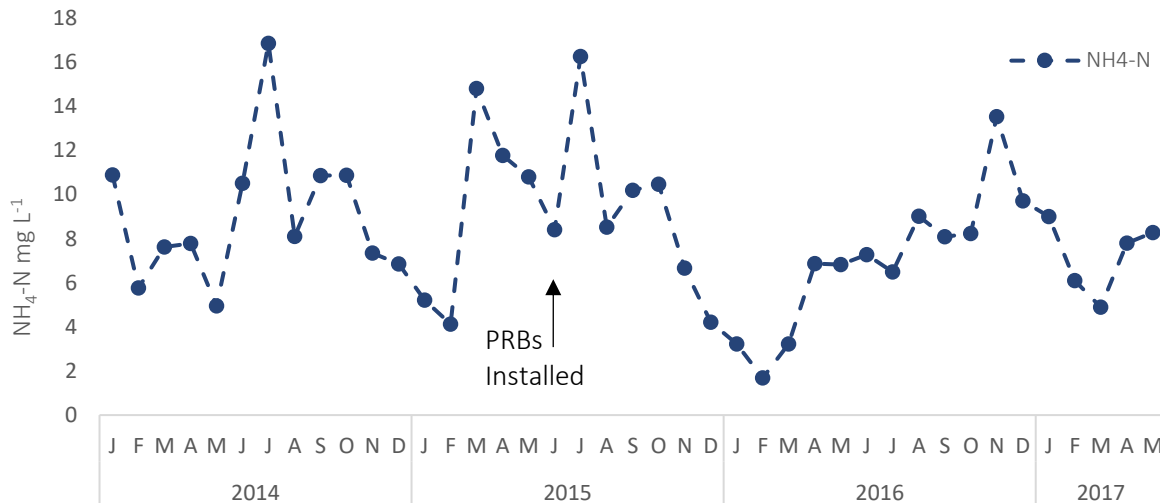
Figure 2. 36: NH$_4$-N concentrations in water collected from OB2 (S5) from January 2014 to May 2017.

Each year saw a fluctuation in NH$_4$-N concentrations. Below, Figure 2.37 shows the yearly data trends. The average ammoniacal nitrogen concentration in OB2 (S5) for 2014 was 9.04 mg L$^{-1}$. 2015 showed an average concentration of 9.29 mg L$^{-1}$ (PRBs were installed in June 2015) and the average concentration for 2016 was 7.02 mg L$^{-1}$ showing a decrease of 2.27 mg L$^{-1}$, from 9.04 mg L$^{-1}$ in 2014 to 7.02 mg L$^{-1}$ in 2016. While this was a decrease in average concentrations, it was a small decrease and still well above the EU limit of 0.175 mg L$^{-1}$.
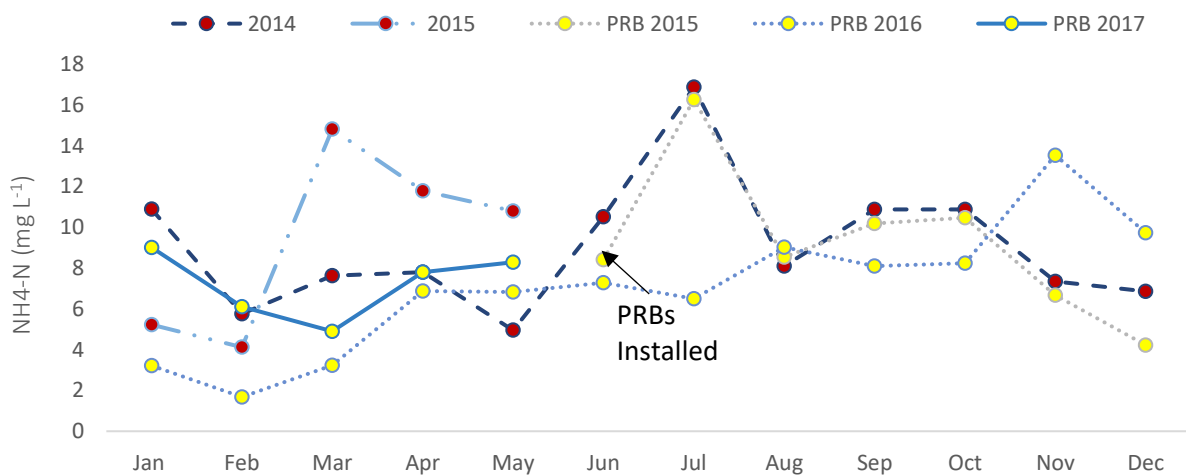


Figure 2. 37: NH$_4$-N concentrations in OB2 (S5), 2014 - 2017. The trendlines denoted by red dots are pre PRB installation, the yellow denote post PRB installation.

## 2.3.7 Weather Data

To investigate other factors that might influence NH$_4$-N, weather data was examined from Shannon Airport, c. 20 km from site. Figure 2.38 below shows rainfall (mm) and on site NH$_4$-N (mg L$^{-1}$) concentrations. Below, Figure 2.39 illustrates the average NH$_4$-N concentration from all

71

sampling wells and rainfall. The correlation between the average rainfall and the NH4-N was tested and showed a correlation coefficient of -0.57 (p value <0.004), illustrated in Figure 2.40 below.
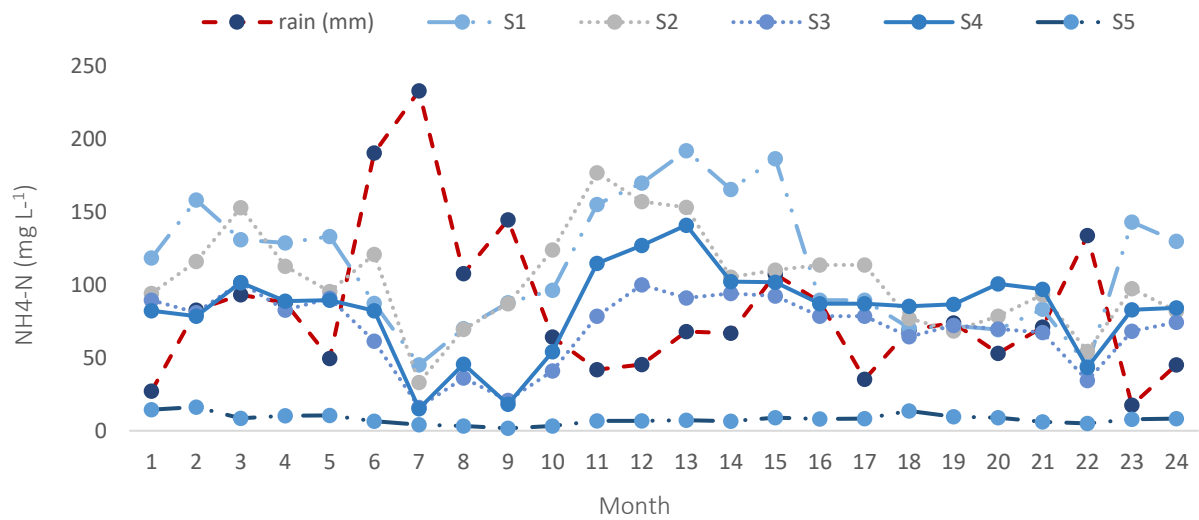


Figure 2. 38: Rainfall (mm) recorded at Shannon Airport and NH$_4$-N concentrations at bioremediation site.
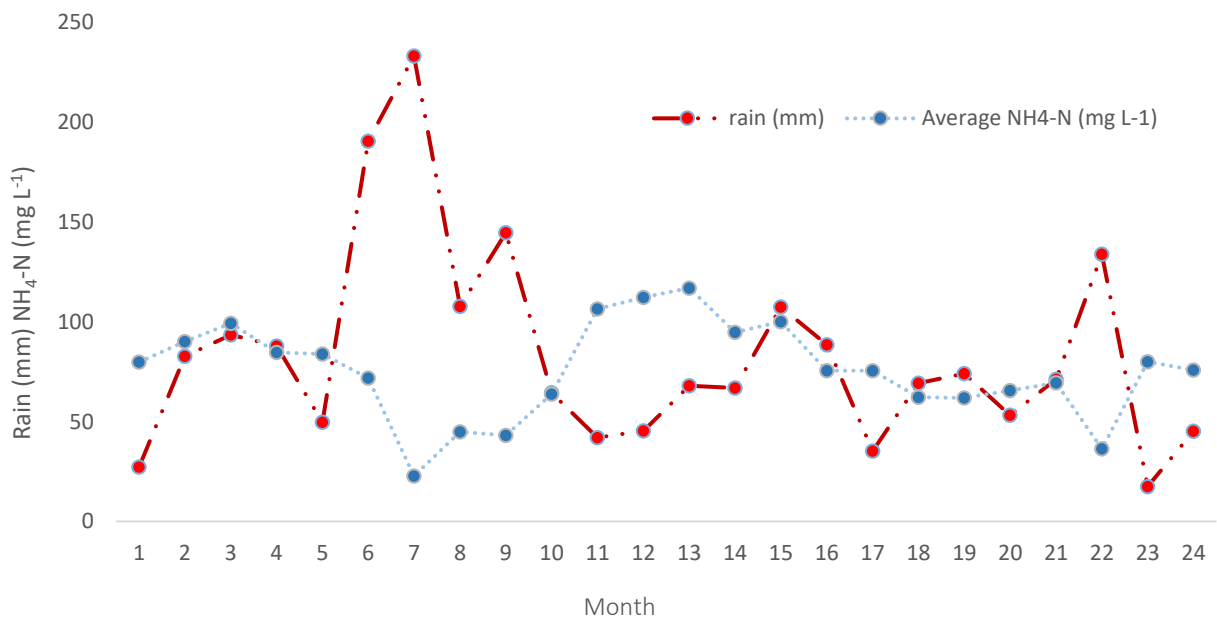


Figure 2. 39: Rainfall (mm) recorded at Shannon Airport and average NH$_4$-N concentrations (from wells S1-S5) at bioremediation site.
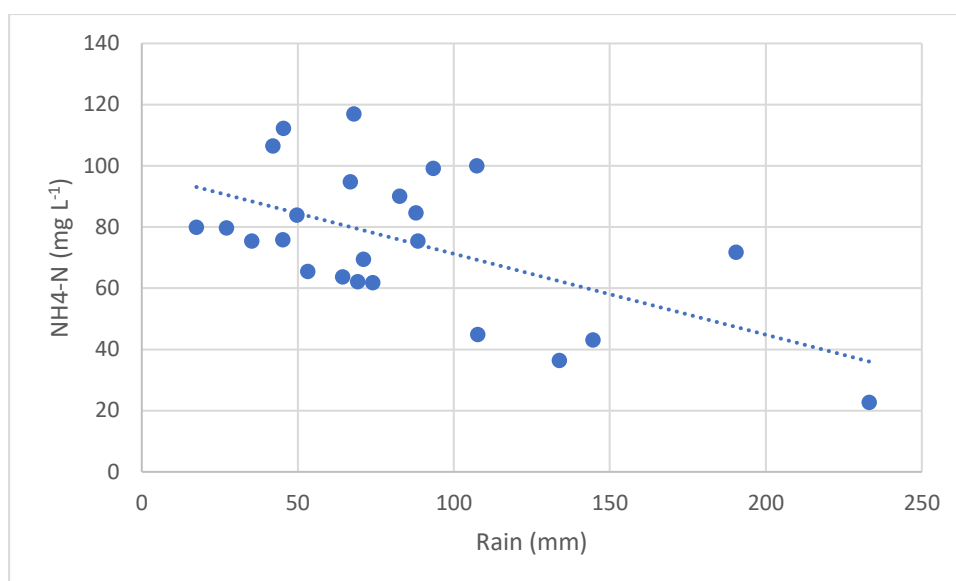
Figure 2. 40: Scattergram showing modest negative correlation (-0.57) between rainfall (mm) and average $NH_4$-N (mg $L^{-1}$) concentrations in monitoring wells S1 – S5.

## 2.4 Discussion

Due to the complicated spatiotemporal differences of land uses, weather, hydrogeology, topography, microbial community structure, etc., complex variabilities in the N concentration in shallow groundwater are noticeable (Zhang et al., 2022). Added to this complexity is the heterogeneity of the pollution source i.e., landfill leachate (Christensen et al., 1994; Kjeldsen et al., 1994; Nooten & Diels, 2008). The parameters used to ascertain the efficacy of the PRBs were the field parameters (pH, DO, temperature, and electrical conductivity) and the chemical results ($NH_4$-N, $NO_2$, $NO_3$ and TOC). The aim of the PRBs were to influence microbial activity so that nitrification would occur in PRB1, cycling $NH_4$-N through to $NO_2$ and $NO_3$ and denitrification would occur in PRB2, cycling $NO_3$ to $N_2$ gas through the intermediary gaseous stages of NO and $N_2O$. Differences in the chemical states of the nitrification stages meant that the products of nitrification could be measured whereby the gaseous products of denitrification could not. Reduction of $NH_4$-N concentrations and increased concentrations of $NO_2$ and $NO_3$ could be measured as indicators of nitrification and efficacy of PRB1 while reductions in $NO_3$ concentrations were the only chemical result that could be used as a metric for denitrification in PRB2, as the gaseous products of denitrification could not be measured onsite.

Of the field parameters measured affecting microbial activity, levels of pH and temperature remained within the optimum range for nitrification to occur in PRB1 and for denitrification to

73

occur in PRB2. Significant differences (p<0.05) in pH between sampling times were noted (and not between wells) and were most likely due to the known correlation between pH and temperature first described by Hamer et al. (1946). Rising temperatures cause molecular vibrations in water which in turn increases the ability of the water to ionise and form more hydrogen bonds, making the water more acidic (and causing pH to decrease). As described in Section 2.2.2, the optimum range for nitrifiers is $6.4 - 7.9$ and $5.5 - 8.0$ for denitrifiers. PRB1 and PRB2 had suitable pH for nitrifiers and denitrifiers, respectively, except for PRB1 in May 17 which had a pH concentration of 8.12.

DO levels in PRB1 remained above $1.0$ mg L$^{-1}$ (optimum $O_2$ concentrations for nitrifiers) at all sampling times except for the last three months of the experiment (March, April, and May 2017) where concentrations were 0.6, 0.3 and 0.9 mg L$^{-1,}$ respectively. DO concentrations in PRB2 also remained above $1.0$ mg L$^{-1}$ apart from three months towards the end of the experiment (January 2017, February 2017, and April 2017). Optimum conditions for denitrifiers are $< 0.5$ mg L$^{-1}$ as outlined in Section 2.2.2, and PRB2 was designed to lower the oxygen concentrations to less than $0.5$ mg L$^{-1}$ to promote anaerobic denitrification. While this was not reached for the majority of the study, the conditions were optimal for aerobic denitrifiers belonging to *Pseudomonadota* (formerly *Proteobacteria*) that work efficiently within a pH range of $7 - 8$ and with DO concentrations of up to 5 mg L$^{-1}$ (Hayatsu et al*.,* 2008; Ji et al., 2015). It should be noted however that during the sampling process of vigorously pumping water to the surface for analysis, oxygenation of the water is likely to have occurred, potentially resulting in an inaccurate reading. Lowering a DO meter into the sampling well would have avoided this.

It was expected that there would be higher electrical conductivity in the wells downstream of the bioremediation site due to the inundation of estuarine (i.e., saline) water from the surface water bodies, though the opposite was true. Electrical conductivity was higher upstream with the highest concentration found in S1 and the lowest concentrations found in the monitoring well closest to the estuary, S5. Mohammad-Pajooh et al. (2017) noticed a positive correlation between electrical conductivity and $NH_4$-N (correlation coefficient of 0.82) and suggested electrical conductivity as an economical and efficient method of testing for $NH_4$-N. While this study showed a correlation between electrical conductivity and DO, there was only a modest positive correlation between electrical conductivity and $NH_4$-N concentrations in two of the sampling wells (S1 and S4/PRB2, correlation coefficient of 0.44 and 0.47, respectively).

Statistical analysis (as described in Section 2.3.4) of $NH_4$-N concentrations indicated a significant difference (p <0.005) between wells though not between sampling dates (contrary to the seasonal correlation noticed by Mohammed-Pajooh et al., 2017). Concentrations of $NH_4$-N were significantly lower in downstream monitoring well S5 and all other monitoring wells. Downstream of PRB1, concentrations of $NH_4$-N were significantly (P<0.005) lower in monitoring well S3 than in upstream monitoring well S1, suggesting an intervention by PRB1 in between. Significantly higher (p<0.005) concentrations of $NO_2$, a product of nitrification, were found downstream in S3 when compared to S2 (PRB1). $NO_3$ concentrations were significantly (p< 0.005) lower downstream of PRB2 in monitoring well S5 than they were in the upstream well S3 suggesting an intervention by PRB2 in between. These statistics show that PRB2 had a significant effect in lowering $NH_4$-N concentrations and increasing $NO_2$ downstream, which signalled nitrification. The downward trend of $NH_4$-N after 11 months of operation coinciding with an increase of $NO_3$ in downstream monitoring well was a good indication of microbial nitrification as seen by Li et al. (2014), discussed in Section 1.5.2. The statistical analysis also showed that PRB2 had a significant effect in lowering concentrations of $NO_3$, signalling denitrification. While there were significant reductions in the concentrations of target contaminant $NH_4$-N, it was still well above the EU groundwater regulation limit of 0.175 mg $L^{-1}$ and the EU surface water limit of 0.14 mg $L^{-1}$.

There was a modest negative correlation noted between NH4-N concentrations and level of rainfall also noted by Zhang et al. (2022) in contaminated shallow groundwater. This negative correlation showed that rainfall is likely to have influenced $NH_4$-N concentration fluctuations, though this would also have been the case before the PRBs were installed. This influence was likely caused by the percolation of the rainwater down through the upper layers of the landfill site reaching the groundwater body, thereby diluting the pollution effects within the shallow groundwater.

A weakness in the design of the bioremediation site was the large gap of 10 m between PRB1 and PRB2. If the PRBs had been designed to be side by side, it would have afforded a better picture of their functioning as there would be substantially fewer external factors to consider (e.g., naturally occurring bioremediation/ attenuation). Also, the large gap meant that the groundwater could have been affected by plumes of contamination that did not pass through PRB1 and conversely, contamination plumes might have been intercepted by PRB1 that were not intercepted by PRB2. While previous hydrological reports were assessed to avoid this in the design phase, constructing

the PRBs side by side would have avoided this uncertainty. Further, a study using piezometers to assess field and chemical parameters in the groundwater before the bioremediation site was installed would have better informed the location and orientation of the PRBs and also allow a more comparable analysis of PRB efficacy. However, these further investigations would significantly have delayed the installation of the bioremediation site and had financial implications that Clare County Council preferred to avoid.

The statistical analysis would have been more robust and powerful if repeat replicates had been taken each month at each sampling well. This could have been achieved for field parameters, though it would have tripled the cost of chemical analysis for Clare County Council.

## 2.5 Conclusion

Designing an *in-situ* bioremediation strategy requires a broad knowledge of a range of different subjects. Initially the pollutant needs to be examined and understood in terms of its source, its chemistry, and the relevant potential solutions. The local site needs to be investigated in terms of its geology, hydrogeology, and topography. The constraints on this bioremediation solution were that it needed to be financially and environmentally sustainable, *in-situ* and if effective could be easily applied to other sites with similar issues.

The only costs from this bioremediation site were the installation of the PRBs (kindly supported by Clare County Council) and the monitoring wells with no on-going maintenance costs. They were environmentally sustainable as they relied on naturally occurring processes and required no energy to run. While they were initially invasive to install, they can be left in place without causing any harm to the local environment. As discussed above in Section 2.3.8, PRB1 was shown to cause a statistically significant reduction in the target contaminant ($NH_4$-N) concentrations and PRB2 was shown to reduce concentrations of $NO_3$, both positive indicators of bioremediation occurring.

The concentrations of $NH_4$-N in downstream monitoring well S5 were significantly lower than all other upstream wells, though still not below the EU limits for groundwater and surface water. Perhaps if monitoring was still occurring on the PRBs after this study was completed further reductions in $NH_4$-N would be noted if bioremediation was only beginning to occur halfway through the experiment. The PRBs have the potential to be a sustainable *in-situ* bioremediation solution for the treatment of ammonia contamination in shallow groundwater. To our knowledge these were the first set of full-scale *in-situ* sequential PRBs designed to bioremediate ammonia and indications of their success is heartening. Perhaps if some adjustments were made as

described in Section 2.3.8 above, NH$_4$-N concentrations could be reduced further to within EU regulation limits.

This chapter has focused on the site assessment, PRB design and installation, and the field and chemical aspects of bioremediation monitoring. The next two chapters, Chapters 3 and 4 focus on the molecular aspects of bioremediation monitoring to supplement the field and chemical monitoring and shed light on the microbial aspects. Chapter 3 discusses the use of functional genes to monitor nitrogen cycling and Chapter 4 takes a broader view of the microbial communities present in the bioremediation site.

# Chapter III. Nitrogen Cycling Functional Gene Distribution in an Ammonia Contaminated Bioremediation Site

## 3.1 Introduction

This chapter focuses on the microbial nitrogen cycling that occurred on the bioremediation site through functional gene analysis. The quantification of nitrogen cycling functional genes using qPCR was employed to complement the chemical analysis discussed in the previous chapter, Chapter 2. Changes in abundances of these genes would provide clarity on the bioremediation efficacy of the PRBs, as well as elucidate the nitrogen cycling processes occurring. Advances in molecular understanding are allowing bioremediation techniques to be utilised and monitored more effectively. This has increased our understanding of processes in the nitrogen cycle as historically, microbial understanding was gleaned from those microbes that could be cultured in the laboratory. Now it is known that some microbes can oxidise ammonia under anaerobic conditions (anammox), some bacteria can oxidise ammonia to nitrate and on to nitrite (comammox), and that archaea play a fundamental role in nitrogen cycling as discussed in Chapter 1. Briefly (detailed in Section 1.2), the nitrogen cycle can be broadly divided into two stages i.e., nitrification and denitrification. Nitrification occurs when ammonia is converted into nitrite and subsequently into nitrate. It was originally thought that this was an exclusively two-step process, but it is now known (Costa et al., 2006; Van Kessel et al., 2015; Daims et al., 2015) that *Nitrospira inoptina*, and presumably other species, are capable of complete ammonia oxidation (comammox). Denitrification occurs then with the sequential reduction of soluble nitrate, through nitrite and gaseous nitric oxide to nitrous oxide and finally dinitrogen (Petersen et al., 2012). Mulder et al., (1995), discovered a new process in the nitrogen cycle whereby ammonia is anaerobically oxidised (annamox) to dinitrogen gas. In most environments, nitrogen cycling is carried out by diverse assemblages of ammonia-oxidizing and nitrite-oxidizing microorganisms (Kuypers et al., 2018), which is why a functional gene approach to studying this process is preferable as it allows for the characterisation and quantification of a group of functionally similar groups (Petersen et al., 2012).

Section 1.4.1 in Chapter 1 describes the enzymes and the functional genes encoding for them involved in catalysing the nitrogen cycle. The functional genes of interest in this study were bacterial and archaeal *amoA* encoding for the enzyme ammonia monooxygenase (*amoA); nirS* and

*nirK* encoding for the enzyme nitrite reductase *(Nir)*; and the functional gene *nosZ* which encodes for the nitrous oxide *(nosZ)* enzyme. By quantifying these functional genes, an insight can be provided into the abundance (or presence/ absence) of different nitrogen cycling groups. These genes are quantified using polymerase chain reaction (PCR) whereby any nucleic acid sequence (e.g., a functional gene) present in a complex sample can be amplified in a cyclical process to generate a large number of identical copies that can be readily analysed (Kubista et al., 2006).

### 3.1.1 Archaeal Vs Bacterial Ammonia Oxidisers

For years, microbiologists considered archaea as extremophiles that thrived in harsh conditions inhospitable to other organisms (Konneke et al., 2005) but advances in molecular ecology have led to a deeper understanding of the archaeal contribution to ammonia oxidation (Dechense et al., 2016). Archaea can constitute between 0 and 10% of total soil prokaryotes (Timonen & Bomberg, 2009) and studies are providing increasing evidence for the global importance of archaeal ammonia oxidisers (Prosser & Nicol, 2008). Leininger et al. (2006) were the first to investigate and compare abundances of bacterial and archaeal ammonia oxidizers, by qPCR amplification of *amoA* genes. They compared the quantity of archaeal and bacterial *amoA* gene copies across 12 different sample types. The results of this study are shown in Figure 3.1 below.
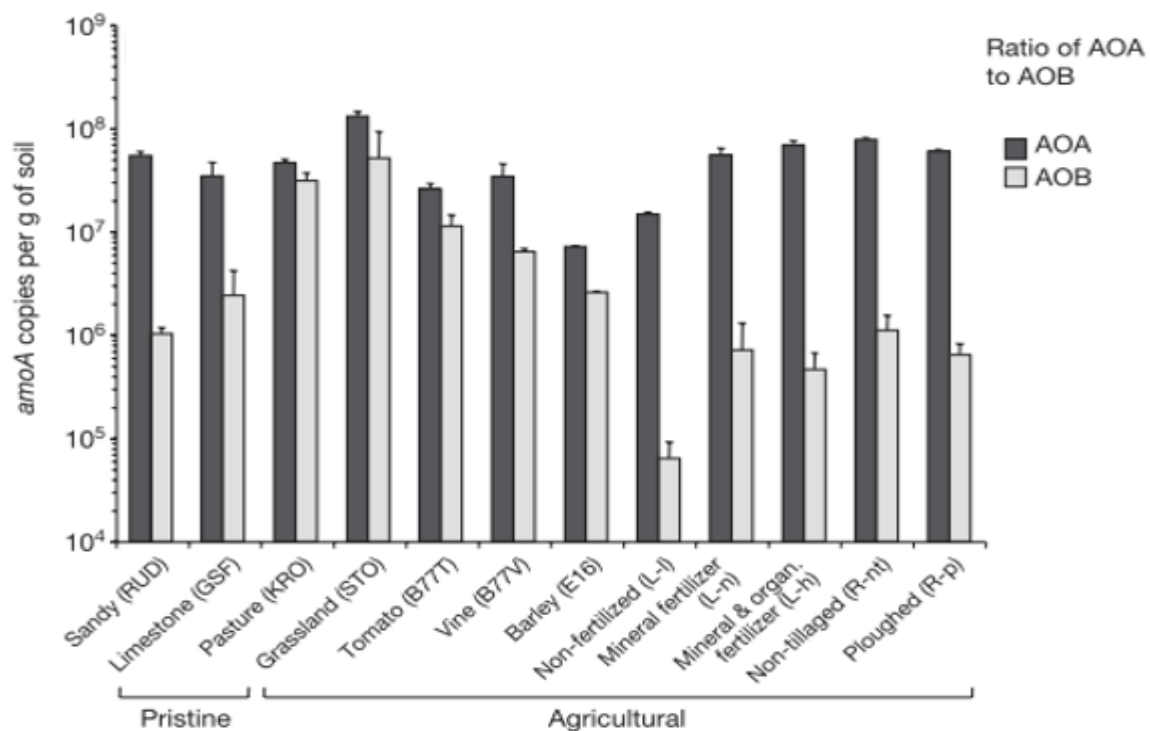


Figure 3. 1: Archaeal *amoA* genes outnumber bacterial *amoA* genes in all 12 sampling points, Leininger et al., (2006).

As can be seen, archaeal *amoA* outnumbered bacterial *amoA* in all sample points. Archaea were also the dominant ammonia oxidiser in coastal and open water environments in a study carried out by Mincer et al., (2007) where *amoA* was used as a functional marker to quantify the distribution of archaeal and bacterial nitrifiers. Nicol et al. (2008) compared the quantity of bacterial and archaeal ammonia oxidisers in acid soils and found that archaea were the most numerous, also noting a negative correlation between AOA and pH in low nutrient groundwater. When studying thaumarchaeal ammonia oxidation in acidic peat soils, Stopnieisek et al. (2010) found that only AOA were present (i.e., no AOB detected) and they were unaffected by the addition of ammonium.  Reed et al. (2010) noted that AOA far exceeded the quantity of AOB in groundwater, though also noticed that AOB numbers increased after urea application. Kelly et al. (2011) found that AOA outstripped AOB quantity in tillage soil under four different treatments. In estuarine sediment, Zhang et al. (2014) detected more archaeal *amoA* than bacterial *amoA* genes. A study carried out on 146 soil samples from North and South America and Antarctica conducted by Bates et al. (2011) found that archaeal content of the soil varied between 0 and >10% (with an average of 2%) and decreased with increasing N content (unlike their bacterial counterparts). Ding et al. (2015) measured AOA and AOB in two soil aquifer treatment systems and found that AOA were predominant. Ouyang et al. (2017) found more AOA in agricultural soils than AOB and noted that sampling time influenced AOA quantity whereas both sampling time and temperature affected AOB numbers.

Other studies compared the abundance of AOA and AOB and found the dominant ammonia oxidisers were bacteria. Limpiyakorn et al. (2010) found that in sewage sludge AOB were more abundant than AOA but as $NH_4$-N concentration decreased, AOA numbers increased. Petersen et al. (2012) analysed soil from five different habitat types and found that AOB were more dominant in all sites and showed strong correlation with potential nitrification rates. In ten different wastewater treatment plants, AOB outnumbered AOA (with no AOA occurring in one site) in a study conducted by Gao et al. (2014). Li et al. (2015) found that AOB were the dominant ammonia oxidiser in estuarine sediment in the Colne estuary, UK. Gwak et al. (2020) investigated the trend of AOBs outnumbering AOA in eutrophic environments and noted that the presence of organic compounds (found in WWTPs) resulted in the inhibition of AOAs.  The study suggested that this is due to the unavailability of bioavailable copper as organic compounds form complexes with metals and thereby remove bioavailable copper for AOAs.

Other studies investigating AOA versus AOB have found mixed results. Hallin et al. (2009) found that AOB and AOA occurred in equal numbers in soil, but that AOB dominated in sewage sludge. Di et al. (2009) found that AOA were more abundant in grassland soils, though AOB were the drivers of nitrification. A study conducted by Bollmann et al. (2014) on two lakes, one oligotrophic, the other meso-/ eutrophic, found that archaea were the dominant ammonia oxidiser in the oligotrophic lake and bacteria were the dominant ammonia oxidiser in the meso-/ eutrophic lake. Hu et al. (2014) carried out seasonal sampling over three years on soil in an inter-tidal wetland and found that in Spring, AOA and AOB occurred in similar quantities, and AOA were more abundant than AOB in Summer and Autumn though absent in Winter. Wang et al. (2014) found that AOA were predominant in reservoirs and riparian zones, but AOB were more abundant in farmland in a reclamation study. Similar to the Di et al. (2015) study, Sterngren et al. (2015) found that AOA were more abundant, but AOB were the dominant ammonia oxidisers in grassland soil.

### 3.1.2 Nitrogen Cycling Functional Gene Abundance

Culturing studies have successfully been carried out on nitrifying cultures (Koops & Pommerening-Roser, 2001; Elbanna et al., 2012; Nakos & Wolcott, 1972), denitrifying cultures (Heylen et al., 2006) and mixed cultures for both nitrifying and denitrifying bacteria (Du et al., 2003). *In-situ* analysis of nitrifying bacterial communities is limited by the fact that most species existing in nature are not necessarily available in culture (Koops & Pommerening-Roser, 2001), which is why microbial composition was mostly investigated through molecular methods in this project.

Some studies have used analysis of functional gene abundance as a measure of nitrogen cycling processes; however, as discussed by Prosser & Nicol (2008), caution must be taken when interpreting abundance data as the presence or high abundance of a functional gene does not mean that the function is operating. Hallin et al. (2009) investigated the relationship between N-cycling communities and ecosystem functioning in a 50-year-old fertilisation experiment. To understand the relationship between the agroecosystem and the nitrogen cycling community the study quantified the abundance of bacterial and archaeal *amoA, nirS, nirK* and *nosZ* functional genes. The quantity of the various nitrifiers and denitrifiers varied depending on the fertiliser treatment (or lack of). As mentioned briefly in Section 3.1.1, Petersen et al. (2012), conducted a study on the abundance of microbial genes associated with nitrogen cycling as indices of biogeochemical processes under five different habitats. To determine the abundance of nitrogen cycling soil bacteria and archaea they quantified several genes using quantitative PCR. The 16S

rRNA gene was used to assess the total number of bacteria and archaea. The *amoA* gene was used to quantify bacterial and archaeal ammonia oxidisers and *nirK, nirS* and *nosZ* genes were used to quantify different groups of denitrifiers. Total bacterial numbers exceeded total archaeal numbers across all sites (3 -5 orders of magnitude). Bacterial *amoA* genes were $8 - 10$ times higher than the abundance of archaeal *amoA* genes. Functional gene *nosZ* was the most abundant denitrifier gene while *nirK* was the least abundant.

Rotthauwe et al. (1997) designed a primer set (amoA-1F/ 2R) for targeting the *amoA* functional gene in ammonia oxidising communities in various aquatic and terrestrial environments and concluded that *amoA* represents a very powerful tool for analysis of indigenous ammonia-oxidising communities. *amoA*-2R is a degenerate primer and Shimomura et al. (2009), designed two non-degenerate substitute reverse primers and noticed no significant difference in quantitative values of *amoA* from environmental samples using real-time PCR. An evaluation of revised PCR primers for more inclusive quantification of AOA and AOB was carried out by Meinhardt et al. (2015). This study found that primer set amoA-1F/2R resulted in similar AOB gene copy numbers as the primer set (GenAOB) designed by themselves in five of eight soil samples. GenAOB returned higher gene copy numbers in the remaining three soil samples, but there was also non target amplification observed in melt curve analysis and gel electrophoresis. Dechesne et al. (2016) warned that caution is warranted when comparing AOB abundances using different qPCR primer sets as their study showed consistent underestimation of AOB when using the amoA-1F/ 2R primer set when compared with AOB-specific primer set: CTO189a/b/c -RT1r for 16S rRNA (Kowalchuk et al., 1997).

An archaeal-focused *amoA* study was conducted by Pester et al. (2012) on an *amoA*-based consensus phylogeny of AOA, which carried out deep sequencing of archaeal *amoA* genes from soils of four geographic regions. This study screened all publicly available entries of the archaeal amoA genes in the NCBI and Camera databases and constructed a consensus archaeal *amoA* tree composed of five monophyletic clusters. Based on this information a primer set (CamoA-19f/ 616R) was designed for conventional PCR that fully matched all *amoA* genes for which sequence information in the target region was available. Meinhardt et al. (2015) compared three sets of primers (Francis et al., 2005; Treusch et al., 2005; Mincer et al., 2007) with their own primer set (GenAOA) in their study investigating PCR primers for more inclusive quantification of AOA and AOB. The study found that the GenAOA primers provided improved quantification of model

mixtures of different *amoA* sequence variants and increased detection of *amoA* in DNA extracted from soils.

To detect denitrifying bacteria in environmental samples Braker et al. (1998) developed conventional PCR primer sets that targeted the *nirK* and *nirS* functional genes. The study concluded that the primer sets (nirK-1F/5R and nirS-1F/6R, respectively) were suitable for the qualitative detection of denitrifying bacteria which was confirmed by analysis of total DNA preparations from aquatic habitats.

To overcome the time consuming and biased MPN-based approach for quantifying bacteria possessing the *nirK* gene, Henry et al. (2004) designed a primer set (nirK876/ nirK1040) to enable quantification of denitrifying bacteria in soils and found the set to be specific and the real-time PCR assay to be linear over 7 orders of magnitude. Following on from this study, Henry et al. (2006) designed a primer set (nosZ-2F/2R) within the region amplified by primers designed by Kloos et al. (2001) to quantify the *nosZ* gene in soils and compare their abundance to functional denitrifying genes *narG* and *nirK* and structural gene 16S rRNA. As expected, 16S rRNA was most abundant in the six soil samples, followed by *narG, nirK* then *nosZ.* The study concluded that the maximum abundance of *nirK* and *nosZ* relative to 16S rRNA was 5 to 6%, showing a low proportion of denitrifiers to total bacteria in soils.  Throback et al. (2004) reassessed PCR primers targeting *nirS, nirK* and *nosZ* for community surveys of denitrifying bacteria. They designed a new primer set to code for the *nirS* functional gene and found that only this primer set (cd3aF/ R3cd) produced an amplicon of the correct size from all samples. To investigate denitrification with the genus *Azospirillum* and other associated bacteria, Kloos et al. (2001) developed a primer set (nosZ-F/R) that targeted the *nosZ* functional gene. *nosZ* functional gene was detected in 11 of the 16 bacterium and each of the 11 bacteria also contained either *nirK* or *nirS.*

## 3.2 Materials and Methods

Chapter 2 describes the materials and methods used to sample water from the bioremediation site and to carry out field parameter testing and laboratory analysis. The materials and methods used for molecular analysis are outlined below.

### 3.2.1 Site Description

As described and illustrated in Chapter 2, a bioremediation study was carried out on a landfill site in Co. Clare, in an effort to reduce ammonia contamination in shallow groundwater. Two permeable reactive barriers were installed to intercept the contamination plume, one to

encourage nitrification, the second to encourage denitrification incorporating sampling wells S2 and S4, respectively. Sampling well S1 was installed upstream and an existing well downstream was incorporated into the bioremediation site as downstream sampling well S5.

### 3.2.2 eDNA Extraction

Molecular analysis required that environmental DNA be extracted from the water samples collected to allow for downstream processes. The DNA extraction method used in this study was the CTAB method as per Barrett et al., (2013) with an adjustment as per Sirisena et al. (2013). This method was chosen due to its effectiveness (discussed in Section 1.4.1) and was more economical than using commercial kits for large number of samples. Three samples of one litre of water were collected from each of the five sampling points (S1, S2, S3, S4 and S5) at the bioremediation site each month. Each litre (x 3) was filtered through a 0.2 μm Sartorius cellulose nitrate filter, resulting in three filters (replicates) per sampling point. Each filter was individually sealed and frozen at -20°C until further processing.

As per Sirisena et al. (2013), each filter was placed in a 15 ml centrifuge tube with 10 ml sterile water and allowed to soak for 5 minutes. Each filter was then abraded with a sterile plastic inoculating loop and the tubes were then centrifuged at 3,000 x g for 20 minutes to recover bacterial cells as a pellet. The pellet was transferred to a sterile 2 ml Eppendorf tube. To each tube 500 μl 1% (w/v) cetyltrimethylammonium bromide (CTAB), 500 μl lysis buffer (1M tris HCL, 0.5 M EDTA, 1 M sucrose) and 20 μl of sterile lysozyme (10 ml L$^{-1}$). The tubes were vortexed for 30 seconds before incubation at 37°C for 30 minutes. 200 μl 10% SDS was added to each tube, then tubes were vortexed briefly and incubated at 70°C for 1 hour. Then 6 μl Proteinase K (1354 U/ ml) was added and the tubes were centrifuged at 15,000 x g for 15 minutes. The supernatant was transferred to fresh 2 ml tubes with equal volume of chloroform/ isoamyl alcohol (24:1) and centrifuged at 10,000 x g for 15 minutes. The top phase was transferred into fresh microcentrifuge tubes with 0.6 volume isopropanol and allowed to precipitate at room temperature for 12 hours. The samples were centrifuged at 10,000 x g for 30 minutes and the supernatant was discarded. 200 μl of 70% ice cold ethanol was added to the remaining pellet and centrifuged at 10,000 x g for 15 minutes. The pellets were allowed to air dry and were then re-suspended in a final volume of 30 μl dH$_2$O. Concentration and purity of the extracted DNA was then measured on a ND-1000 spectrophotometer. The DNA was then purified using a slight modification of the Roche High Pure PCR Template Preparation Kit. To each 30 μl sample, 170 μl sterile phosphate buffer saline

solution was added. Following this, 200 µl binding buffer was added along with 100 µl isopropanol and mixed. The remainder of the procedure was carried out as per the Roche High Pure PCR Template Preparation Kit Protocol. The samples were then stored in labelled Eppendorf tubes at -20°C until further use.

### 3.2.3 Positive Standard Preparation

To allow for a positive control to be used in downstream molecular analysis, positive standards were prepared. The primers used to create positive standards are described in Table 3.1.

Reference sequences for the bacterial *amoA* gene (from *Nitrosomonas europaea*, 450 bp) and archaeal *amoA* gene (from *Nitrosarchaeum limnia*, 672 bp) were obtained from Genbank. Sequences were synthesised commercially and cloned into plasmid vectors in competent *E. coli* cells (MWG-Eurofins, Germany). Plasmid DNA was extracted using the GenElute™ Plasmid Miniprep kit (Sigma Aldrich) and used as standards for bacterial and archaeal *amoA* PCR reactions. To ensure the correct gene was present, samples were sent for commercial sequencing (https://eurofinsgenomics.eu/en/). BLAST (Altschul et al., 1990) was used to confirm the correct genes were sequenced for use as standards for bacterial and archaeal *amoA* PCR and *Nitrosomonas europea* (100% identical) and archaeon enrichment clone (99.66% identical) were confirmed for bacterial and archaeal *amoA* respectively.

For *nosZ*, a standard was prepared by amplifying the *nosZ* gene (using primer set nosZ-F/R (Kloos et al., 2000)) from DNA extracted from a revived NCIMB culture of *Pseudomonas denitrificans* (NCIMB 1656). The PCR products were then cleaned using DNA clean & Concentrator™-5 (Zymo Research) and cloned using pGEM-T Easy vector kit (Promega) into prepared competent cells.

The competent cells were prepared by inoculating an *Escherichia coli* colony from an LB plate into 2 ml LB liquid medium and incubated overnight in a shaking incubator. The culture was chilled on ice for 15 minutes and then centrifuged at 3,300 x g at 4°C for 10 minutes. The supernatant was discarded, and the pellet was re-suspended in 35 ml cold 0.1 M CaCl$_2$ solution. The cells were chilled on ice for 30 minutes and then centrifuged at 3,300 x g for 10 minutes. After the supernatant was removed the pellet was re-suspended in 6 ml 0.1 M CaCl$_2$ solution and 15% glycerol. Finally, 0.4 – 0.5 ml of the cell suspension was pipetted into 1.5 ml centrifuge tubes, frozen on dry ice and transferred to a -80°C freezer.

The competent cells now containing the cleaned PCR products were grown on LB/ ampicillin (100 ug L$^{-1}$) agar. The cells were blue/ white screened and positive cells were then streaked for isolated

colonies. These were grown overnight in LB/ampicillin broth and underwent a plasmid preparation using GenElute™ Plasmid Miniprep kit (Sigma Aldrich). To ensure the correct gene was present samples were sent for commercial sequencing (https://eurofinsgenomics.eu/en/). BLAST (Altschul et al., 1990) was used to confirm the correct gene was sequenced for use as standards for *nosZ* PCR and was confirmed as *Pseudomonas denitrificans* (86% identical).

To create a *nirK* standard, PCR (using primer set nirK-1F/5R (Braker et al., (1998)) was carried out on eDNA extracted from water that was collected from the bioremediation site. PCR products were then cleaned and concentrated using DNA clean & Concentrator™-5 (Zymo Research). However, since there was a high quantity of non-specific products also, post-PCR a gel extraction was necessary.

Another PCR was performed on this *nirK* PCR product using the same primers to determine whether the correct DNA template had amplified. This second product was transformed into competent cells and underwent plasmid extraction as described above for *nosZ*. The insert of this plasmid DNA was sequenced to ensure that the appropriate gene was present (confirmed through BLAST to be *Pseudomonas stutzeri* (99.72% identical)), and it was then used as a positive standard for the remainder of the trial.

A positive standard for the *nirS* functional gene was prepared as *nirK* above using primer set nirS32F/ nirS64R (this study) and was confirmed to be *Acidovorax carolinensis* (92.34% identical).

For the 16S rRNA gene standard, DNA was extracted from a pure culture of *Escherichia coli* by the boil preparation method (Queipo-Ortuno et al., 2008). The samples were centrifuged at 15,000 × g for 15 min. The supernatant was removed, and the pellet was resuspended in molecular biology-grade water and centrifuged at 15,000 × *g* for 10 min. The supernatant was removed, and the pellet was resuspended in 40 µl of molecular biology-grade water, before being subjected to boiling at 100°C in a water bath for 10 min, cooled on ice, and centrifuged at 15,000 × *g* for 10 s before it was stored at −20°C. This was then used as the positive control.

All samples were DNA sequenced commercially (https://eurofinsgenomics.eu/en/) to ensure that the correct gene was present. Post PCR products showing the correct size band on agarose gels were prepared with 5 pmol SP6 or T7 sequencing primers. The sequences are included in Appendix B.

### 3.2.4 Culturing

To grow cultures of nitrifiers, groundwater was collected from PRB1 and enriched in nitrifier enrichment medium (NEM) as per Elananna et al. (2012) based on a media described by Nakos & Walcot (1979) and another NEM described by Du et al (2003). These media were inoculated with water from the site every quarter and incubated aerobically @28°C for three weeks before samples of the broth were taken and stored in 30% glycerol and at -80°C. To pick cultures from agar plates, agar was added to these media and plates were streaked with the enrichment broth inoculated with water from PRB1 from the bioremediation site. Concurrently, nutrient agar plates were inoculated with samples from PRB1 and were grown aerobically (to select for aerobic nitrifiers) @28°C.

To grow cultures of denitrifiers, groundwater was collected from PRB2 and enriched in denitrifier enrichment medium (DEM) described by Heylen et al. (2006) and another DEM described by Du et al. (2003). The NEM and DEM were inoculated with water from the site every quarter and incubated anaerobically for three weeks before samples were taken and stored in 30% glycerol at -80°C. To pick cultures from these media, agar was added, and plates were streaked with the enriched media. Concurrently, nutrient agar plates were inoculated with samples from PRB2 and were grown anaerobically (to select for aerobic nitrifiers) @28°C.

Cultures were isolated and were then enriched in LB broth overnight @ 37°C. A boil preparation was then carried out as described in Section 3.2.3 above and the sample was stored at -20°C.

### 3.2.5 Conventional PCR

Conventional PCR was used to amplify full gene fragments from the bioremediation site so they could be used as standards for qPCR analysis once the genes was confirmed to be correct. Conventional PCR was carried out using an Applied Biosystems 2720 thermal biocycler. The assay was standardised across all genes of interest unless otherwise specified. The oligonucleotide primers were supplied by Eurofins Genomics (Germany) and diluted with sterile ultra-pure water as per manufacturer's instructions and are displayed in Table 3.1 below. These were then mixed and diluted to a 25 µM primer mix. PCR reactions were performed in a 15 µl assay containing 10 µM each primer, 7.5 µl 2X GoTaq Hot Start Green Master Mix (Promega) and 1 µl DNA. The cycling conditions varied across the genes and are displayed in Table 3.1. PCR products were then visualised via agarose gel electrophoresis. Unless otherwise stated, gels were 0.8% agarose and 1

x TAE buffer and underwent electrophoresis for a duration of 45 minutes at 200 volts and 120 mAmps (50 ml gels) and 250 volts and 180 mAmps (100 ml gels).

Table 3. 1: Primers and thermal cycling conditions used for conventional PCR in this study

| Gene | Primer | Sequence (5'-3) | Size | Run Conditions | Thermal Profile | Reference |
|---|---|---|---|---|---|---|
| Bacterial amoA | amoA-1F | GGG GTT TCT ACT GGT GGT | 491 | Limpyakorn et al., (2011) | 94°C x 2 min (94°C x 30 s, 55°C x 45 s, 72°C x 45 sec) x 33, 72°C x 10 min | Rotthauwe et al. (1997) |
| | amoA-2R | CCC CTC KGS AAG CCT TCT TC | | Horz et al., (2000) | 95 x 5 min (94°C x 1 min, 62°C x 90 sec, 72°C x 90 sec) x 30, 72 x 10 min | |
| Archaeal amoA | CamoA-19f | ATG GTC TGG YTW AGA CG | 709 | Pester et al., (2012) | 5 min x 95 °C, (95 °C x 1 min, 55 °C x 90 s, 72°C x 90 s) x 30, 72°C x 5 min | Pester et al., (2012) |
| | CamoA-616r | GCC ATC CAB CKR TAN GTC CA | | | | |
| nirK | nirK-1F | GGM ATG GTK CCS TGG CA | 514 | Braker et al., (1998) | 5 min x 95°C, (30 s x 95°C, [40 s x 45°C- 40°C (-0.5°C/cycle)], 40 s x 72°C) x 10, (30 s x 95°C, 40 s x 45°C x 72°C, 40 s x 72°C) x 20, 7 min x 72°C | Braker et al., (1998) |
| | nirK-5R | GCC TCG ATC AGR TTR TGG | | | | |
| | | | | Throback et al., (2004) | 5 min x 95 °C, (95 °C x 1 min, 55 °C x 90 s, 72°C x 90 s) x 30, 72°C x 5 min | |
| nirS | nirS-1F | CCT AYT GGC CGC CRC ART | 890 | Braker et al., (1998) | 5 min x 95°C, (30 s x 95°C, [40 s x 45°C- 40°C (-0.5°C/cycle)], 40 s x 72°C) x 10, (30 s x 95°C, 40 s x 45°C x 72°C, 40 s x 72°C) x 20, 7 min x 72°C | Braker et al., (1998) |
| | nirS-6R | CGT TGA ACT TRC CGG T | | | | |
| | | | | Throback et al., (2004) | 5 min x 95 °C, (95 °C x 1 min, 55 °C x 90 s, 72°C x 90 s) x 30, 72°C x 5 min | |
| | nirS- 8F | TAC CAY CCS GAR CCG CGC GT | 480 | This Study | 94°C x 5 min; (94°C x 1 min, 55°C x 1 min, 72°C x 30 s) x 30, 72°C x 8 min | This study |
| | nirS- 16R | GGR TGS GTC TTS AYG AAC AG | | | | |
| | nirS- 32F | TWC CAY CCS GAR CCS CGC GT | 480 | This Study | 94°C x 5 min; (94°C x 1 min, 55°C x 1 min, 72°C x 30 s) x 30, 72°C x 8 min | This study |
| | nirS- 64R | GGR TGS GWY TTS AYG AAC AG | | | | |
| nosZ | NosZ-F | CGY TGT TCM TCG ACA GCC AG | 699 | Kloos et al., (2001) | 97°C x 7 min; 1 x (94°C x 20 s, 65°C x 30 s, 72°C x 40 s), 2 x (94°C x 20 s, 62°C x 30 s, 72°C x 40 s); 3 x (94°C x 20 s, 59°C x 30 s, 72°C x 40 s); 5 x (94°C x 20 s, 57°C x 30 s, 72°C x 40 s) 24 x (94°C x 20 s, 55°C x 30 s, 72°C x 40 s), 72°C x 10 min | Kloos et al., (2001) |
| | NosZ-R | CAT GTG CAG NGC RTG GCA GAA | | | | |
| 16S rRNA | F27 | AGA GTT TGA TC(A/C) TGG CTC AG | 1465 | Heuer et al., (1997) | 5 min x 94°C, (94°C x 1 min, 63°C x 1 min, 72°C x 2 min) x 35, 72°C x 10 min | Heuer et al., (1997) |
| | R1492 | TAC GG(C/T) TAC CTT GTT ACG ACT T | | | | |

### 3.2.6 Real-Time PCR

Molecular analysis using qPCR was chosen so that the nitrogen cycling functional genes could be quantified across the bioremediation site at quarterly intervals during the two-year study. Table 3.2 below displays the primer sets and thermal cycling conditions used for qPCR. Some of the conditions were adjusted from the original to cater for differences in instrumentation, e.g., the 7300 Real Time System will not allow for an extension time of less than 29 seconds so the cycling conditions for the Meinhardt et al. (2011) primers were adjusted to include an extension time of 29 seconds rather than 13 seconds. Also, a dissociation stage of 95°C x 15 s, 60°C x 30 s and 95°C x 15s was added to each run. Unless otherwise stated the assay used for real time PCR was a 15 µl reaction composed of: 1X Sybr (FastStart Universal Sybr green master (Rox)), 5 µM each primer (final concentrations), 2µl DNA template and was carried out in an Applied Biosystems 7300 Real time PCR system. Samples were run in duplicate. A serial dilution (10-fold unless otherwise stated) of the positive standards were included in each run so that a standard curve could be generated and evaluated to assess gene copy number (GCN) of the target gene.

Table 3. 2:Primers and thermal cycling conditions used for qPCR in this study.

| | Primer | Sequence (5'-3) | Size | Run Conditions | Cycling Conditions | Reference |
|---|---|---|---|---|---|---|
| Bacterial *amoA* | amoA-1F<br>amoA-2R | GGG GTT TCT ACT GGT GGT<br>CCC CTC KGS AAG CCT TCT TC | 491 | Petersen et al., (2012) | 94°C x 5 min (94°C x 30 s,  55°C x 45 s, 72°C x 1 min) x 40 + Dissociation Stage | Rotthauwe et al., (1997) |
| | amoA-1Fmod<br>Gen-AOB-R | CTG GGG TTT CTA CTG GTG GTC<br>GCA GTG ATC ATC CAG TTG GG | 130 | Meinhardt et al., (2015) | 95°C x 5 min (95°C x 10 s,  58°C x 10 s, 72°C x 29 sec) x 45 | Meinhardt et al., (2015) |
| Archaeal *amoA* | Gen-AOA-F<br>Gen-AOA-R | ATA GAG CCT CAA GTA GGA AAG TTC TA<br>CCA AGC GGC CAT CCA GCT GTA TGT CC | 140 | Meinhardt et al., (2015) | 95°C x 5 min (95°C x 10 s,  55°C x 10 s, 72°C x 29 sec) x 45 + Dissociation Stage | Meinhardt et al,. (2015) |
| *nirK* | nirK876-F<br>nirK1040-R | ATY GGC GGV CAY GGC GA<br>GCC TCG ATC AGR TTR TGG TT | 165 | Machine Default | 50°C x 2 min, 95°C x 10 min (95°C x 15 s,  60°C x 1 min) x 40 + Dissociation Stage | Henry et al., (2004) |
| *nirS* | nirSCd3a-F-m<br>nirSR3cd-m | AAC GYS AAG GAR ACS GG<br>GAS TTC GGR TGS GTC TTS AYG AA | 425 | Machine Default | 50°C x 2 min, 95°C x 10 min (95°C x 15 s,  60°C x 1 min) x 40 + Dissociation Stage | Throback et al., (2004) |
| | nirS RealT F4<br>nirS RealT R16 | CCG GTY TCC TTC ACG TTS AC<br>CCG  GTY TCC TTS ACR TTS AC | 80 | This Study | 50°C x 2 min, 95°C x 10 min (95°C x 15 s,  56°C x 30 s,72°C x 30 s) x 40 + Dissociation stage | This Study |
| *nosZ* | nosZ-2F<br>nosZ-2R | CGC RAC GGC AAS AAG GTS MSS GT<br>CAK RTG CAK SGC RTG GCA GAA | 267 | Machine Default | 50°C x 2 min, 95°C x 10 min (95°C x 15 s,  60°C x 1 min) x 40 + Dissociation Stage | Henry et al., (2006) |
| *16S rRNA* | Eub-338F<br>Eub-518R | ACA TCC TAC GGG AGG C<br>CGTATTACCGCGGCTGCTGG | 200 | Fierer et al., (2005) | 95°C x 15 min (95°C x 1 min,  53°C x 30 s, 72°C x 1 min) x 45 + Dissociation Stage | Amann et al., (1990) |

91

## 3.3 Results and Discussion

### 3.3.1 Culturing

The results of the culturing that was carried out from water collected from the PRBs as described in Section 3.2.4 are presented in Table 3.3 below.

Table 3. 3: Culturing results showing microbial growth on NEM (nitrifier enrichment medium) and DEM (denitrifier enrichment medium) and nutrient agar

|  | NEM & DEM (Du et al., 2003) | NEM (Elbanna et al., 2012) | DEM (Heylen et al., 2006) | Nutrient Agar |
|---|---|---|---|---|
| Nitrifier (aerobic) | No Growth | No Growth | n/a | Growth |
| Denitrifier (anaerobic) | No Growth | n/a | No Growth | Growth |

Growth on the agar plates were noted on the nutrient agar plates only. The nutrient agar plates that were inoculated with groundwater collected from PRB1 and incubated aerobically produced white and orange colonies that were streaked for isolation. The nutrient agar plates that were inoculated from water collected from PRB2 and incubated aerobically produced white colonies that were streaked for isolated colonies and grown aerobically and anaerobically. DNA was extracted from the colonies using the boil prep method described in Section 3.2.3. and used for PCR optimisation.

## 3.3 Results and Discussion

### 3.3.2 PCR Optimisation

The results of conventional PCR primer and thermal cycling condition optimisation for the six genes of interest are outlined below. The associated gel images are displayed in Appendix C.

#### 3.3.2.1 16S rRNA

*16S rRNA* conventional PCR was carried out with the primers and thermal cycling conditions described previously in Table 3.1. Performing *16s rRNA* detection on the environmental samples tested the integrity of the eDNA by confirming whether there was any detectable bacterial or archaeal DNA present, as amplification should occur because the *16S rRNA* structural gene is found in all bacteria and archaea. December 2015 eDNA samples were used in dilution series to check for inhibition (i.e., 1:1000, 1:500, 1:100, and 1:50), and at higher DNA quantities to check for concentration issues (i.e., 1 µl, 2 µl and 3 µl) and the resulting gel image is displayed in Appendix C, Figure C.1. Amplification occurred in all samples with higher

concentrations of DNA. 16S PCR was also performed on the August 2015 samples to check the integrity of this eDNA. Knowing that low concentrations were potentially an issue, the August 2015 sample amplifications were carried out with 1 µl and 2 µl DNA concentrations. The gel image can be seen below in Appendix C, Figure C.2. Strong bands of appropriate size (1465 bp) were seen in both 1 µl and 2 µl PCR products with the exception of sample S3. This indicated that no bacterial or archaeal DNA was present in the sample. *16S* PCR was carried out on all samples prior to functional gene PCR to ensure that DNA was present.

### 3.3.2.2 Bacterial *amoA*

The primer set used for bacterial *amoA* conventional PCR was designed by Rotthauwe et al. (1997), previously outlined in Table 3.1, and resulted in a PCR product size of 491 bp. A PCR method described by Horz et al. (2000) was initially used as described in Table 3.1. Figure C.3 in Appendix C, shows the resulting gel images after PCR was carried out on DNA samples extracted from the landfill groundwater in July 2015, October 2015, and December 2015. The results were poor, with faint amplification in only four of the 30 samples. This poor amplification could indicate inappropriate cycling conditions, inhibitors in the DNA or low target DNA concentrations.

In order to test the cycling conditions, conditions from a study carried out by Limpiyakorn et al. (2011), described in Table 3.1, were used along with the same primers (amoA-1F and amoA-2R). This run consisted of an initial step of an extra minute and an annealing step 7°C lower. Lower annealing temperatures allow the primers to be less stringent though also usually result in non-specific amplification. The results can be seen in Figure C.4 in Appendix C. A mirror run using the Horz et al. (2000) cycling conditions was also performed to compare the efficacy of the two PCR cycling conditions and can also be seen in Figure C.4. Sample S2.2 from December 2015 was chosen for comparative purposes as amplification did occur previously and samples December 2015 S1.2 and S3.2 were used. To test for inhibition a "spike" of 1 µl positive bacterial *amoA* DNA (as described in Section 3.2.3) was added to each sample to see if amplification occurred. It was thought that if the environmental DNA contained inhibitors, they would not allow a spike in the eDNA to amplify. Finally, to test for gene concentration issues, assays were used with diluted concentrations of DNA ($10^{-1}$ to $10^{-4}$) and also larger concentrations of DNA were used in the PCR assays (2 µl and 3 µl). The results can be seen in Figure C.4 also. The results from the PCR using the Limpiyakorn et al. (2011) cycling conditions were similar though slightly better than the amplification seen after using the Horz et al. (2000)

bacterial *amoA* PCR protocol, with faint amplification occurring in the diluted samples. This indicated that the cycling conditions were not the issue. The higher concentrations of the environmental DNA were more successful, indicating a concentration issue rather than an inhibition issue.

To test this further, the better performing cycling conditions (Limpyakorn et al., 2011) were repeated using the July 2015 samples with DNA volumes of 1 µl, 2 µl and 3 µl. Gel image Figure C.5, Appendix C. As can be seen from the resulting gel image, June 2015 samples S1, S2, S4 and S5 amplified. Poor amplification occurred in sample S3, so another PCR was performed with 1:10 dilution and a 1 µl, 2 µl and 3 µl DNA volume recipe in duplicate (Figure C.6, Appendix C) along with samples spiked with positive standard (described in Section 3.2.3) samples to check for inhibition. Amplification occurred in the spiked samples, indicating inhibitors were not present, and in the positive control. Amplification occurred in the eDNA samples also with the best results noted in the 1 µl DNA recipe.

Considering the issue with samples not amplifying suggested concentration rather than inhibition factors, another 2 µl DNA volume recipe was carried out on all the July, October and December 2015, samples, Figures C.7 and C.8, Appendix C. Ten samples showed strong bands of appropriate size. Eight samples showed no product and the remaining samples showed faint bands. A gradient PCR was then carried out to establish the most appropriate annealing temperature (54°C – 58°C). The samples used were a positive standard and eDNA; both were used undiluted and in 1:10 dilution. Figure C.9 displays the resulting gel image. The standards amplified (both concentrated and diluted samples) though there was no amplification in the environmental DNA sample. The annealing step of 57 °C appeared to work best from this image.

Finally, a PCR was carried out as per Rotthauwe et al. (1997), described in Table 3.1, and the resulting gel image can be seen in Appendix C, Figure C.10. The Rotthauwe cycling conditions showed non-specific amplification in some of the samples. For the remainder of the study the cycling conditions described by Limpiyakorn et al. (2011) were used and the PCR assays contained 2 µl eDNA.

To test whether the cultures grown on the nutrient agar inoculated with groundwater collected from the PRBs (as described in Section 3.2.4) possessed the bacterial functional gene *amoA*, a PCR was carried out from all samples grown from PRB 1 and PRB 2 and the gel image, Figure C.11, shows the result in Appendix C. Bacterial *amoA* was present in the samples collected from

PRB 1 and did not amplify in the samples collected from PRB 2. This indicated that the PRBs could be functioning as intended, i.e., PRB1 was promoting bacteria possessing the *amoA* functional gene, and these bacteria were absent from PRB 2 which was aimed at promoting the growth of anaerobic denitrifiers.

### 3.3.2.3 Archaeal amoA

The primer set used for archaeal *amoA* conventional PCR was designed by Pester et al. (2012), described in Table 3.1., and results in a product size of 709 bp. An initial PCR was carried out on eDNA and on positive standards. The cycling conditions used can be seen in Table 3.1, and the resulting gel image Figure C.12 is displayed in Appendix C. As can be seen, amplification occured in the positive standard but not at all in the eDNA samples (January 2015), suggesting a problem with the DNA (i.e. inhibition or concentration) rather than an issue with the primers or cycling conditions. A different set of environmental DNA was used (July, October and December, 2015) as these samples showed amplfication of the bacterial *amoA* functional gene. The results are displayed in Figures C.13 and C.14, Appendix C. As can be seen from the two gel images very faint bands of appropriate size appeared in some samples (most in July 2015, less in October and none in December 2015). To further test whether there was a concentration or inhibition issue with the DNA, trouble shooting was carried out on the October 2015 samples. PCR was performed on 1 µl, 2 µl and 4 µl DNA recipes and spiked DNA samples and can be seen in gel image, Figure C.15, Appendix C. The spiked DNA samples contained 1 µl eDNA and also 1 µl of positive archaeal *amoA* DNA sample. This amplification showed that there was concentration issue rather than an inhibition one. The 2 µl sample worked best in this example so another PCR was carried out on the samples collected from July, October and December 2015 using a 2 µl DNA recipe (gel images can be seen in Figures C.16 and C.17, Appendix C).

This PCR was much more successful than the 1 µl DNA recipe carried out previously showing the eDNA was of a low concentration and 2 µl was necessary to provide enough target DNA for the primers to identify. Some samples still did not amplify so a dilution series ($10^{-1}$ to $10^{-4}$) and higher DNA concentration PCR assays was carried out on these samples, gel images displayed in Figures C.18 and C.19, Appendix C. As can be seen on the gel images there was poor amplification in the samples. Faint amplification can be seen in the higher DNA concentration samples of October S3.2 and December S1.2. Using the DNA concentrations that worked best for each sample (2 µl Dec S1.2, 3 µl for the remainder) another PCR was then carried out with

DNA samples in duplicate, Figure C.20, Appendix C. Amplification could be seen in October S1.1 though no amplification occurred previously. Very faint amplification occurred in the remaining samples and at this point it was considered that the archaeal *amoA* gene was present in very low concentrations.

Due to the large amount of troubleshooting that was required and the finite amount of eDNA it was decided to designate one month's eDNA samples to troubleshooting, and August 2015 was chosen as there were no fluctuations in the field or chemical parameters for that month. Archaeal *amoA* PCR was performed on samples from August 2015. The resulting gel image can be seen in Figure C.21, Appendix C.  There appeared to be amplification in all five samples tested from August 2015. Considering the PCR cycling conditions appeared to be working effectively and there appeared to be no inhibition in the eDNA samples, it was concluded at this point that in some samples the archaeal *amoA* functional gene was either not present, or present at very low concentrations.

Archaeal *amoA* PCR was performed on the cultures grown on the nutrient agar that was inoculated from water samples collected from PRB 1 and PRB 2 as described in section 3.3.3.2. The resulting gel image is displayed in Figure C.22, Appendix C. The gel image suggests no archaeal *amoA* gene was present in isolates cultured from water collected from PRB 1 or PRB 2. Archaeal ammonia oxidisers do not respond to culturing and Klein et al. (2022) found that agar inhibits the growth of some AOA.

### 3.3.2.4 nirK

As described in Section 3.2.3, positive standards were prepared by carrying out PCR on laboratory cultures and eDNA to isolate the 514 bp gene. To determine whether the *nirK* gene was present in cultures grown from the PRBs, and in revived cultures of *P. denitrificans*, PCR (as per Braker et al., 1998) was performed on these samples and the PCR products were then visualised on an agarose gel, Figure C.23, Appendix C. The expected product (514 bp) did not appear to be present in the PRB cultures or in *P. denitrificans.* Another PCR was carried out with cycling conditions as per Throback et al. (2004) and visualised using 1.5% agarose gel, Figure C.24, Appendix C. There was no obvious amplification of the 514 bp n*irK* gene and the gel showed non-specific amplification. Another PCR was carried out using the Throback et al. (2004) cycling conditions on *P. denitrificans*, PRB cultures and also on August 2015 samples to determine whether the *nirK* gene was present in the bioremediation site, gel images in Figure C.25, Appendix C.  The August 2015 samples showed non-specific amplification with some wells

(i.e., A1, A4) possibly displaying the 514 bp *nirK* gene. Faint amplification is seen in the denitrifier culture above possibly with appropriate bands of 514 bp occurring through there was a lot of non-specific amplification. Further *nirK* PCR was carried out on the August samples so that PCR product could be extracted from the gel, transformed into competent cells and the plasmid extracted (as described in Section 3.2.3) so that it could be used as a positive standard. The plasmid preps were visualised on an agarose gel post-PCR, Figure C.26, Appendix C. The gel extraction and transformation were successful, though contamination of the non-template control was noted. The post-PCR products were confirmed as *nirK* through sequencing as described in Section 3.2.3. It was determined that the primer set nirK-1F/5R (Braker et al., 1998) and Throback et al. (2004) cycling conditions were appropriate for the remainder of the study and the *nirK* plasmid preps were used as a positive standard for the reminder of the study.

### 3.3.2.5 nirS

Conventional PCR was carried out on *Pseudomonas denitrificans* and the denitrifier cultures grown from water samples collected from PRB2. The cycling conditions and primers used (Braker et al., 1998) are outlined in Table 3.1. The PCR products were visualised on an agarose gel to check whether the appropriate 890 bp product was present, Figure C.27, Appendix C. The correct 890 bp product was found in the *P. denitrificans* PCR products though there was a high amount of nonspecific amplification. There was no band of appropriate size visualised on the denitrifier culture PCR products. In an effort to ascertain whether a different annealing temperature would reduce the high amount of nonspecific amplification, a gradient PCR was carried out using *P. denitrificans* DNA and the PCR products were visualised on an agarose gel, Figure C.28, Appendix C. Faint bands appear around the 890 bp mark though nonspecific amplification occurred at all temperatures. Fortunato et al. (2009) found amplification of *nirS* to be poorly reproducible, so focused on denitrifying genes *nirK* and *nosZ* only. For this study an independent set of *nirS* primers was designed by aligning all publicly available complete *nirS* sequences using the Genbank database (https://www.ncbi.nlm.nih.gov/genbank/) and searching for conserved regions that could provide suitable primer target sites. Two degenerate primers, nirS8F/ nirS16R, were selected to amplify a 480-bp fragment. The specificity of the primers was tested in silico using MEGA 7 Software. To compare this new primer set and nirS-1F/ nirS-6R (Braker et al., 1998), a *nirS* PCR was performed on eDNA extracted from water collected in August and December 2015, Figure C.29, Appendix C. Both

primer sets amplified the target product, 890 bp and 480 bp, respectively. The new primer set showed nonspecific amplification though significantly less than the Braker et al. (1998) primer set. In an effort to reduce nonspecific amplification further, another primer set was designed, nirS32F and nirS64R using the same method as described to design nirS8F/16R. *nirS* PCR was performed again on eDNA to compare the three primer sets and the PCR products were visualised on an agarose gel, Figure C.30, Appendix C

Primer set nirS32F/ 64R showed the least amount of nonspecific amplification. A gradient PCR was carried out on eDNA using this primer set (not pictured) where it was determined that 55°C was the most appropriate annealing temperature. To create a positive standard for *nirS*, a 50 µl PCR was carried out using the nirS32F/ nirS64R primer set and the PCR product was extracted, transformed into competent cells and the plasmid extracted (as described in Section 3.2.2). PCR was performed on the plasmid preps and the PCR products were sent for sequencing (as per Section 3.2.3), where it was determined that the primer set was amplifying the appropriate *nirS* gene. The BLAST (Altschul et al., 1990) results showed the sequence to be 92.34% identical to *Acidovorax carolinensis* first isolated from a contaminated site in North Carolina in 2002 and described by Singleton et al. (2018) as an aerobic neutrophile with affinity for $NH_4$. These *nirS* plasmid preps were used as a positive standard for the remainder of the experiment.

### 3.3.2.6 nosZ

The cycling conditions used for conventional *nosZ* PCR as per Kloos et al. (2000) are outlined in Table 3.1. Positive standards were prepared for *nosZ* as described in Section 3.2.3. *nosZ* PCR was performed on four plasmid preps to determine whether the cloning procedure was successful and the 699 bp gene had amplified (figure C.31, Appendix C). The gel image shows that the positive standard procedure was successful, and that the PCR was working well with the *nosZ* primers and cycling conditions as per Kloos et al. (2001). These were used as positive standards for the remainder of the experiment. To check the efficacy of the primers and cycling conditions on the eDNA, a *nosZ* PCR was performed on DNA extracted from groundwater collected in July 2016, S1 and S2, gel image displayed in Figure C.32, Appendix C. No product was seen in S1, and a product of correct size was seen in S2. *nosZ* PCR was performed on the isolates grown on nutrient agar that was inoculated from water samples collected from PRB 1 and PRB 2 as described in Section 3.3.1. The PCR products were visualised on an agarose gel (Figure C.33, Appendix C). There were faint bands of correct size (699 bp) appearing in one

white colony from PRB1 and strong bands of expected size from the orange colony. The PCR products from the aerobically grown isolates from water sampled from PRB2 showed bands of correct size and faint bands appeared in the anaerobically grown cultures from PRB2. This suggested that *nosZ* was ubiquitous across the bioremediation site. As discussed in Chapter 2, Section 2.3.3 aerobic denitrifiers belonging to *Pseudomonadota* (formerly *Proteobacteria*) work efficiently with DO concentrations of up to 5 mg L$^{-1}$ (Hayatsu et al*.,* 2008; Ji et al., 2015).

### 3.3.3 Real-time PCR Optimisation

The results of the qPCR primer and thermal cycling condition optimisation for the six genes of interest are outlined below. The associated amplification plots and gel images are displayed in Appendix D.

#### *3.3.3.1 16S rRNA*

A 10-fold serial dilution of the *16S* positive standards (DNA extracted from *E. coli*) was prepared (as described in Section 3.2.6) for *16S* qPCR which was performed using the primers and cycling conditions described in Table 3.2 so that the performance of the qPCR could be validated, and the gene copy number (GCN) could be calculated for the target gene. The GCN was calculated using the equation of the line displayed on the standard curve once the coefficient of the correlation (R$^2$) was >0.99. Figure 3.2 below shows the dilution, GNC, Ct value and melting point (Tm) of the positive standards and the standard curve generated. The 1:1000 dilution of the positive standard was removed to ensure an R$^2$ value of > 0.99. This standard curve was used to calculate the *16S* GCN of the eDNA.



| Dillution | GCN | Ct | Tm |
|---|---|---|---|
| 1 | 4.25E+07 | 7.14 | 80.9 |
| 1 | 4.25E+07 | 7.03 | 80.9 |
| 1:10 | 4.25E+06 | 9.16 | 80.9 |
| 1:10 | 4.25E+06 | 9.04 | 80.9 |
| 1:100 | 4.25E+05 | 13.25 | 80.9 |
| 1:100 | 4.25E+05 | 13.27 | 80.9 |
| 1:10000 | 4.25E+03 | 18.98 | 80.9 |
| 1:10000 | 4.25E+03 | 20.21 | 80.9 |
| 1:100000 | 4.25E+02 | 22.66 | 80.6 |
| 1:100000 | 4.25E+02 | 22.94 | 80.6 |
| NTC | - | 25.69 | 77.4 |
| NTC | - | 27.72 | 75.5 |
| NTC | - | 26.58 | 78.9 |

Chart: y = -3.2316x + 31.263, R² = 0.9933; axes: Ct (y-axis) vs log Gene Copy Number (16S) (x-axis).
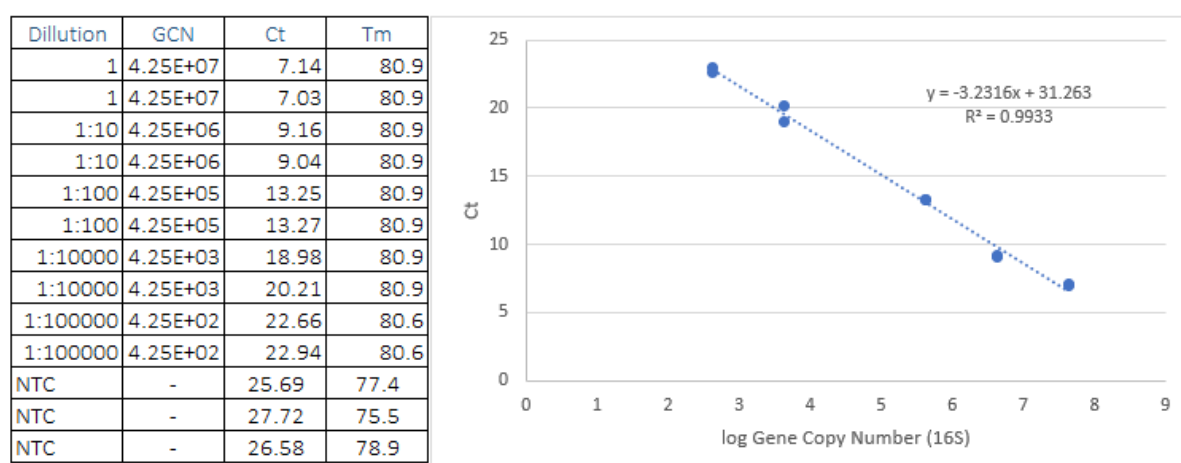
Figure 3. 2: *16S* positive standard qPCR results (Ct and Tm values), the standard curve displaying the line equation, R$^2$ value of >0.99 and gene copy numbers (GCN)

Considering the structural gene *16S rRNA* is present in all bacteria and archaea, it was expected that amplification would occur in all samples. Real-time qPCR was carried out on eDNA collected from the bioremediation site in December 2015 using the primers and cycling conditions described in Table 3.2 in Section 3.2.5. The qPCR products were visualised on an agarose gel, displayed in Figures D.1, Appendix D. Bands of appropriate size (200 bp) appeared in all samples. The melt curve analysis is displayed in Figure D.2, Appendix D. The December 2015 eDNA samples showed an average dissociation of 79°C, while the positive standards (DNA extracted from *Escherichia coli*) displayed an average dissociation at 80°C.

### 3.3.3.2 Bacterial amoA

As outlined in Table 3.2, two qPCR primer sets for bacterial *amoA* qPCR were trialled for use in this study. Rotthauwe et al. (1997) designed primers for use in conventional PCR, but these have also been successfully used for qPCR (Leininger et al., 2006; Kelly et al., 2011). Meinhardt et al. (2015) carried out a study to evaluate qPCR primers being used for ammonia-oxidizers and designed their own primers in an attempt for more inclusive quantification of ammonia oxidising archaea and bacteria. Thermal cycling conditions used initially were as per Leininger et al. (2006) with default dissociation stage added, as described in Table 3.2. Thermal cycling conditions as per Petersen et al. (2012) were also trialled with the addition of the instrument's default dissociation step.

Meinhardt et al. (2011) primers were used at the outset as described in Table 3.2. A trial run was performed using the eDNA samples from July, October and December 2015, the amplification plot can be seen in Figure D.3, Appendix D. The run was unsuccessful, only the standards amplified, crossing the threshold line at cycle number (Ct value) 20. The remaining eDNA crossed the threshold at Ct 33 along with the NTCs (Non-Template Controls). To test for inhibition of the eDNA, the qPCR was re-run and spiked samples were included. The amplification plot is displayed in Figure D.4, Appendix D. Again, only the standards amplified and none of the eDNA or the spiked samples. This could indicate inhibition or concentration issues. To troubleshoot further, another qPCR was performed using 15 µl assays with up to 5 µl DNA template and also spiked DNA samples, Figure D.5, Appendix D. The standards amplified, some of the spiked samples and none of the eDNA samples. This showed that the Meinhardt et al. (2011) primers were not amplifying the eDNA samples, so a qPCR using the Rotthauwe et al. (1997) primers (see Table 3.2) were used for qPCR performed on the July 2015 samples, as conventional PCR had showed that the bacterial *amoA* gene was present in these

samples (amplification plot displayed in Figure D.6, Appendix D). This appeared to be an improvement, so the eDNA qPCR products were visualised on an agarose gel (Figure D.7, Appendix D) to determine whether the 491 bp product was present. There was no amplification of the bacterial *amoA* gene (490 bp). An increased reaction volume (50 µl reaction) qPCR was performed, and the post qPCR products were visualised on an agarose gel, (Figure D.8, Appendix D). Again, there was amplification of the standards but not of the eDNA. Another qPCR with the Rotthauwe et al. (1997) primers using August 2015 DNA samples, spiked August 2015 eDNA, and October 2015 eDNA was carried out. October 2015 samples were selected as they had amplified using conventional PCR and the Rotthauwe et al. (1997) primers. These qPCR products were then visualised on a 1% agarose gel (Figures D.9 and D.10, Appendix D). Amplification occurred in most of the August eDNA samples, spiked and un-spiked. This suggested that bacterial *amoA* gene concentration was the issue, rather than inhibition and that if the bacterial *amoA* gene was present in the DNA it was in low concentration. It was decided to use the Rotthauwe et al. (1997) primers with the Petersen et al. (2012) cycling conditions as described in Table 3.2 for all subsequent runs.

Once the primer set and cycling conditions were determined, a 10-fold serial dilution of the bacterial *amoA* positive standards (plasmid prep of a cloned *amoA* sequence from *Nitrosomonas europea*) was prepared (as described in Section 3.2.6) for bacterial *amoA* qPCR so that a standard curve could be generated to allow for validation of the assay and quantification of the bacterial *amoA* gene in the eDNA samples, Figure 3.3 below.

| Dillution | GCN | Ct | Tm |
|---|---|---|---|
| 1 | 1.08E+11 | 9.3 | 81.3 |
| 1.00 | 1.08E+11 | 8.66 | 81.3 |
| 1:10 | 1.08E+10 | 10.94 | 81.6 |
| 1:10 | 1.08E+10 | 11.61 | 81.6 |
| 1:100 | 1.08E+09 | 16.53 | 81.6 |
| 1:100 | 1.08E+09 | 16.3 | 81.3 |
| 1:1000 | 1.08E+08 | 17.53 | 81.3 |
| 1:1000 | 1.08E+08 | 17.57 | 81.3 |
| 1:10000 | 1.08E+07 | 21.22 | 80.9 |
| 1:10000 | 1.08E+07 | 22 | 80.9 |
| 1:1000000 | 1.08E+05 | 28.26 | 81.6 |
| 1:1000000 | 1.08E+05 | 28 | 81.6 |
| 1:10000000 | 1.08E+04 | 33.43 | 81.6 |
| 1:10000000 | 1.08E+04 | 33.5 | 82 |
| 1:100000000 | 1.08E+03 | 35.71 | 82 |
| 1:100000000 | 1.08E+03 | 35.26 | 81.6 |
| NTC | - | 32.75 | 79.1 |
| NTC | - | UND | 77.6 |
| NTC | - | 38.67 | 87.1 |



Figure 3. 3: Bacterial *amoA* positive standard qPCR results (Ct and Tm values), the standard curve displaying the line equation, $R^2$ value of >0.99 and gene copy numbers (GCN)

This standard curve was used to calculate the Bacterial *amoA* GCN of the eDNA.

### 3.3.3.3 Archaeal *amoA*

Archaeal *amoA* qPCR primers from the Meinhardt et al. (2011) study were used for this work. The thermal profile for was adjusted from the cycling conditions suggested by Meinhardt et al. (2011), (described in Table 3.2) due to differences in thermal cyclers and with the addition of the instrument's default dissociation stage. Figure D.11, Appendix D, shows the amplification plot after performing archaeal *amoA* qPCR on the August 2015 samples and spiked August 2015 samples. The standards and spiked samples amplified while there was poor amplification in the August 2015 samples, with the amplification curves crossing the threshold line along with the NTCs. Considering the spiked samples amplified successfully this would suggest that the archaeal *amoA* gene was not present or at very low concentrations in the environmental DNA samples. A 10-fold serial dilution of the archaeal *amoA* positive standards (plasmid prep of a cloned *amoA* sequence from *Nitrosarchaeum limnia*) was prepared (as described in Section 3.2.6) for archaeal *amoA* qPCR so that a standard curve could be generated to allow for validation of the assay and quantification of the archaeal *amoA* gene in the eDNA samples Figure 3.4 below.

| Dillution | GCN | Ct | Tm |
|---|---|---|---|
| 1 | 1.01E+10 | 12.77 | 76.9 |
| 1 | 1.01E+10 | 12.65 | 76.9 |
| 1:10 | 1.01E+09 | 16.5 | 77.3 |
| 1:10 | 1.01E+09 | 16.72 | 77.3 |
| 1:100 | 1.01E+08 | 21.12 | 77.3 |
| 1:10000 | 1.01E+06 | 27.2 | 77.3 |
| 1:10000 | 1.01E+06 | 26.96 | 77.3 |
| 1:100000 | 1.01E+05 | 29.89 | 77.3 |
| 1:100000 | 1.01E+05 | 30.29 | 76.9 |
| 1:1000000 | 1.01E+04 | 32.34 | 74.2 |
| 1:1000000 | 1.01E+04 | 31.9 | 73.9 |
| NTC | - | 30.3 | 72.9 |
| NTC | - | 31.21 | 72 |
| NTC | - | 40.27 | - |
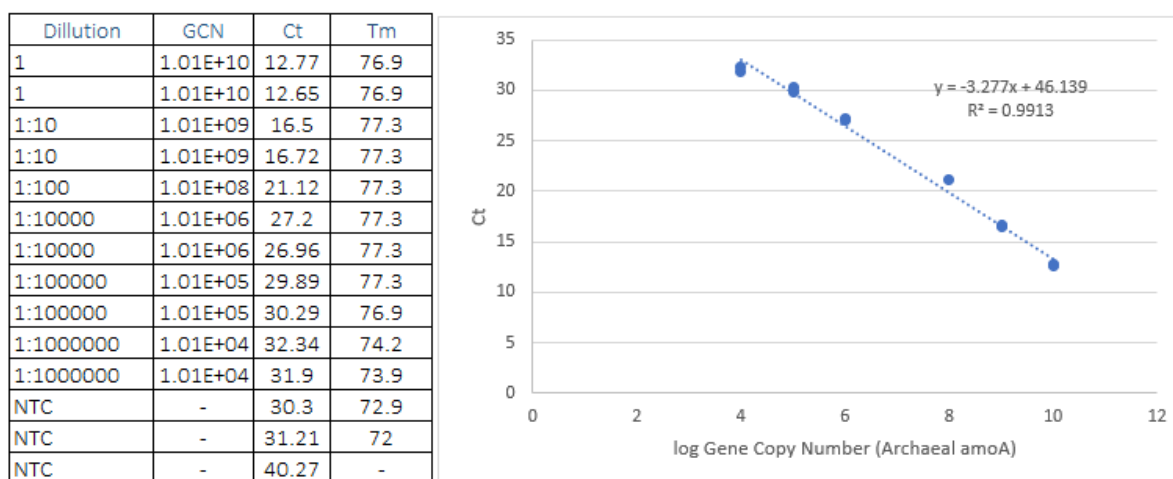


Figure 3. 4: Archaeal *amoA* positive standard qPCR results (Ct and Tm values), the standard curve displaying the line equation, $R^2$ value of >0.99 and gene copy numbers (GCN)

### *3.3.3.4 nirK*

A primer set designed by Henry et al. (2004) was used for real-time *nirK* qPCR (resulting in a 165 bp product). Primer set and thermal cycling conditions are described in Table 3.2. A dilution series of the *nirK* positive standard (described in Section 3.2.3) was prepared for *nirK* qPCR archaeal *amoA* qPCR so that a standard curve could be generated to allow for validation of the assay and quantification of the *nirK* gene in the eDNA samples Figure 3.5 below.

| Dillution | GCN | Ct | Tm |
|---|---|---|---|
| 1 | 1.90E+10 | 13.2 | 87.4 |
| 1 | 1.90E+10 | 13.15 | 87.4 |
| 1 | 1.90E+10 | 13 | 87.7 |
| 01:10 | 1.90E+09 | 16.08 | 87.7 |
| 01:10 | 1.90E+09 | 15.76 | 87.7 |
| 01:100 | 1.90E+08 | 19.38 | 87.4 |
| 01:100 | 1.90E+08 | 19.43 | 87.4 |
| 01:100 | 1.90E+08 | 19.42 | 87.4 |
| 01:200 | 1.04E+08 | 20.69 | 87.7 |
| 01:200 | 1.04E+08 | 20.54 | 87.7 |
| 01:200 | 1.04E+08 | 20.42 | 87.7 |
| 01:500 | 3.80E+07 | 22.29 | 87.7 |
| 01:500 | 3.80E+07 | 22.21 | 87.7 |
| NTC | - | 24.84 | 84.2 |
| NTC | - | 24.77 | 84.2 |
| NTC | - | 25.32 | 83.8 |
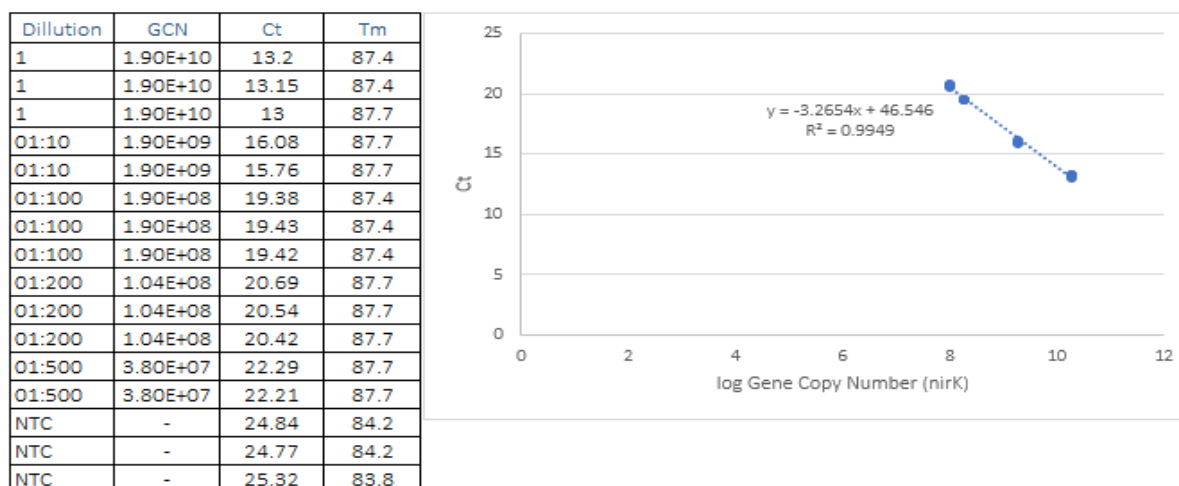


Figure 3. 5: *nirK* positive standard qPCR results (Ct and Tm values), the standard curve displaying the line equation, $R^2$ value of >0.99 and the gene copy numbers (GCN)

The qPCR products were visualised on an agarose gel (Figure D.12, Appendix D). Each of the positive standard dilutions showed PCR product of 165 bp band when visualised on an agarose gel, confirming that the primers were appropriate. To ascertain whether the touchdown cycling conditions were needed or whether the instrument's default cycling conditions were sufficient, a *nirK* qPCR was carried out using both sets of cycling conditions. The qPCR products

from both were visualised on an agarose gel (Figure D.13, Appendix D). The appropriate 165 bp amplicon was visualised after the touchdown cycling conditions and the instrument's default cycling conditions. It was noted that the NTC of the touchdown showed signs of contamination. It was determined that the Henry et al (2004) primer set, and instrument's default cycling conditions would be appropriate for *nirK* real-time PCR for the remainder of the experiment.

### 3.3.3.5 nirS

A primer set designed by Throback et al. (2004) for *nirS* real-time PCR was used initially. The eDNA did not amplify and had Ct values similar to that of the NTCs. Since *nirS* primers were designed for conventional PCR and worked well, it was decided to design primers for real-time PCR also. The forward primer from the set designed for conventional PCR nirS-8F was used and a new reverse primer, nirS-4R was designed (using the same method as described in Section 3.3.2.5) to result in an 80 bp product. Based on the thermal cycling conditions used for the conventional PCR, a thermal cycling profile was devised (described in Table 3.2) and concluded with a dissociation stage. A *nirS* qPCR was carried out on four plasmid extractions that were prepared as a positive standard (a plasmid prep of a cloned *amoA* sequence from *Acidovorax carolinensis* described in Section 3.2.3) and the qPCR products were visualised on an agarose gel, shown in Figure D.14, Appendix D. The correct band size (80 bp) was present with little nonspecific amplification. A standard curve was be generated to allow for further validation of the assay and quantification of the *nirS* gene in the eDNA samples Figure 3.6 below.

| Dillution | GCN | Ct | Tm |
|-----------|----------|-------|------|
| 1:100 | 4.37E+07 | 11.64 | 80 |
| 1:100 | 4.37E+07 | 11.34 | 80.3 |
| 1:10000 | 4.37E+06 | 15.35 | 80.3 |
| 1:10000 | 4.37E+06 | 15.03 | 80.3 |
| 1:55000 | 8.75E+05 | 17.89 | 80.3 |
| 1:55000 | 8.75E+05 | 17.61 | 80.3 |
| 1:100000 | 4.37E+05 | 18.97 | 80.6 |
| 1:100000 | 4.37E+05 | 18.45 | 80.3 |
| 1:550000 | 8.75E+04 | 20.81 | 80.3 |
| 1:550000 | 8.75E+04 | 20.75 | 80.3 |
| 1:1000000 | 4.37E+04 | 22.21 | 80 |
| 1:1000000 | 4.37E+04 | 22.59 | 79.6 |
| 1:5500000 | 4.37E+03 | 25.04 | 80 |
| 1:5500000 | 4.37E+03 | 25.26 | 80.3 |
| NTC | - | 30.56 | 75.1 |
| NTC | - | 30.89 | 74.8 |
| NTC | - | 30.46 | 74.8 |



Scatter plot: Ct versus log Gene Copy Number (nirS), with line equation $y = -3.433x + 37.951$ and $R^2 = 0.9954$.

Figure 3. 6: *nirS* positive standard qPCR results (Ct and Tm values), the standard curve displaying the line equation, $R^2$ value of >0.99 and the gene copy numbers (GCN)

### 3.3.3.6 nosZ

Real-time Primers for *nosZ* qPCR were designed by Henry et al. (2006) within the region amplified by Kloos et al. (2001). The thermal cycling conditions used by Henry et al. (2006) were not compatible with Applied Biosystems 7300, so a standard thermal profile was used as described in Table 3.2.

A 10-fold serial dilution of the *nosZ* positive standards (plasmid prep of a cloned *amoA* sequence from *Pseudomonas denitrificans*) was prepared (as described in Section 3.2.6) for *nosZ* qPCR. This generated a standard curve, displayed in Figure 3.7 below that validated the assay and allowed *nosZ* GCN in the eDNA samples to be calculated.

| Dillution | GCN | Ct | Tm |
|---|---|---|---|
| 1:10000 | 1.15E+06 | 18.61 | 82.9 |
| 1:10000 | 1.15E+06 | 18.67 | 82.6 |
| 1:55000 | 2.30E+05 | 21.05 | 82.6 |
| 1:55000 | 2.30E+05 | 20.9 | 82.6 |
| 1:100000 | 1.15E+05 | 22.26 | 82.6 |
| 1:100000 | 1.15E+05 | 22.03 | 82.2 |
| 1:1000000 | 1.15E+04 | 26.67 | 82.2 |
| 1:1000000 | 1.15E+04 | 26.11 | 82.6 |
| 1:10000000 | 1.15E+03 | 29.07 | 82.6 |
| 1:10000000 | 1.15E+03 | 29.69 | 82.9 |
| NTC | - | 30.65 | 81.4 |
| NTC | - | 37.12 | 81.4 |
| NTC | - | 35.49 | 81.9 |
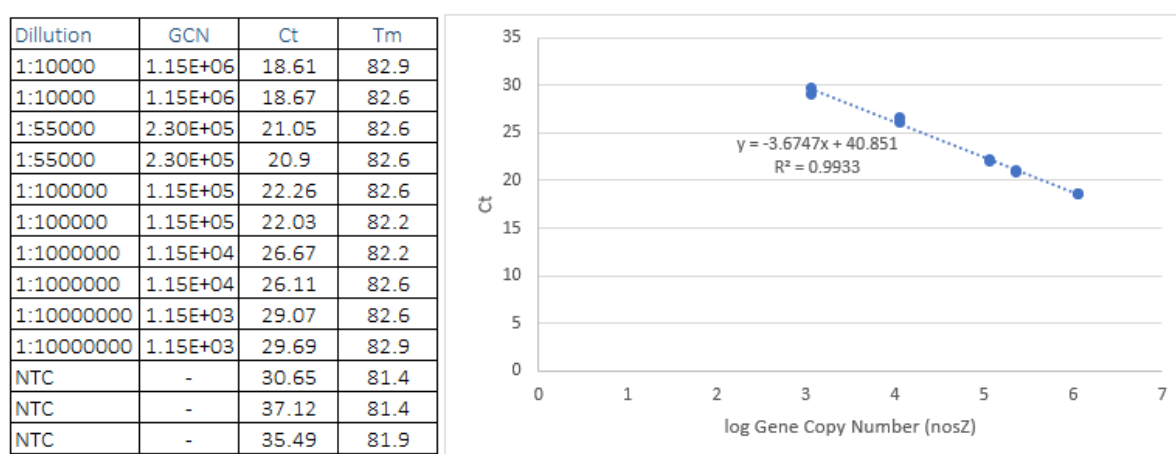
Figure 3. 7: *nosZ* positive standard qPCR results (Ct and Tm values), the standard curve displaying the line equation, $R^2$ value of >0.99 and the calculated gene copy numbers (GCN)

### 3.3.4 Functional Gene Abundance

The initial aspiration of the experiment was to quantify the gene copy numbers using qPCR so that their fluctuations in abundance over time could be compared with the chemical results. Gene copy number was calculated for each gene using the line equation on the standard curves generated for each gene. The qPCR results containing the Ct values, Tm values and GCN for the eDNA are presented in Appendix E. However, after troubleshooting, it became clear that the eDNA contained very low concentrations of some of the functional genes and that comparisons between genes could not be relied upon. Therefore, it was decided that presence/ absence would be used *in lieu* of quantification. Presence was determined when there was a dissociation curve in the melt curve analysis of the eDNA that matched that of the standards and the Ct values were greater than those of the non-template controls for any of the replicates i.e., if a gene was deemed present in any one of the replicates (e.g., S1.1), it was deemed present in that sample (e.g., S1).  Further validation was provided by visualising the

post qPCR products on agarose gels and inspecting them for the appropriate bands. The tables presented in Appendix E are highlighted green when a corresponding qPCR product has been visualised on an agarose gel. For example, Figure 3.8 below shows post bacterial *amoA* qPCR products visualised on an agarose gel.
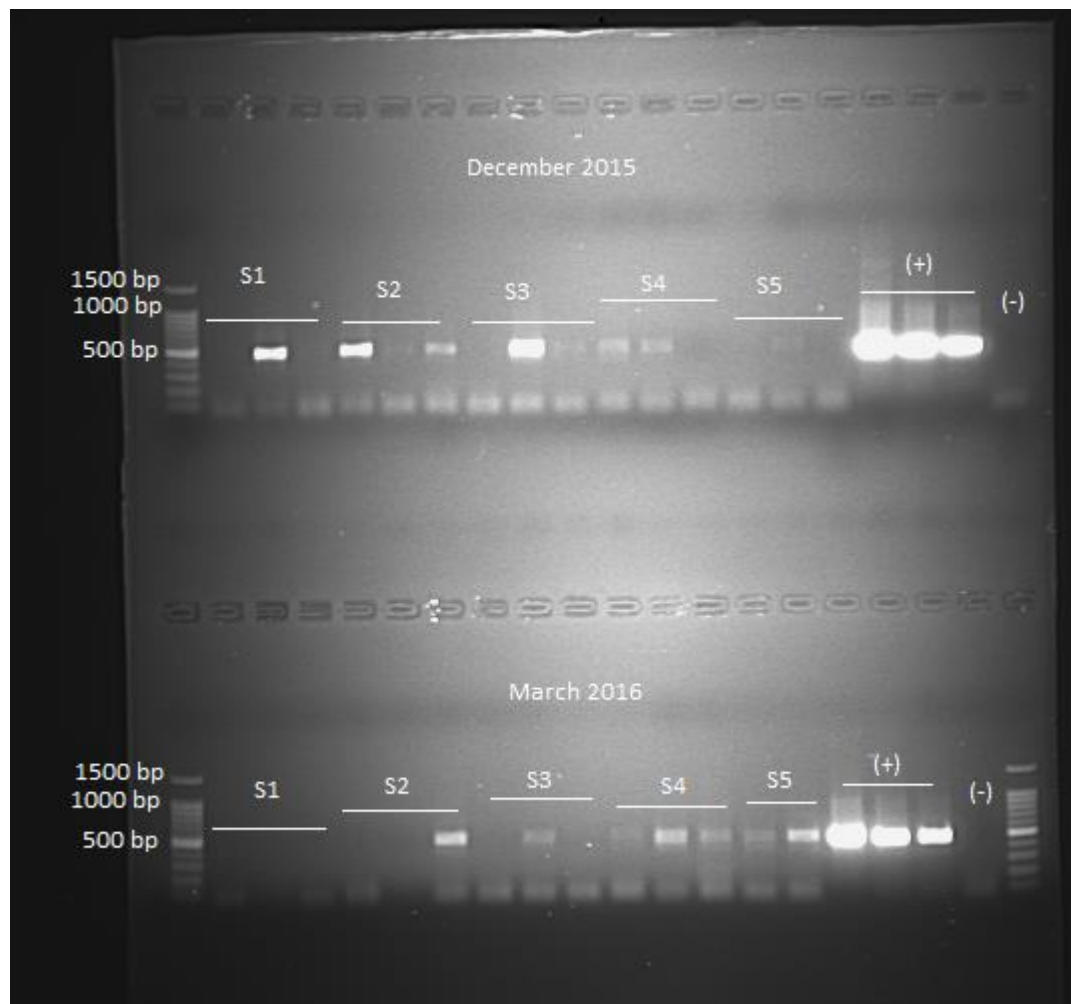


Figure 3. 8: Post bacterial *amoA* qPCR products (790 bp) of December 2015 and March 2016 samples S1-S5 and visualised on an agarose gel (+) Positive control was a plasmid prep of a cloned *amoA* sequence from *Nitrosomonas europea*

Below, Table 3.4 shows the presence or absence of the five-nitrogen cycling functional genes in groundwater collected from the five sampling wells at the bioremediation site at three monthly intervals over two years (i.e., 40 sampling points per functional gene). The structural gene *16S rRNA* was present in all wells at all sampling times as expected.

Table 3. 4: Presence/ absence of the five nitrogen cycling functional genes assessed in the bioremediation sampling wells over two-year experiment

| | Bacterial *amoA* | | | | | Archaeal *amoA* | | | | | *nirS* | | | | | *nirK* | | | | | *nosZ* | | | | |
|---|---|---|---|---|---|---|---|---|---|---|---|---|---|---|---|---|---|---|---|---|---|---|---|---|---|
| | S1 | PRB1 | S3 | PRB2 | S5 | S1 | PRB1 | S3 | PRB2 | S5 | S1 | PRB1 | S3 | PRB2 | S5 | S1 | PRB1 | S3 | PRB2 | S5 | S1 | PRB1 | S3 | PRB2 | S5 |
| June 2015 | Absent | Absent | Present | Present | Present | Absent | Absent | Absent | Absent | Absent | Present | Present | Present | Present | Present | Present | Present | Present | Present | Present | Present | Present | Present | Present | Present |
| Sept 2015 | Present | Present | Present | Present | Present | Absent | Present | Present | Present | Present | Present | Present | Present | Present | Present | Present | Present | Present | Present | Present | Present | Present | Present | Present | Present |
| Dec 2015 | Present | Present | Present | Absent | Absent | Present | Present | Absent | Present | Present | Present | Present | Absent | Present | Present | Present | Present | Present | Present | Present | Present | Present | Present | Present | Present |
| Mar 2016 | Absent | Present | Present | Absent | Absent | Absent | Absent | Absent | Absent | Present | Present | Present | Present | Present | Present | Present | Present | Present | Present | Present | Present | Present | Present | Present | Present |
| Jun 2016 | Absent | Absent | Absent | Absent | Absent | Absent | Absent | Absent | Absent | Present | Present | Present | Present | Present | Present | Present | Present | Present | Present | Present | Absent | Present | Present | Present | Present |
| Sept 2016 | Absent | Absent | Absent | Absent | Absent | Absent | Absent | Absent | Absent | Absent | Present | Present | Present | Present | Present | Present | Present | Present | Present | Present | Present | Present | Present | Present | Absent |
| Dec 2016 | Present | Present | Absent | Present | Absent | Absent | Absent | Absent | Absent | Absent | Present | Present | Present | Present | Present | Present | Present | Present | Present | Present | Present | Present | Present | Present | Present |
| Mar 2017 | Present | Present | Absent | Absent | Absent | Absent | Absent | Present | Absent | Absent | Present | Present | Present | Present | Present | Present | Present | Present | Present | Present | Present | Present | Present | Present | Present |

Present    Absent

Bacterial *amoA* was confirmed present in just over half of the sampling points (i.e., 21 of 40). The gene was found in eDNA from water samples taken from all wells in the bioremediation site, suggesting that the PRBs had little influence on their abundance. Bacterial *amoA* was not found during the June and September 2016 sampling events, confirmed by repeated qPCR runs, though the gene was present in the following two sampling events, December 2016, and March 2017. This does not concur with the hypothesis that nitrification could be occurring in PRB1 after month 10 as was the interpretation of the increasing $NO_3$ concentrations and concurrent decrease in $NH_4$-N in PRB1 as discussed in Section 2.3.8.

Archaeal *amoA* was absent from upstream well S1 throughout all sampling events and was not detected in the initial month, June 2015. The gene was detected in PRB1 and all downstream wells in water collected during the following sampling month, September 2015, and was only intermittently detected thereafter. This was to be expected considering that archaea comprise less than 10% of total soil prokaryotes (Timonen & Bomberg, 2009).

The results showed that denitrifying microbes appeared to be more prevalent than nitrifying ones. Of the denitrifying genes, *nirK* was ubiquitous across the bioremediation site at all sampling times and *nirS* occurred in 39 of the sampling events, while *nosZ* was found in 38 of the 40 sampling events. While there was little difference in the abundance of the denitrifying functional genes, it was the opposite to what Petersen et al. (2012) found, with *nirK* being the most abundant and *nosZ* the least abundant of the three genes. As discussed in Section 3.3.2.6, denitrifying aerobes can work efficiently with DO concentrations of up to 5 mg $L^{-1}$. The standard for *nirS* amplified and sequenced from DNA extracted from the water samples collected from the bioremediation site was identified as *Acidovorax carolinensis* and described as an aerobe. The culturing results showed that the *nosZ* functional gene was present in cultures grown aerobically from PRB1.

### 3.3.5 Functional Genes and Field Parameters

To determine whether the field parameters influenced bacterial and archaeal *amoA* functional gene abundance (i.e., if they might be related to bacterial and/or archaeal *amoA* presence or absence), these results were compared with the field parameters that were measured at each sampling point, i.e., pH, DO, temperature, and electrical conductivity. Table 3.5 below shows the pH of the groundwater sample collected and whether the bacterial and/ or archaeal *amoA* functional gene was detected in its eDNA.

Table 3. 5: Presence (highlighted blue)/ absence (highlighted grey) of bacterial and archaeal *amoA* functional genes and associated pH results

| pH | Bacterial *amoA* | | | | | Archaeal *amoA* | | | | |
|---|---|---|---|---|---|---|---|---|---|---|
| | S1 | PRB1 | S3 | PRB2 | S5 | S1 | PRB1 | S3 | PRB2 | S5 |
| June 2015 | 6.6 | 6.6 | 6.6 | 6.6 | 6.5 | 6.6 | 6.6 | 6.6 | 6.6 | 6.5 |
| Sept 2015 | 6.7 | 6.7 | 6.7 | 6.6 | 6.4 | 6.7 | 6.7 | 6.7 | 6.6 | 6.4 |
| Dec 2015 | 6.5 | 6.9 | 7.1 | 7 | 6.9 | 6.5 | 6.9 | 7.1 | 7 | 6.9 |
| Mar 2016 | 7 | 7.1 | 7.1 | 7.1 | 7 | 7 | 7.1 | 7.1 | 7.1 | 7 |
| Jun 2016 | 7.1 | 7.3 | 7.3 | 7.3 | 7.2 | 7.1 | 7.3 | 7.3 | 7.3 | 7.2 |
| Sept 2016 | 6.9 | 7 | 7 | 6.9 | 7.1 | 6.9 | 7 | 7 | 6.9 | 7.1 |
| Dec 2016 | 7.5 | 7.5 | 8.1 | 8.3 | 8.4 | 7.5 | 7.5 | 8.1 | 8.3 | 8.4 |
| Mar 2017 | 7.5 | 7.8 | 6.9 | 6.9 | 6.9 | 7.5 | 7.78 | 6.9 | 6.9 | 6.9 |

As can be seen from Table 3.5, pH does not affect the presence or absence of the bacterial or archaeal *amoA* functional genes. Bacterial *amoA* was detected in samples that had a pH range of 6.5 – 7.5 and was absent from samples with a pH range of 6.4 – 8.4. Archaeal *amoA* was detected in samples with a pH range from 6.4 – 7.2 and absent from samples with a pH range of 6.5 – 8.4. This corroborated the findings of the study conducted by Nicol et al. (2009) which showed a negative correlation between AOA and pH and saw a significant decrease in AOA gene copy numbers once pH reached 7.3. Table 3.6 below shows the archaeal and bacterial amoA results along with DO concentrations (mg L$^{-1}$).

Table 3. 6: Presence (highlighted blue)/ absence (highlighted grey) of bacterial and archaeal *amoA* functional genes and associated DO (DO) concentrations (mg L$^{-1}$)

| DO | Bacterial *amoA* | | | | | Archaeal *amoA* | | | | |
|---|---|---|---|---|---|---|---|---|---|---|
| | S1 | PRB1 | S3 | PRB2 | S5 | S1 | PRB1 | S3 | PRB2 | S5 |
| June 2015 | 2.5 | 1.9 | 1.7 | 1.6 | 1.2 | 2.5 | 1.9 | 1.7 | 1.6 | 1.2 |
| Sept 2015 | 4.5 | 3.2 | 6.0 | 2.7 | 1.9 | 4.5 | 3.2 | 6.0 | 2.7 | |
| Dec 2015 | 4.9 | 5 | 4.2 | 4.1 | 3.6 | 4.9 | 5 | 4.2 | 4.1 | 3.6 |
| Mar 2016 | 3.9 | 3.4 | 4.3 | 2.9 | 1.9 | 3.9 | 3.4 | 4.3 | 2.9 | 1.9 |
| Jun 2016 | 2.8 | 2.3 | 2.5 | 2.3 | 2.5 | 2.8 | 2.3 | 2.5 | 2.3 | 2.5 |
| Sept 2016 | 0.6 | 1.8 | 2 | 1.6 | 2.5 | 0.6 | 1.8 | 2 | 1.6 | 2.5 |
| Dec 2016 | 3.6 | 2.5 | 1.5 | 1.5 | 1.6 | 3.6 | 2.5 | 1.5 | 1.5 | 1.6 |
| Mar 2017 | 0.2 | 0.6 | 0.5 | 1 | 2.1 | 0.2 | 0.6 | 0.5 | 1 | 2.1 |

DO range did not affect the presence or absence of the bacterial or archaeal *amoA* functional genes. Bacterial *amoA* was detected in samples that had a DO concentration of 0.6 – 5.96 (mg L$^{-1}$) and was absent from samples with a DO range of 1.5 – 4.9 (mg L$^{-1}$). Archaeal *amoA* was detected in samples with a D.O range of 1.2 – 3.6 (mg L$^{-1}$) and absent from samples with a D.O range of 0.6 – 5.96 (mg L$^{-1}$). This shows that DO was not an inhibiting factor on the presence of

ammonia oxidising bacteria or archaea, though Wiszniowski et al. (2006) recommended a minimum DO concentration of 1.0 mg L$^{-1}$. Table 3.7 below shows the archaeal and bacterial *amoA* results along with associated temperature recordings.

Table 3. 7: Presence (highlighted blue)/ absence (highlighted grey) of bacterial and archaeal *amoA* functional genes and associated temperature recordings (°C).

| | Bacterial *amoA* | | | | | Archaeal *amoA* | | | | |
|---|---|---|---|---|---|---|---|---|---|---|
| | S1 | PRB1 | S3 | PRB2 | S5 | S1 | PRB1 | S3 | PRB2 | S5 |
| June 2015 | 14.7 | 15.8 | 15.2 | 15.3 | 13 | 14.7 | 15.8 | 15.2 | 15.3 | 13 |
| Sept 2015 | 15.4 | 15.4 | 15.3 | 16.6 | 15.5 | 15.4 | 15.4 | 15.3 | 16.6 | 15.5 |
| Dec 2015 | 12.6 | 13.2 | 12 | 11.7 | 12.2 | 12.6 | 13.2 | 12 | 11.7 | 12.2 |
| Mar 2016 | 12 | 12.1 | 12 | 8 | 8.7 | 12 | 12.1 | 12 | 8 | 8.7 |
| Jun 2016 | 16.6 | 14.6 | 14.6 | 14.2 | 14 | 16.6 | 14.6 | 14.6 | 14.2 | 14 |
| Sept 2016 | 13.7 | 13.4 | 13.1 | 13.3 | 12.2 | 13.7 | 13.4 | 13.1 | 13.3 | 12.2 |
| Dec 2016 | 11.5 | 10.7 | 12.6 | 12.3 | 11.4 | 11.5 | 10.7 | 12.6 | 12.3 | 11.4 |
| Mar 2017 | 12.1 | 12.1 | 12.2 | 11.6 | 11.8 | 12.1 | 12.1 | 12.2 | 11.6 | 11.8 |

Temperature did not affect the presence or absence of the bacterial or archaeal *amoA* functional genes. Bacterial *amoA* was detected in samples that had a temperature range of 10.7 – 16.6°C and was absent from samples with a temperature ranging between 8 and 16.6°C. Archaeal *amoA* was detected and absent in samples with a temperature range of 8 to 16.6°C. C (within the range of 5 – 40°C prescribed by Wiszniowski et al, 2006) and was absent from samples with a temperature ranging between 8 and 16.6°C, showing that temperature was not an inhibiting factor. Archaeal *amoA* was both detected and absent in samples with a temperature range of 8 to 16.6°C. Ouyang et al. (2017) showed that temperature influenced AOBs and not AOAs but also showed optimum temperature for AOBs as 31°C and 41°C for AOAs, temperatures that were never reached during this study. Table 3.8 below shows the archaeal and bacterial amoA results along with associated electrical conductivity results.

Table 3. 8: Presence (highlighted blue)/ absence (highlighted grey) of bacterial and archaeal *amoA* functional genes and electrical conductivity results (μS/cm)

| | Bacterial *amoA* | | | | | Archaeal *amoA* | | | | |
|---|---|---|---|---|---|---|---|---|---|---|
| | S1 | PRB1 | S3 | PRB2 | S5 | S1 | PRB1 | S3 | PRB2 | S5 |
| June 2015 | 1797 | 1524 | 1470 | 1498 | 986 | 1797 | 1524 | 1470 | 1498 | 986 |
| Sept 2015 | 1680 | 1590 | 1466 | 1388 | 908 | 1680 | 1590 | 1466 | 1388 | 908 |
| Dec 2015 | 1235 | 1285 | 1472 | 958 | 846 | 1235 | 1285 | 1472 | 958 | 846 |
| Mar 2016 | 1326 | 1141 | 895 | 1100 | 642 | 1326 | 1141 | 895 | 1100 | 642 |
| Jun 2016 | 1899 | 1555 | 1187 | 1470 | 1023 | 1899 | 1555 | 1187 | 1470 | 1023 |
| Sept 2016 | 1359 | 1444 | 1217 | 1213 | 867 | 1359 | 1444 | 1217 | 1213 | 867 |
| Dec 2016 | 1695 | 1970 | 2110 | 2170 | 1148 | 1695 | 1970 | 2110 | 2170 | 1148 |
| Mar 2017 | 1408 | 1838 | 1716 | 1661 | 1275 | 1408 | 1838 | 1716 | 1661 | 1275 |

Electrical conductivity did not affect the presence or absence of the bacterial or archaeal *amoA* functional genes. Bacterial *amoA* was detected in samples that had an electrical conductivity range of 846 - 1970 (µS/cm) and was absent from samples with an electrical conductivity range of 642 and 2170 (µS/cm). Archaeal *amoA* was detected in samples with an electrical conductivity range of 642 - 2110 (µS/cm) and absent from samples with an electrical conductivity range of 867 - 2170 (µS/cm).

### 3.3.6 Functional Genes and Chemical Results

To determine whether the chemical parameters monitored influenced the abundance of bacterial and archaeal *amoA* functional genes, these results were compared, i.e., $NH_4$-N, $NO_2$, $NO_3$ and TOC. Table 3.9 below shows the archaeal and bacterial *amoA* results along with associated $NH_4$-N (mg $L^{-1}$) results.

Table 3. 9: Presence (highlighted blue)/ absence (highlighted grey) of bacterial and archaeal *amoA* functional genes and associated $NH_4$-N concentrations (mg $L^{-1}$)

| | Bacterial *amoA* | | | | | Archaeal *amoA* | | | | |
|---|---|---|---|---|---|---|---|---|---|---|
| | S1 | PRB1 | S3 | PRB2 | S5 | S1 | PRB1 | S3 | PRB2 | S5 |
| June 2015 | 119 | 94.11 | 89.5 | 82.26 | 14.4 | 119 | 94.11 | 89.5 | 82.26 | 14.4 |
| Sept 2015 | 129 | 112.9 | 82.7 | 88.8 | 10.2 | 129 | 112.9 | 82.7 | 88.8 | 10.2 |
| Dec 2015 | 45.1 | 33.13 | 16.1 | 15.2 | 4.22 | 45.1 | 33.13 | 16.1 | 15.2 | 4.22 |
| Mar 2016 | 96.3 | 124.1 | 41 | 54.11 | 3.23 | 96.3 | 124.1 | 41 | 54.11 | 3.23 |
| Jun 2016 | 192 | 153.3 | 91 | 141 | 7.28 | 192 | 153.3 | 91 | 141 | 7.28 |
| Sept 2016 | 89.5 | 113.6 | 78.7 | 87.22 | 8.09 | 89.5 | 113.6 | 78.7 | 87.22 | 8.09 |
| Dec 2016 | 72.1 | 68.44 | 72.2 | 86.66 | 9.72 | 72.1 | 68.44 | 72.2 | 86.66 | 9.72 |
| Mar 2017 | 44.7 | 54.49 | 34.4 | 43.44 | 4.94 | 44.7 | 54.49 | 34.4 | 43.44 | 4.94 |

$NH_4$-N concentration did not appear to influence the presence or absence of the bacterial or archaeal *amoA* functional genes. Bacterial *amoA* was detected in samples with $NH_4$-N concentrations of 3.23 - 129 mg $L^{-1}$ and was absent from samples with $NH_4$-N concentrations ranging between 4.22 and 192 mg $L^{-1}$. Archaeal *amoA* was detected in samples with $NH_4$-N concentrations ranging between 3.23 and 113 mg $L^{-1}$ and absent from samples with a $NH_4$-N range of 4.94 and 192 mg $L^{-1}$. This indicated that $NH_4$-N concentrations did not appear to affect AOAs as suggested by Limpiyakorn et al. (2010) and corroborated the findings by Stopnieisek et al. (2010) who found that AOA were unaffected by the presence of ammonium. The absence of the archaeal *amoA* functional gene may be due to the presence of organic compounds which results in the inhibition of AOAs as per Gwak et al. (2020). Table 3.10 below shows the archaeal and bacterial amoA results along with associated $NO_2$ (mg $L^{-1}$) results.

Table 3. 10: Presence (highlighted blue)/ absence (highlighted grey) of bacterial and archaeal *amoA* functional genes and associated $NO_2$ concentrations (mg $L^{-1}$)

| | Bacterial *amoA* | | | | | Archaeal *amoA* | | | | |
|---|---|---|---|---|---|---|---|---|---|---|
| | S1 | PRB1 | S3 | PRB2 | S5 | S1 | PRB1 | S3 | PRB2 | S5 |
| June 2015 | 0.24 | 0.02 | 0.05 | 0.04 | 0.02 | 0.24 | 0.02 | 0.05 | 0.04 | 0.02 |
| Sept 2015 | 1.83 | 0.02 | 0.02 | 0.02 | 0.02 | 1.83 | 0.02 | 0.02 | 0.02 | 0.02 |
| Dec 2015 | 0.02 | 0.02 | 0.02 | 0.02 | 0.02 | 0.02 | 0.02 | 0.02 | 0.02 | 0.02 |
| Mar 2016 | 0.02 | 0.02 | 0.4 | 0.02 | 0.02 | 0.02 | 0.02 | 0.4 | 0.02 | 0.02 |
| Jun 2016 | 0.02 | 0.02 | 0.18 | 0.02 | 0.02 | 0.02 | 0.02 | 0.18 | 0.02 | 0.02 |
| Sept 2016 | 0.02 | 0.02 | 0.17 | 0.02 | 0.02 | 0.02 | 0.02 | 0.17 | 0.02 | 0.02 |
| Dec 2016 | 0.02 | 0.02 | 0.37 | 0.02 | 0.02 | 0.02 | 0.02 | 0.37 | 0.02 | 0.02 |
| Mar 2017 | 0.1 | 0.02 | 0.02 | 0.02 | 0.02 | 0.1 | 0.02 | 0.02 | 0.02 | 0.02 |

$NO_2$ concentrations were mostly conserved below the method detection limit and do not appear to have affected the presence or absence of the bacterial or archaeal *amoA* functional genes. Bacterial *amoA* was detected in samples that had $NO_2$ concentrations of $0.02 - 1.83$ mg $L^{-1}$ and was absent from samples with $NO_2$ concentrations ranging between 0.02 and 0.37 mg $L^{-1}$. Archaeal *amoA* was detected only in samples with $NO_2$ concentrations less than the MDL of 0.02 mg $L^{-1}$ and absent from samples with a $NO_2$ range of 0.02 and 1.83 mg $L^{-1}$. Table 3.11 below shows the archaeal and bacterial *amoA* results along with associated $NO_3$ (mg $L^{-1}$) results.

Table 3. 11: Presence (highlighted blue)/ absence (highlighted grey) of bacterial and archaeal *amoA* functional genes and associated $NO_3$ concentrations (mg $L^{-1}$)

| | Bacterial *amoA* | | | | | Archaeal *amoA* | | | | |
|---|---|---|---|---|---|---|---|---|---|---|
| | S1 | PRB1 | S3 | PRB2 | S5 | S1 | PRB1 | S3 | PRB2 | S5 |
| June 2015 | 0.2 | 0.2 | 0.2 | 0.2 | 0.2 | 0.2 | 0.2 | 0.2 | 0.2 | 0.2 |
| Sept 2015 | 19.8 | 0.2 | 0.3 | 0.2 | 1.2 | 19.8 | 0.2 | 0.3 | 0.2 | 1.2 |
| Dec 2015 | 0.2 | 0.2 | 0.2 | 0.2 | 0.2 | 0.2 | 0.2 | 0.2 | 0.2 | 0.2 |
| Mar 2016 | 0.5 | 0.6 | 1.2 | 0.5 | 0.5 | 0.5 | 0.6 | 1.2 | 0.5 | 0.5 |
| Jun 2016 | 0.2 | 0.2 | 1.9 | 0.2 | 0.2 | 0.2 | 0.2 | 1.9 | 0.2 | 0.2 |
| Sept 2016 | 0.2 | 0.2 | 0.7 | 0.2 | 0.2 | 0.2 | 0.2 | 0.7 | 0.2 | 0.2 |
| Dec 2016 | 0.2 | 0.2 | 3.9 | 0.2 | 0.2 | 0.2 | 0.2 | 3.9 | 0.2 | 0.2 |
| Mar 2017 | 1 | 0.2 | 0.2 | 0.2 | 0.2 | 1 | 0.2 | 0.2 | 0.2 | 0.2 |

Concentrations of $NO_3$ were also mostly below the MDL and remained low, except for a spike in upstream well S1 in September 2015 where $NO_3$ concentrations reached 19.8 mg $L^{-1}$. Bacterial *amoA* was detected in samples that had $NO_3$ concentrations of $0.2 - 19.8$ mg $L^{-1}$ and was absent from samples with $NO_3$ concentrations ranging between 0.2 and 3.9 mg $L^{-1}$. Archaeal *amoA* was detected in samples with $NO_3$ concentrations of up to 1.2 mg $L^{-1}$. Table 3.12 below shows the archaeal and bacterial amoA results along with associated TOC (mg $L^{-1}$) results.

Table 3. 12: Presence (highlighted blue)/ absence (highlighted grey) of bacterial and archaeal *amoA* functional genes and associated TOC concentrations (mg L$^{-1}$)

| | Bacterial *amoA* | | | | | Archaeal *amoA* | | | | |
|---|---|---|---|---|---|---|---|---|---|---|
| | S1 | PRB1 | S3 | PRB2 | S5 | S1 | PRB1 | S3 | PRB2 | S5 |
| June 2015 | 37 | 28 | 22 | 35 | 42 | 37 | 28 | 22 | 35 | 42 |
| Sept 2015 | 32 | 20 | 18 | 46 | 19 | 32 | 20 | 18 | 46 | 19 |
| Dec 2015 | 5 | 7 | 3 | 2 | 2 | 5 | 7 | 3 | 2 | 2 |
| Mar 2016 | 2 | 2 | 4 | 6 | 10 | 2 | 2 | 4 | 6 | 10 |
| Jun 2016 | 20 | 2 | 2 | 2 | 5 | 20 | 2 | 2 | 2 | 5 |
| Sept 2016 | 15 | 34 | 23 | 2 | 9 | 15 | 34 | 23 | 2 | 9 |
| Dec 2016 | 21 | 14 | 6 | 25 | 10 | 21 | 14 | 6 | 25 | 10 |
| Mar 2017 | 15 | 21 | 30 | 18 | 10 | 15 | 21 | 30 | 18 | 10 |

It appeared that total organic carbon concentrations did not affect the presence or absence of the bacterial or archaeal *amoA* functional genes. Bacterial *amoA* was detected in samples that had TOC concentrations of 2 - 46 mg L$^{-1}$ and was absent from samples with TOC concentrations ranging between 2 and 37 mg L$^{-1}$. Archaeal *amoA* was detected in samples with TOC concentrations ranging between 2 and 46 mg L$^{-1}$ and absent from samples with a NH$_4$-N range of 2 and 42 mg L$^{-1}$.

The least abundant gene found was archaeal *amoA*, detected in nine of the 40 sampling wells. As discussed in Section 3.1.1, archaeal ammonia oxidisers are often undetected in environments where there are high ammonia concentrations, though as seen in Table 3.6, the archaeal *amoA* functional gene was detected in a water sample that contained NH$_4$-N concentrations of 113 mg L$^{-1}$. Archaea are less abundant than bacteria in the environment though bacterial *amoA* was only detected in just over half of the sampling events when it would be expected that they be more prevalent. As discussed above, there was no obvious field or chemical parameter in the bioremediation site that seemed to influence the presence or absence of either archaeal or bacterial *amoA*.

Unlike nitrification there was no chemical parameter measured on the bioremediation site that could provide an insight into denitrification and thereby only the functional genes can be used as a measure of denitrification success. *nirS*, *nirK* and *nosZ* functional genes occurred in all wells. It makes sense that *nirK* and *nirS* would share a similar abundance to *nosZ* because as previously described in Section 3.1.2, the *nosZ* functional gene occurs in species that also possess the *nirK* or *nirS* functional genes.

As mentioned in Section 3.1, care must be taken when ascribing function to the detection of functional genes. It must also be considered that all primers, particularly those used for archaeal and bacterial *amoA* (despite trouble shooting) were not equally efficient in amplifying functional genes, especially in eDNA extracted from heavily contaminated groundwater. Due to the finite nature of eDNA extracted from each sampling point in time, trialling and trouble shooting was restricted.

## 3.4 Conclusion

Functional gene analysis was used to gain a further insight into the efficacy of the PRBs at bioremediating ammonia from shallow groundwater. Structural gene *16S rRNA* gene and five nitrogen cycling functional genes were monitored over the 24-month study from each of the five monitoring wells. New primer sets were designed to amplify the *nirS* functional gene for conventional and qPCR and worked well. The new primer set nirS32F/ nirS64R was used to create a positive standard from eDNA extracted from the bioremediation site and the resulting sequence revealed the gene to belong to *Acidovorax carolinensis*, a bacterium isolated from a contaminated site in North Carolina and first described and named in 2018.

Bacterial *amoA* was shown to be present in the cultures that were grown aerobically on nutrient agar that was inoculated by water collected from PRB1 and was not detected in the cultures grown anaerobically from PRB2. *NirK* was (potentially) amplified from the anaerobically grown cultures that were inoculated from PRB2. The *nosZ* gene was amplified from the cultures grown aerobically from PRB1 and from the cultures grown anaerobically from PRB2 indicating that denitrifiers capable of anaerobic and anaerobic growth existed in the bioremediation site. This corroborates the suggestion made in Chapter 2, Section 2.3.8 that denitrification could be occurring aerobically.

The GCN results were not used to compare functional gene abundance as it was felt that the GCN between functional genes were not relative to each other due to the extremely low concentrations of the target genes in the eDNA and therefore should not be used for comparative purposes. The presence and/ or absence of functional genes were used instead. Both nitrifying and denitrifying microbial genes were detected in all sampling wells in the bioremediation site but did not show preference for either PRB over time. It should be remembered that there could be nitrogen cycling microbes present in the bioremediation site that were not detected by the primers used. The database itself used for primer design is biased

towards those microbes that can be cultured and identified from metagenomics DNA. While it was disappointing that the GCN could not be relied upon to analyse the abundance of nitrogen cycling functional genes, it is now known that nitrogen cycling microbes were present in the bioremediation site and that bioremediation as suspected in Chapter 2, could be taking place.

Chapter 4 delves into the amplicon sequencing results from the bioremediation site and thereby will shed light on the efficacy of the primers used (by detailing the species of microbes present) and will also highlight any trends or correlations occurring between field, chemical and microbial analysis.

# Chapter IV: Next Generation Sequencing of eDNA extracted from a bioremediation site with emphasis on nitrogen cycling microbial communities

## 4.1 Introduction

Groundwater and the saturated terrestrial underground forms the largest habitat for microorganisms on earth with up to 40% of the prokaryotic biomass hidden within it (Griebler & Lueders, 2009). Identifying key degraders and microbial structure in highly polluted waters and soils can lead to optimised assemblies of microbial communities capable of addressing new problem sites (Czapilicki & Gunsch, 2016). Advances in next-generation sequencing (NGS) have allowed comprehensive biological environmental inquiry feasible in bioremediation (Czapilicki & Gunsch, 2016) and two common amplicon sequencing platforms used in environmental sequencing are Illumina and Ion Torrent (Salipante et al., 2014). They work on the principle that 16S rRNA amplicon sequencing can be targeted specifically against bacteria, they do not require the availability of reference genome sequences and can be employed in cases where only trace amounts or poor-quality bacterial DNA templates are available (Salipant et al., 2014). Illumina uses sequencing-by-synthesis wherein bases are recognised (through unique light signals) as they bind to elongating light signals (Illumina, 2016). Ion Torrent also uses sequencing-by-synthesis, but detects protons released when nucleotides become incorporated into the DNA (Czaplicki & Gunsch, 2016) through detection of pH changes.

This chapter focuses on the amplicon sequencing results from the analysis carried out on eDNA extracted from the two permeable reactive barriers installed on the bioremediation site.

### 4.1.1 Microbial Communities in Contaminated Groundwater

Rolling et al. (2000a) noted that knowledge of the composition of microbial communities in landfill leachate polluted aquifers could have the potential for intrinsic bioremediation. As such, they conducted microbial community analysis on water and sediments collected from an aquifer that was polluted by a neighbouring landfill using anaerobic cultivation and denaturing gel electrophoresis (DGGE). The results showed that there was a significant difference observed in the microbial community of the groundwater and in the associated sediment. Differences were also noted in the polluted groundwater when compared with nonpolluted groundwater. These findings were confirmed when Roling et al. (2000b) combined community-level physiological

profiling and most probable number-Biolog methods on water collected from the same landfill using piezometers spread across the aquifer, rather than just four sampling points, and found that both substrate richness and functional diversity were significantly enhanced in the plume of pollution. To investigate this further, Roling et al. (2001) combined DGGE with sequencing cloned 16S DNA and found there was a strong correlation between community profiles and hydro-chemical parameters in groundwater, though not noted in the sediment samples, supporting the hypothesis that bacteria attached to sediment particles and formed biofilms usually consisting of stable communities which were less influenced by changing environmental factors.

Tian et al. (2004) conducted molecular analysis on groundwater polluted by leachate and seawater. They found that 95.9% of the randomly selected sequences belonged to bacteria with *Pseudomonadota* (formerly *Proteobacteria*), (63.5%) being the dominant division. A Malaysian study assessing microbial diversity in both active and closed landfills carried out by Zainun & Simarani (2018) found that the prevalent bacterial communities also belonged to the phylum *Pseudomonadota* in both open and closed landfills (55.7%). The study also noticed that archaea were absent from closed landfills and constituted a minor part of the active landfill represented by the phylum *Euryarchaeota.*

## 4.1.2 Nitrogen Cyclers

As described previously there are many microbial niches within the nitrogen cycle. This study has focused on five functional genes that catalyse important steps therein. The microbes that possess these genes are the AOA, AOB and denitrifying bacteria. This chapter also looks at the nitrite oxidising bacteria (NOB) that utilise the *NxrA* functional gene to catalyse the second nitrification step. There are five genera of known *amoA* possessing ammonia oxidising bacteria (Koops et al., 2005; Samocha et al., 2019): *Nitrosomonas*, *Nitrosospira*, *Nitrosococcus*, *Nitrosolobus* and *Nitrosovibrio*. There are four (NxrA functional gene possessing) genera of nitrite oxidising bacteria (Daims et al., 2015; Teske et al., 1994; Freitag et al., 2005), though investigations on NOB diversity and community structure are few (Hayatsu et al., 2008).

Ammonia oxidising archaea were grouped into a new *Thaumarchaeota* phylum (Brochier-Armanet et al., 2008) and represent up to 30% of the prokaryotic community in the marine environment and 3% of the soil environment (Ren et al., 2019). The phylum *Thaumarchaeota* encompasses all known ammonia oxidising archaeon within which there are four major clusters (Pester et al., 2012). These can be further divided into four monophyletic clusters: *Nitrosotalea*, *Nitrososphaera*, *Nitrosopumilus* and one non-monophyletic, *Nitrosocaldus* (Cao et al., 2013).

Denitrifying bacteria are polyphyletic (Zumft, 1997) and unlike AOA and AOB (and NOB) they do not fit into any one taxonomic group (Fortunato et al., 2009). They are widely though thinly distributed across various taxonomic groups of prokaryotes (Jeter & Ingrahan, 1981). Denitrifiers occur in the genera *Acidovorax, Azospira, Bacillus, Dechloromonas, Desulfovibrio, Flavobacterium, Hyphomicrobium, Meganema, Rhizobium, Rhodobacter, Rhodoplanes* and *Thiobacillus* (Zhang et al., 2016).

## 4.2 Materials and Methods

Some of the methods used have been described in Chapters 2 and 3 so only a brief synopsis is included where this is the case.

### 4.2.1 Site Description

As described and illustrated in Chapter 2, a bioremediation experiment was carried out on a landfill site in Co. Clare, in an effort to reduce ammonia contamination in shallow groundwater. Two permeable reactive barriers were installed to intercept the contamination plume, one to encourage nitrification, the second to encourage denitrification incorporating sampling wells S2 and S4, respectively. Sampling well S1 was installed upstream and an existing well downstream was incorporated into the bioremediation site as downstream sampling well S5.

### 4.2.2 DNA extraction

Groundwater was collected from each of the monitoring wells each month for in field monitoring and chemical and molecular analysis. DNA was extracted from these samples as described in Chapter 3, Section 3.2.2 and the eDNA was stored at -20°C until used for downstream molecular analysis.

### 4.2.3 Amplicon Sequencing

Due to economic constraints, it was decided to use ion-torrent PGM (discussed in Section 1.4.5.1) to investigate the microbial community profile and to use samples from the PRBs only (excluding upstream and downstream wells) to send for amplicon sequencing. After discussion with the sequencing lab (Molecular Research LP Laboratories (Mr. DNA)), ten samples at six-monthly intervals were chosen to chronicle the changes in both PRBs over the two-year experiment (i.e., DNA from PRB1 and PRB2 collected from June 2015, November 2015, June 2016, November 2016, and March 2017). A model community standard (ZymoBIOMICS™) was also sent as a quality control. Samples from November 2015 and the model community standard were sequenced initially then the remaining samples were sequenced together. 20 µl of each sample

was transferred to a 1.5 ml Eppendorf tube and sent under chain of custody at room temperature to Molecular Research LP.

When in discussion with Molecular Research LP Labs regarding the amplicon target and whether to target the 16S structural gene or the archaeal and bacterial *amoA* genes, it was advised that the archaea assay was not as primer efficient and the length of the archaea *amoA* allows only analysis of the first 280bp of the amplicon. The functional genes were already targeted using qPCR so targeting the 16S gene was a useful additional approach to analysing the microbial community within the groundwater. Finally, if the bacterial and archaeal *amoA* genes were targeted for amplicon sequencing, due to budgetary constraints it meant that there would be no focus on the denitrifying functional genes.

The 16S rRNA gene V4 variable region PCR primers 515/806 were used in a single-step 30 cycle PCR using the HotStarTaq Plus Master Mix Kit (Qiagen, USA) under the following conditions: 94°C for 3 minutes, followed by 28 cycles (5 cycle used on PCR products) of 94°C for 30 seconds, 53°C for 40 seconds and 72°C for 1 minute, after which a final elongation step at 72°C for 5 minutes was performed. Sequencing was performed on an Ion Torrent PGM following the manufacturer's guidelines. Sequence data were processed using a proprietary analysis pipeline (MR DNA, Shallowater, TX, USA). In summary, sequences were depleted of barcodes and primers, then sequences <150 bp removed, sequences with ambiguous base calls and with homopolymer runs exceeding 6 bp were also removed. Sequences were then denoised, OTUs generated, and chimeras removed. Operational taxonomic units (OTUs) were defined by clustering at 3% divergence (97% similarity). Final OTUs were taxonomically classified using BLASTn against a database derived from RDPII http://rdp.cme.msu.edu) and NCBI (www.ncbi.nlm.nih.gov). Abundances of archaea and bacterial genes were expressed as a percentage of total archaea and bacteria sequences amplified, respectively.

### 4.2.4 Statistical Analysis

To compare the diversity of the nitrogen cycling communities in the PRBs, the Shannon Diversity Index ($H'$) and Shannon Equitability Index were calculated in Microsoft Excel based on the percentage of N-cycling genes as percentages of total sequences amplified (Kim et al., 2017). The higher the Diversity index, the higher the "richness" of the community. The Shannon Equitability Index was calculated to determine the evenness of the community i.e., to measure how similar the abundances of different species were in the community. This normalises the Shannon diversity index to a value between 0 and 1, where 1 indicates complete evenness. To

test for correlations between nitrogen cycling gene abundance and the results of the chemical analysis, Pearson's correlation test was performed in Microsoft Excel and p values were extrapolated to test for significance and the Bonferroni correction was applied. The changes in the abundance of archaeal and bacterial groups in PRB1 and PRB2 at six monthly intervals were analysed by non-metric multidimensional scaling (nMDS) using Primer 7 software (Primer-E, Plymouth, UK) with Bray-Curtis similarity index (Castro-Gutiérrez et al., 2017).

## 4.3 Results and Discussion

The results from Molecular LP Laboratories returned a dataset of bacterial and archaeal sequences amplified from each sample of eDNA extracted from PRB1 and PRB2 at six monthly intervals and at the end of the study (i.e., June 2015, November 2015, June 2016, November 2016, and March 2017), ten samples in total. The datasets described the DNA identified from Kingdom level down to species and strain level where possible. As discussed in Section 4.2.3, the primers used to amplify the 16S rRNA gene were universal primers 515/806 and were not specific to bacteria and archaea. They were designed to target the V4 region which can detect most archaea and bacteria (Gilbert et al., 2010), though studies that use primers specific for bacteria and archaea supplemented by universal ones allow an in-depth evaluation of the microbial diversity (Adamiak et al., 2018). It should be remembered that the amplicon sequencing results are subject to primer bias and these results represent what was sequenced and do not necessarily give a complete picture of the microbial diversity present in the PRBs. Furthermore, the microbial communities amplified and identified from the DNA extracted from the water may not be representative of the microbial communities found in the sediment, as found by Roling et al. (2001). Also, as discussed in Section 3.1.2, microbes possessing nitrogen cycling functional genes does not mean that those genes are being expressed (Prosser et al., 2008). The sequencing data were searched and examined for any microbes known to be nitrogen cyclers, though this does not mean that the results presented below are exhaustive, as there may be microbes that have the ability to catalyse parts of the nitrogen cycle that are as yet unknown. This is particularly the case with denitrifiers as they do not fit comfortably into any one taxon as discussed in Section 4.1.2.

## 4.3.1 Archaea Vs Bacteria

Of the DNA amplified and sequenced the vast majority was bacterial DNA with some archaeal DNA as per Figure 4.1, below.
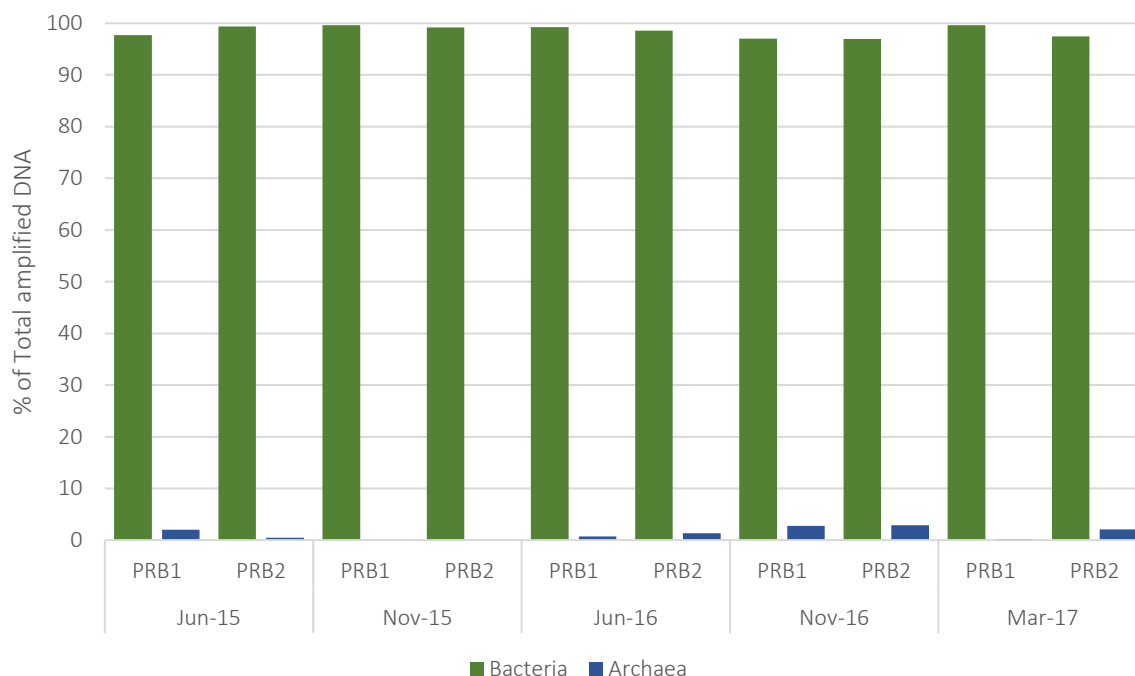
As discussed in Chapter 3, Section 3.1.1, archaea can constitute between 0 and 10% of total soil prokaryotes (Timonen and Bomberg, 2009) with an average of 2% (Bates et al., 2010). The bacterial domain dominated in the DNA amplified from the bioremediation site comprising from 97.04% of total DNA sequenced (November 2016 in PRB2) to 99.65% (March 2017 in PRB1). Archaeal DNA that was amplified consisted of between 0.09% (November 2015 in PRB1) and 2.88% (November 2016 in PRB2) of DNA extracted and amplified from the two PRBs. Except for eDNA collected in June 2015, PRB2 contained a higher quantity of amplified archaeal sequences than PRB1.

## 4.3.2 Archaeal Diversity in Permeable Reactive Barriers

The diversity of the archaeal DNA amplified from the samples belonged to four phyla, as shown in Figure 4.2 below, with most of the archaeal sequences belonging to the Euryarchaeota phylum (from 88% of total archaeal amplicons in PRB1 in June 2015 to 98.81% in PRB1 in June 2016) which Zainun & Simarani (2008) also found in the soil of active landfills, though they found no archaeal DNA at all in a closed landfill.

Ammonia oxidising archaea belong to the phylum *Thaumarchaeota* (Brochier-Armanet et al., 2008) which contributed to between 0% (PRB1 in November 2015) and 9.01% (PRB1 in March 2017) of total archaeal amplicons. Only PRB2 in November 2015 contained amplified DNA that belonged to the acidophilic phylum *Parvarchaeota*. Chen et al. (2018) isolated genomes belonging to this phylum in acid mine drainage and hot springs (they were absent from soil, peat, hyper saline conditions, or freshwater) and described the phylum as anaerobic. DO concentrations in PRB2 in November 2015 were 1.9 mg L$^{-1}$. While this is a low concentration, it was not the lowest that was seen in either PRB over the two-year period, though it was the only time point where DNA belonging to the phylum *Parvarchaeota* was detected. Below, Figure 4.3 shows the genera of archaea identified in the PRB that comprised over 1% of total archaeal sequences.
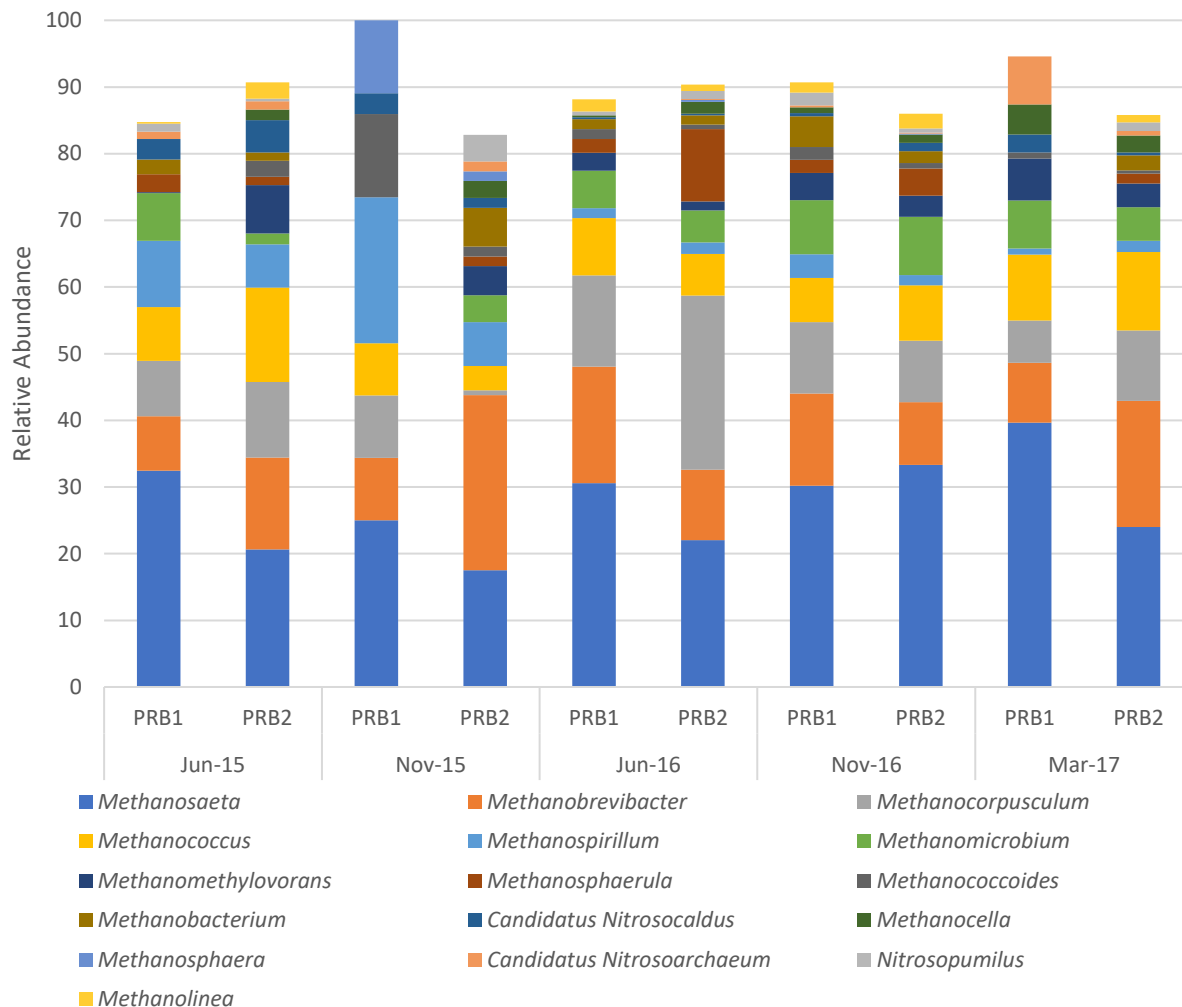
Figure 4. 3: Relative abundance of archaeal genera identified in PRB 1 and 2 on the bioremediation site

As can be seen from Figure 4.3, the highest percentage of archaeal DNA sequences belonged to archaeal genera associated with methane cycling archaea (e.g., *Methanosaeta* and *Methanobrevibacter*). Three nitrogen cycling genera that comprised more than 1% of total archaeal DNA amplicons were *Candidatus nitrosocaldus, Candidatus nitrosoarchaeum* and *Nitrosopumilus.* Two other nitrogen cycling archaeal genera were identified comprising less than 1% of archaeal DNA amplicons i.e., *Candidatus nitrososphaera* and *Candidatus nitrosotalea.* The genus *Candidatus nitrososphaera* was only identified from DNA extracted from water sampled from PRB1 in June 2015 (comprising 2.17 % of total amplified archaeal DNA) and was not identified thereafter. This would indicate that this genus was present in the overburden of the landfill before the bioremediation site was installed in June 2015, and the altered conditions caused by the installation of bioremediation site were unsuitable. Lehtovirta-Morley et al. (2011) describe *Candidatus nitrosotalea* as an obligate acidophile with optimum pH conditions of 5.0.

123

As seen from Table 3.5 in Chapter 3, archaeal *amoA* genes were only detected in samples that had a pH value of 7.2 or less.

To test whether the PRBs influenced the community structure in the amplified archaeal communities, the changes in the abundance of archaeal genera (>1% of total archaeal genera amplified) in both PRBs over the 24-month study were analysed by non-metric multidimensional scaling (nMDS) using Primer 7 software (Primer-E, Plymouth, UK) with Bray-Curtis similarity index, Figure 4.4 below. The software used was a trial version and the images were superimposed with a watermark that could not be removed.
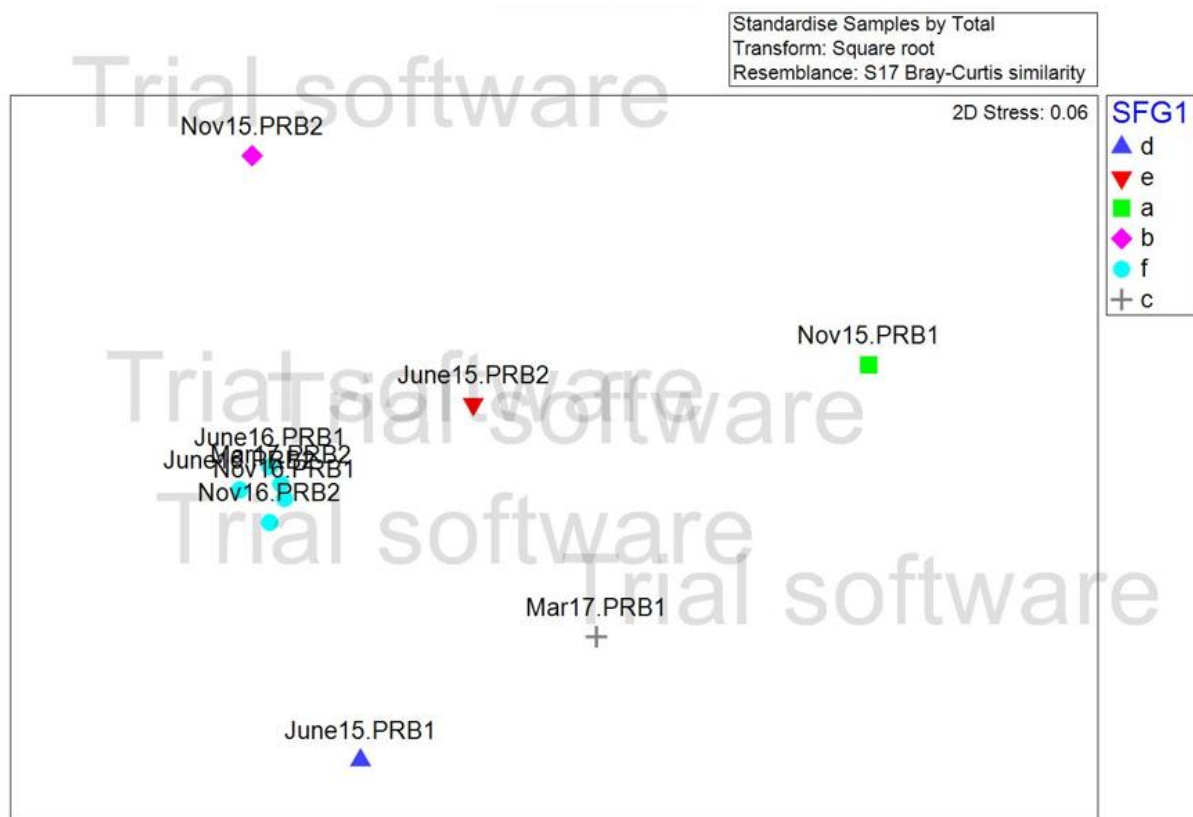


Figure 4. 4: Cluster and non-metric multidimensional scaling (nMDS) analysis of abundance of archaeal amplicons in PRBs

There was no clustering of samples that showed high similarity or fidelity to either PRB. It would have been expected that if clusters were to form it would be per PRB as they were designed to encourage the growth of different groups of nitrogen cyclers. There was no clustering according to season either.

Below, Figures 4.5 to 4.14, show the most abundant (>1% of total archaeal sequences) archaeal taxa found in PRB1 and PRB2 over the five sampling points in time with ammonia oxidising

archaea highlighted in colour. Where possible, the archaea were identified to species and strain level.
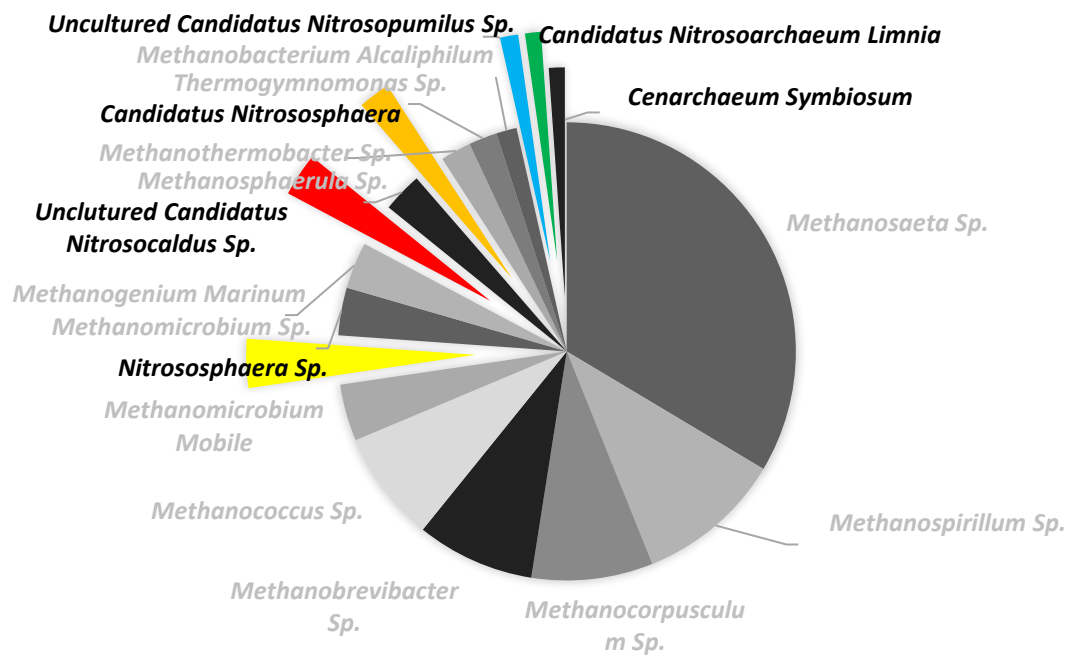


Figure 4. 5: Archaeal species occuring above 1% of total archaeal sequences amplified from eDNA extracted from water sample collected from PRB1 in June 2015, with AOA outlined in colour
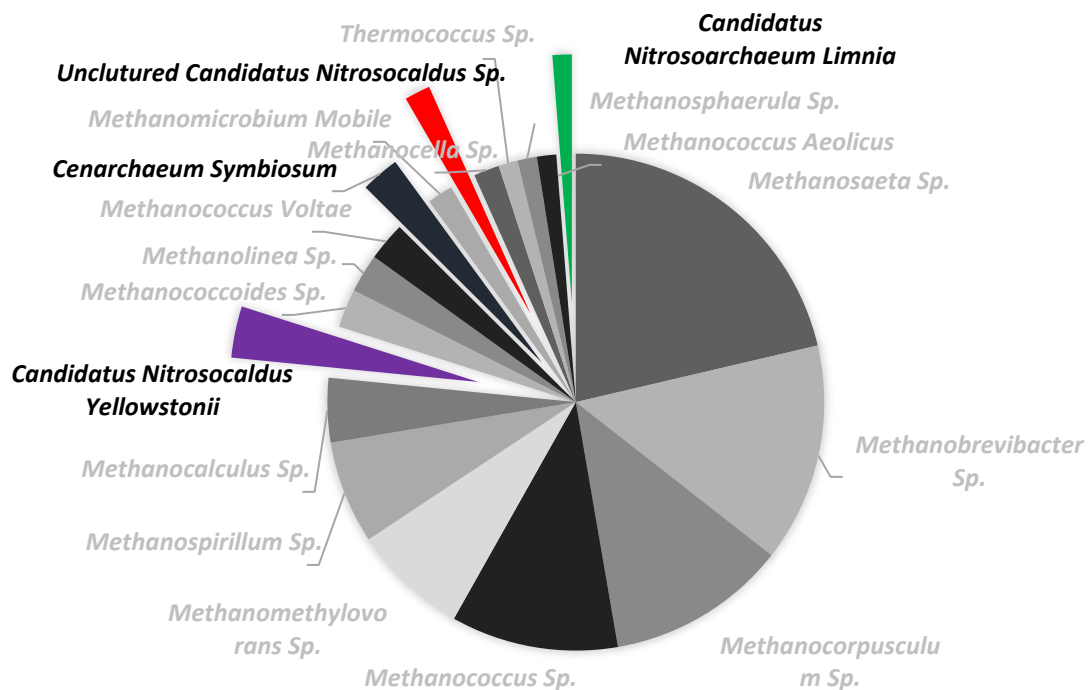


Figure 4. 6: Archaeal species occuring above 1% of total archaeal sequences amplified from eDNA extracted from water sample collected from PRB2 in June 2015, with AOA outlined in colour
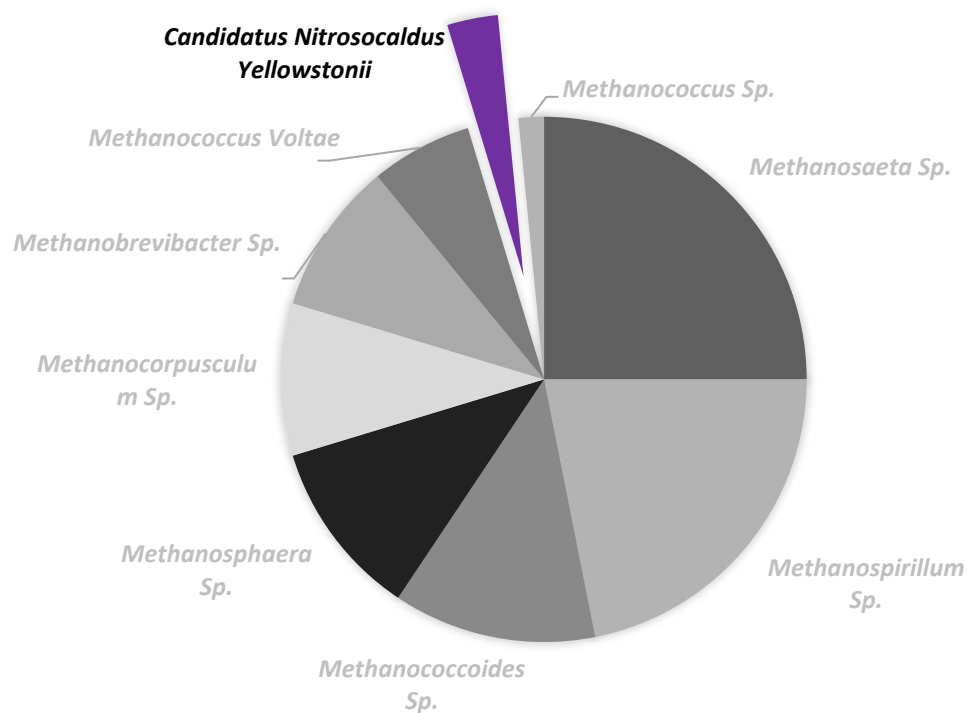
Figure 4. 7: Archaeal species occuring above 1% of total archaeal sequences amplified from eDNA extracted from water sample collected from PRB1 in November 2015, with AOA outlined in colour
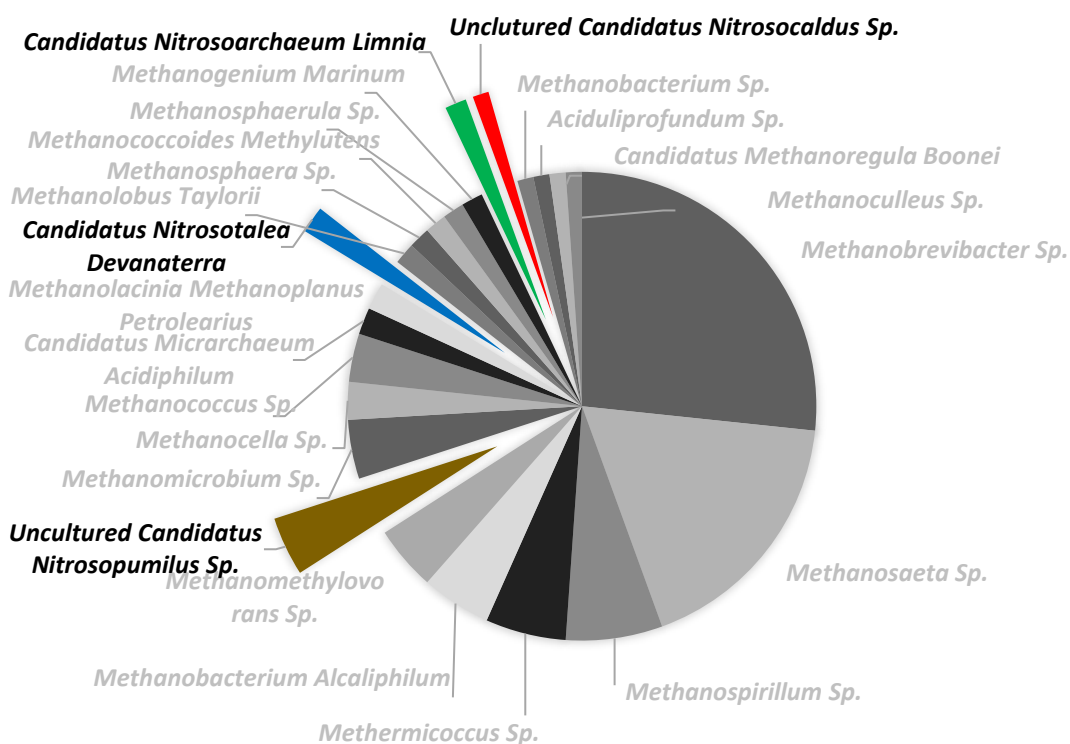


Figure 4. 8: Archaeal species occuring above 1% of total archaeal sequences amplified from eDNA extracted from water sample collected from PRB2 in Niovember 2015, with AOA outlined in colour
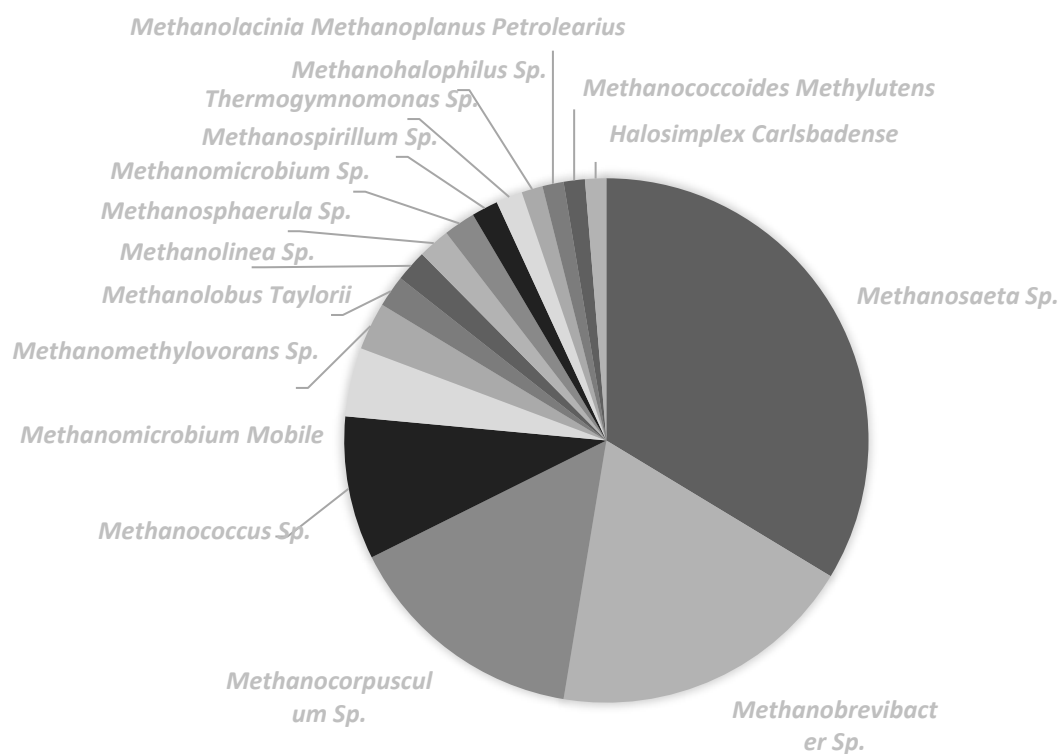
Figure 4. 9: Archaeal species occuring above 1% of total archaeal sequences amplified from eDNA extracted from water sample collected from PRB1 in June 2016, with AOA outlined in colour
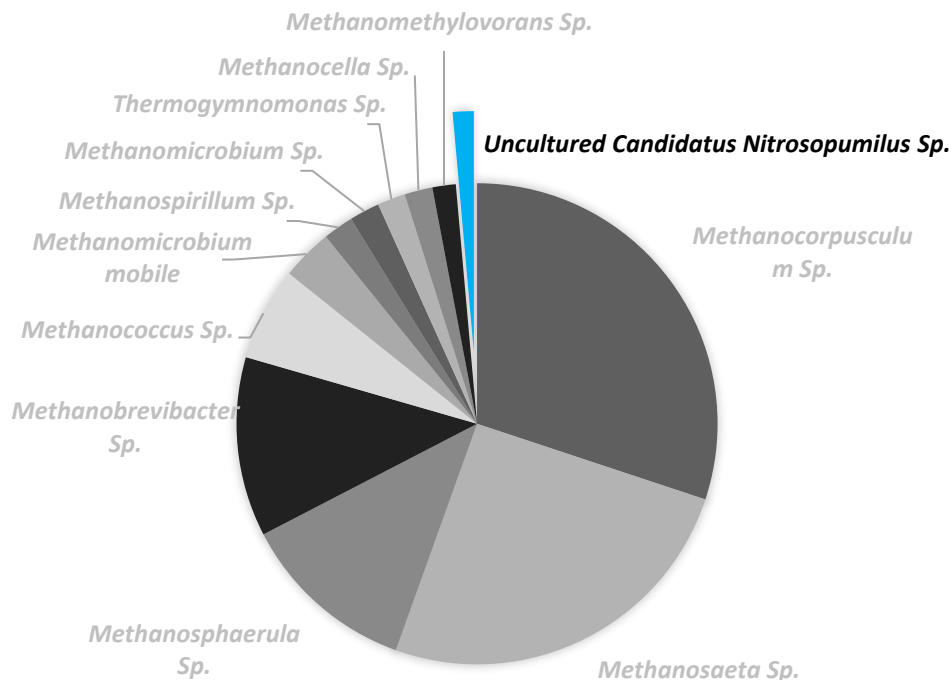


Figure 4. 10: Archaeal species occuring above 1% of total archaeal sequences amplified from eDNA extracted from water sample collected from PRB2 in June 2016, with AOA outlined in colour
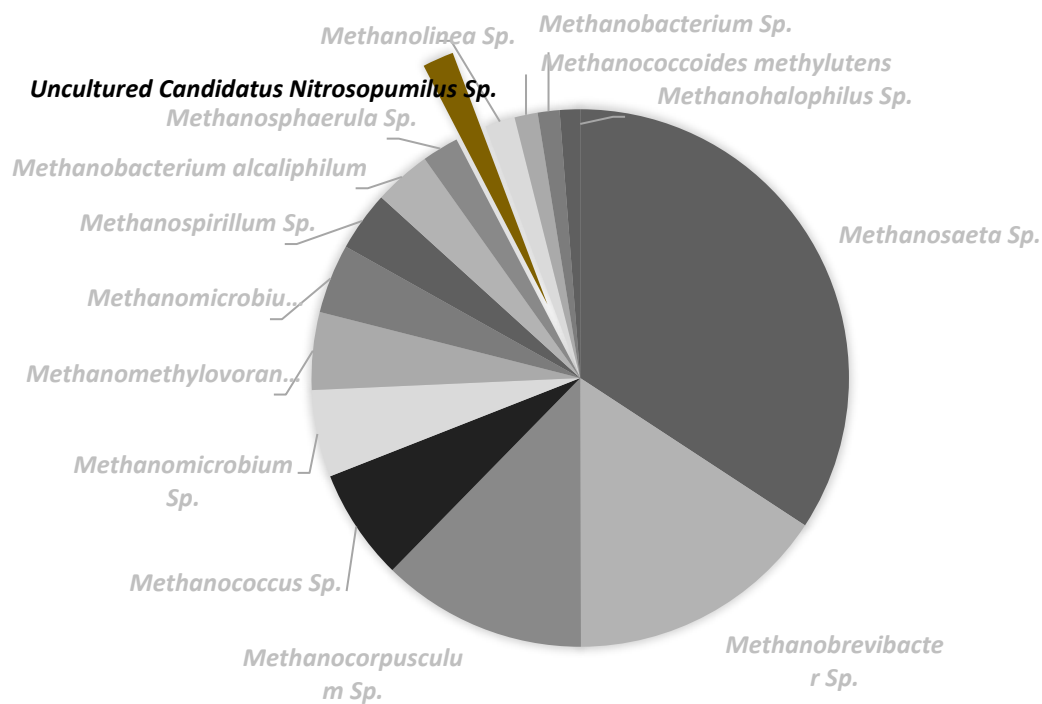
Figure 4. 11: Archaeal species occuring above 1% of total archaeal sequences amplified from eDNA extracted from water sample collected from PRB1 in November 2016, with AOA outlined in colour
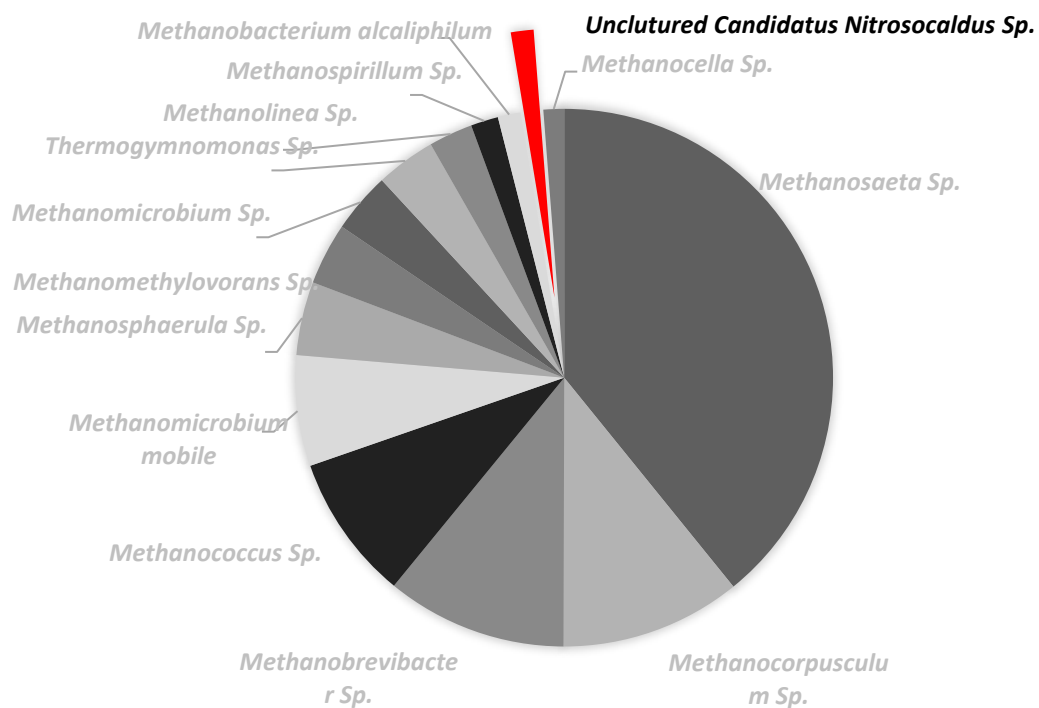


Figure 4. 12: Archaeal species occuring above 1% of total archaeal sequences amplified from eDNA extracted from water sample collected from PRB2 in November 2016, with AOA outlined in colour
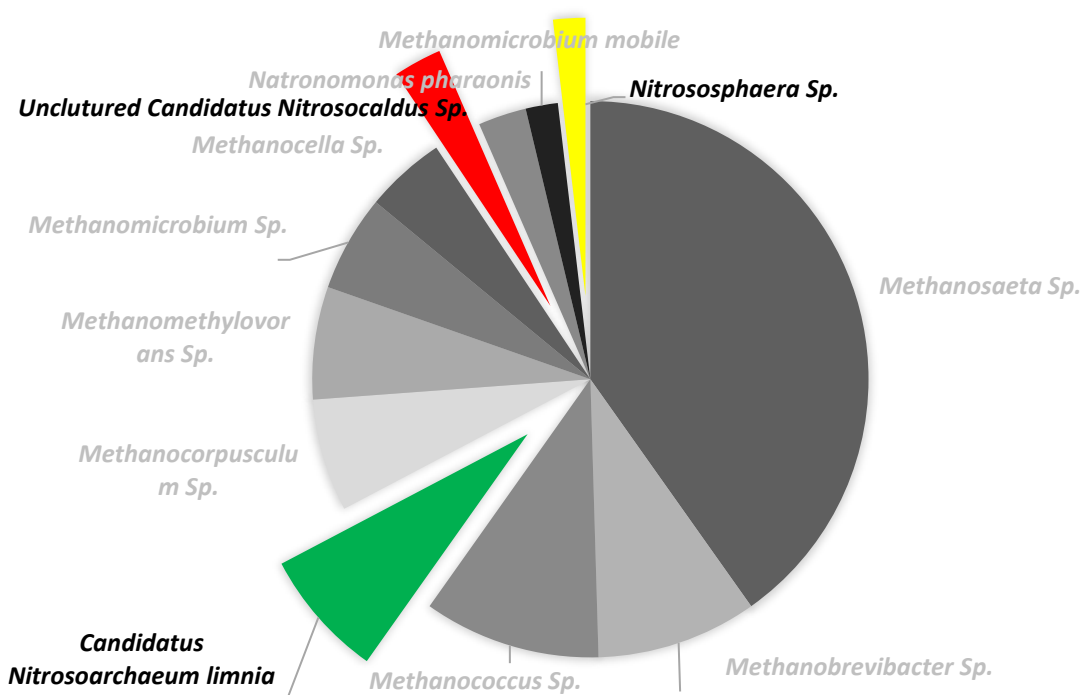
Figure 4. 13: Archaeal species occuring above 1% of total archaeal sequences amplified from eDNA extracted from water sample collected from PRB1 in March 2017, with AOA outlined in colour
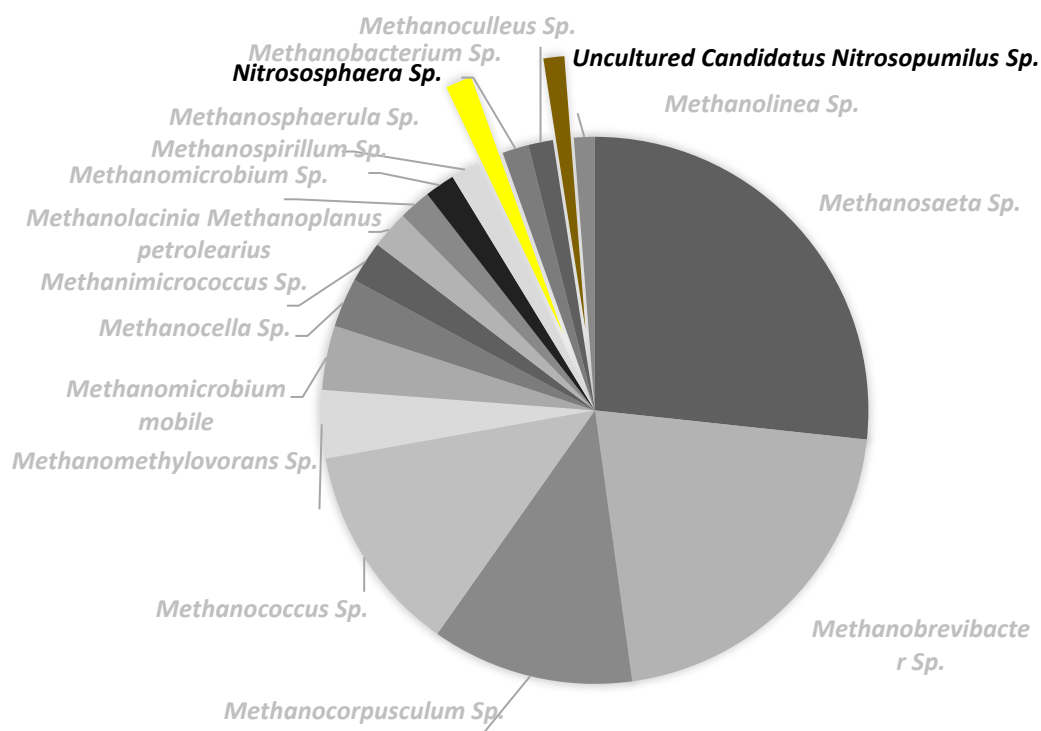


Figure 4. 14: Archaeal species occuring above 1% of total archaeal sequences amplified from eDNA extracted from water sample collected from PRB2 in March 2017, with AOA outlined in colour

As can be seen from the results, the major archaeal species were methanogens, as expected in a groundwater body that is beneath, and contaminated by, an unlined landfill. Almost one

quarter of total archaeal amplicons across the bioremediation site were *Methanosaeta* sp. Only the sample collected in June 2016 in PRB1 did not contain any AOA with relative abundances greater than 1% of total archaeal amplicons. The sample collected in June 2015 in PRB1 contained the greatest number of AOA over 1% abundance, with five AOA identified: uncultured *Candidatus Nitrosopumilus* sp. (colour coded green in the above graphs) and *Candidatus nitrosocaldus* sp. (red) and *Candidatus nitrososphaera* (orange), *Candidatus nitrosoarchaeum limnia* (green) and *Crenarchaeon symbiosum* (navy).

### 4.3.3 AOA Diversity in Permeable Reactive Barriers

Eleven archaeal ammonia oxidisers were revealed (Martens-Habbena et al., 2009; Spang et al., 2012; Pester et al., 2012; Mosier et al., 2012; Zhalnina et al., 2014; De la Tore et al., 2008; Daebeler et al., 2018; Prosser & Nicol, 2015; Lehtovirta et al., 2016; Schelper & Nicol, 2010) to be present in the PRBs, illustrated in Figure 4.15 below.
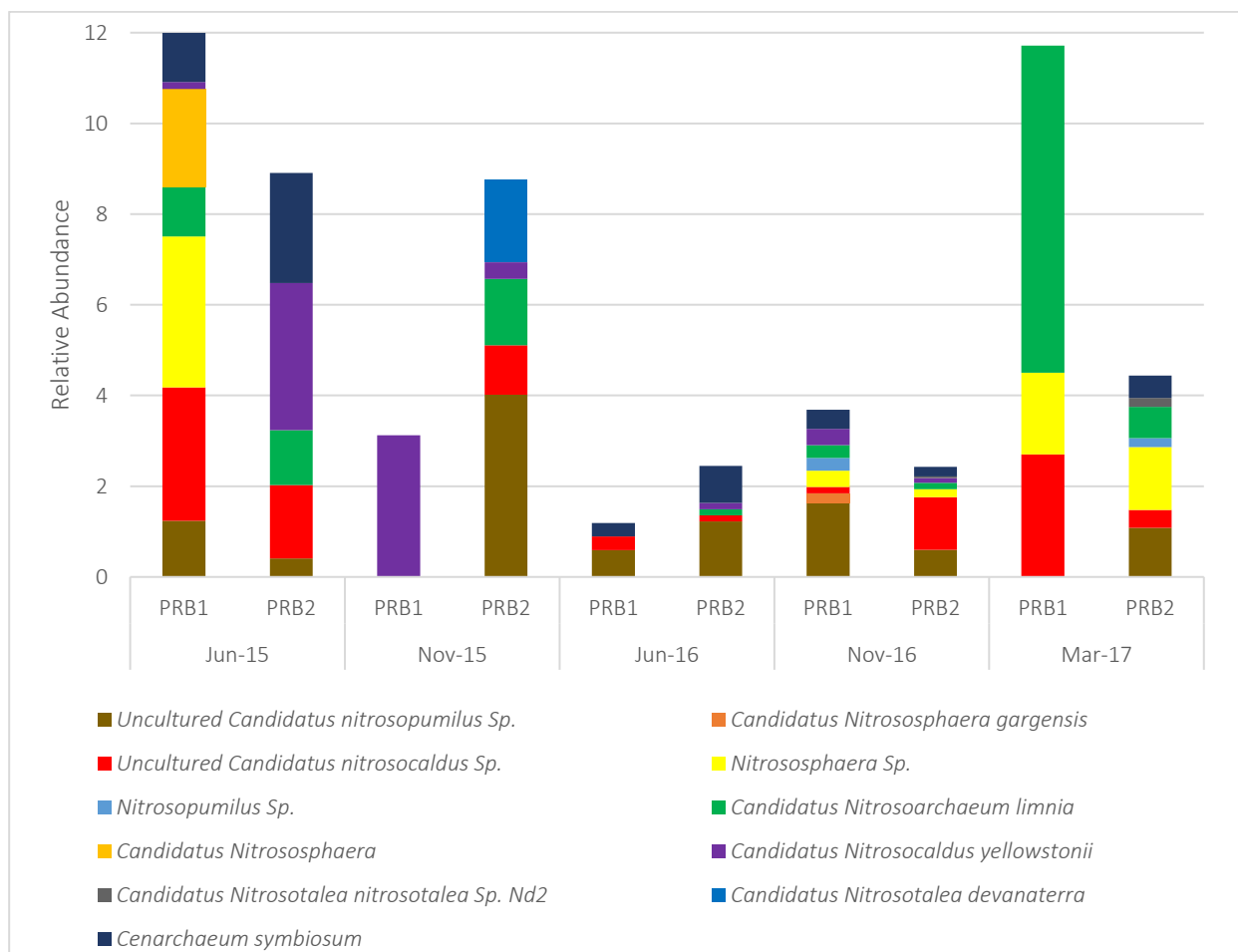


Figure 4. 15: AOA percentage of total archaeal sequences found in PRB1 and 2 on the bioremediation site

Figure 4.15 shows the relative abundance of AOAs as a percentage of archaeal DNA. As shown, the highest quantity of AOA amplicons (12% of total archaeal amplicons; 0.24 % of total 16S rRNA

amplicons) was found in PRB1 in June 2015 when the PRBs were installed. The most AOA diverse sampling point occurred in PRB1, November 2016, with eight AOA occurring which accounted for 2.76% of total amplified archaeal DNA or 1.10% of the total amplified 16S rRNA sequences. *Crenarchaeum symbiosiom* is a symbiont, dwelling within the tissues of sea sponges and has never been cultured. It is included here though it has never been proven to be an ammonia oxidiser, but it is known to contain the *amoA* gene (Schleper & Nicol, 2010). This may indicate that there is a significant influx of sea water into the bioremediation site. The most prevalent AOA found in the PRBs was uncultured *Candidatus nitrosocaldus* sp., occurring in both PRBs at all sampling times except PRB1 in November 2015. *Candidatus nitrosocaldus yellowstonii, Candidatus nitrosotalea* sp. and *Candidatus nitrososphaera gargensis* are thermophiles, and the latter is an obligate acidophile, preferring a pH of <5 (Hatzenpichler et al., 2007; Lehtovirta-Morley et al., 2016). *Candidatus nitrosocaldus yellowstonii* is an aerobic ammonia oxidiser (Prosser & Nicol, 2015) and occurred in both PRB1 and PRB2 (as do the other AOAs), possibly verifying that that anaerobic conditions were not reached in PRB2.

### 4.3.4 Bacterial Diversity in Permeable Reactive Barriers

Thirty-one bacterial phyla were identified from the bioremediation site. Below, Figure 4.16 shows the dominant phyla (comprising more than 1%) of total DNA amplified from the eDNA collected from the PRBs.
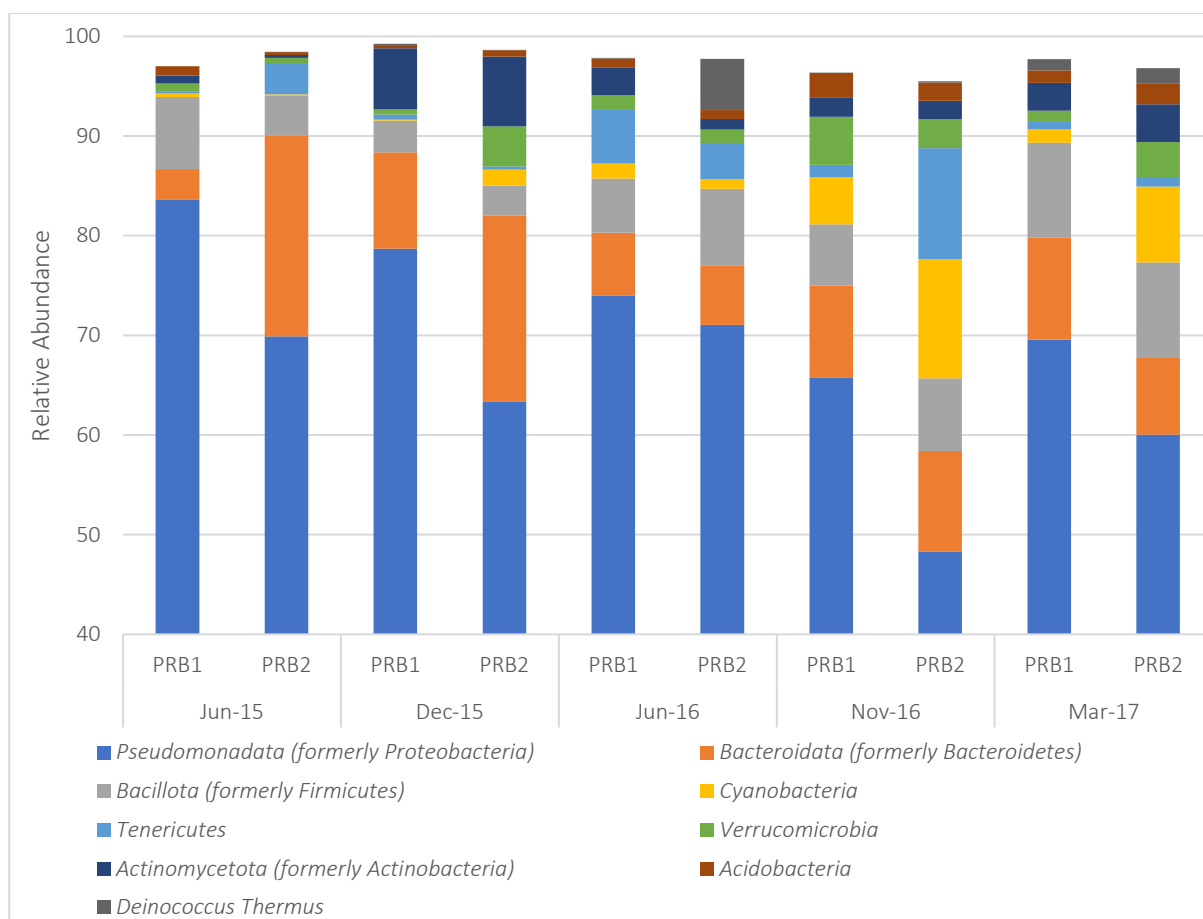
Figure 4. 16: Dominant bacterial phyla identified in the PRBs over two-year study period

The most dominant phylum was *Pseudomonadota* (formerly *Proteobacteria*) ranging in abundance from 48% (PRB2 in November 2016) to 84% (PRB1 in June 2015) with an average of 68%. This is concurrent with other studies described in Section 4.1.1.  Tian et al. (2004) carried out a study on groundwater polluted by landfill leachate and found that 63.5% of the microbial community belonged to the phylum *Pseudomonadota.* Zainun & Simarani (2018) also found the dominant microbial community to be *Pseudomonadota* (55.7%) during work that they carried out on landfills.  Bacteroidetes and Firmicutes were the next most abundant phyla. Of the bacterial genera, 887 were amplified from both PRBS. The dominant (i.e., >1% of total bacterial amplicons) bacterial genera are illustrated in Figure 4.17 below.
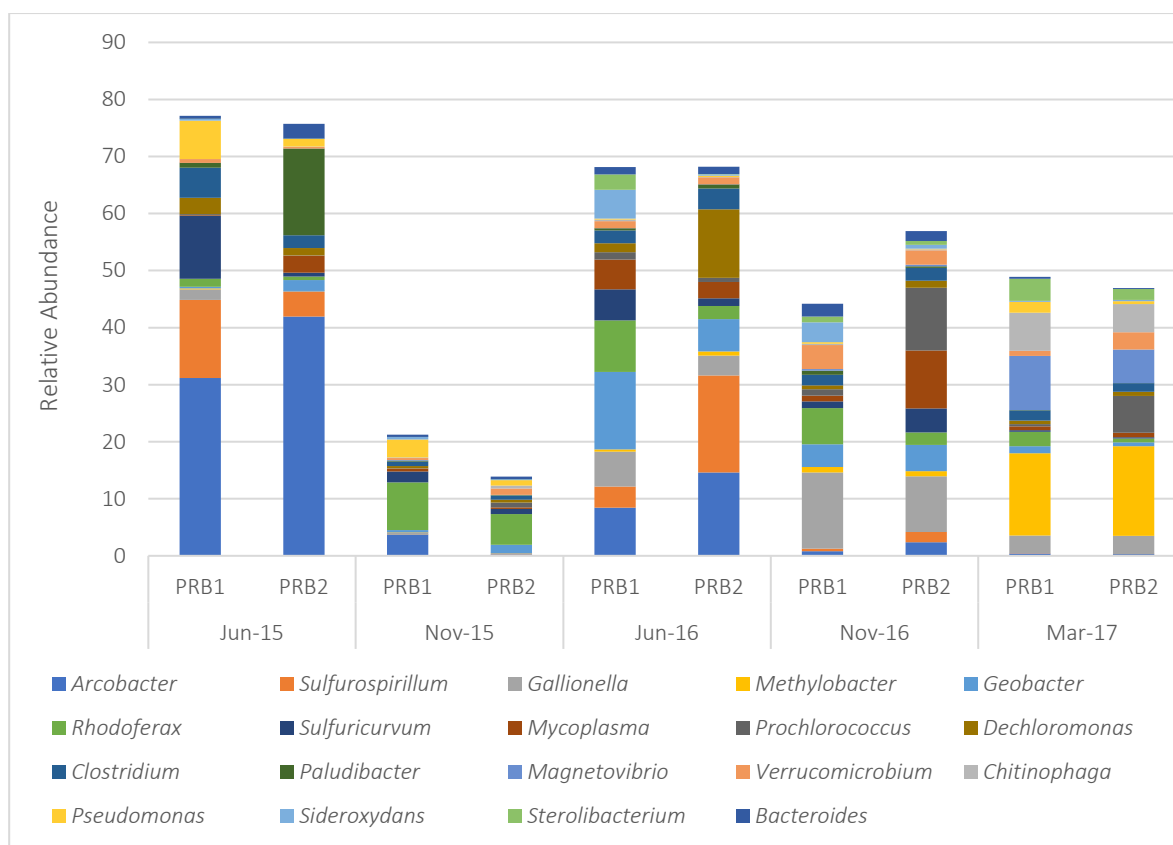
Figure 4. 17: Relative abundance of dominant (i.e., >1%) bacterial genera identified in the bioremediation site

The dominant genera varied more over time than between the two PRBs. November 2015 showed the least commonality with the other sampling times. This may be due to the addition of ORC which was added in November 2015, or may be due to the disruption caused by the construction and installation of the bioremediation site (in June 2015) before the native bacterial communities re-established themselves. This shift in dominant genera did not occur with the archaeal genera, which was contrary to the study carried out by Roling et al. (2001) which noted that pollution plumes affected archaeal community structure more than bacterial community structure. To test whether the PRBs influenced the community structure in the amplified bacterial communities, the changes in the relative abundance of bacterial genera (>1% of total bacterial genera amplified) in both PRBs over the 24-month study were analysed by non-metric multidimensional scaling (nMDS) using Primer 7 software (Primer-E, Plymouth, UK) with Bray-Curtis similarity index, Figure 4.18 below.
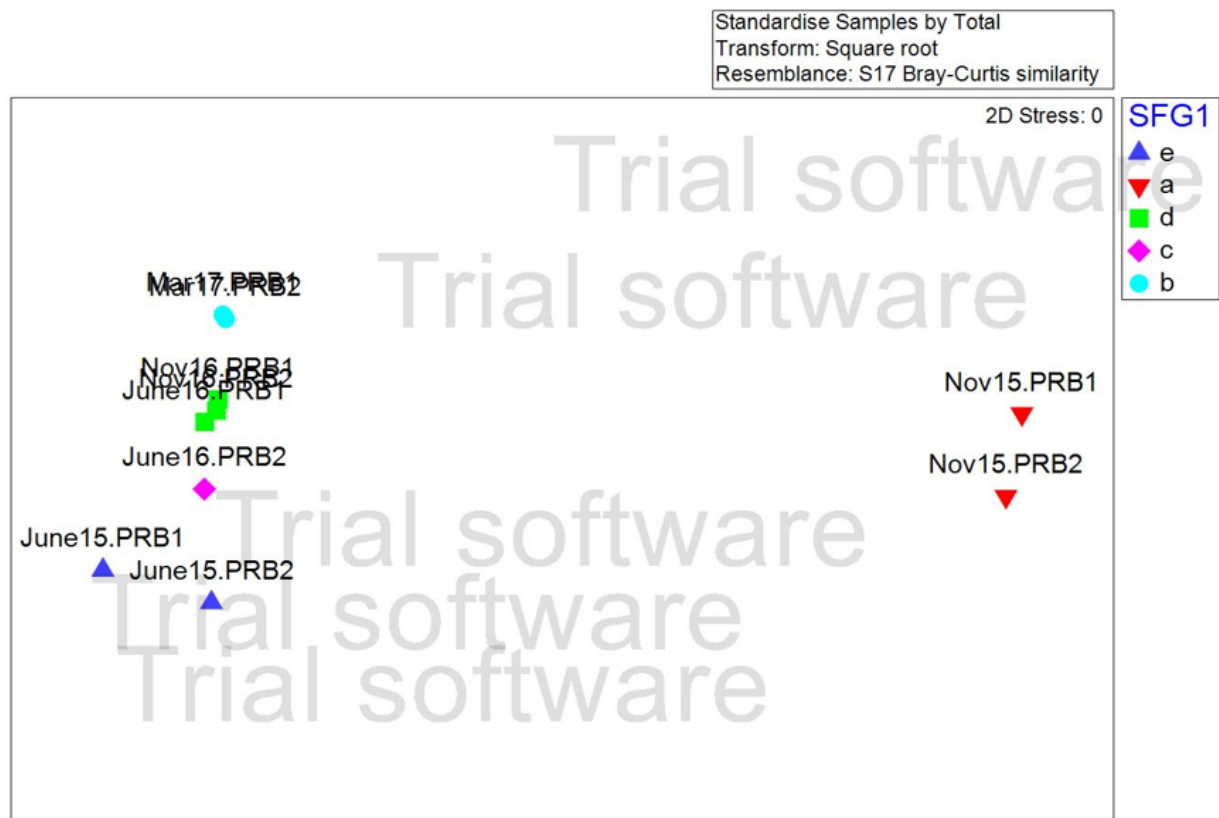
Figure 4. 18: Cluster and non-metric multidimensional scaling (nMDS) analysis of abundance of bacterial amplicons in PRBs

There was no clustering of samples that showed high similarity or fidelity to either PRB. It would have been expected that if clusters were to form it would be per PRB as they were designed to encourage the growth of different groups of nitrogen cyclers. There was no clustering according to season either. It was noted that the samples that amplified from November 2015 in both PRBs showed high dissimilarity to the other samples. This was most likely due to batch effect because the November 2015 samples were sent one year prior to the remaining samples. The dissimilarity could be due to technical differences or differences in the reference library over the intervening time period or any other unwanted variation introduced by confounding factors that are not related to any factors of interest (Wang & LêCao, 2020). This difference was not noted in the archaeal samples though this is likely due to the much smaller quantity of amplified archaeal DNA. Figures 4.19 to 4.28 below show the most abundant genes/ species (i.e., >1% of total bacterial DNA amplified) identified in the PRBs with nitrogen cyclers highlighted in colour.
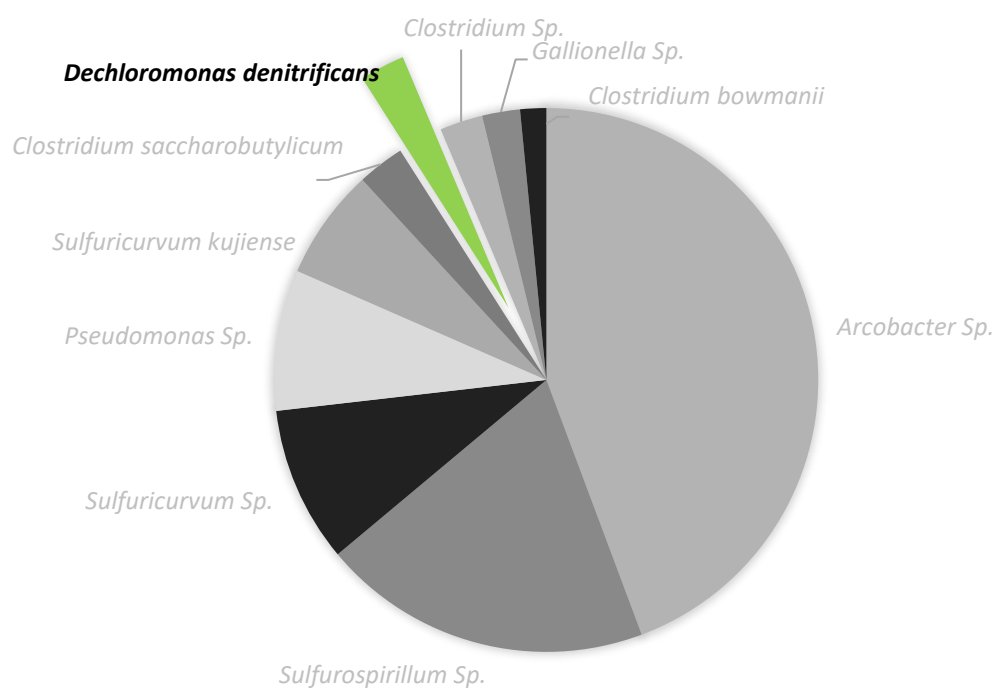
Figure 4. 19: Bacterial species occuring above 1% of total bacterial sequences amplified from eDNA extracted from water sample collected from PRB1 in June 2015, with AOB outlined in colour
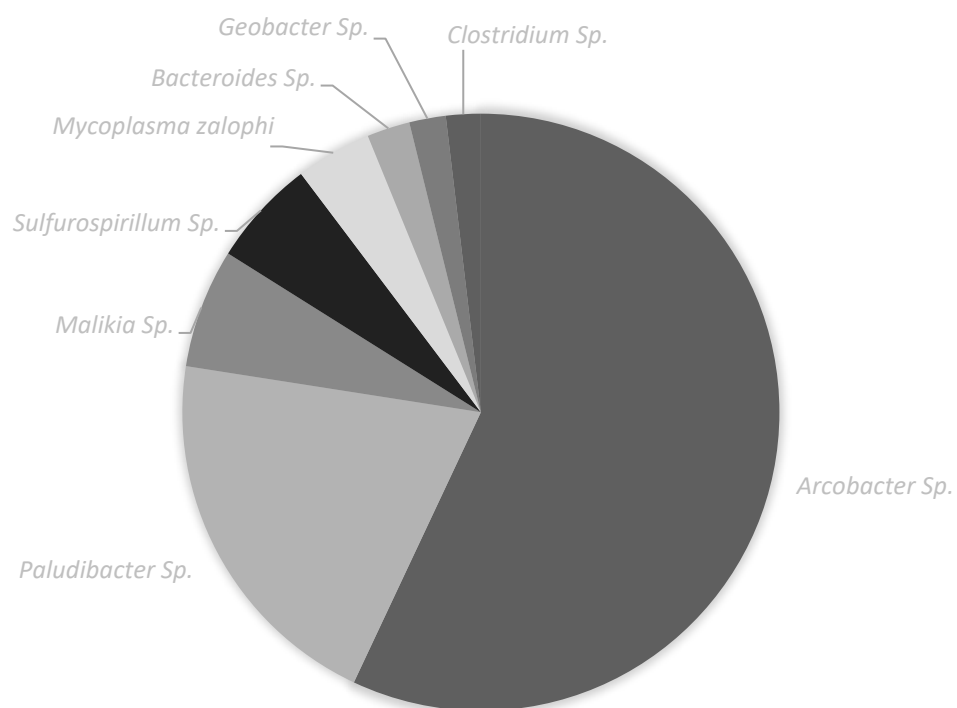


Figure 4. 20: Bacterial species occuring above 1% of total bacterial sequences amplified from eDNA extracted from water sample collected from PRB2 in June 2015, with AOB outlined in colour

135
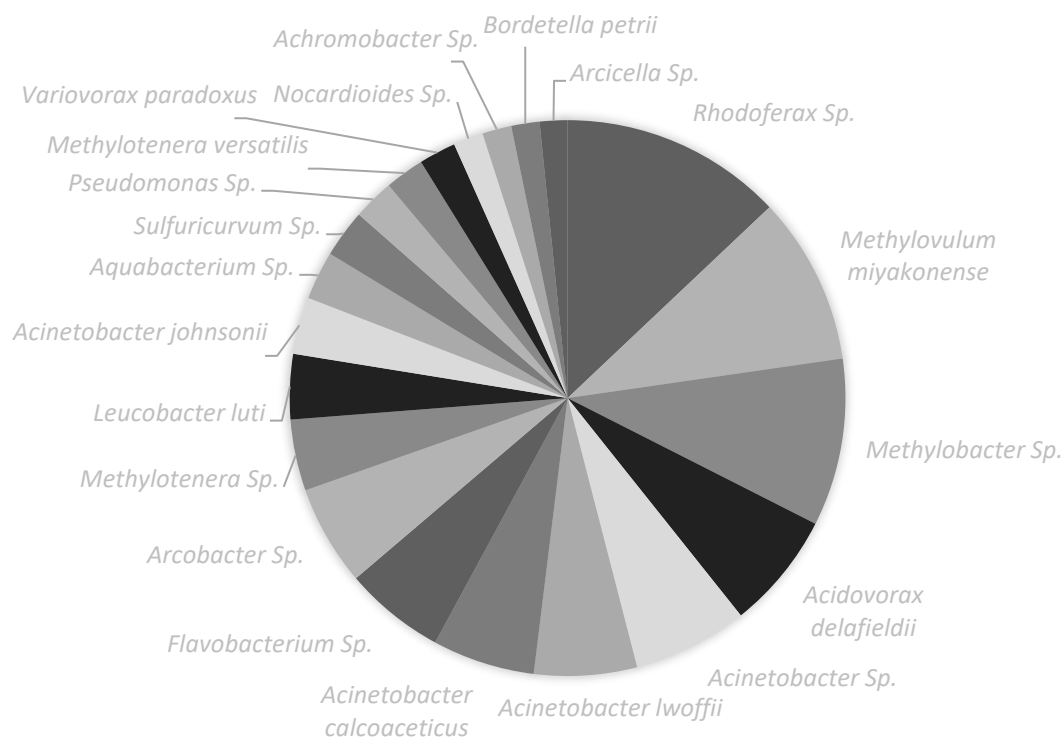
Figure 4. 21: Bacterial species occuring above 1% of total bacterial sequences amplified from eDNA extracted from water sample collected from PRB1 in November 2015, with AOB outlined in colour
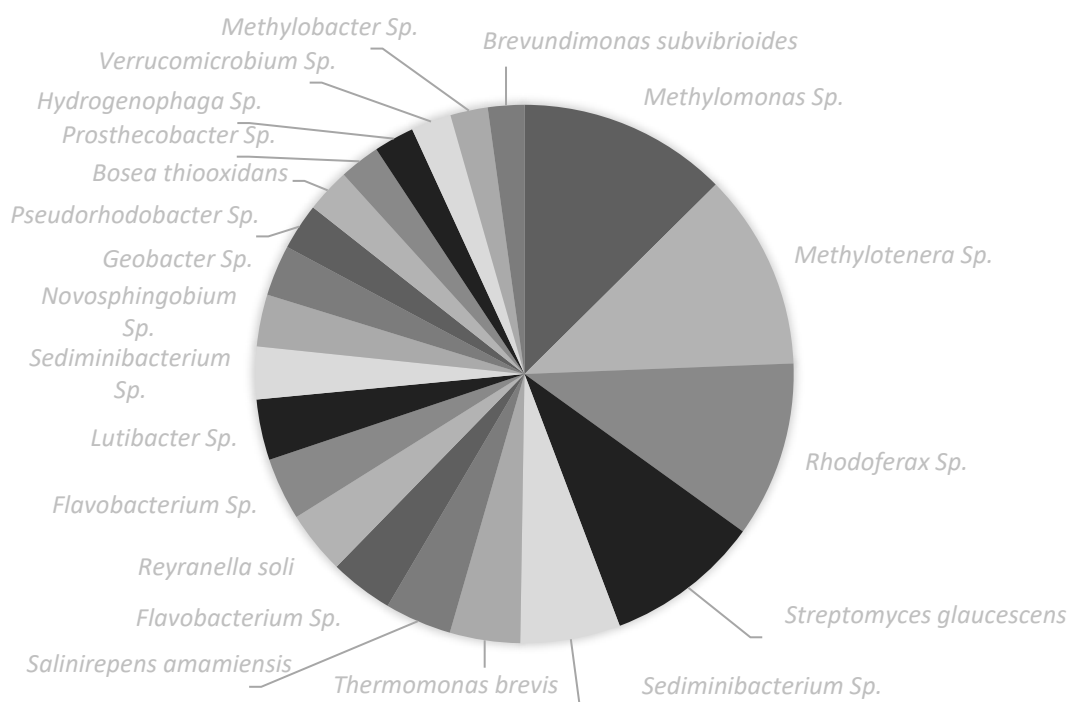


Figure 4. 22: Bacterial species occuring above 1% of total bacterial sequences amplified from eDNA extracted from water sample collected from PRB2 in November 2015, with AOB outlined in colour
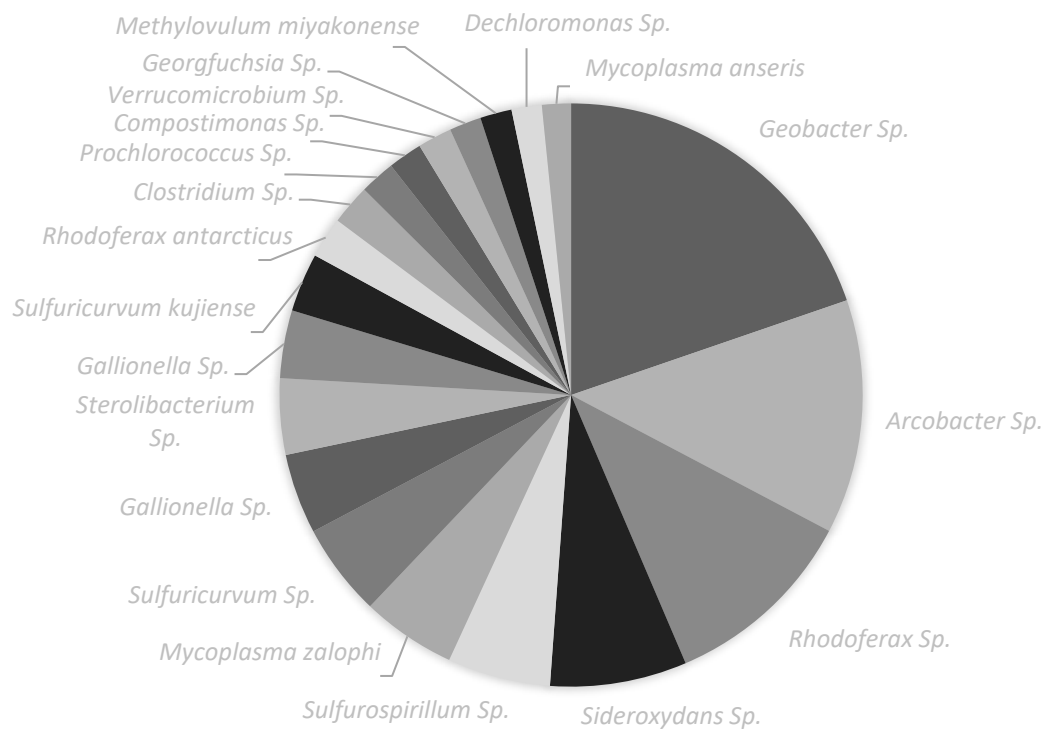
Figure 4. 23: Bacterial species occuring above 1% of total bacterial sequences amplified from eDNA extracted from water sample collected from PRB1 in June 2016, with AOB outlined in colour
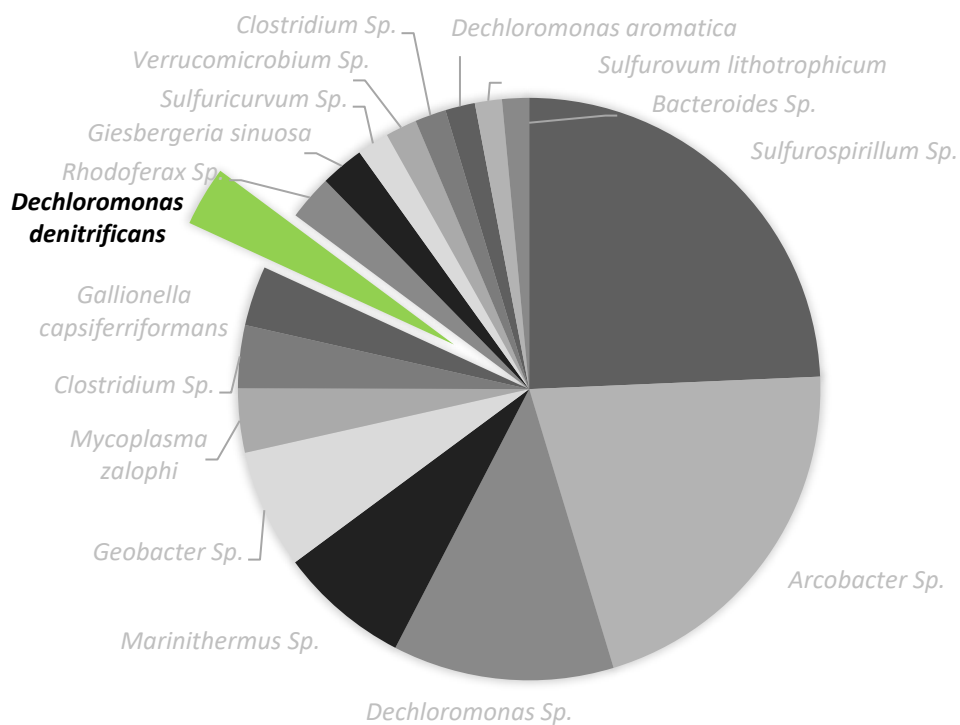


Figure 4. 24: Bacterial species occuring above 1% of total bacterial sequences amplified from eDNA extracted from water sample collected from PRB12 in June 2016, with AOB outlined in colour
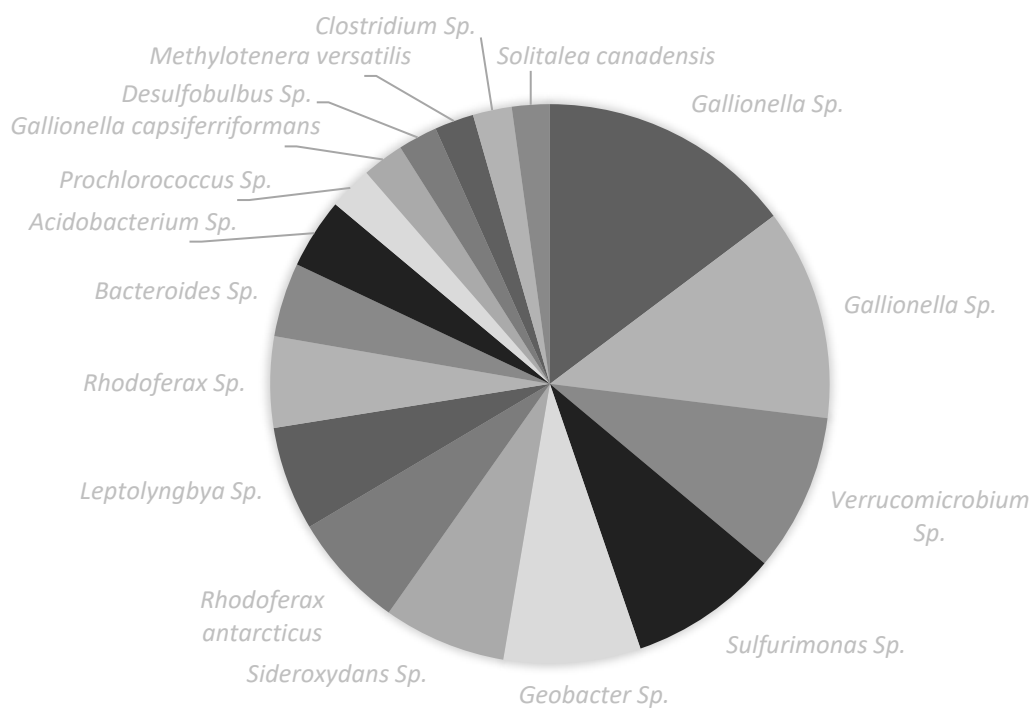
Figure 4. 25: Bacterial species occuring above 1% of total bacterial sequences amplified from eDNA extracted from water sample collected from PRB1 in November 2016, with AOB outlined in colour
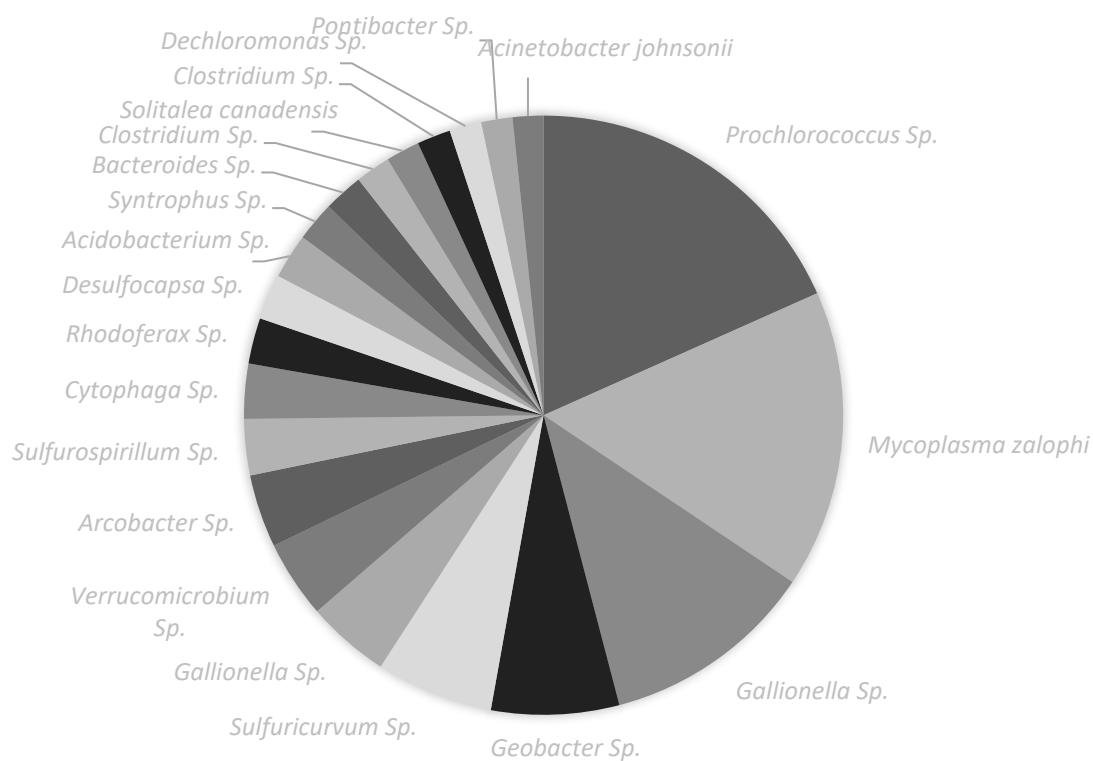


Figure 4. 26: Bacterial species occuring above 1% of total bacterial sequences amplified from eDNA extracted from water sample collected from PRB2 in November 2016, with AOB outlined in colour
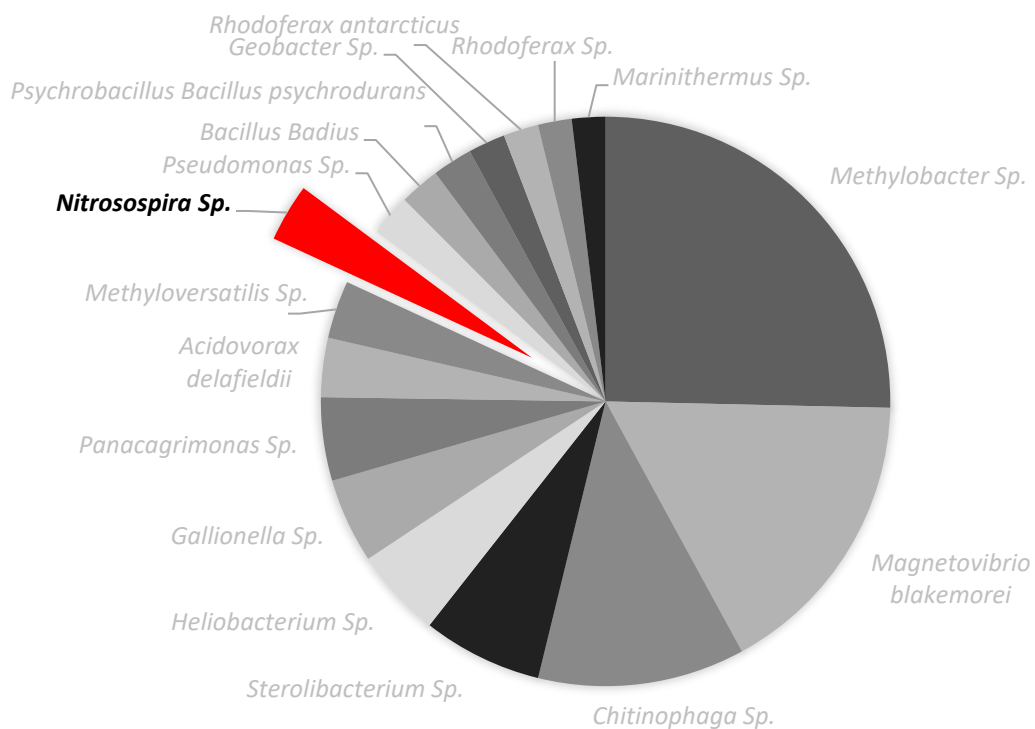
Figure 4. 27: Bacterial species occuring above 1% of total bacterial sequences amplified from eDNA extracted from water sample collected from PRB1 in March 2017, with AOB outlined in colour
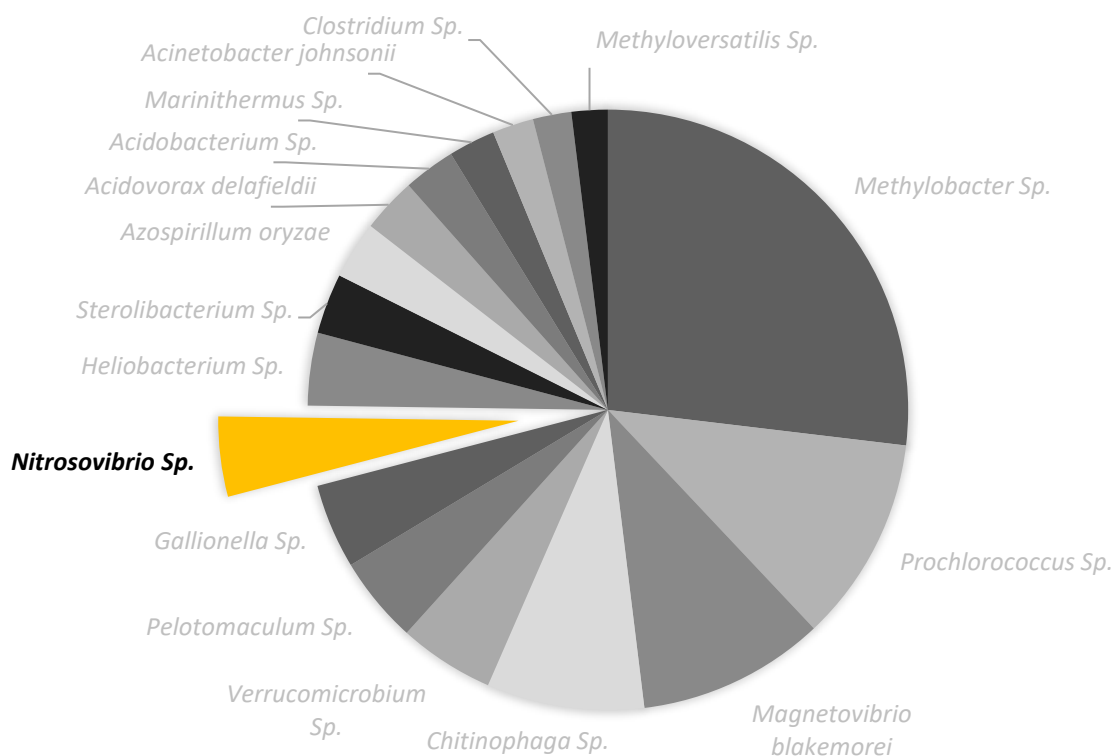


Figure 4. 28: Bacterial species occuring above 1% of total bacterial sequences amplified from eDNA extracted from water sample collected from PRB2 in March 2017, with AOB outlined in colour

While bacteria were the dominant Kingdom, nitrogen cyclers comprised only a small portion of that. The denitrifier *Dechloromonas denitrificans* comprised over 1% of the total bacterial amplicons in PRB1, June 2015 and again in PRB2, June 2016 and was the only nitrogen cycler represented until ammonia oxidiser *Nitrosospira* sp. occurred in PRB1, March 2017. Another ammonia oxidiser, *Nitrosovibrio* sp. also occurred for the first time in March 2017, in PRB2. Methane cyclers (e.g., *Methyloversatilis* sp., *Methanobacter* sp.) were sometimes the dominant genera/ species with sulphur-loving genera/ species (e.g., *Sulfurospirillum* sp., *Sulufuricurvum* sp.) occurring also.

## 4.3.5 Nitrifier diversity in Permeable Reactive Barriers

Six bacterial ammonia oxidisers amplified and were identified (Samocha, 2019; Shaw et al., 2006; Malinowski et al., 2020; Meinecke et al., 1989; Ida et al., 2004; Campbell et al., 2011) from the eDNA extracted from the bioremediation site and their relative abundances are illustrated in Figure 4.29 below.
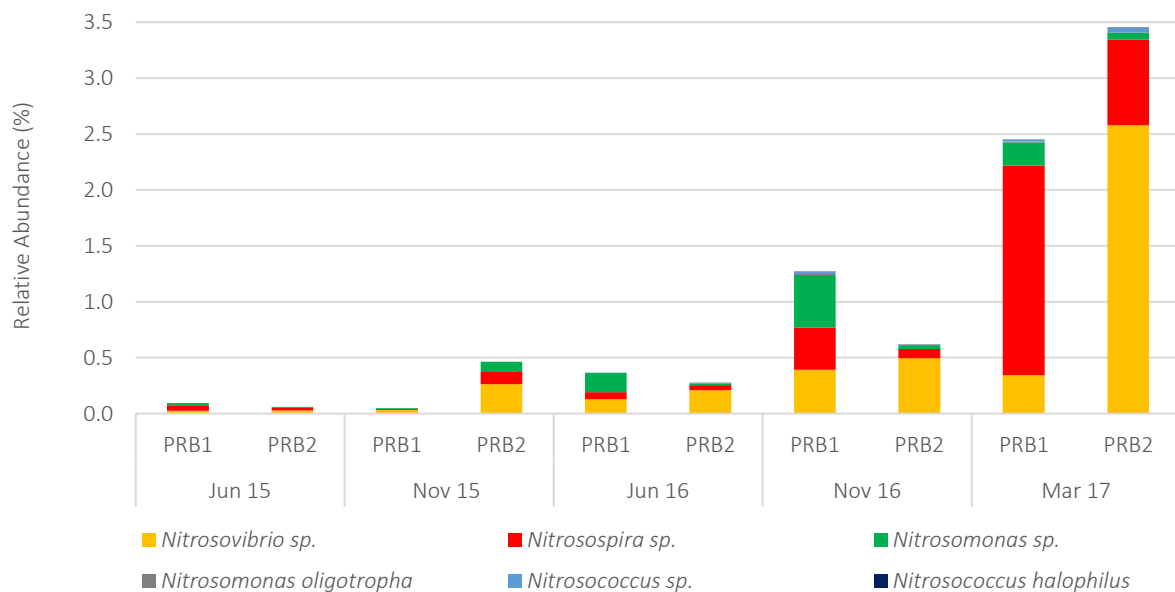


Figure 4. 29: Relative abundance of ammonia oxidising bacteria in the PRBs over two-year period

The highest abundance of amplified ammonia oxidisers occurred in the eDNA extracted from the sample collected in PRB2 in March 17, representing 3.42% of total amplified bacterial DNA (3.36 % of total 16S rRNA amplicons). In June 2015 the amplified AOB abundance was at its lowest in both PRBs with 0.09% amplified AOB of total amplified DNA in PRB1 and 0.05% in PRB2. As was hoped, the quantity of AOBs increased over time in PRB1 though this also occurred in PRB2 which was not intended. This increase was mainly due to an increase in abundance of *Nitrosovibrio* sp.

and *Nitrosospira* sp. Three nitrite oxidising bacteria (NOB) were also identified (Hayatsu et al., 2008; Koops & Stehr, 1991; Teske et al., 1994; Daims et al., 2015; Poly et al., 2008; Freitag et al., 2005), illustrated below in Figure 4.30.
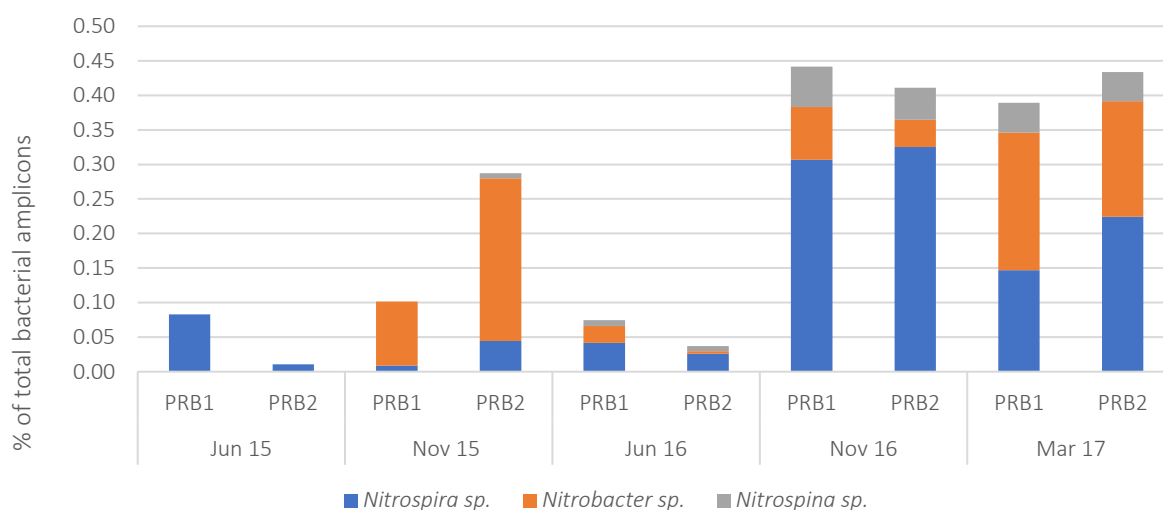


Figure 4. 30: Relative abundance of nitrite oxidising bacteria in the PRBs over two-year period

Initially the quantities of AOB and NOB were similar but over time AOB became the dominant nitrifier increasing over the second half of the study. The quantity of NOBs did not follow the intended pattern being prevalent in both PRBs and ranged between 0.00994% of total amplified DNA in PRB2 in June 2015 and 0.4289168 in PRB1 in November 2016. The conditions in PRB2 were within acceptable limits for NOB in terms of pH (with a median pH of 7.0 in both PRBs) and DO with median concentrations of 2.03 mg $L^{-1}$ and 1.88 mg $L^{-1}$ in PRB1 and PRB2, respectively. As described by Wiszniowski et al. (2006), favourable DO concentrations for aerobic nitrification are ≥ 1mg $L^{-1}$.

## 4.3.6 Denitrifying Diversity in Permeable Reactive Barriers

As described in Section 4.1.2 denitrifying bacteria do not fit comfortably into one taxon. Denitrifiers were identified by searching the amplicon sequencing results for known denitrifying bacteria (Kloos et al., 2001; Throback et al., 2004; Jeter & Ingraham 1981; Wei et al., 2015; Sorokin et al., 2007; Patureau et al., 1998; Anderson et al., 2020; Fahrback et al., 2006; Helen et al., 2016; Toon et al., 2005; Auclair et al., 2012; Berghaust et al., 2010). Some bacteria were only identified to genus level so potentially some denitrifiers have been missed. Below, Figure 4.31 illustrates the thirteen potential denitrifying bacteria identified in the bioremediation site.
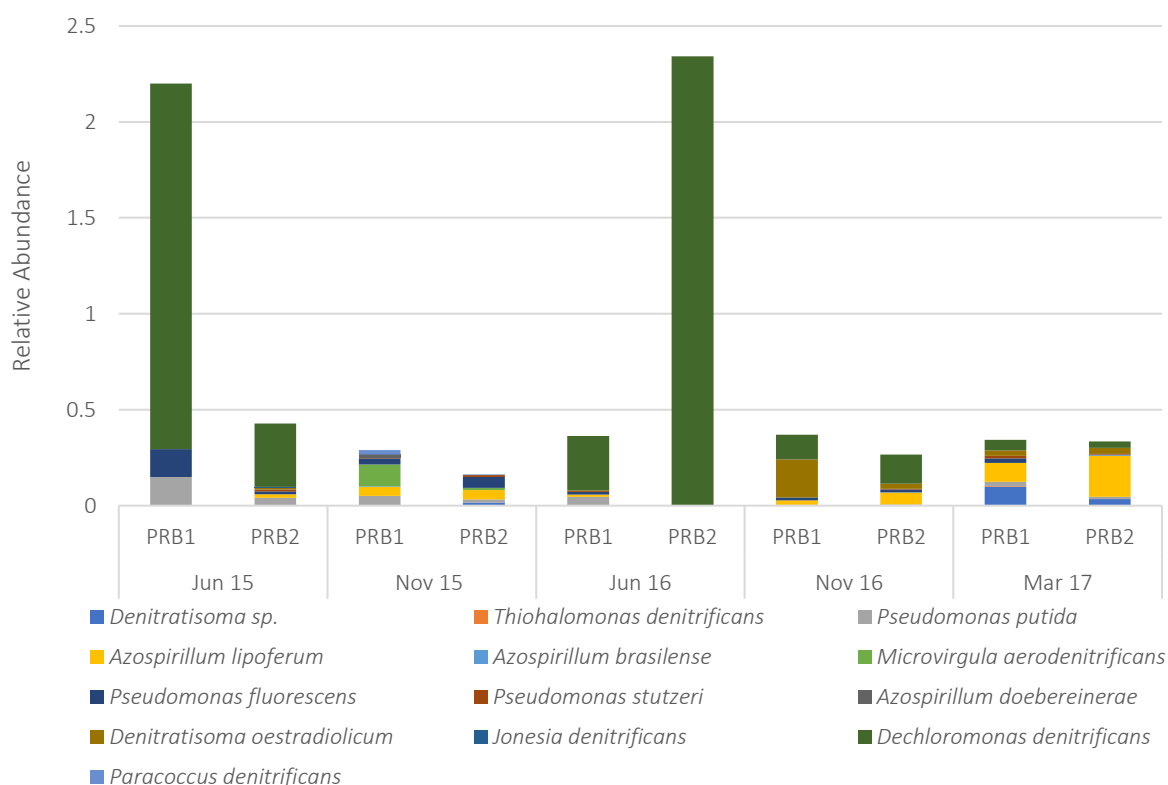
Figure 4. 31: Relative abundance of denitrifying bacteria identified in the PRBs over the two-year study period.

Denitrifying bacterial abundance would remain below 0.32% of total amplified bacterial DNA if not for *Dechloromonas denitrificans* which was responsible for total amplified denitrifying bacterial abundance in PRB2 in June 2016 constituting 2.34% of total amplified bacterial DNA alone. This bacterium was identified as a *nosZ* possessing bacterium (Yoon et al., 2016 & Horn et al., 2005) and made up 5.23% of a total of 7.11% amplified denitrifying bacterial DNA. The remaining bacteria were identified as possessing *nirS, nirK, nosZ* and/ or a combination of two of these genes. *Paracoccus denitrificans*, found only in November 2015 in both PRBs, was identified as possessing a "full suite" of denitrifying genes (Berghaust et al., 2010). While these bacteria were identified as possessing denitrifying genes it should be remembered that this does not mean that the genes were being expressed and also genes could have been amplified from as of yet unknown denitrifiers.

### 4.3.7 Relative Abundance of Nitrogen Cyclers

As discussed in Section 4.2.3, it was decided to target the 16S gene for amplicon sequencing rather than the bacterial or archaeal *amoA*. Of the five genera of known *amoA* possessing ammonia oxidising bacteria previously described in Section 4.1.2, four of the genera amplified and were identified in this study, but *Nitrosobolus* was not. Of the four bacterial nitrite oxidising

genera, *Nitrobacter, Nitrospina* and *Nitrospina* amplified and were identified from the bioremediation site, while *Nitrococcus* was not. Each of the major archaeal ammonia oxidising clusters belonging to the phylum *Thaumarchaeota* amplified and were identified in both PRBs on the bioremediation site. The sequencing results were searched for any known denitrifiers as described in Section 4.3.6. The percentage of total amplified DNA was calculated for each of the four nitrogen cycling communities amplified, Figure 4.32 below.
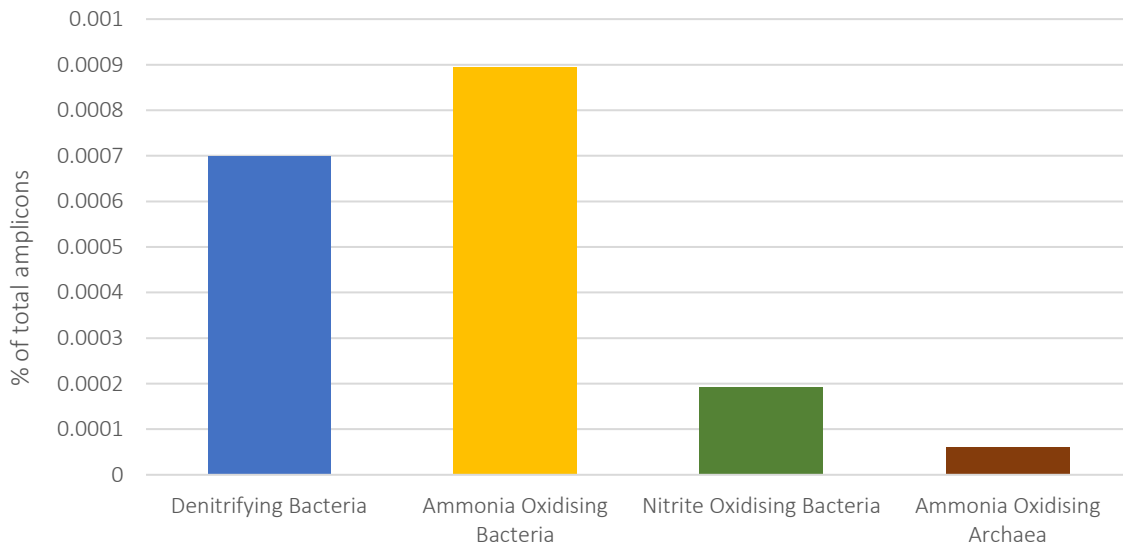


Figure 4. 32: Relative abundance of total denitrifying bacteria, AOB, NOB and AOA as a percentage of total amplified DNA from all 10 samples

As can be seen, the highest quantity of amplified nitrogen cycler DNA was represented by AOB, and the AOA were the least abundant. This corroborated the findings of Limpyakorn et al. (2010), Petersen et al. (2012), Gao et al. (2014), Li et al. (2015) and Gwak et al. (2020) as discussed in Chapter 3, Section 3.1.1 who also noted that AOB were the dominant ammonia oxidisers. Limpyakorn et al. (2010) also noticed that AOA numbers increased significantly once the $NH_4$-N concentration fell below 11 mg $L^{-1}$. The lowest $NH_4$-N concentration occurring in PRB1 was 33.13 mg $L^{-1}$ with an average of 104 mg $L^{-1}$ and the lowest concentration in PRB2 was 15.2 mg $L^{-1}$ with an average concentration of 83 mg $L^{-1}$. Gwak et al. (2020) suggested that the presence of organic compounds (likely to be prevalent in water contaminated by leachate) inhibits AOA. They suggest that considering the high affinity of organic compounds for metals, bioavailable copper (Cu) is removed. A common feature of AOA is the central role of Cu in their metabolism as it is used as a cofactor to many key proteins in AOA including the ammonia monooxygenase (AMO), which performs ammonia oxidation (Reyes et al., 2020). This could be a contributing factor to the low abundance of AOA in groundwater that is polluted by landfill leachate.

The Shannon Diversity Index (SDI) and Shannon Equitability Index (SEI) were calculated for all the nitrogen cyclers amplified and also for the nitrogen cyclers per PRB, Table 4.1 below.

Table 4. 1: The Shannon Diversity Index and Shannon Equitability Index of nitrogen cyclers per PRB

| | Both PRBs | | PRB1 | | PRB2 | |
|---|---|---|---|---|---|---|
| | SDI | SEI | SDI | SEI | SDI | SEI |
| Denitrifying Bacteria | 1.23 | 0.44 | 1.47 | 0.56 | 0.62 | 0.23 |
| Ammonia Oxidising Bacteria | 1.04 | 0.58 | 1.05 | 0.59 | 0.75 | 0.42 |
| Nitrite Oxidising Bacteria | 0.92 | 0.84 | 0.93 | 0.85 | 0.59 | 0.53 |
| Ammonia Oxidising Archaea | 2.00 | 0.83 | 1.89 | 0.86 | 1.90 | 0.87 |

While the AOA were the least abundant, they had the highest SDI of 2.0 and an SEI of 0.83. The denitrifiers were the next most diverse group with an SDI of 1.23 and an SEI of 0.44. AOB had an SDI of 1.04 and an SEI of 0.58. NOB showed the least diversity with an SDI of 0.92 and an SEI of 0.84. Figure 4.33 below shows the four different groups of nitrogen cyclers and their abundance in PRB1 and PRB2 as a percentage of total amplicons.
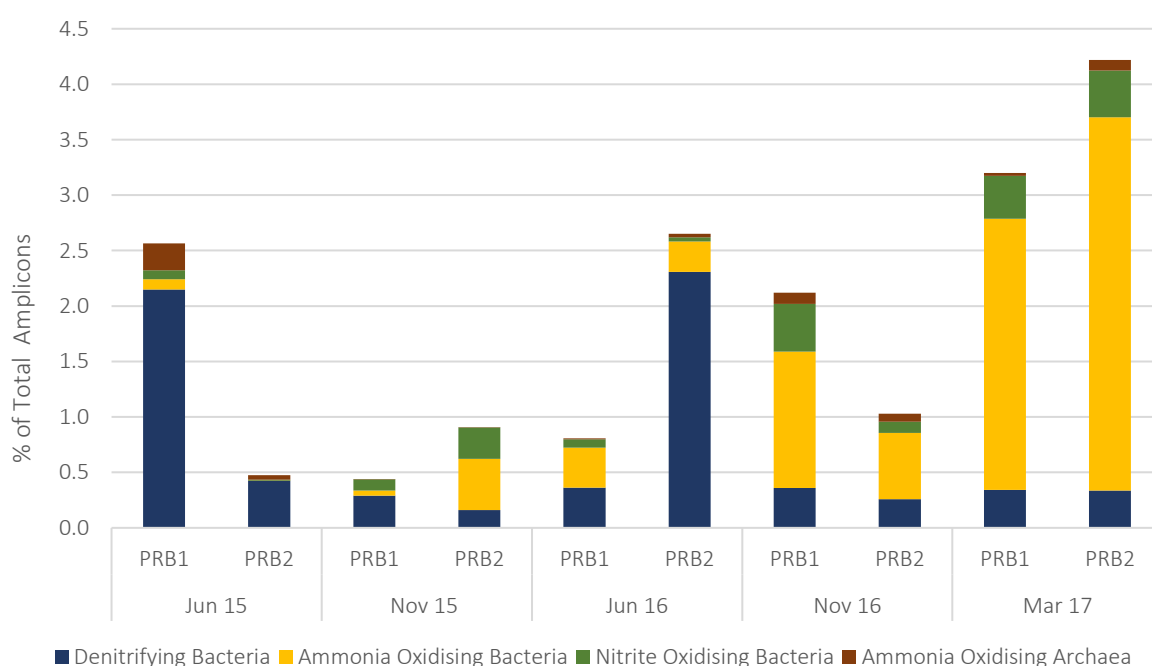


Figure 4. 33: Relative abundance of nitrogen cyclers in PRB1 and PRB2 for the duration of the two-year sampling period

The eDNA collected from PRB1 in June 2015 contained the highest amount of AOA amplicons, suggesting that the original overburden contained archaeal numbers that were never reached again through manipulation of the bioremediation site. Of the nitrogen cyclers that were amplified, denitrifiers were the most abundant in this sample though it was the intention of the experiment to increase nitrifier abundance in PRB 1 and denitrifier abundance in PRB2. This

happened in June 2016 in PRB2 with AOB and NOB occurring in PRB1 as hoped. However, denitrifier abundance decreased thereafter and AOB and NOB abundance increased in both PRBs, not as intended. Figures 4.34 and 4.35 below show nitrogen cycler abundance per PRB.
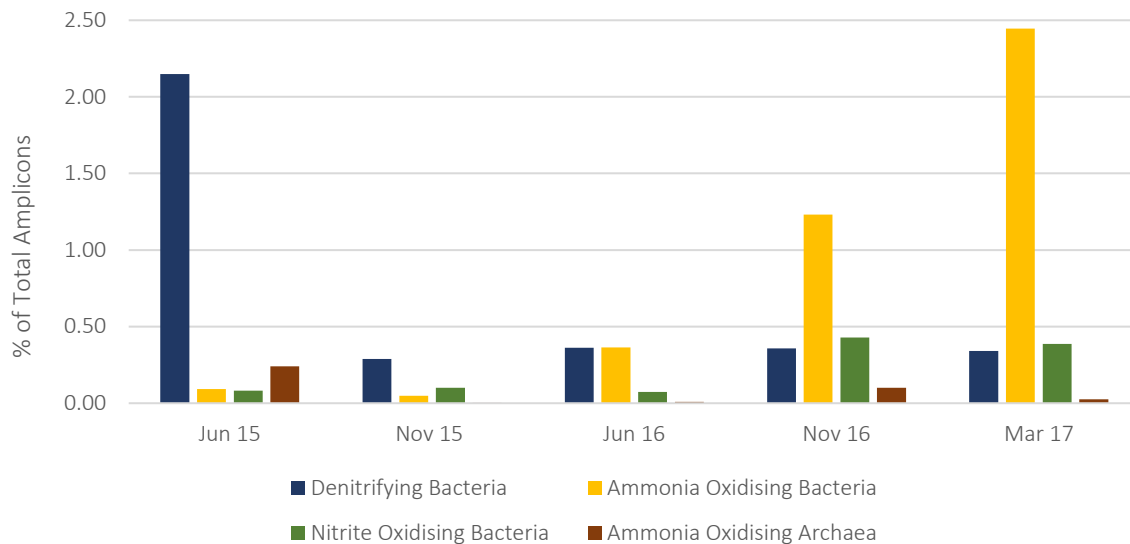


Figure 4. 34: Relative abundance of AOB, NOB, denitrifying bacteria, and AOA in PRB1

In PRB1, the denitrifier quantity decreased once the PRBs were installed and remained lowered for the remainder for the study. AOB and NOB increased in abundance from June 2016 until the end of the study. This indicated that the alteration to favour ammonia oxidisers over denitrifiers in PRB1 was achieved. As discussed in Chapter 2, Li et al. (2014) found that nitrification began to occur in their pilot scale PRB after 10 months of operation. As can be seen in Figure 4.35 below, AOB and NOB began to increase from June 16 (i.e., twelve months after installation) which corroborated these findings. The chemical results also showed a consistently higher concentration of nitrate in monitoring well S3, downstream of PRB1 indicating that nitrification could have been occurring. The Shannon indices for the nitrogen cyclers showed the same order of diversity as those calculated for both PRBs, i.e., AOA showing most diversity followed by denitrifiers then AOB and lastly NOB.
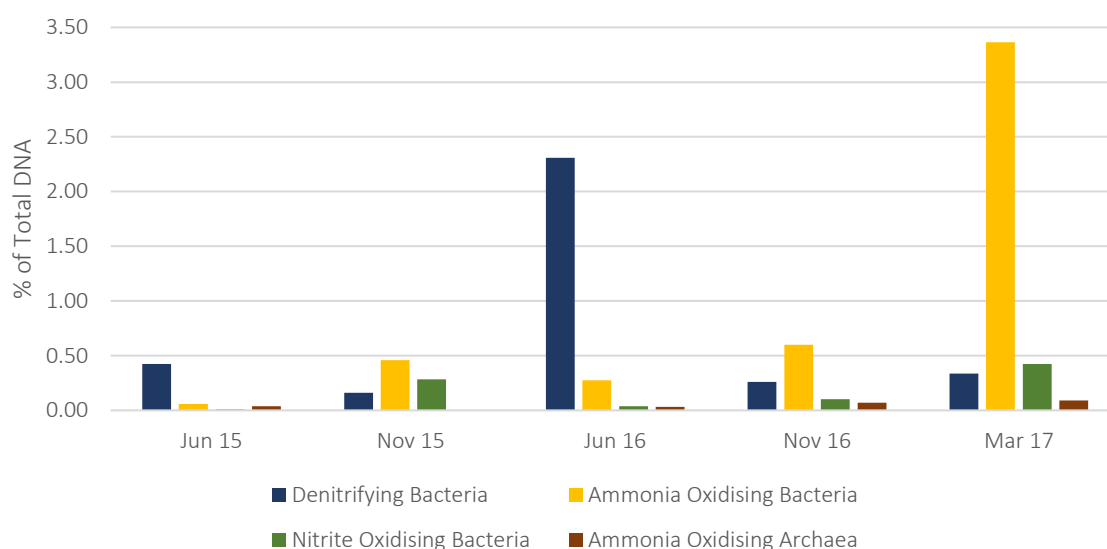
Figure 4. 35: Relative abundance of AOB, NOB, denitrifying bacteria, and AOA in PRB2

There was a higher total number of nitrogen cycler amplicons in PRB2 overall. AOB amplicons increased over time in PRB2, as in PBR1, though it was intended to promote the abundance of denitrifiers over nitrifiers in PRB2 i.e., to create anaerobic conditions. As discussed in Section 2.3.8, aerobic conditions prevailed in PRB2 for the duration of the study. In the graph above, Figure 4.35 shows the highest amplified and identified abundance of denitrifiers occurred in June 2016 where the DO concentrations were 2.3 mg L$^{-1}$ at the time of sampling. This spike in the abundance of denitrifiers was due to an increase in sequences of *Dechloromonas denitrificans,* an N$_2$O producing, *nosZ* possessing microbe (Horn et al., 2005; Yoon et al., 2016) that reduces nitrate to dinitrogen anaerobically (Singh et al., 2009). This would indicate that anaerobic conditions are prevailing in PRB2 at least periodically and that measuring the DO concentrations in water after it has been pumped to the surface is not a true reflection of the oxygen content of the water within the PRBs, as suggested previously in Section 2.3.3. The increase in AOB in PRB2 in March 2017 was due to an increase in sequences of *Nitrosovibro* sp., an ammonia oxidising bacterium which is a prevalent AOB (Meinecke et al., 1989).

The Shannon Index showed highest diversity in the AOA community (SDI of 1.9 and SEI of 0.87) and then AOB (SDI 0.75 and SEI of 0.42) despite the fact that amplified AOA were of the lowest abundance. The denitrifiers showed an SDI of 0.62 and an SEI of 0.23 with the NOB again showing the lowest diversity with an SDI of 0.59 and an SEI of 0.53. As previously mentioned, the abundance of denitrifiers is likely to be underestimated and therefore their diversity is likely to be underestimated also.

## 4.3.8 Chemical Correlations

To ascertain whether field and chemical parameters (Chapter 2) affected the abundance of amplicons from the nitrogen cycling communities, Pearson's test was performed in Microsoft Excel and the p values extrapolated to reveal the significance of any correlations. The cells are highlighted according to whether they are of statistical significance (yellow illustrates a p value of < 0.5, green illustrates a Bonferroni corrected p value of < 0.005). The negative numbers denote negative correlations while positive numbers describe a positive correlation. Nitrate and nitrite concentrations were below the method detection limits for these sampling times so were excluded from the correlation tests. The results are displayed in Table 4.2 below.

Table 4. 2: Correlation results between nitrogen cyclers (relative abundance of amplicons of ammonia oxidising bacteria (AOB), nitrite oxidising bacteria (NOB), ammonia oxidising archaea (AOA) and denitrifying bacteria (DB)) and field and chemical parameters (ammoniacal nitrogen ($NH_4$-N), total organic carbon (TOC), DO (DO), pH, electrical conductivity (EC), and temperature (Temp))

| | $NH_4$-N | TOC | DO | pH | EC | Temp |
|---|---|---|---|---|---|---|
| AOB | -0.74 | -0.25 | -0.83 | 0.36 | 0.53 | -0.90 |
| NOB | -0.73 | -0.04 | -0.72 | 0.48 | 0.06 | -0.92 |
| AOA | -0.26 | -0.13 | -0.16 | -0.39 | 0.05 | 0.17 |
| DB | 0.38 | -0.41 | 0.36 | -0.21 | -0.14 | 0.45 |

| | |
|---|---|
| 0.00 - 0.19 | Very weak correlation |
| 0.20 -0.39 | Weak correlation |
| 0.40 - 0.69 | Modest correlation |
| 0.70 - 0.89 | Strong correlation |
| 0.90 - 1.00 | Very strong correlation |

The strong correlations had p values of less than the Bonferroni corrected p value of <0.005 meaning that they are statistically significant. The AOA showed no correlation with field or chemical parameters. The AOB and NOB showed similar correlations, both displaying strong negative correlations with $NH_4$-N and DO and a very strong negative correlation with temperature. The average DO concentrations during the sampling months that water was collected for amplicon sequencing analysis was 1.6 mg L$^{-1}$. Park & Noguera (2004) found that lower concentrations of DO provided an apparent advantage to the *Nitrosomonas europaea* though this bacterium was not identified on the bioremediation site.  Quyang et al. (2017) noticed that temperature affected AOB numbers but not AOA. Their study found that the optimum temperature for AOA was 41°C and 31°C for AOB, which makes the very strong negative correlation with temperature surprising, especially considering the temperature on the bioremediation site had a modest range of 7.9°C to 18.1°C. The strong negative correlation between AOB and $NH_4$-N is unexpected as AOB are associated with higher nutrient concentrations (Hallin et al., 2009; Bollmann et al., 2014). The AOB showed a modest positive correlation with electrical conductivity while NOB showed a modest positive correlation with pH.

Considering that the nitrogen cycling communities are such a small proportion of the overall microbial community in the contaminated groundwater it should be remembered that there may be other influencing factors. Also, as mentioned previously by Rolling et al. (2000b), there was a significant difference noted in polluted aquifer groundwater and the corresponding sediment, indicating that microbial assessment of groundwater might not be a true reflection of the bioremediation capacity of the soil.

## 4.3.9 Amplicon sequencing vs qPCR Results

Previously in Chapter 3, Section 3.3.4, the presence/ absence of the five functional genes of interest (archaeal and bacterial *amoA,* (present in AOA and AOB) and *nirS, nirK* and *nosZ* (present in denitrifying bacteria)) was assessed using qPCR and gel electrophoresis. The denitrifying genes were ubiquitous while both archaeal and bacterial *amoA* functional genes were more sporadic. Table 4.3 below shows the presence/ absence results overlain with the AOA and AOB percentages of total amplified DNA.

Table 4. 3: Presence/ Absence of bacterial and archaeal *amoA* and relative abundance percentages of AOA and AOB amplicons

| | AOB | | AOA | |
|---|---|---|---|---|
| | PRB1 | PRB2 | PRB1 | PRB2 |
| Jun-15 | 0.092 | 0.059 | 0.241 | 0.038 |
| Nov-15 | 0.049 | 0.459 | 0.000 | 0.002 |
| Jun-16 | 0.363 | 0.274 | 0.008 | 0.033 |
| Nov-16 | 1.231 | 0.598 | 0.102 | 0.070 |
| Mar-17 | 2.445 | 3.365 | 0.025 | 0.093 |

Gene Present
Gene Absent

As can be seen from the table above, there was no correlation between the qPCR (presence/ absence) results and the amplicon sequencing results. For example, the presence/ absence results concluded that the bacterial *amoA* gene was present in PRB 2 in June 15 (AOB 0.059% of amplified DNA) and absent from PRB2 in March 2017 which had a much higher (x56) relative abundance of AOB amplicons (3.365%). Similarly, the qPCR results concluded that the archaeal gene was present in PRB1 in November 2015, when this sample showed the lowest concentration of AOA amplicons.

The differences in these results are most likely due to the fact that different assays were used for the functional gene analysis and the amplicon sequencing. The qPCR used primers specifically aimed at target genes while the amplicon sequencing targeted the *16S rRNA* gene with the aim of identifying microbes. These microbes can only be identified if they have already been isolated,

sequenced and described. Similarly (and conversely), the functional gene analysis could be amplifying functional genes that are not ascribed as yet to any known microbes. An example of this is that a bacterium (*Acidovorax carolinensis*) from the bioremediation site was identified because its *nirS* gene was targeted, amplified, and sequenced. The amplicon sequencing did not identify *Acidovorax carolinensis* though did identify "*Acidovorax* sp".

The qPCR results showed that archaeal *amoA* was mostly absent/ beneath the limit of detection and the results of the amplicon sequencing show that of the amplified sequences, archaea only comprised a small portion (between 0.09% and 2.88%) compared to bacteria. While the functional gene analysis and the amplicon sequencing results were not in alignment, they were complimentary to each other and allowed a better understanding of the microbial communities.

### 4.3.10 Limitations of Sequencing Data

Ion torrent sequencing is becoming less popular (due to its comparatively higher error rate (Salipante et al., 2014)) as costs of other sequencing methods reduce e.g., illumina. Bragg et al., (2013), Deagle et al., (2013) and Salipante et al., (2014) when analysing ion-torrent generated data, observed that a fraction of 16S rRNA sequence reads were prematurely truncated which was highly dependent on both the orientation in which sequencing was performed and the specific organism from which the sequence was derived indicating species bias.

Also, the amplicon sequencing data should have been rarefied (at added cost). Rarefaction is a normalization tool initially developed for ecological diversity analyses to allow for sample comparison without associated bias from differences in sample size (Woese et al., 1990). This is accomplished by reducing the number of observations to a size threshold shared among several samples through random subsampling of the observations. Though some argue that it is inappropriate for detection of differentially abundant species as it returns a high rate of false positives in tests for species that are differentially abundant across sample classes (McMurdie & Holmes, 2014). While there was quality control included in the amplicon sequencing (a model community standard (ZymoBIOMICS™) was sequenced alongside the eDNA samples) a control to check for contamination in the filtration and eDNA extraction steps should also have been sequenced but was not due to budgetary constraints. For the purposes of this study however the amplicon sequencing data provides a relative analysis on the community structure as the same biases and limitations would be the same across all the samples.

## 4.5 Conclusion

The aim of this chapter was to evaluate the nitrogen cycling microbial communities of the PRBs through the use of amplicon sequencing namely Ion Torrent sequencing technology and to relate this back to the bioremediation strategy. As discussed above in Section 4.3.9 the amplicon sequencing provided a broad overview of the microbial communities of the bioremediation site, and this complemented the functional gene analysis which was much more targeted.

However, it should be remembered that the amplicon sequencing results provided information on known nitrogen cyclers only. There was also another limitation, particularly in relation to the denitrifying community that do not fit into a neat taxonomic group and thereby many denitrifying microbes were very likely missed.

The nitrogen cycling community in PRB1 altered as designed over the course of the two-year study period, with AOB and NOB genes becoming more abundant possibly indicating an increase in nitrification and were responsible for the reductions in $NH_4$-N concentrations in PRB1 and caused the concurrent downstream increases in nitrite and nitrate concentrations. The increase in amplified AOB and NOB from month 12 onwards corroborates the results seen in Chapter 2 that suggested nitrification beginning to occur in month 10.  However, the microbial community in PRB2 did not appear to be adjusted as hoped, with lower denitrifier abundance and diversity than PRB1. Though as stated previously, the amplicon sequencing results have very likely vastly underestimated the abundance of denitrifiers. Also, the amplicon sequencing results are based on amplicons from eDNA extracted from groundwater rather than from the more stable microbial environments of sediment that are less influenced by external factors, meaning that these results may not be a true reflection of the bioremediation capacity of the site.

# General Conclusion

The scope of this study was wide ranging and required a broad understanding of an array of different subjects because designing an *in-situ* bioremediation strategy requires a knowledge of a range of different subjects.

To design an appropriate bioremediation site specific to Doora landfill to reduce high $NH_4$-N contamination in groundwater, a desk-based scoping exercise was performed initially. This involved detailed investigations of previous hydrogeological surveys and contamination monitoring that had been carried out previously on the site by environmental consultancies commissioned by Clare County Council. It also involved using online resources such as the National Biodiversity Data Centre and Geological Survey Ireland to better inform the design of the bioremediation strategy. Laboratory testing in the form of bench tests and column experiments were carried out to test the viability of locally sourced reactive materials. Once the contamination issues and the hydrogeology of the site were understood, and the reactive materials selected and tested, the concept design of sequential PRBs could be physically realised on site. The chosen design saw two PRBs installed to intercept the contaminated groundwater plume before the contamination reached the surface water boundaries of the landfill and supplemented with monitoring wells upstream and downstream. The first PRB was designed to promote the activity of ammonia oxidising microbes to cycle $NH_4$-N through the nitrification phase of the nitrogen cycle. The selected reactive material, locally sourced limestone, was chosen to increase the pH and DO concentrations of the groundwater and to allow for surface attachment, which are requirements of autotrophic nitrifiers. The second PRB was designed to cycle the nitrification product of $NO_3$ through the denitrification phase of the nitrogen cycle to the gaseous end product of dinitrogen gas. The selected reactive material, locally sourced mulch, was chosen to decrease the pH and DO concentrations of the groundwater and to provide a carbon source, requirements for heterotrophic denitrifiers.

As this was a novel study, in-depth monitoring was required. The monthly field and chemical monitoring were supplemented by molecular investigations, namely functional gene analysis (through qPCR) and microbial community assessment (through amplicon sequencing) for a 24-month period. pH, DO, temperature, and electrical conductivity were monitored onsite each month and samples were collected for chemical analysis (i.e., $NH_4$-N, $NO_2$, $NO_3$ and TOC). Water was also collected so that eDNA could be extracted for further downstream molecular analysis.

Statistical analysis was applied to the field and chemical monitoring results. The field parameters that the study hoped to influence (i.e., pH and DO) did not show statistically significant differences between wells, though the pH parameters in both PRB1 and PRB2 were appropriate for nitrifiers and denitrifiers, respectively. DO concentrations in PRB1 remained at optimal conditions (i.e., >1.0 mg L$^{-1}$) for 21 of the 24-month period in PRB1, though they were not optimal for denitrifiers in PRB2 (i.e., below 0.5 mg L$^{-1}$). While the DO concentrations were not ideal for anaerobic denitrifiers as hoped, the conditions were optimal for aerobic denitrifiers belonging to *Pseudomonadota* (formerly *Proteobacteria*) that work efficiently within a pH range of $7 - 8$ and with DO concentrations of up to 5 mg L$^{-1}$. This was illustrated by the discovery of *Acidovorax carolinensis,* which is described as an aerobe that possesses the denitrifying functional gene *nirS*, from the bioremediation site.

The statistical analysis showed that the concentrations of NH$_4$-N in downstream monitoring well S5 were significantly (p<0.005) lower than all other upstream wells (though still not below the EU limits for groundwater and surface water). PRB1 was shown to cause a significant (P<0.005) reduction in the target contaminant (NH$_4$-N) concentrations and PRB2 was shown to significantly (p<0.005) reduce concentrations of NO$_3$, both positive indicators of bioremediation occurring as designed. If bioremediation was only beginning to occur after one year in operation perhaps further reductions in NH$_4$-N would be noted if the bioremediation site was being monitored.

The functional gene analysis was used to gain a further insight into the efficacy of the PRBs at bioremediating ammonia from shallow groundwater. Structural gene *16S rRNA* and five nitrogen cycling functional genes (i.e., bacterial, and archaeal *amoA, nirS, nirK* and *nosZ*) were monitored quarterly over the 24-month study from each of the five monitoring wells. New primer sets were designed to amplify the *nirS* functional gene for conventional and qPCR and worked well and could be trialled for future use in other studies. The new primer set nirS32F/ nirS64R was used to create a positive standard from eDNA extracted from the bioremediation site and the resulting sequence revealed the gene to belong to *Acidovorax carolinensis*, an aerobic bacterium isolated from a contaminated site in North Carolina and first described and named in 2018. The functional gene analysis showed that denitrifying microbes were ubiquitous across the bioremediation site and (supported by the culturing results) corroborated the indication discussed in Chapter 2 that aerobic denitrification was occurring in PRB2.

The gene copy number (GCN) results were not used to compare functional gene abundance as it was felt that the GCN between functional genes were not relative due to the extremely low

concentrations of the target genes in the eDNA and therefore should not be used for comparative purposes. The presence and/ or absence of functional genes were used instead. Both nitrifying and denitrifying microbial genes were detected in all sampling wells in the bioremediation site but did not show preference for either PRB over time. It should be remembered that there could be nitrogen cycling microbes present in the bioremediation site that were not detected by the primers used. The database itself used for primer design is biased towards those microbes that can be cultured and identified from metagenomics DNA. While it was disappointing that the GCN could not be relied upon to analyse the abundance of nitrogen cycling functional genes, it showed that nitrogen cycling microbes were present in the bioremediation site and that bioremediation as suspected in Chapter 2, could be taking place.

There has been much debate (as discussed in Section 4.1.2) regarding who are the heavy lifters in terms of ammonia oxidisation - archaea or bacteria. The microbial community data set generated by this study revealed that of the amplicons sequenced the vast majority were bacterial (from 97.04% to 99.65% of total amplicons sequenced). Of the sequences amplified belonging to nitrogen cyclers $8.94 \times 10^{-4}$ % belonged to bacterial ammonia oxidisers while even fewer belonged to archaeal ammonia oxidisers i.e., $6.09 \times 10^{-6}$ % The amplicon sequencing revealed a wide array of microbial communities and the analysis showed that the nitrogen cycling community in PRB1 altered as designed over the course of the two-year study period, with AOB and NOB genes becoming more abundant and a reduction in the abundance of genes of known denitrifying genera, possibly indicating an increase in nitrification and a concurrent downstream increase in nitrate concentrations. The increase in amplified AOB and NOB from month 12 onwards corroborates the results seen in Chapter 2.

As far as can be seen, these were the first set of full-scale *in-situ* sequential PRBs designed to bioremediate ammonia and indications of their success are heartening. The hypothesis of this study was "PRBs can provide an environmentally and economically sustainable solution to ammonia contamination in shallow groundwater" and was accepted. The only costs from the bioremediation site were the installation of the PRBs (kindly supported by Clare County Council) and the monitoring wells with no on-going maintenance costs. They were also environmentally sustainable. Their scope is wide ranging and if refined further they could be readily applied to other sites once the proper local investigations take place. There are numerous sites across Ireland (e.g., Tramore Beach in Waterford) where landfills have been located (following the now outdated "dilute and disperse" model) next to surface water receptors. It is hoped that the

knowledge generated from this study could be used to inform bioremediation strategies for contaminated sites like these in future. Similar scoping exercises would need to be performed to fully understand the contamination issues to the site and a bespoke bioremediation strategy would be tailored to it.

The bioremediation site is still in place in Doora landfill. Potentially, with the permission of Clare County Council, the site could be monitored again for chemical analysis to ascertain whether $NH_4$-N concentrations have been further reduced. Pending the chemical analysis, the PRBs could be adjusted or added to, to address some of the issued highlighted in this study. For instance, a zeolite barrier (as used by some studies outlined in Chapter 1) could be installed on the site to align with PRB1. This would remove the unknown between the two PRBs as are currently installed and would allow for adsorption of the $NH_4$-N thereby adding another (and more immediate though short-term) remediation strategy.

# Bibliography

Abiriga, D., Jenkins, A., Alfsnes, K., Vestgarden, L. S., & Klempe, H. (2021). Characterisation of the bacterial microbiota of a landfill-contaminated confined aquifer undergoing intrinsic remediation. *Science of the Total Environment*, *785*, 147349.

Adamiak, J., Otlewska, A., Tafer, H., Lopandic, K., Gutarowska, B., Sterflinger, K., & Piñar, G. (2018). First evaluation of the microbiome of built cultural heritage by using the Ion Torrent next generation sequencing platform. *International Biodeterioration & Biodegradation*, *131*, 11-18.

Addy, K., Gold, A. J., Christianson, L. E., David, M. B., Schipper, L. A., & Ratigan, N. A. (2016). Denitrifying Bioreactors for Nitrate Removal: A Meta-Analysis. *Journal of Environmental Quality*, *45*(3), 873–881.

Altschul, S. F., Gish, W., Miller, W., Myers, E. W., & Lipman, D. J. (1990). Basic local alignment search tool. *Journal of molecular biology*, *215*(3), 403-410.

Amann, R. I., Ludwig, W., & Schleifer, K. H. (1995). Phylogenetic identification and in situ detection of individual microbial cells without cultivation. *Microbiological Reviews*, *59*(1), 143–169.

Anderson, E. L., Jang, J., Venterea, R. T., Feyereisen, G. W., & Ishii, S. (2020). Isolation and characterization of denitrifiers from woodchip bioreactors for bioaugmentation application. *Journal of Applied Microbiology*, *129*(3), 590-600.

Auclair, J., Parent, S., & Villemur, R. (2012). Functional diversity in the denitrifying biofilm of the methanol-fed marine denitrification system at the Montreal Biodome. *Microbial Ecology*, *63*(4), 726-735.

Bates, S. T., Berg-Lyons, D., Caporaso, J. G., Walters, W. A., Knight, R., & Fierer, N. (2011). Examining the global distribution of dominant archaeal populations in soil. *The ISME journal*, *5*(5), 908-917.

Bedessem, M. E., Edgar, T. V, & Roll, R. (1994). Nitrogen removal in laboratory model leachfields with organic-rich layers. *Journal of Environmental Quality*, *34*(3), 936–942.

Beauchamp, E. G., Trevors, J. T. & Paul, J. W. (1989). Carbon sources for bacterial denitrification. *Adv. Soil Sci.* 10, 113–142.

Bergaust, L., Mao, Y., Bakken, L. R., & Frostegård, A. (2010). Denitrification response patterns during the transition to anoxic respiration and posttranscriptional effects of suboptimal pH on nitrogen oxide reductase in Paracoccus denitrificans. *Applied and environmental microbiology*, *76*(19), 6387-6396.

Bharagava, R. N., Purchase, D., Saxena, G., & Mulla, S. I. (2019). Applications of metagenomics in microbial bioremediation of pollutants: from genomics to environmental cleanup. In *Microbial diversity in the genomic era* (pp. 459-477). Academic Press.

Bier, R.L., Bernhardt, E.S., Boot, C.M., Graham, E.B., Hall, E.K., Lennon, J.T., Nemergut, D.R., Osborne, B.B., Ruiz-González, C., Schimel, J.P. & Waldrop, M.P. (2015). Linking microbial community structure and microbial processes: an empirical and conceptual overview. *FEMS microbiology ecology*, *91*(10).

Bock, E., & Wagner, M. (2006). Oxidation of inorganic nitrogen compounds as an energy source. *The prokaryotes*, *2*, 457-495.

Böhlke, J. K., Smith, R. L., & Miller, D. N. (2006). Ammonium transport and reaction in contaminated groundwater: Application of isotope tracers and isotope fractionation studies. *Water Resources Research*, *42*(5).

Bollmann, A., Bullerjahn, G. S., & McKay, R. M. (2014). Abundance and diversity of ammonia-oxidizing archaea and bacteria in sediments of trophic end members of the Laurentian Great Lakes, Erie and Superior. PLoS One, 9(5), e97068.

Bouskill, N., Tang, T., Riley, W., & Brodie E. (2012). Trait-based representation of biological nitrifrication: model development, testing, and predicted community composition. *Frontiers in Microbiology (*3) 364 - 381.

Bragg, L. M., Stone, G., Butler, M. K., Hugenholtz, P., & Tyson, G. W. (2013). Shining a light on dark sequencing: characterising errors in Ion Torrent PGM data. *PLoS computational biology*, *9*(4), e1003031.

Braker, G., Fesefeldt, A., & Witzel, K. P. (1998). Development of PCR primer systems for amplification of nitrite reductase genes (nirK and nirS) to detect denitrifying bacteria in environmental samples. *Applied and environmental microbiology*, *64*(10), 3769-3775.

Brennan, R. B., Healy, M. G., Morrison, L., Hynes, S., Norton, D., & Clifford, E. (2016). Management of landfill leachate: The legacy of European Union Directives. *Waste management*, *55*, 355-363.

Brennan, R. B., Healy, M. G., Morrison, L., Hynes, S., Norton, D., & Clifford, E. (2017). Suitability of municipal wastewater treatment plants for the treatment of landfill leachate. *Wexford, Ireland: Environmental Protection Agency*.

Brochier-Armanet, C., Boussau, B., Gribaldo, S., & Forterre, P. (2008). Mesophilic Crenarchaeota: proposal for a third archaeal phylum, the Thaumarchaeota. *Nature Reviews Microbiology*, *6*(3), 245-252.

Calli, B., Mertoglu, B., Roest, K., & Inanc, B. (2006). Comparison of long-term performances and final microbial compositions of anaerobic reactors treating landfill leachate. *Bioresource Technology*, *97*(4), 641–647. https://doi.org/10.1016/j.biortech.2005.03.021

Campbell, M. A., Chain, P. S., Dang, H., El Sheikh, A. F., Norton, J. M., Ward, N. L., ... & Klotz, M. G. (2011). Nitrosococcus watsonii sp. nov., a new species of marine obligate ammonia-oxidizing bacteria that is not omnipresent in the world's oceans: calls to validate the names 'Nitrosococcus halophilus' and 'Nitrosomonas mobilis'. *FEMS microbiology ecology*, *76*(1), 39-48.

Cameron, E. S., Schmidt, P. J., Tremblay, B. J. M., Emelko, M. B., & Müller, K. M. (2021). Enhancing diversity analysis by repeatedly rarefying next generation sequencing data describing microbial communities. *Scientific reports*, *11*(1), 1-13.

Cao, H., Auguet, J. C., & Gu, J. D. (2013). Global ecological pattern of ammonia-oxidizing archaea. *PloS one*, *8*(2), e52853.

Carley, B.N. and Mavinic, D.S. (1991). The effects of external carbon loading on nitrification and denitrification of a high-ammonia landfill leachate. *Research Journal of the Water Pollution Control Federation*, pp.51-59.

Casciotti, K. L., & Ward, B. B. (2001). Dissimilatory Nitrite Reductase Genes from Autotrophic Ammonia-Oxidizing Bacteria. *Applied and Environmental Microbiology*, *67*(5), 2213–2221.

Castro-Gutiérrez, V., Masís-Mora, M., Diez, M. C., Tortella, G. R., & Rodríguez-Rodríguez, C. E. (2017). Aging of biomixtures: effects on carbofuran removal and microbial community structure. *Chemosphere*, *168*, 418-425.

Chen, L. X., Méndez-García, C., Dombrowski, N., Servín-Garcidueñas, L. E., Eloe-Fadrosh, E. A., Fang, B. Z., ... & Shu, W. S. (2018). Metabolic versatility of small archaea Micrarchaeota and Parvarchaeota. *The ISME journal*, *12*(3), 756-775.

Chen, R., Yao, J., Ailijiang, N., Liu, R., Fang, L., Chen, Y. (2019). Abundance and diversity of nitrogen-removing microorganisms in the UASB-anammox reactor. *PLos one* 14(4),

p.e0215615.

Christensen, T. H., Kjeldsen, P., Albrechtsen, H., Heron, G., Nielsen, P. H., Bjerg, P. L., & Holm, P. E. (1994). Attenuation of landfill leachate pollutants in aquifers. *Critical Reviews in Environmental Science and Technology*, *24*(2), 119–202.

Chan, 2009. Overview of Historic Unlicenced Waste Disposal Sites in Ireland. Office of Environmental Enforcement, The Environmental Protection Agency, Ireland.

Costa, E., Pérez, J. & Kreft, J.U. (2006). Illustration of the kinetic theory of optimal pathway length. *Trends in Microbiology*, *5*(14), 213-219.

Colloff, M.L., Wakelin, S.A., Fomez, D & Rogers S.L. (2008). Detection of nitrogen cycle genes in soils for measuring the effects of changes in land use and management. *Soil Biology & Biochemistry,* 40(7), 1637 - 1645.

Conte, J., Potoczniak, M. J., & Tobe, S. S. (2018). Using synthetic oligonucleotides as standards in probe-based qPCR. *Biotechniques*, *64*(4), 177-179.

Crutzen, P. J. (1970). The influence of nitrogen oxides on the atmospheric ozone content. *Quarterly Journal of the Royal Meteorological Society*, *96*(408), 320–325.

Czaplicki, L. M., & Gunsch, C. K. (2016). Reflection on molecular approaches influencing state-of-the-art bioremediation design: culturing to microbial community fingerprinting to omics. *Journal of Environmental Engineering*, *142*(10), 03116002.

Daebeler, A., Herbold, C. W., Vierheilig, J., Sedlacek, C. J., Pjevac, P., Albertsen, M., … & Wagner, M. (2018). Cultivation and genomic analysis of "Candidatus Nitrosocaldus islandicus," an obligately thermophilic, ammonia-oxidizing thaumarchaeon from a hot spring biofilm in Graendalur Valley, Iceland. *Frontiers in microbiology*, *9*, 193.

Daims, H., Elena, V., Palatinszky, M., Vierheilig, J., Bulaev, A., Kirkegaard, R. H., Bergen, M. Von, & Rattei, T. (2015). Complete nitrification by Nitrospira bacteria. *Nature*, *528*(7583), 504–509.

Dalsgaard, T., Thamdrup, B., & Canfield, D. E. (2005). Anaerobic ammonium oxidation (anammox) in the marine environment. *Research in Microbiology*, *156*(4), 457–464.

Dalton, H., & Brand-Hardy, R. (2003). Nitrogen, the essential public enemy. *Journal of Applied Ecology*, 40 (5), 771–781.

Deagle, B. E., Thomas, A. C., Shaffer, A. K., Trites, A. W., & Jarman, S. N. (2013). Quantifying sequence proportions in a DNA-based diet study using Ion Torrent amplicon sequencing: which counts count? *Molecular Ecology Resources*, *13*(4), 620-633.

Dechesne, A., Musovic, S., Palomo, A., Diwan, V. and Smets, B.F., 2016. Underestimation of ammonia-oxidizing bacteria abundance by amplification bias in amoA-targeted qPCR. *Microbial biotechnology*, *9*(4), pp.519-524.

De Jong, F. (2007). *Marine eutrophication in perspective: on the relevance of ecology for environmental policy*. Springer Science & Business Media.

Demeke, T., & Jenkins, G. R. (2010). Influence of DNA extraction methods, PCR inhibitors and quantification methods on real-time PCR assay of biotechnology-derived traits. *Analytical and bioanalytical chemistry*, *396*(6), 1977-1990.

De la Torre, J. R., Walker, C. B., Ingalls, A. E., Könneke, M., & Stahl, D. A. (2008). Cultivation of a thermophilic ammonia oxidizing archaeon synthesizing crenarchaeol. *Environmental microbiology*, *10*(3), 810-818.

Department for Environment, Food and Rural Affairs (Defra), (2006). Post-conciliation Partial Regulatory Impact Assessment. Groundwater Proposals under Article 17 of the Water Framework Directive. Draft final report. Defra, London.

Desai, C., Pathak, H., & Madamwar, D. (2010). Advances in molecular and "-omics" technologies

to gauge microbial communities and bioremediation at xenobiotic/anthropogen contaminated sites. *Bioresource Technology*, *101*(6), 1558–1569.

Di, H. J., Cameron, K. C., Shen, J. P., Winefield, C. S., O'Callaghan, M., Bowatte, S., & He, J. Z. (2009). Nitrification driven by bacteria and not archaea in nitrogen-rich grassland soils. *Nature Geoscience*, *2*(9), 621–624.

Ding, K., Wen, X., Li, Y., Shen, B., & Zhang, B. (2015). Ammonia-oxidizing archaea versus bacteria in two soil aquifer treatment systems. Applied microbiology and biotechnology, 99(3), 1337-1347.

Du, Q., Liu, S., Cao, Z., & Wang, Y. (2005). Ammonia removal from aqueous solution using natural Chinese clinoptilolite. *Separation and purification technology*, *44*(3), 229-234.

Du, Q., Liu, S., Cao, Z. & Wang, Y. (2005). Ammonia removal from aqueous solution using natural Chinese clinoptilolite. *Separation and purification technology*, *44*(3), 229-234.

Ehrig, H.J. (1989). Leachate quality in: Christensen, T.H., Cossu, R., Stegman, R. (Eds.), Sanitary Landfilling: Process, Technology, and Environmental Impact. Academic Press, New York.

Elbanna, K., El-Shahawy, R. M., & Atalla, K. M. (2012). A new simple method for the enumeration of nitrifying bacteria in different environments. *Plant, Soil and Environment*, *58*(1), 49-53.

EPA. (2003). Towards setting guideline values for the protection of groundwater- Interim Report. Environmental Protection Agency.

EPA, "EPA Licensed Sites Report on Waste Enforcement," 2015.

EPA (2021) https://www.epa.ie/news-releases/news-releases-2021/ireland-continues-to-be-in-non-compliance-with-the-eu-national-emissions-ceiling-directive.php Accessed October, 2021.

Fahrbach, M., Kuever, J., Meinke, R., Kämpfer, P., & Hollender, J. (2006). Denitratisoma oestradiolicum gen. nov., sp. nov., a 17β-oestradiol-degrading, denitrifying betaproteobacterium. *International Journal of Systematic and Evolutionary Microbiology*, *56*(7), 1547-1552.

Farman, J. C., Gardiner, B. G., & Shanklin, J. D. (1985). Large losses of total ozone in Antarctica reveal seasonal ClOx/NOx interaction. *Nature*, *315*(6016), 207–210.

Faris, B., & Vlassopoulos, D. (2003). A systematic approach to in situ bioremediation in groundwater. *Remediation Journal: The Journal of Environmental Cleanup Costs, Technologies & Techniques*, *13*(2), 27-52.

Fehily Timoney & Co. (1992). Doora Landfill Site Ground Investigation. Clare County Council.

Fehily Timoney & Co. (1998a). Section C.6 of Waste Licence Application Document, Doora Landfill. Clare County Council.

Fehily Timoney & Co. (1998b). Hydrogeological Cross Sections, Doora Landfill. Clare County Council.

Fehily Timoney & Co. (2004). Submission on Trial Hole Investigations, Doora Landfill. Clare County Council.

Felske, A., Wolterink, A., Van Lis, R., De Vos, W. M., & Akkermans, A. D. L. (1999). Searching for predominant soil bacteria: 16S rDNA cloning versus strain cultivation. *FEMS Microbiology Ecology*, *30*(2), 137–145.

Fierer, N., Jackson, J. A., Vilgalys, R., & Jackson, R. B. (2005). Assessment of soil microbial community structure by use of taxon-specific quantitative PCR assays. *Applied and environmental microbiology*, *71*(7), 4117-4120.

Fortunato, C. S., Carlini, D. B., Ewers, E., & Bushaw-Newton, K. L. (2009). Nitrifier and denitrifier molecular operational taxonomic unit compositions from sites of a freshwater estuary of Chesapeake Bay. *Canadian Journal of Microbiology*, *55*(3), 333-346.

Fowler, J., Cohen, L. and Jarvis, P., 2013. *Practical statistics for field biology*. John Wiley & Sons

Fowler, D., Coyle, M., Skiba, U., Sutton, M. A., Cape, J. N., Reis, S., Sheppard, L. J., Jenkins, A., Grizzetti, B., Galloway, N., Vitousek, P., Leach, A., Bouwman, A. F., Butterbach-bahl, K., Dentener, F., Stevenson, D., Amann, M., & Voss, M. (2013). *The global nitrogen cycle in the twenty- first century*. Philosophical Transactions of the Royal Society B: Biological Sciences, *368*(1621), p.20130164.

Francis, C. A., Roberts, K. J., Beman, J. M., Santoro, A. E., & Oakley, B. B. (2005). Ubiquity and diversity of ammonia-oxidizing archaea in water columns and sediments of the ocean. *Proceedings of the National Academy of Sciences of the United States of America*, *102*(41), 14683–14688.

Francis, C. A., Beman, J. M., & Kuypers, M. M. (2007). New processes and players in the nitrogen cycle: the microbial ecology of anaerobic and archaeal ammonia oxidation. *The ISME Journal*, *1*(1), 19–27.

Freitag, T. E., Chang, L., Clegg, C. D., & Prosser, J. I. (2005). Influence of inorganic nitrogen management regime on the diversity of nitrite-oxidizing bacteria in agricultural grassland soils. *Applied and environmental microbiology*, *71*(12), 8323-8334.

Galloway, J. N., Leach, A. M., Bleeker, A., & Erisman, J. W. (2013). A chronology of human understanding of the nitrogen cycle. *Philosophical Transactions of the Royal Society B: Biological Sciences*, *368*(1621).

Galloway, J. N., Aber, J. D., Erisman, J. W., Seitzinger, S. P., Howarth, R. W., Cowling, E. B., & Cosby, B. J. (2003). The nitrogen cascade. *BioScience*, *53*(4), 341–356.

Galvão, T. C., Mohn, W. W., & De Lorenzo, V. (2005). Exploring the microbial biodegradation and biotransformation gene pool. *Trends in Biotechnology*, *23*(10), 497–506.

Gao, J., Luo, X., Wu, G., Li, T., & Peng, Y. (2014). Abundance and diversity based on amoA genes of ammonia-oxidizing archaea and bacteria in ten wastewater treatment systems. *Applied microbiology and biotechnology*, *98*(7), 3339-3354.

Garrett, K. E., & Hudson, A. L. (2005). Large-scale application of in-situ remediation to remove nitrate from groundwater. *Federal Facilities Environmental Journal*, *16*(1), 97–108.

Gavaskar, A. R. (1999). Design and construction techniques for permeable reactive barriers. *Journal of Hazardous Materials*, *68*(1–2), 41–71.

Gavaskar, A., Gupta, N., Sass, B., Janosy, R., & Hicks, J. (2000). *Design guidance for application of permeable reactive barriers for groundwater remediation.* Battelle Columbus Operations OH.

Gibert, O., Pomierny, S., Rowe, I., & Kalin, R. M. (2008). Selection of organic substrates as potential reactive materials for use in a denitrification permeable reactive barrier (PRB). *Bioresource Technology*, *99*(16), 7587–7596.

Gilbert, Jack A., Folker Meyer, Dion Antonopoulos, Pavan Balaji, C. Titus Brown, Christopher T. Brown, Narayan Desai et al. "Meeting report: the terabase metagenomics workshop and the vision of an Earth microbiome project." *Standards in genomic sciences* 3, no. 3 (2010): 243-248.

Golab, A. N., Peterson, M. A., & Indraratna, B. (2006). Selection of potential reactive materials for a permeable reactive barrier for remediating acidic groundwater in acid sulphate soil terrains. *Quarterly Journal of Engineering Geology and Hydrogeology*, *39*(2), 209–223.

Gómez, M. A., Hontoria, E., & González-lópez, J. (2002). *Effect of DO concentration on nitrate removal from groundwater using a denitrifying submerged filter*. *90*, 267–278.

Gorham, E. (1998). Acid deposition and its ecological effects: A brief history of research. *Environmental Science and Policy*, *1*(3), 153–166.

Grennfelt, P., Engleryd, A., Forsius, M., Hov, Ø., Rodhe, H., & Cowling, E. (2020). Acid rain and air pollution: 50 years of progress in environmental science and policy. *Ambio*, *49*(4), 849–864.

Griebler, C., & Lueders, T. (2009). Microbial biodiversity in groundwater ecosystems. *Freshwater biology*, *54*(4), 649-677.

Gruber, N., Galloway, J. (2008). An Earth-system perspective of the global nitrogen cycle. *Nature* 451 (7176)**,** 293–296.

GSI (2021). Geological Survey Ireland. Groundwater Data and Maps, Public Viewer. Available at: https://www.gsi.ie/en-ie/data-and-maps/Pages/Groundwater.aspx. Accessed December 2016.

Gupta N. (2019). DNA Extraction and Polymerase Chain Reaction. J Cytol. 2019 Apr-Jun;36(2):116-117. doi: 10.4103/JOC.JOC_110_18. PMID: 30992648

Gwak, J. H., Jung, M. Y., Hong, H., Kim, J. G., Quan, Z. X., Reinfelder, J. R., ... & Rhee, S. K. (2020). Archaeal nitrification is constrained by copper complexation with organic matter in municipal wastewater treatment plants. *The ISME journal*, *14*(2), 335-346.

Hallin, S., Jones, C.M., Schloter, M. and Philippot, L. (2009). Relationship between N-cycling communities and ecosystem functioning in a 50-year-old fertilization experiment. *The ISME journal*, *3*(5), 597-605.

Hamer, W.J., Pinching, G.D. and Acree, S.F. (1946). pH standards at various temperatures; aqueous solutions of acid potassium phthalate. *Journal of research of the National Bureau of Standards*, *36*,47-62.

Hatzenpichler, R., Lebedeva, E. V., Spieck, E., Stoecker, K., Richter, A., Daims, H., & Wagner, M. (2008). A moderately thermophilic ammonia-oxidizing crenarchaeote from a hot spring. *Proceedings of the National Academy of Sciences*, *105*(6), 2134-2139.

Hayatsu, M., Tago, K., & Saito, M. (2008). Various players in the nitrogen cycle: Diversity and functions of the microorganisms involved in nitrification and denitrification. *Soil Science and Plant Nutrition*, *54*(1), 33–45.

HC, 2018. UK Progress on Reducing Nitrate Pollution, House of Commons Environmental Audit Committee. Eleventh Report of Session 2017 − 19. *London, UK.*

Heid, C. A., Stevens, J., Livak, K. J., & Williams, P. M. (1996). Real Time Quantitative PCR. *Genome Research* 6(10), 986–994.

Helen, D., Kim, H., Tytgat, B., & Anne, W. (2016). Highly diverse nirK genes comprise two major clades that harbour ammonium-producing denitrifiers. *BMC genomics*, *17*(1), 1-13.

Helsel, D.R. (2005). More than obvious: better methods for interpreting nondetect data. *Environmental science & technology*, *39*(20), 419A-423A.

Henry, S., Baudoin, E., López-Gutiérrez, J. C., Martin-Laurent, F., Brauman, A., & Philippot, L. (2004). Quantification of denitrifying bacteria in soils by nirK gene targeted real-time PCR. *Journal of microbiological methods*, *59*(3), 327-335.

Henry, S., Bru, D., Stres, B., Hallet, S., & Philippot, L. (2006). Quantitative detection of the nosZ gene, encoding nitrous oxide reductase, and comparison of the abundances of 16S rRNA, narG, nirK, and nosZ genes in soils. *Applied and environmental microbiology*, *72*(8), 5181-5189.

Heuer, H., Krsek, M., Baker, P., Smalla, K., & Wellington, E. (1997). Analysis of actinomycete communities by specific amplification of genes encoding 16S rRNA and gel-electrophoretic separation in denaturing gradients. *Applied and environmental microbiology*, *63*(8), 3233-3241.

Heylen, K., Vanparys, B., Wittebolle, L., Verstraete, W., Boon, N., & Vos, P. De. (2006). Cultivation of Denitrifying Bacteria : Optimization of Isolation Conditions and Diversity Study. *Applied*

and environmental microbiology 72(4), 2637–2643.

Horn, M. A., Ihssen, J., Matthies, C., Schramm, A., Acker, G., & Drake, H. L. (2005). Dechloromonas denitrificans sp. nov., Flavobacterium denitrificans sp. nov., Paenibacillus anaericanus sp. nov. and Paenibacillus terrae strain MH72, N2O-producing bacteria isolated from the gut of the earthworm Aporrectodea caliginosa. *International journal of systematic and evolutionary microbiology*, *55*(3), 1255-1265.

Horz, H. P., Rotthauwe, J. H., Lukow, T., & Liesack, W. (2000). Identification of major subgroups of ammonia-oxidizing bacteria in environmental samples by T-RFLP analysis of amoA PCR products. *Journal of microbiological methods*, *39*(3), 197-204.

Hou, G., Liu, F., Liu, M., Kong, X., Li, S., Chen, L., ... & Chen, H. (2014). Performance of a permeable reactive barrier for in situ removal of ammonium in groundwater. *Water Science and Technology: Water Supply*, *14*(4), 585-592.

Hu, Z., Meng, H., Shi, J.H., Bu, N.S., Fang, C.M. & Quan, Z.X. (2014). Community size and composition of ammonia oxidizers and denitrifiers in an alluvial intertidal wetland ecosystem. *Frontiers in microbiology*, *5*, 371.

Huang, G., Liu, F., Yang, Y., Deng, W., Li, S., Huang, Y., & Kong, X. (2015). Removal of ammonium-nitrogen from groundwater using a fully passive permeable reactive barrier with oxygen-releasing compound and clinoptilolite. *Journal of Environmental Management*, *154*, 1–7.

Ida, T., Satoh, M., Yabe, R., Takahashi, R., & Tokuyama, T. (2004). Identification of genus Nitrosovibrio, ammonia-oxidizing bacteria, by comparison of N-terminal amino acid sequences of phosphoglycerate kinase. *Journal of bioscience and bioengineering*, *98*(5), 380-383.

Ilies, P. & Mavinic, D.S. (2001). The effect of decreased ambient temperature on the biological nitrification and denitrification of a high ammonia landfill leachate. *Water research*, *35*(8), 2065-2072.

Illumina (2016). "An introduction to next generation sequencing technology". 1-15 International Organization for Standardization (2005) ISO21571:2005. Foodstuffs—methods of analysis for the detection of genetically modified organisms and derived products—nucleic acid extraction.

Irish Geotechnical Services (1998) Investigation at Doora Landfill Site. Clare County Council.

Irish times (1998). "*Clare residences win case against local dump*". December 19, 1998.

ITRC. (1999). *Regulatory Guidance for Permeable Reactive Barriers Designed to Remediate Inorganic and Radionuclide Contamination*. Interstate Technology Regulatory Cooperation Permeable Reactive Barriers Work Group.

Jeter, R. M., & Ingraham, J. L. (1981). The denitrifying prokaryotes. In *The prokaryotes* (pp. 913-925). Springer, Berlin, Heidelberg.

Jetten, M.S., Schmid, M., Schmidt, I., Wubben, M., Van Dongen, U., Abma, W., Sliekers, O., Revsbech, N.P., Beaumont, H.J., Ottosen, L. and Volcke, E. (2002). Improved nitrogen removal by application of new nitrogen-cycle bacteria. *Reviews in Environmental science and biotechnology*, *1*(1), 51-63.

Ji, B., Yang, K., Zhu, L., Jiang, Y., Wang, H., Zhou, J., & Zhang, H. (2015). Aerobic denitrification: a review of important advances of the last 30 years. *Biotechnology and bioprocess engineering*, *20*(4), 643-651.

Jickells, T., Baker, A.R., Cape, J.N., Cornell, S.E. & Nemitz, E. (2013). The cycling of organic nitrogen through the atmosphere. *Philosophical Transactions of the Royal Society B: Biological Sciences*, *368*(1621), p.20130115.

Jokela, J.P.Y., Kettunen, R.H., Sormunen, K.M. & Rintala, J.A. (2002). Biological nitrogen removal

from municipal landfill leachate: low-cost nitrification in biofilters and laboratory scale in-situ denitrification. *Water Research*, *36*(16), 4079-4087.

Jonnson, J.A. & Sagulenko, E. (2011). Beyond the bacterium: planctomycetes challenge our concepts of microbial structure and function. *Nature Reviews Microbiology*, *9*(6), 403-413.

Jun, D., Yongsheng, Z., Weihong, Z., & Mei, H. (2009). Laboratory study on sequenced permeable reactive barrier remediation for landfill leachate-contaminated groundwater. *Journal of Hazardous Materials*, 161(1), 224–230.

Kärrman, E., & Jönsson, H. (2001). Including oxidisation of ammonia in the eutrophication impact category. T*he International Journal of Life Cycle Assessment,* 6(1), 29–33.

Kelleghan, D. B., Hayes, E.T., Everard, T. & Curran, T.P. (2020). *Assessment of the Impact of Ammonia Emissions from Intensive Agriculture Installations on Special Areas of Conservation and Special*

Kelly, J. J. (2003). Molecular techniques for the analysis of soil microbial processes: functional gene analysis and the utility of DNA microarrays. *Soil science*, *168*(9), 597-605.

Kelly, J. J., Policht, K., Grancharova, T., & Hundal, L. S. (2011). Distinct responses in ammonia-oxidizing archaea and bacteria after addition of biosolids to an agricultural soil. *Applied and Environmental Microbiology*, 77(18), 6551–6558.

Kennedy, N., & Egger, K. N. (2010). Impact of wildfire intensity and logging on fungal and nitrogen-cycling bacterial communities in British Columbia forest soils. *Forest Ecology and Management*, *260*(5), 787–794.

Kim, Y.M., Park, H., Cho, K.H. and Park, J.M. (2013). Long term assessment of factors affecting nitrifying bacteria communities and N-removal in a full-scale biological process treating high strength hazardous wastewater. *Bioresource technology*, *134*, pp.180-189.

Kim, M., & Chun. (2014). 16S rRNA Gene-Based Identification of *Bacteria* and *Archaea* using the EzTaxon Server. *Methods in microbiology, 41,* 61-74.

Kim, B. R., Shin, J., Guevarra, R. B., Lee, J. H., Kim, D. W., Seol, K. H., ... & Isaacson, R. E. (2017). Deciphering diversity indices for a better understanding of microbial communities. *Journal of Microbiology and Biotechnology*, *27*(12), 2089-2093.

Kjeldsen, P., Barlaz, M.A., Rooker, A.P., Baun, A., Ledin, A. & Christensen, T.H. (2002). Present and long-term composition of MSW landfill leachate: a review. *Critical reviews in environmental science and technology*, *32*(4), 297-336.

Klein, Timothy, Lianna Poghosyan, J. Elaine Barclay, J. Colin Murrell, Matthew I. Hutchings, and Laura E. Lehtovirta-Morley. "Cultivation of ammonia-oxidising archaea on solid medium." *FEMS microbiology letters* 369, no. 1 (2022): fnac029.

Kloos, K., Mergel, A., Rösch, C. & Bothe, H. (2001). Denitrification within the genus Azospirillum and other associative bacteria. *Functional Plant Biology*, *28*(9), 991-998.

Koops, H. P., & Stehr, G. (1991). Classification of eight new species of ammonia-oxidizing bacteria: Nitrosomonas communis sp. nov., Nitrosomonas ureae sp. nov., Nitrosomonas aestuarii sp. nov., Nitrosomonas marina sp. nov., Nitrosomonas nitrosa sp. nov., Nitrosomonas eutropha sp. nov., Nitrosomonas oligotropha sp. nov. and Nitrosomonas halophila sp. nov. *Microbiology*, *137*(7), 1689-1699.

Koops, H. P., & Pommerening-Röser, A. (2001). Distribution and ecophysiology of the nitrifying bacteria emphasizing cultured species. *FEMS Microbiology ecology*, *37*(1), 1-9.

Koops, H. P., Purkhold, U., Pommerening-Röser, A., Timmermann, G., & Wagner, M. (2005). The lithoautotrophic ammonia-oxidizing bacteria. *Bergey's manual of systematic bacteriology, volume two: the proteobacteria, part A introductory essays, Springer*, 141-147.

Knapp, M. F. (2005). Diffuse pollution threats to groundwater: A UK water company perspective.

*Quarterly Journal of Engineering Geology and Hydrogeology*, *38*(1), 39–51.

Knowles, R. (1982). Denitrification. *Microbiological Reviews*, *46*(1), 43–70.

Kong, X., Bi, E., Liu, F., Huang, G., & Ma, J. (2015). Laboratory column study for evaluating a multimedia permeable reactive barrier for the remediation of ammonium contaminated groundwater. *Environmental Technology (United Kingdom)*, *36*(11), 1433–1440.

Könneke, M., Bernhard, A.E., José, R., Walker, C.B., Waterbury, J.B. & Stahl, D.A. (2005). Isolation of an autotrophic ammonia-oxidizing marine archaeon. *Nature*, *437*(7058), 543-546.

Koops, H.P., Purkhold, U., Pommerening-Röser, A., Timmermann, G. and Wagner, M., 2003. The prokaryotes: an evolving electronic resource for the microbiological community.

Kowalchuk, G. A., Stephen, J. R., De Boer, W. I. E. T. S. E., Prosser, J. I., Embley, T. M., & Woldendorp, J. W. (1997). Analysis of ammonia-oxidizing bacteria of the beta subdivision of the class Proteobacteria in coastal sand dunes by denaturing gradient gel electrophoresis and sequencing of PCR-amplified 16S ribosomal DNA fragments. *Applied and environmental microbiology*, *63*(4), 1489-1497.

Kruempelbeck, I. & Ehrig, H. (1999). Long-term behaviour of municipal solid waste landfills in Germany, in Sardinia 99, Seventh International Waste Management and Landfill Symposium, 4- 8 October, S. Margherita di Pula, Cagliari, Proceedings vol. I, Christensen, T. H., Cossu, R., and Stegmann, R. Eds., CISA — Environmental Sanitary Engineering Centre, Cagliari, Italy, 1999.

Kuai, L., & Verstraete, W. (1998). Ammonium Removal by the Oxygen-Limited Autotrophic Nitrification-Denitrification System. *Applied Environmenal Biology*, *64*(11), 4500–4506.

Kubista, M., Andrade, J. M., Bengtsson, M., Forootan, A., Jonák, J., Lind, K., Sindelka, R., Sjöback, R., Sjögreen, B., Strömbom, L., Ståhlberg, A. & Zoric N. (2006). The real-time polymerase reaction. *Molecular Aspects of Medicine*, 27(95-125).

Kulikowska, D. & Klimiuk, E. (2008). The effect of landfill age on municipal leachate composition. *Bioresource technology*, 99(13), 5981-5985.

Külköylüoğlu, O., Dügel, M., & Kılıç, M. (2007). Ecological requirements of Ostracoda (Crustacea) in a heavily polluted shallow lake, Lake Yeniçağa (Bolu, Turkey). In *Ostracodology—Linking Bio-and Geosciences* (pp. 119-133). Springer, Dordrecht.

Kuypers, M., Marchant, H. & Kartal, B. (2018). The microbial nitrogen-cycling network. *Nature Reviews Microbiology* 16(5), 263–276.

Langille, M. G. I., Zaneveld, J., Caporaso, J. G., Mcdonald, D., Knights, D., Reyes, J. A., Clemente, J. C., Burkepile, D. E., Thurber, R. L. V., Knight, R., Beiko, R. G., & Huttenhower, C. (2013). Predictive functional profiling of microbial communities using 16S rRNA marker gene sequences. *Nature Biotechnology*, 1–10.

Lehtovirta-Morley, L. E., Sayavedra-Soto, L. A., Gallois, N., Schouten, S., Stein, L. Y., Prosser, J. I., & Nicol, G. W. (2016). Identifying potential mechanisms enabling acidophily in the ammonia-oxidizing archaeon "Candidatus Nitrosotalea devanaterra". *Applied and Environmental Microbiology*, *82*(9), 2608-2619.

Leininger, S., Urich, T., Schloter, M., Schwark, L., Qi, J., Nicol, G. W., Prosser, J. I., Schuster, S. C., & Schleper, C. (2006). Archaea predominate among ammonia-oxidizing prokaryotes in soils. *Nature*, *442*(August), 806–809.

Levy-Booth, D, Prescott, C., & Grayston (2014). Microbial functional genes involved in nitrogen fixation, nitrification and denitrification in forest ecosystems. *Soil Biology and Biochemistry* 75 (11-25).

Loman, N. J., Misra, R. V., Dallman, T. J., Constantinidou, C., Gharbia, S. E., Wain, J., & Pallen, M. J. (2012). Performance comparison of benchtop high-throughput sequencing

platforms. *Nature biotechnology*, *30*(5), 434-439.

Li, X. R., Xiao, Y. P., Ren, W. W., Liu, Z. F., Shi, J. H., & Quan, Z. X. (2012). Abundance and composition of ammonia-oxidizing bacteria and archaea in different types of soil in the Yangtze River estuary. *Journal of Zhejiang University SCIENCE B*, *13*(10), 769-782.

Li, S., Huang, G., Kong, X., Yang, Y., Liu, F., Hou, G., & Chen, H. (2014). Ammonium removal from groundwater using a zeolite permeable reactive barrier: a pilot-scale demonstration. *Water Science & Technology*, *70*(9), 1540.

Li, J., Nedwell, D. B., Beddow, J., Dumbrell, A. J., McKew, B. A., Thorpe, E. L., & Whitby, C. (2015). amoA gene abundances and nitrification potential rates suggest that benthic ammonia-oxidizing bacteria and not archaea dominate N cycling in the Colne estuary, United Kingdom. *Applied and Environmental Microbiology*, *81*(1), 159–165.

Limpiyakorn, T., Sonthiphand, P., Rongsayamanont, C., & Polprasert, C. (2011). Bioresource technology abundance of amoA genes of ammonia-oxidizing archaea and bacteria in activated sludge of full-scale wastewater treatment plants. *Bioresource Technology*, *102*(4), 3694–3701.

Liu, S. J., Jiang, B., Huang, G. Q., & Li, X. G. (2006). Laboratory column study for remediation of MTBE-contaminated groundwater using a biological two-layer permeable barrier. *Water Research*, *40*(18), 3401–3408.

Lv, P., Luo, J., Zhuang, X., Zhang, D., Huang, Z., & Bai, Z. (2017). Diversity of culturable aerobic denitrifying bacteria in the sediment, water and biofilms in Liangshui River of Beijing, China. *Scientific Reports*, *7*(1), 1–12.

Majone, M., Verdini, R., Aulenta, F., Rossetti, S., Tandoi, V., Kalogerakis, N., Agathos, S., Puig, S., Zanaroli, G., & Fava, F. (2015). In situ groundwater and sediment bioremediation: Barriers and perspectives at European contaminated sites. *New Biotechnology*, *32*(1), 133–146.

Malik, S., Beer, M., Megharaj, M., & Naidu, R. (2008). The use of molecular techniques to characterize the microbial communities in contaminated soil and water. *Environment International*, *34*(2), 265–276.

Malinowski, M., Alawi, M., Krohn, I., Ruff, S., Indenbirken, D., Karrasch, M., ... & Pommerening-Röser, A. (2020). Deep amoA amplicon sequencing reveals community partitioning within ammonia-oxidizing bacteria in the environmentally dynamic estuary of the River Elbe. *Scientific reports*, *10*(1), 1-11.

Martens-Habbena, W., Berube, P. M., Urakawa, H., de La Torre, J. R., & Stahl, D. A. (2009). Ammonia oxidation kinetics determine niche separation of nitrifying Archaea and Bacteria. *Nature, 431 (7226), 976-979.*

Matsuzaka, E., Nomura, N., Maseda, H., Otagaki, H., Nakajima-Kambe, T., Nakahara, T., & Uchiyama, H. (2003). Participation of Nitrite Reductase in Conversion of NO2- to NO3- in a Heterotrophic Nitrifier, Burkholderia cepacia NH-17, with Denitrification Activity. *Microbes and Environments*, *18*(4), 203–209. https://doi.org/10.1264/jsme2.18.203

McMurdie, P. J., & Holmes, S. (2014). Waste not, want not: why rarefying microbiome data is inadmissible. *PLoS computational biology*, *10*(4), e1003531.

Milne, I., Seager, J., Mallett, M. & Sims I. (2000). Effects of short-term pulsed ammonia exposure on fish. *Environmental Toxicology and Chemistry* 19(12), 2929-2936.

Mincer, T. J., Church, M. J., Taylor, L. T., Preston, C., Karl, D. M., & DeLong, E. F. (2007). Quantitative distribution of presumptive archaeal and bacterial nitrifiers in Monterey Bay and the North Pacific Subtropical Gyre. *Environmental microbiology*, *9*(5), 1162-1175.

Meincke, M., Krieg, E., & Bock, E. (1989). Nitrosovibrio spp., the dominant ammonia-oxidizing bacteria in building sandstone. *Applied and Environmental Microbiology*, *55*(8), 2108-2110.

Meinhardt, K. A., Bertagnolli, A., Pannu, M. W., Strand, S. E., Brown, S. L., & Stahl, D. A. (2015). Evaluation of revised polymerase chain reaction primers for more inclusive quantification of ammonia-oxidizing archaea and bacteria. *Environmental Microbiology Reports*.

Meyer-Dombard, D. A. R., Bogner, J. E., & Malas, J. (2020). A review of landfill microbiology and ecology: A call for modernization with 'next generation'technology. *Frontiers in Microbiology*, *11*, 1127.

Mohammad-pajooh, E., Weichgrebe, D., & Cuff, G. (2017). Municipal landfill leachate characteristics and feasibility of retrofitting existing treatment systems with deammonification – A full scale survey. *Journal of Environmental Management*, *187*, 354–364.

Morris, M.A., Crann & Gerard, J. (2009). Corn Bomb : A Short History of Nitrogen 1660 – 2008. RHA Projects.

Morris, S., Garcia-Cabellos, G., Enright, D., Ryan, D., & Enright, A. M. (2018). Bioremediation of landfill leachate using isolated bacterial strains. *Int. J. Environ. Bioremed. Biodegrad*, *6*(1), 26-35.

Mosier, A. C., Allen, E. E., Kim, M., Ferriera, S., & Francis, C. A. (2012). Genome sequence of "Candidatus Nitrosoarchaeum limnia" BG20, a low-salinity ammonia-oxidizing archaeon from the San Francisco Bay estuary.

Mountjoy, K.J., Pringle, E.K., Choi, M. & Gowdy, W. (2003) October. The use of permeable reactive barriers for in-situ remediation of groundwater contaminants. In *Remediation technologies symposium, Banff*.

Mulder, A., van de Gaff, A. A., Robertson, L. A., Kuenen, J. G. (1995). Anaerobic ammonium oxidation discovered in a denitrifying fluidized bed reactor. *FEMS Microbiology Ecology*, (*16)*, 177–184.

Nakos, G. G., & Wolcott, A. R. (1972). Bacteriostatic effect of ammonium on *Nitrobacter agilis* in mixed culture withNitrosomonas europaea. *Plant and Soil*, *36*(1), 521-527.

Niu, S., Classen, A.T., Dukes, J.S., Kardol, P., Liu, L., Luo, Y., Rustad, L., Sun, J., Tang, J., Templer, P.H. & Thomas, R. Q. (2016). Global patterns and substrate-based mechanisms of the terrestrial nitrogen cycle. *Ecology letters*, *19*(6), 697-709.

Nicol, G. W., Leininger, S., Schleper, C., & Prosser, J. I. (2008). The influence of soil pH on the diversity, abundance and transcriptional activity of ammonia oxidizing archaea and bacteria. *Environmental microbiology*, *10*(11), 2966-2978.

Nocker, A., Burr, M., & Camper A., 2007. Genotypic Microbial Commuinity Proifiling: A Critical Technical Review. *Microbial Ecology 54, 276 - 289.*

Nooten, T.V., Diels, L. & Bastiaens, L. (2008). Design of a multifunctional permeable reactive barrier for the treatment of landfill leachate contamination: laboratory column evaluation. *Environmental science & technology*, *42*(23), 8890-8895.

Okada, N., Nomura, N., Nakajima-Kambe, T., & Uchiyama, H. (2005). Characterization of the Aerobic Denitrification in Mesorhizobium sp. Strain NH-14 in Comparison with that in Related Rhizobia. *Microbes and Environments*, *20*(4), 208–215. https://doi.org/10.1264/jsme2.20.208

Okano, Y., Hristova, K. R., Christian, M., Jackson, L. E., Denison, R. F., Lebauer, D., Scow, K. M., Leutenegger, C. M., & Gebreyesus, B. (2004). Application of real-Time PCR to study effects of ammonium on population size of ammonia-oxidizing bacteria in soil. *Applied and*

*Environmental Microbiology*, *70*(2), 1008–1016.

Queipo-Ortuño, M. I., De Dios Colmenero, J., Macias, M., Bravo, M. J., & Morata, P. (2008). Preparation of bacterial DNA template by boiling and effect of immunoglobulin G as an inhibitor in real-time PCR for serum samples from patients with brucellosis. *Clinical and Vaccine Immunology*, *15*(2), 293-296.

Ouyang, Y., Norton, J. M., & Stark, J. M. (2017). Ammonium availability and temperature control contributions of ammonia oxidizing bacteria and archaea to nitrification in an agricultural soil. *Soil Biology and Biochemistry*, *113*, 161-172.

Pace, N. R. (1997). A molecular view of microbial diversity and the biosphere. *Science*, *276*(5313), 734-740.

Panigrahi, S., Velraj, P., & Rao, T. S. (2019). Functional microbial diversity in contaminated environment and application in bioremediation. In *Microbial diversity in the genomic era* (pp. 359-385). Academic Press.

Paiva-Cavalcanti, M., Regis-da-Silva, C. G., & Gomes, Y. M. (2010). Comparison of real-time PCR and conventional PCR for detection of leishmania (leishmania) infantum infection: A mini-review. *Journal of Venomous Animals and Toxins Including Tropical Diseases*, *16*(4), 537–542.

Park, H. D., & Noguera, D. R. (2004). Evaluating the effect of DO on ammonia-oxidizing bacterial communities in activated sludge. *Water research*, *38*(14-15), 3275-3286.

Patterson, B. M., Grassi, M. E., Robertson, B. S., Davis, G. B., Smith, a. J., & McKinley, A. J. (2004). Use of Polymer Mats in Series for Sequential Reactive Barrier Remediation of Ammonium-Contaminated Groundwater: Field Evaluation. *Environmental Science & Technology*, *38*(24), 6846–6854.

Patureau, D., Godon, J. J., Dabert, P., Bouchez, T., Bernet, N., Delgenes, J. P., & Moletta, R. (1998). Microvirgula aerodenitrificans gen. nov., sp. nov., a new gram-negative bacterium exhibiting co-respiration of oxygen and nitrogen oxides up to oxygen-saturated conditions. *International Journal of Systematic and Evolutionary Microbiology*, *48*(3), 775-782.

Pester, M., Rattei, T., Flechl, S., Gröngröft, A., Richter, A., Overmann, J., ... & Wagner, M. (2012). amoA-based consensus phylogeny of ammonia-oxidizing archaea and deep sequencing of amoA genes from soils of four different geographic regions. *Environmental Microbiology*, *14*(2), 525-539.

Petersen, D. G., Blazewicz, S. J., Firestone, M., Herman, D. J., Turetsky, M., & Waldrop, M. (2012). Abundance of microbial genes associated with nitrogen cycling as indices of biogeochemical process rates across a vegetation gradient in Alaska. *Environmental microbiology*, *14*(4), 993-1008.

Pollard, P. C. (2006). A quantitative measure of nitrifying bacterial growth. *Water Research*, *40*(8), 1569–1576.

Poly, F., Wertz, S., Brothier, E., & Degrange, V. (2008). First exploration of Nitrobacter diversity in soils by a PCR cloning-sequencing approach targeting functional gene nxrA. *FEMS microbiology ecology*, *63*(1), 132-140.

Priestly, J. (1774). Experiments and observations on different kinds of air, vol. 1. London, UK: W. *Bowyer and J. Nicjols.*

Prescott L. M., Harley J. P. & Klein D.A. Microbiology 5th edition, Mc Craw-Hill, Newyork, 2002, 10-14.

Prosser, J. I., & Embley, T. (2002). Cultivation-based and molecular approaches to characterisation of terrestrial and aquatic nitrifiers. *Antonie van Leeuwenhoek*, *81*(1), 165-

179.

Prosser, J. I., & Nicol, G. W. (2008). Relative contributions of archaea and bacteria to aerobic ammonia oxidation in the environment. *Environmental microbiology*, *10*(11), 2931-2941.

Prosser, J. I., & Nicol, G. W. (2012). Archaeal and bacterial ammonia- oxidisers in soil : the quest for niche specialisation and differentiation. *Trends in Microbiology*, *20*(11), 523–531.

Prosser, J. I., & Nicol, G. W. (2015). Candidatus Nitrosotalea. *Bergey's Manual of Systematics of Archaea and Bacteria*, 1-7.

Qiu, X., Wang, T., Zhong, X., Du, G., & Chen, J. (2012). Screening and Characterization of an Aerobic Nitrifying-denitrifying Bacterium from Activated Sludge. *Biotechnology and Bioprocess Engineering*, *17*(2), 353–360.

Radojevic, M. & Harrison E.M. (1992) Atmospheric Acidity: sources, consequences and abatement. Barking, UK: Elsevier Science Publishers Ltd.

Reed, D. W., Smith, J. M., Francis, C. A. & Fujita, Y. (2010). Responses of ammonia-oxidizing bacterial and archaeal populations to organic nitrogen amendments in low-nutrient groundwater. *Applied and Environmental Microbiology*, *76*(8), 2517–2523.

Ren, M., Feng, X., Huang, Y., Wang, H., Hu, Z., Clingenpeel, S., ... & Luo, H. (2019). Phylogenomics suggests oxygen availability as a driving force in Thaumarchaeota evolution. *The ISME journal*, *13*(9), 2150-2161.

Reyes, C., Hodgskiss, L. H., Kerou, M., Pribasnig, T., Abby, S. S., Bayer, B., ... & Schleper, C. (2020). Genome wide transcriptomic analysis of the soil ammonia oxidizing archaeon Nitrososphaera viennensis upon exposure to copper limitation. *The ISME journal*, *14*(11), 2659-2674.

Reynolds, T. D., & Richards, P. A. C. (1995). *Unit operations and processes in environmental engineering* (No. 628.162 R333u Ej. 1). PWS Publishing Company.

Richardson, J.P. & Nicklow, J.W. (2002). In situ permeable reactive barriers for groundwater contamination. *Soil and Sediment Contamination*, *11*(2), 241-268.

Rivett, M. O., Buss, S. R., Morgan, P., Smith, J. W. N., & Bemment, C. D. (2008). Nitrate attenuation in groundwater: a review of biogeochemical controlling processes. *Water Research*, *42*(16), 4215–4232.

Robertson, W. D., & Cherry, J. A. (1995). In Situ Denitrification of Septic-System Nitrate Using Reactive Porous Media Barriers: Field Trials. *Ground Water*, *33*(1),

Robertson, W.D., Blowes, D.W., Ptacek, C.J. & Cherry, J.A. (2000). Long-term performance of in situ reactive barriers for nitrate remediation. *Groundwater*, *38*(5), 689-695.

Robertson, W. D., Vogan, J. L., & Lombardo, P. S. (2008). Nitrate removal rates in a 15-year-old permeable reactive barrier treating septic system nitrate. *Ground Water Monitoring and Remediation*, *28*(3), 65–72.

Roehl, K.E., Meggyes, T., Simon, F.G. & Stewart, D.I., eds. (2005). Long-termPerformance of Permeable Reactive Barriers. Gulf Professional Publishing.

Röling, W., van Breukelen B. M., Braster, M., Goeltom, M., Groen, J., & van Verseveld H. W. (2000a). Analysis of Microbial Communities in a Landfill Leachate Polluted Aquifer using a New Method for Anaerobic Physiological Profiling and 16S rDNA Based Fingerprinting. *Microbial Ecology*, *40*(3), 177–188.

Röling, W. F., Van Breukelen, B. M., Braster, M., & Van Verseveld, H. W. (2000b). Linking microbial community structure to pollution: Biolog-substrate utilization in and near a landfill leachate plume. *Water science and technology*, *41*(12), 47-53.

Röling, W. F., van Breukelen, B. M., Braster, M., Lin, B., & van Verseveld, H. W. (2001). Relationships between microbial community structure and hydrochemistry in a landfill

leachate-polluted aquifer. *Applied and Environmental Microbiology*, *67*(10), 4619-4629.

Rotthauwe, J.H., Witzel, K.P. & Liesack, W. (1997). The ammonia monooxygenase structural gene amoA as a functional marker: molecular fine-scale analysis of natural ammonia-oxidizing populations. *Applied and environmental microbiology*, *63*(12), 4704-4712.

Santoro, E. (2016). The do-it-all nitrifier. Microbiology, Sciencemag.org. 351(6271).

Salipante, S. J., Kawashima, T., Rosenthal, C., Hoogestraat, D. R., Cummings, L. A., Sengupta, D. J., ... & Hoffman, N. G. (2014). Performance comparison of Illumina and ion torrent next-generation sequencing platforms for 16S rRNA-based bacterial community profiling. *Applied and environmental microbiology*, *80*(24), 7583-7591.

Samocha, T. M. (2019). *Sustainable biofloc systems for marine shrimp*. Academic Press.

Sauder, L. A., Ross, A. A., & Neufeld, J. D. (2016). Nitric oxide scavengers differentially inhibit ammonia oxidation in ammonia-oxidizing archaea and bacteria. *FEMS Microbiology Letters*, *363*(7).

Scala, D. J., & Kerkhof, L. J. (1998). Nitrous oxide reducatse (*nosZ*) gene-specific PCR primers for detection of denitrifiers and three *nosZ* genes from marine sediments. *FEMS Microbiology Letters* 162 (61-68).

Schipper, L. A., Robertson, W. D., Gold, A. J., Jaynes, D. B., & Cameron, S. C. (2010). Denitrifying bioreactors: An approach for reducing nitrate loads to receiving waters. *Ecological Engineering*, *36*(11), 1532–1543.

Schleper, C., & Nicol, G. W. (2010). Ammonia-oxidising archaea–physiology, ecology and evolution. *Advances in microbial physiology*, *57*, 1-41.

Selman, M., Greenhalgh, S., Diaz, R., & Sugg, Z. (2008). Eutrophication and Hypoxia in Coastal areas: a Global assessment of the State of Knowledge. *World Resources Institute*, *1*, 1–6.

Shaw, L. J., Nicol, G. W., Smith, Z., Fear, J., Prosser, J. I., & Baggs, E. M. (2006). Nitrosospira spp. can produce nitrous oxide via a nitrifier denitrification pathway. *Environmental Microbiology*, *8*(2), 214-222.

Shimomura, Y., Morimoto, S., Hoshino, Y. T., Uchida, Y., Akiyama, H., & Hayatsu, M. (2009). Comparison among amoA primers suited for quantification and diversity analyses of ammonia-oxidizing bacteria in soil. *Microbes and environments*, 1110280329-1110280329.

Singh, A., Van Hamme, J. D., Voordouw, G., & Ward, O. P. (2009). Petroleum microbiology. *Encyclopedia of Microbiology (Third Edition)*, 443-456.

Singleton, D. R., Lee, J., Dickey, A. N., Stroud, A., Scholl, E. H., Wright, F. A., & Aitken, M. D. (2018). Polyphasic characterization of four soil-derived phenanthrene-degrading Acidovorax strains and proposal of Acidovorax carolinensis sp. nov. *Systematic and applied microbiology*, *41*(5), 460-472.

Siripong, S., & Rittmann, B. E. (2007). Diversity study of nitrifying bacteria in full-scale municipal wastewater treatment plants. *Water Research*, *41*(5), 1110–1120.

Smil, V. (2001). *Enriching the Earth: Fritz Harber, Carl Bosch and the transformation of world food production*. Cambridge, MA: Massachusetts Institute of Technology.

Smith, D. S., Maxwell, P. W., & De Boer, S. H. (2005). Comparison of several methods for the extraction of DNA from potatoes and potato-derived products. *Journal of agricultural and food chemistry*, *53*(26), 9848-9859.

Smith, J. I., & Nicol, G. W. (2008). Relative contributions of archaea and bacteria to aerobic ammonia oxidation in the environment. *Environmental Microbiology*, *10*(11), 2931–2941.

Smith, C. J., & Osborn, M. (2009). Advantages and limitations of quantitative PCR (Q-PCR)-based approaches in microbial ecology. *FEMS Microbiology Ecology*, *67*(1), 6–20.

SNC- Environment (2013). Doora Landfill Porewater Sampling Programme. Clare County Council.

SNC- Environment (2014). Doora Landfill Hydrogeological Report. Clare County Council.

Sorokin, D. Y., Tourova, T. P., Braker, G., & Muyzer, G. (2007). Thiohalomonas denitrificans gen. nov., sp. nov. and Thiohalomonas nitratireducens sp. nov., novel obligately chemolithoautotrophic, moderately halophilic, thiodenitrifying Gammaproteobacteria from hypersaline habitats. *International journal of systematic and evolutionary microbiology*, *57*(7), 1582-1589.

Spang, A., Poehlein, A., Offre, P., Zumbrägel, S., Haider, S., Rychlik, N., ... & Wagner, M. (2012). The genome of the ammonia-oxidizing C andidatus N itrososphaera gargensis: insights into metabolic versatility and environmental adaptations. *Environmental microbiology*, *14*(12), 3122-3145.

Sreejith, K. R., Ooi, C. H., Jin, J., Dao, D. V., & Nguyen, N. T. (2018). Digital polymerase chain reaction technology—recent advances and future perspectives. *Lab on a Chip*, *18*(24), 3717-3732.

Staley, J.T. & Konopka, A. (1985). Measurement of in situ activities of nonphotosynthetic microorganisms in aquatic and terrestrial habitats. *Annual review of microbiology*, *39*(1), 321-346.

Starr, R. C. & Cherry, J. A. (1994). In situ remediation of contaminated ground water: The funnel-and-gate system. *Groundwater*, *32*(3), 465-476.

Statutory Instrument (2009). S.I. No 9/2010- European Communities Environmental Objectives (Groundwater) Regulations 2009 as ammended (S.I. No. 149 of 2012 and S.I. No. 366 of 2016). Dublin; Government of Ireland.

Statutory Instrument (2010). S.I. No. 272/2009- European Communities Environmental Objectives (Surface Water) Regulations 2010. Dublin; Government of Ireland.

Stopnisek, N., Gubry-Rangin, C., Höfferle, S., Nicol, G. W., Mandic-Mulec, I., & Prosser, J. I. (2010). Thaumarchaeal ammonia oxidation in an acidic forest peat soil is not influenced by ammonium amendment. *Applied and environmental microbiology*, *76*(22), 7626-7634.

Stein, L. & Klotz, M. (2016) The Nitrogen Cycle, Current Biology 36 (3) 94-98.

Sterngren, A. E., Hallin, S., & Bengtson, P. (2015). Archaeal ammonia oxidizers dominate in numbers, but bacteria drive gross nitrification in N-amended grassland soil. *Frontiers in microbiology*, *6*, 1350.

Stokstad, E. (2014). Ammonia Pollution From Farming May Excact Hefty Health Cost. *Air Pollution, Science* 343.

Strock, J.S. (2008). Ammonification. *Encyclopaedia of Ecology, 162–165.*

Strous, M., Pelletier, E., Mangenot, S., Rattei, T., Lehner, A., Taylor, M. W., Horn, M., Daims, H., Bartol-Mavel, D., Wincker, P., Barbe, V., Fonknechten, N., Vallenet, D., Segurens, B., Schenowitz-Truong, C., Médigue, C., Collingro, A., Snel, B., Dutilh, B. E., ... Le Paslier, D. (2006). Deciphering the evolution and metabolism of an anammox bacterium from a community genome. *Nature*, *440*(7085), 790–794.

Suenaga, H. (2012). Targeted metagenomics: A high-resolution metagenomics approach for specific gene clusters in complex microbial communities. *Environmental Microbiology*, *14*(1), 13–22.

Tatsi, A.A. & Zouboulis, A.I. (2002). A field investigation of the quantity and quality of leachate from a municipal solid waste landfill in a Mediterranean climate (Thessaloniki, Greece). *Advances in Environmental Research*, *6*(3), 207-219.

Terry, C. F., Harris, N., & Parkes, H. C. (2002). Detection of genetically modified crops and their derivatives: critical steps in sample preparation and extraction. *Journal of AOAC International*, *85*(3), 768-774.

Teske, A., Alm, E., Regan, J. M., Toze, S., Rittmann, B. E., & Stahl, D. A. (1994). Evolutionary relationships among ammonia-and nitrite-oxidizing bacteria. *Journal of bacteriology*, *176*(21), 6623-6630.

Treusch, A. H., Leininger, S., Kletzin, A., Schuster, S. C., Klenk, H. P., & Schleper, C. (2005). Novel genes for nitrite reductase and Amo-related proteins indicate a role of uncultivated mesophilic crenarchaeota in nitrogen cycling. *Environmental microbiology*, *7*(12), 1985-1995.

Thiruvenkatachari, R., Vigneswaran, S., & Naidu, R. (2008). Permeable reactive barrier for groundwater remediation. *Journal of Industrial and Engineering Chemistry*, *14*(2), 145–156.

Throback, I.N., Enwall, K., Jarvis, A. & Hallin, S. (2004). Reassessing PCR primers targeting *nirS, nirK* and *nosZ* genes for sommunity surveys of denitrifying bacteria with DGGE. *FEMS Microbiology Ecology* 49, 401-417.

Timonen, S., & Bomberg, M. (2009). Archaea in dry soil environments. *Phytochemistry Reviews*, *8*(3), 505-518.

Torsvik, V. & Øvreås, L., 2002. Microbial diversity and function in soil: from genes to ecosystems. *Current opinion in microbiology*, *5*(3), 240-245.

Trodd W., & O'Boyle S. (2020). Water quality in 2019; An Indicators Report. Environemtal Protection Agency. Johnstown Castle, Wexford.

United States Environmental Protection Agency. Technology Innovation Office and Environmental Management Support (Firm), 1999. *Field applications of in situ remediation technologies: Permeable reactive barriers*. DIANE Publishing.

United States Geological Survey (USGS). (2020). Mineral Commodity Summaries 2020. In *U.S Department of The Interior, U.S Geological Survey* (Issue 703).

Valdi, M. (2001). Bioremediation; An Overview. *Pure Applied Chemisrty* 73, 1163-1172.

Van de Graaf, A.A., De Bruijn, P., Robertson, L.A., Jetten, M.S.M., & Kuenen, J.G. (1996). Autotrophic growth of anaerobic ammonium-oxidizing micro-organisms in a fluidized bed reactor. *Microbiology* 142, 2187-2196.

Van-Nooten, T., Diels, L., & Bastiaens, L. (2010). Design of a multibarrier for the treatment of landfill leachate contamination: laboratory column evaluation. *4th International Symposium: Permeable Reactive Barriers and Reactive Zones*, *42*(23), 34.

Van Kessel, M. A. H. J., Speth, D. R., Albertsen, M., Nielsen, P. H., Op Den Camp, H. J. M., Kartal, B., Jetten, M. S. M., & Lücker, S. (2015). Complete nitrification by a single microorganism. *Nature*, *528*(7583), 555–559.

Vidali, M. "Bioremediation. an overview." *Pure and applied chemistry* 73.7 (2001): 1163-1172.

Vitousek, P. M., Aber, J. D., Howarth, R. W., Likens, G. E., Matson, A., Schindler, D. W., Schlesinger, W. H., & Tilman, D. G. (1997). Human Alteration Of The Global Nitrogen Cycle: Sources And Consequences. *Ecological Applications*, *7*(3), 737–750.

Vitousek, P. M., Menge, D. N., Reed, S. C. & Cleveland, C. C. (2013). Biological nitrogen fixation: rates, patterns and ecological controls in terrestrial ecosystems. *Philosophical Transactions of the Royal Society B: Biological Sciences*, *368*(1621), p.20130119.

Wakida, F. T., & Lerner, D. N. (2005). Non-agricultural sources of groundwater nitrate: a review and case study. *Water Research*, *39*(1), 3–16.

Wang, Y., Hammes, F., Boon, N., & Egli, T. (2007). Quantification of the filterability of freshwater bacteria through 0.45, 0.22, and 0.1 μm pore size filters and shape-dependent enrichment of filterable bacterial communities. *Environmental science & technology*, *41*(20), 7080-7086.

Wang, X., Wang, C., Bao, L., & Xie, S. (2014). Abundance and community structure of ammonia-oxidizing microorganisms in reservoir sediment and adjacent soils. *Applied microbiology and biotechnology*, *98*(4), 1883-1892.

Wang, Y., & LêCao, K. A. (2020). Managing batch effects in microbiome data. *Briefings in bioinformatics*, *21*(6), 1954-1970.

Ward, B. B. (2011). Measurement and distribution of nitrification rates in the oceans. In *Methods in Enzymology* 486, 307–323. Academic Press Inc.

Ward, B. B., Jensen, M. M. (2014). The Microbial Nitrogen Cycle. *Frontiers in Microbiology, 5(553).*

Warneke, S., Schipper, L. A., Bruesewitz, D. A., Mcdonald, I., & Cameron, S. (2011). Rates , controls and potential adverse effects of nitrate removal in a denitrification bed, *37*, 511–522. https://doi.org/10.1016/j.ecoleng.2010.12.006

Wei, W., Isobe, K., Nishizawa, T., Zhu, L., Shiratori, Y., Ohte, N., ... & Senoo, K. (2015). Higher diversity and abundance of denitrifying microorganisms in environments than considered previously. *The ISME journal*, *9*(9), 1954-1965.

Whale, A. S., & Huggett, J. F. (2012). Cowen S, Speirs V, Shaw J, Ellison S, Foy CA and Scott DJ: Comparison of microfluidic digital PCR and conventional quantitative PcR for measuring copy number variation. *Nucleic Acids Res*, *40*, e82.

WHO. (2003). 12.6 Ammonia. *Ammonia in Drinking-Water. Background Document for Preparation of WHO Guidelines for Drinking-Water Quality*, 303–306.

Wiszniowski, J., Robert, D., Surmacz-Gorska, J., Miksch, K. & Weber, J. V. (2006). Landfill leachate treatment methods: A review. *Environmental chemistry letters*, *4*(1), 51-61.

Woese, C. R. (1987). Bacterial evoloution. *Microbial Reviews, 51(2),* 221 - 271.

Woese, C. R., Kandler, O., & Wheelis, M. L. (1990). Towards a natural system of organisms: proposal for the domains Archaea, Bacteria, and Eucarya. *Proceedings of the National Academy of Sciences*, *87*(12), 4576-4579.

Woese, C.R., & Fox, G. E. (1997). Phylogenetic structure of the prokaryotic domain: The primary kingdoms. *Proceedings of the National Academy of Sciences of the United States of America, 74, 5088 - 5090.*

Wurts, 2003. Daily pH cycle and ammonia toxicity. *World Aquaculture* 34(2): 20-21.

Yokoyama, K., Yumura, M., Honda, T., & Ajitomi, E. (2016). Characterization of denitrification and net N2O-reduction properties of novel aerobically N2O-reducing bacteria. *Soil Science and Plant Nutrition*, *62*(3), 230–239. https://doi.org/10.1080/00380768.2016.1178076

Yoon, S., Nissen, S., Park, D., Sanford, R. A., & Löffler, F. E. (2016). Nitrous oxide reduction kinetics distinguish bacteria harboring clade I NosZ from those harboring clade II NosZ. *Applied and environmental microbiology*, *82*(13), 3793-3800.

Zainun, M. Y., & Simarani, K. (2018). Metagenomics profiling for assessing microbial diversity in both active and closed landfills. *Science of the Total Environment*, *616*, 269-278.

Zhalnina, K. V., Dias, R., Leonard, M. T., Dorr de Quadros, P., Camargo, F. A., Drew, J. C., ... & Triplett, E. W. (2014). Genome sequence of Candidatus Nitrososphaera evergladensis from group I. 1b enriched from Everglades soil reveals novel genomic features of the ammonia-oxidizing archaea. *PLos one*, *9*(7), e101648.

Zhang, J., Chiodini, R., Badr, A., & Zhang, G. (2011). The impact of next-generation sequencing on genomics. *Journal of genetics and genomics*, *38*(3), 95-109.

Zhang, X., Agogué, H., Dupuy, C., & Gong, J. (2014). Relative Abundance of Ammonia Oxidizers, Denitrifiers, and Anammox Bacteria in Sediments of Hyper-Nutrified Estuarine Tidal Flats and in Relation to Environmental Conditions. *CLEAN–Soil, Air, Water*, *42*(6), 815-823.

Zhang, S., Pang, S., Wang, P., Wang, C., Guo, C., Addo, F. G., & Li, Y. (2016). Responses of bacterial community structure and denitrifying bacteria in biofilm to submerged macrophytes and nitrate. *Scientific Reports*, *6*(1), 1-10.

Zhang, H., Yan, Z., Wang, X., Ganova, M., Chang, H., Lassakova, S., ... & Neuzil, P. (2021). Determination of advantages and limitations of qPCR duplexing in a single fluorescent channel. *ACS omega*, *6*(34), 22292-22300.

Zhang, D., Wang, P., Cui, R., Yang, H., Li, G., Chen, A., & Wang, H. (2022). Electrical conductivity and DO as predictors of nitrate concentrations in shallow groundwater in Erhai Lake region. *Science of The Total Environment*, *802*, 149879.

Zhuang, X., Han, Z., Bai, Z., Zhuang, G., & Shim, H. (2010). Progress in decontamination by halophilic microorganisms in saline wastewater and soil. *Environ. Pollution* 158, 1119–1126.

Zhou, J., He, Z., Yang, Y., Deng, Y., Tringe, S. G., & Alvarez-cohen, L. (2015). High-Throughput Metagenomic Technologies for Complex Microbial Community Analysis : Open and Closed Formats. *MBio, 6*(1), 1–17.

Zou, S., Yao, S., & Ni, J. (2014). High-efficient nitrogen removal by coupling enriched autotrophic-nitrification and aerobic-denitrification consortiums at cold temperature. *Bioresource Technology*, *161*, 288–296.

# Appendix A: Bioremediation Site Field and Chemical Results over 24 months

Table A. 1: pH concentrations in the five monitoring wells over 24-month period

|  | pH | S1 | S2 | S3 | S4 | S5 |
|---|---|---|---|---|---|---|
| 1 | June 15 | 6.6 | 6.6 | 6.6 | 6.6 | 6.5 |
| 2 | July 15 | 6.7 | 6.6 | 6.7 | 6.7 | 6.5 |
| 3 | Aug 15 | 6.7 | 6.7 | 6.8 | 6.5 | 6.6 |
| 4 | Sept 15 | 6.7 | 6.7 | 6.7 | 6.6 | 6.4 |
| 5 | Oct 15 | 6.8 | 6.9 | 7.0 | 6.9 | 6.6 |
| 6 | Nov 15 | 6.8 | 7.0 | 7.0 | 6.9 | 7.7 |
| 7 | Dec 15 | 6.5 | 6.9 | 7.1 | 7.0 | 6.9 |
| 8 | Jan 16 | 6.5 | 6.9 | 7.0 | 7.0 | 7.0 |
| 9 | Feb 16 | 6.8 | 6.9 | 7.3 | 7.0 | 6.9 |
| 10 | Mar 16 | 7.0 | 7.1 | 7.1 | 7.1 | 7.0 |
| 11 | Apr 16 | 6.6 | 7.2 | 7.3 | 7.1 | 7.5 |
| 12 | May 16 | 6.6 | 6.9 | 7.0 | 6.9 | 6.7 |
| 13 | June 16 | 7.1 | 7.3 | 7.3 | 7.3 | 7.2 |
| 14 | July 16 | 7.0 | 7.2 | 7.1 | 6.9 | 6.9 |
| 15 | Aug 16 | 7.0 | 7.0 | 7.1 | 7 | 6.5 |
| 16 | Sept 16 | 6.9 | 7.0 | 7.0 | 6.9 | 7.1 |
| 17 | Oct 16 | 7.2 | 7.6 | 8.0 | 7.6 | 7.0 |
| 18 | Nov 16 | 6.9 | 7.3 | 7.2 | 7.5 | 7.5 |
| 19 | Dec 16 | 7.5 | 7.5 | 8.1 | 8.3 | 8.4 |
| 20 | Jan 17 | 7.1 | 7.0 | 7.8 | 7.9 | 7.6 |
| 21 | Feb 17 | 7.2 | 7.1 | 7.2 | 8.2 | 7.1 |
| 22 | Mar 17 | 7.5 | 7.8 | 7.0 | 6.9 | 6.9 |
| 23 | Apr 17 | 7.1 | 6.8 | 7.0 | 7.0 | 6.8 |
| 24 | May 17 | 7.8 | 8.1 | 8.3 | 7.8 | 7.0 |

Table A. 2: DO concentrations in the five monitoring wells over 24-month period

|  | DO mg $L^{-1}$ | S1 | S2 | S3 | S4 | S5 |
|---|---|---|---|---|---|---|
| 1 | June 15 | 2.5 | 1.9 | 1.7 | 1.6 | 1.2 |
| 2 | July 15 | 1.05 | 2.15 | 0.78 | 1.86 | 0.98 |
| 3 | Aug 15 | 1.4 | 1.6 | 0.2 | 1.2 | 1.8 |
| 4 | Sept 15 | 4.46 | 3.18 | 5.96 | 2.66 | 1.95 |
| 5 | Oct 15 | 2.6 | 1.3 | 0.4 | 1.8 | 2.7 |
| 6 | Nov 15 | 2.5 | 2.2 | 0.8 | 1.9 | 1.6 |
| 7 | Dec 15 | 4.9 | 5 | 4.2 | 4.1 | 3.6 |
| 8 | Jan 16 | 4.1 | 3.6 | 4.3 | 3.7 | 3.8 |
| 9 | Feb 16 | 3.6 | 3.9 | 4.9 | 3.3 | 3.9 |
| 10 | Mar 16 | 3.9 | 3.4 | 4.3 | 2.9 | 1.9 |
| 11 | Apr 16 | 3.4 | 3.1 | 2.6 | 2.3 | 2.3 |
| 12 | May 16 | 2.5 | 2.2 | 2.5 | 2.3 | 2.4 |
| 13 | June 16 | 2.8 | 2.3 | 2.5 | 2.3 | 2.5 |

| | | | | | |
|---|---|---|---|---|---|---|
| 14 | July 16 | 5.6 | 2.4 | 2.4 | 2.8 | 3.1 |
| 15 | Aug 16 | 1.6 | 1.8 | 2.3 | 1.7 | 2.3 |
| 16 | Sept 16 | 0.6 | 1.8 | 2 | 1.6 | 2.5 |
| 17 | Oct 16 | 2 | 1.6 | 2.9 | 2.5 | 3.2 |
| 18 | Nov 16 | 1.8 | 1.1 | 0.8 | 1.9 | 2.1 |
| 19 | Dec 16 | 3.6 | 2.5 | 1.5 | 1.5 | 1.6 |
| 20 | Jan 17 | 1.2 | 1.4 | 0.9 | 0.9 | 1.1 |
| 21 | Feb 17 | 0.1 | 1.1 | 0.7 | 0.4 | 0.3 |
| 22 | Mar 17 | 0.2 | 0.6 | 0.5 | 1 | 2.1 |
| 23 | Apr 17 | 3.1 | 0.3 | 0.5 | 0.5 | 1.3 |
| 24 | May 17 | 3.1 | 0.9 | 1 | 1.3 | 2 |

Table A. 3: Temperature in the five monitoring wells over 24-month period

| | Temp °C | S1 | S2 | S3 | S4 | S5 |
|---|---|---|---|---|---|---|
| 1 | June 15 | 14.7 | 15.8 | 15.2 | 15.3 | 13 |
| 2 | July 15 | 13.3 | 13.4 | 13.5 | 14 | 14.2 |
| 3 | Aug 15 | 13.6 | 14 | 14.3 | 14.3 | 13.1 |
| 4 | Sept 15 | 15.4 | 15.4 | 15.3 | 16.6 | 15.5 |
| 5 | Oct 15 | 15.2 | 15 | 15 | 14.8 | 15.2 |
| 6 | Nov 15 | 14 | 15 | 13.9 | 13.7 | 13 |
| 7 | Dec 15 | 12.6 | 13.2 | 12 | 11.7 | 12.2 |
| 8 | Jan 16 | 11.8 | 11.6 | 10.2 | 8.3 | 11 |
| 9 | Feb 16 | 11.6 | 11.9 | 9 | 7.9 | 10.5 |
| 10 | Mar 16 | 12 | 12.1 | 12 | 8 | 8.7 |
| 11 | Apr 16 | 12.5 | 12.4 | 12.4 | 10.7 | 10 |
| 12 | May 16 | 13.1 | 11.7 | 12.5 | 10.9 | 10.3 |
| 13 | June 16 | 16.6 | 14.6 | 14.6 | 14.2 | 14 |
| 14 | July 16 | 18.1 | 17.7 | 15.8 | 16.6 | 14.9 |
| 15 | Aug 16 | 16.3 | 15.6 | 14.4 | 14 | 14.3 |
| 16 | Sept 16 | 13.7 | 13.4 | 13.1 | 13.3 | 12.2 |
| 17 | Oct 16 | 11.4 | 10.7 | 9.6 | 9.8 | 9.5 |
| 18 | Nov 16 | 12.8 | 12.6 | 12.9 | 12.8 | 12.6 |
| 19 | Dec 16 | 11.5 | 10.7 | 12.6 | 12.3 | 11.4 |
| 20 | Jan 17 | 10.6 | 10.1 | 10.8 | 10.9 | 10 |
| 21 | Feb 17 | 11.7 | 11.3 | 10.8 | 11.5 | 10.9 |
| 22 | Mar 17 | 12.1 | 12.1 | 12.2 | 11.6 | 11.8 |
| 23 | Apr 17 | 16.8 | 12.7 | 13.2 | 13.1 | 13 |
| 24 | May 17 | 11.5 | 11 | 11.3 | 11.8 | 11.5 |

Table A. 4: Electrical conductivity in the five monitoring wells over 24-month period

| | Electrical Conductivity mg L$^{-1}$ | S1 | S2 | S3 | S4 | S5 |
|---|---|---|---|---|---|---|
| 1 | June 15 | 1797 | 1524 | 1470 | 1498 | 986 |
| 2 | July 15 | 1904 | 1715 | 1403 | 1330 | 936 |
| 3 | Aug 15 | 1785 | 1756 | 1506 | 1518 | 1164 |
| 4 | Sept 15 | 1680 | 1590 | 1466 | 1388 | 908 |
| 5 | Oct 15 | 1489 | 1543 | 1398 | 1365 | 984 |
| 6 | Nov 15 | 1291 | 1550 | 1476 | 1326 | 900 |
| 7 | Dec 15 | 1235 | 1285 | 1472 | 958 | 846 |
| 8 | Jan 16 | 1324 | 1523 | 854 | 895 | 698 |
| 9 | Feb 16 | 1121 | 1183 | 638 | 566 | 520 |
| 10 | Mar 16 | 1326 | 1141 | 895 | 1100 | 642 |
| 11 | Apr 16 | 1548 | 1704 | 1116 | 1347 | 719 |
| 12 | May 16 | 1460 | 1492 | 953 | 1325 | 829 |
| 13 | June 16 | 1899 | 1555 | 1187 | 1470 | 1023 |
| 14 | July 16 | 1580 | 1598 | 1349 | 1422 | 787 |
| 15 | Aug 16 | 1970 | 1494 | 1242 | 1371 | 889 |
| 16 | Sept 16 | 1359 | 1444 | 1217 | 1213 | 867 |
| 17 | Oct 16 | 869 | 1239 | 1161 | 1247 | 860 |
| 18 | Nov 16 | 1203 | 1410 | 1302 | 1178 | 926 |
| 19 | Dec 16 | 1695 | 1970 | 2110 | 2170 | 1148 |
| 20 | Jan 17 | 1855 | 1888 | 1869 | 2110 | 1335 |
| 21 | Feb 17 | 1830 | 2140 | 1280 | 2110 | 1357 |
| 22 | Mar 17 | 1408 | 1838 | 1716 | 1661 | 1275 |
| 23 | Apr 17 | 2510 | 2400 | 1753 | 2170 | 1320 |
| 24 | May 17 | 2720 | 2220 | 1599 | 1942 | 1325 |

Table A. 5: NH$_4$-N concentrations in the five monitoring wells over 24-month period

| | NH$_4$-N mg L$^{-1}$ | S1 | S2 | S3 | S4 | S5 |
|---|---|---|---|---|---|---|
| 1 | June 15 | 118.52 | 94.11 | 89.51 | 82.26 | 14.41 |
| 2 | July 15 | 158.34 | 116.21 | 80.96 | 78.54 | 16.26 |
| 3 | Aug 15 | 131.15 | 153.03 | 101.64 | 101.6 | 8.53 |
| 4 | Sept 15 | 128.84 | 112.87 | 82.67 | 88.8 | 10.19 |
| 5 | Oct 15 | 133.18 | 95.47 | 90.97 | 89.53 | 10.47 |
| 6 | Nov 15 | 87.42 | 121.01 | 61.52 | 82.39 | 6.67 |
| 7 | Dec 15 | 45.1 | 33.13 | 16.09 | 15.2 | 4.22 |
| 8 | Jan 16 | 69.94 | 69.47 | 36.14 | 45.65 | 3.22 |
| 9 | Feb 16 | 87.73 | 87.07 | 20.78 | 18.29 | 1.68 |
| 10 | Mar 16 | 96.29 | 124.1 | 41.01 | 54.11 | 3.23 |
| 11 | Apr 16 | 155.22 | 176.89 | 78.57 | 114.75 | 6.87 |
| 12 | May 16 | 169.98 | 157.22 | 100.07 | 127.07 | 6.83 |
| 13 | June 16 | 192.12 | 153.32 | 91.01 | 141.02 | 7.28 |
| 14 | July 16 | 165.62 | 105.43 | 94.17 | 102.24 | 6.5 |

| 15 | Aug 16 | 186.57 | 110.16 | 92.46 | 101.86 | 9.02 |
|----|--------|--------|--------|-------|--------|------|
| 16 | Sept 16 | 89.52 | 113.64 | 78.68 | 87.22 | 8.09 |
| 17 | Oct 16 | 89.52 | 113.64 | 78.68 | 87.22 | 8.24 |
| 18 | Nov-16 | 70.37 | 77.1 | 64.43 | 85.33 | 13.53 |
| 19 | Dec-16 | 72.09 | 68.44 | 72.15 | 86.66 | 9.72 |
| 20 | Jan-17 | 69.39 | 78.67 | 69.78 | 100.8 | 9.01 |
| 21 | Feb-17 | 83.49 | 93.31 | 67.41 | 97 | 6.1 |
| 22 | Mar-17 | 44.65 | 54.49 | 34.42 | 43.44 | 4.94 |
| 23 | Apr-17 | 143.09 | 97.41 | 68.34 | 82.99 | 7.8 |
| 24 | May-17 | 129.99 | 82.12 | 74.46 | 84.19 | 8.28 |

Table A. 6: $NO_2$ concentrations in the five monitoring wells over 24-month period

|  | $NO_2$ mg $L^{-1}$ | S1 | S2 | S3 | S4 | S5 |
|----|-----------|------|------|------|------|------|
| 1 | June 15 | 0.24 | 0.02 | 0.05 | 0.04 | 0.02 |
| 2 | July 15 | 0.02 | 0.02 | 0.02 | 0.02 | 0.02 |
| 3 | Aug 15 | 0.09 | 0.02 | 0.02 | 0.02 | 0.02 |
| 4 | Sept 15 | 1.83 | 0.02 | 0.02 | 0.02 | 0.02 |
| 5 | Oct 15 | 0.36 | 0.02 | 0.02 | 0.02 | 0.02 |
| 6 | Nov 15 | 0.02 | 0.02 | 0.02 | 0.02 | 0.02 |
| 7 | Dec 15 | 0.02 | 0.02 | 0.02 | 0.02 | 0.02 |
| 8 | Jan 16 | 0.02 | 0.02 | 0.02 | 0.02 | 0.02 |
| 9 | Feb 16 | 0.02 | 0.02 | 0.08 | 0.05 | 0.02 |
| 10 | Mar 16 | 0.02 | 0.02 | 0.4 | 0.02 | 0.02 |
| 11 | Apr 16 | 0.02 | 0.06 | 0.14 | 0.02 | 0.02 |
| 12 | May 16 | 0.02 | 0.07 | 0.16 | 0.02 | 0.02 |
| 13 | June 16 | 0.02 | 0.02 | 0.18 | 0.02 | 0.02 |
| 14 | July 16 | 0.13 | 0.02 | 0.2 | 0.02 | 0.02 |
| 15 | Aug 16 | 0.13 | 0.02 | 0.59 | 0.02 | 0.02 |
| 16 | Sept 16 | 0.02 | 0.02 | 0.17 | 0.02 | 0.02 |
| 17 | Oct 16 | 0.02 | 0.02 | 0.17 | 0.02 | 0.02 |
| 18 | Nov 16 | 0.71 | 0.02 | 0.39 | 0.02 | 0.02 |
| 19 | Dec 16 | 0.02 | 0.02 | 0.37 | 0.02 | 0.02 |
| 20 | Jan 17 | 0.29 | 0.05 | 0.35 | 0.02 | 0.02 |
| 21 | Feb 17 | 0.47 | 0.05 | 0.19 | 0.02 | 0.02 |
| 22 | Mar 17 | 0.1 | 0.02 | 0.02 | 0.02 | 0.02 |
| 23 | Apr 17 | 0.11 | 0.02 | 0.12 | 0.02 | 0.02 |
| 24 | May 17 | 0.02 | 0.02 | 0.02 | 0.02 | 0.02 |

Table A. 7: NO$_3$ concentrations in the five monitoring wells over 24-month period

|    | NO$_3$ mg L$^{-1}$ | S1 | S2 | S3 | S4 | S5 |
|----|------|------|------|------|------|------|
| 1  | June 15 | 0.2 | 0.2 | 0.2 | 0.2 | 0.2 |
| 2  | July 15 | 0.8 | 0.8 | 0.7 | 0.8 | 0.2 |
| 3  | Aug 15 | 0.2 | 0.2 | 0.2 | 0.2 | 0.3 |
| 4  | Sept 15 | 19.8 | 0.2 | 0.3 | 0.2 | 1.2 |
| 5  | Oct 15 | 2.1 | 0.5 | 0.5 | 0.4 | 0.3 |
| 6  | Nov 15 | 0.3 | 0.4 | 0.3 | 0.3 | 0.3 |
| 7  | Dec 15 | 0.2 | 0.2 | 0.2 | 0.2 | 0.2 |
| 8  | Jan 16 | 0.2 | 0.2 | 0.2 | 0.2 | 0.2 |
| 9  | Feb 16 | 0.2 | 0.2 | 0.2 | 2 | 0.2 |
| 10 | Mar 16 | 0.5 | 0.6 | 1.2 | 0.5 | 0.5 |
| 11 | Apr 16 | 0.8 | 1.1 | 1.7 | 0.8 | 0.8 |
| 12 | May 16 | 0.4 | 0.4 | 3.5 | 0.4 | 0.4 |
| 13 | June 16 | 0.2 | 0.2 | 1.9 | 0.2 | 0.2 |
| 14 | July 16 | 1.5 | 0.4 | 6.4 | 0.4 | 0.2 |
| 15 | Aug 16 | 0.8 | 0.3 | 9.1 | 0.3 | 0.4 |
| 16 | Sept 16 | 0.2 | 0.2 | 0.7 | 0.2 | 0.2 |
| 17 | Oct 16 | 0.2 | 0.2 | 0.7 | 0.2 | 0.2 |
| 18 | Nov 16 | 7.8 | 0.2 | 10.7 | 0.2 | 0.2 |
| 19 | Dec 16 | 0.2 | 0.2 | 3.9 | 0.2 | 0.2 |
| 20 | Jan 17 | 6.2 | 0.2 | 5.3 | 0.2 | 0.2 |
| 21 | Feb 17 | 1.6 | 0.6 | 3.2 | 0.3 | 0.2 |
| 22 | Mar 17 | 1 | 0.2 | 0.2 | 0.2 | 0.2 |
| 23 | Apr 17 | 0.2 | 0.2 | 0.12 | 0.2 | 0.2 |
| 24 | May 17 | 0.2 | 0.2 | 0.2 | 0.2 | 0.2 |

Table A. 8: TOC concentrations in the five monitoring wells over 24-month period

|    | TOC mg L$^{-1}$ | S1 | S2 | S3 | S4 | S5 |
|----|------|------|------|------|------|------|
| 1  | June 15 | 37 | 28 | 22 | 35 | 42 |
| 2  | July 15 | 23 | 7 | 2 | 2 | 39 |
| 3  | Aug 15 | 11 | 2 | 2 | 37 | 16 |
| 4  | Sept 15 | 32 | 20 | 18 | 46 | 19 |
| 5  | Oct 15 | 9 | 13 | 7 | 6 | 5 |
| 6  | Nov 15 | 43 | 67 | 39 | 54 | 28 |
| 7  | Dec 15 | 5 | 7 | 3 | 2 | 2 |
| 8  | Jan 16 | 25 | 2 | 26 | 9 | 8 |
| 9  | Feb 16 | 13 | 18 | 5 | 2 | 8 |
| 10 | Mar 16 | 2 | 2 | 4 | 6 | 10 |
| 11 | Apr 16 | 72 | 2 | 4 | 2 | 2 |
| 12 | May 16 | 64 | 74 | 39 | 60 | 12 |
| 13 | June 16 | 20 | 2 | 2 | 2 | 5 |
| 14 | July 16 | 25 | 15 | 17 | 17 | 11 |
| 15 | Aug 16 | 41 | 32 | 26 | 31 | 19 |

| 16 | Sept 16 | 15 | 34 | 23 | 2 | 9 |
|----|---------|----|----|----|----|----|
| 17 | Oct 16  | 15 | 34 | 23 | 2 | 3 |
| 18 | Nov 16  | 27 | 27 | 28 | 35 | 5 |
| 19 | Dec 16  | 21 | 14 | 6 | 25 | 10 |
| 20 | Jan 17  | 11 | 14 | 18 | 12 | 2 |
| 21 | Feb 17  | 6 | 2 | 9 | 14 | 2 |
| 22 | Mar 17  | 15 | 21 | 30 | 18 | 10 |
| 23 | Apr 17  | 30 | 21 | 23 | 18 | 12 |
| 24 | May 17  | 14 | 7 | 8 | 8 | 9 |

## Appendix B: DNA Sequences of Functional Gene Positive Standards

### Bacterial *amoA*

AATCGTTGTAGAAGGCACATTGCTGTCGATGGCTGATTACATGGGACATCTGTATGTTCGTACAGGTA
CACCCGAGTATGTTCGTCATATTGAGCAAGGTTCACTGCGTACCTTTGGTGGTCATACCACAGTTATTG
CAGCATTCTTCTCTGCGTTCGTATCAATGTTGATGTTCACCGTATGGTGGTATCTTGGAAAAGTTTACTG
TACAGCCTTTTTCTACGTTAAAGGTAAAAGAGGTCGTATCGTACATCGCAATGATGTTACCGCATTCGG
TGAAGAAGGCTTTCCAGAGGGGATCAAATAAAACCTGCGGCCGCAAGCTTGGATCCGAATTCCTGTGT
GAAATTGTTATCCGCTCACAATTCCACACAACATACGAGCCGGAAGCATAA

### Archaeal *amoA*

CAAGGAGTGCTTGTTCTTCTTTGTGGCCCAATAGGCTAAATCAAGCAACATTGCTGATGGTAACCAAAC
TGGTGTTACAATGAAGTCATATGGATATCCTAGTGCAAACCATGCACCTTTTGCTATCCATGTGTATACT
GTCATAATTAGGGCGTAATACGTCGCTGTTCCTGGAACACCTGTAAATGTCAGGTAGTATGTTGCACCT
ACCGCGAGCATCAATGTTTGTGATATTGAAAATACCACAAAGGATGTCCAAGCCCAGTCAGTATAGAA
AATGTAGTCTCCTGCATTAATTGTTAACAGTGTAGAGTTAACTGCAACTACTACTATGAATAAGTAGTG
AGTACATCGTCTTAGCCAGACCATTATGAACTAGACCTGCGGCCGCAAGCTTGGATCCGAATTCCTGTG
TGAAATTGTTATCCGCTCACAATTCCACACAACATACGAGCCGGAAGCATAAAGTGTAAAGCCTGGGg
TGCCTAATGAGTGAGCTAACTCACATTAATTGCGTTGC

### *nirS*

GgnagCTCTCCcaTATGGTCGACcTGCAGGCGGCCGCGAaTTCACTAGTGATTGGGTGGGACTTGATGA
ACAGCGCGCCGCCGCCTGGGCCCTTGAGCTTGGCAACTTCCTTGAACGCGTATTGCTTGTGCTTCTTGG
GGtnGgTCCCAATCAGCGAGATGGTGTCATCACCCAGATGGCCGGTGGACCACACGGGGCCGAACTTA
GGATGGATGAAGTTGGCGCCACGGCCGGGGTGGGgAaTCTTGCCCACATCGACGACAGCCTCCATCTT
GCnntCCTTGgCGT

### *nirK*

cacgCcggCCGAgCCnCCGCGCAcgaaccAGGTCTCCaGATTCTTCAgCGGTGGGTTGtcgAaCTTGCCGGT
CTCCcaTACccagtcgCcgTGccngccnnnnnCnGCATCCAGCTCGGCATAGCTGAGTTGCCGGCTGCCGCA
TGCTACGGCAATGGCGTCCGGCTGCGACCTGACCTGCTCTTCGAGCATGTGGTTCAGCGGTTTGCCGA
GCCAGTAACCGGCTTCGCGGTAGCGTTCGGCGAAGGCCTGGGGCCAACGACTGAAGGGCGTCAGGCT
CATACCGCCTCCCGTTCGAGACCGAACGCGCTGAGCATGGTGCCGAACTTGGTGCCCGTCTCGCGCCA
TTCGGATTCCGGACAGGACGCCGAAACCAGCCCCGCTCCGGCAAACAGGCGCACCTGGCGTTGATGA
ATGACGCCGCAGCGAATCACCACCGCCCATTCGCCATgCccGCcantaaaa

### *nosZ*

catATGGTCGACCTGCAGGCGGCCGCGAATTCACTAGTGATTCATGTGCAGAGCGTGGCAGAACCAGC
TGCAGTAGTACCAGTACGCGCCGGCCTTGTCTGCAGTGAAGGTGATCGAGGAGGTCTGTTGCGGGCT
GATCTCCATGCTCACCCCGTGGTTGACCATGACGAAACCGTGGGAAACGTCCTCGATCTGGTCGATGT
TGGTGATGATCACCGTGACCTCGTCGCCCTGCTTGACGGTGAACTCGTTGATGCCGAAGGACGGCGCC
ATGGAGATCATGTACACCCGCACCTTGTTGCCATCGCGAATGATCTTGCTATCGCTGGTCAGGTTGATG
CCGTCGGCTTCCGCCATCTTCACTGTTTCTGCGAAGAAGGGGTCGTTGCGGTCCCAGATCTTC

179

TTGGTACGCAGTTGATCGCGGCGAGCCATGATGCAGTCGTGCGGTTCGGCAAAGGTGGGGCCGTCGT
GTACCAGCACCATCTCTTCACCGGAAATGTCGATCAACTGGTCGTTTTCCGGGTGCAGAGGGCCGACC
GGCAGGAAGCGGTCCTTGGAGAACTTGGACAGCACCACCAGCCACTGACCATCGGCTTCGCTGGTTTC
GCACAGCGAGGCGTGGGTATGCCCAGGCTGGTAATGCACGTCGAGCTTCTGCTTGATGTAGTTGACGT
TGTCGCCGTTATAGGCACGGATGGCATCTTCGATGTTCCACTTGACCACCTGGCTGTCGAGGAACAAC
GAATCGAATTCCcGCGGCCGCCATGGCGGCCGGgaGCATGCGACGTCGGGCCCAATTCGCCCTATAGT
GAGTCGTATTACAATTCACTGGCCGTCGTTTTACAACGTCGTGACTGGGAA

# Appendix C: Agarose Gel Images from PCR optimisation
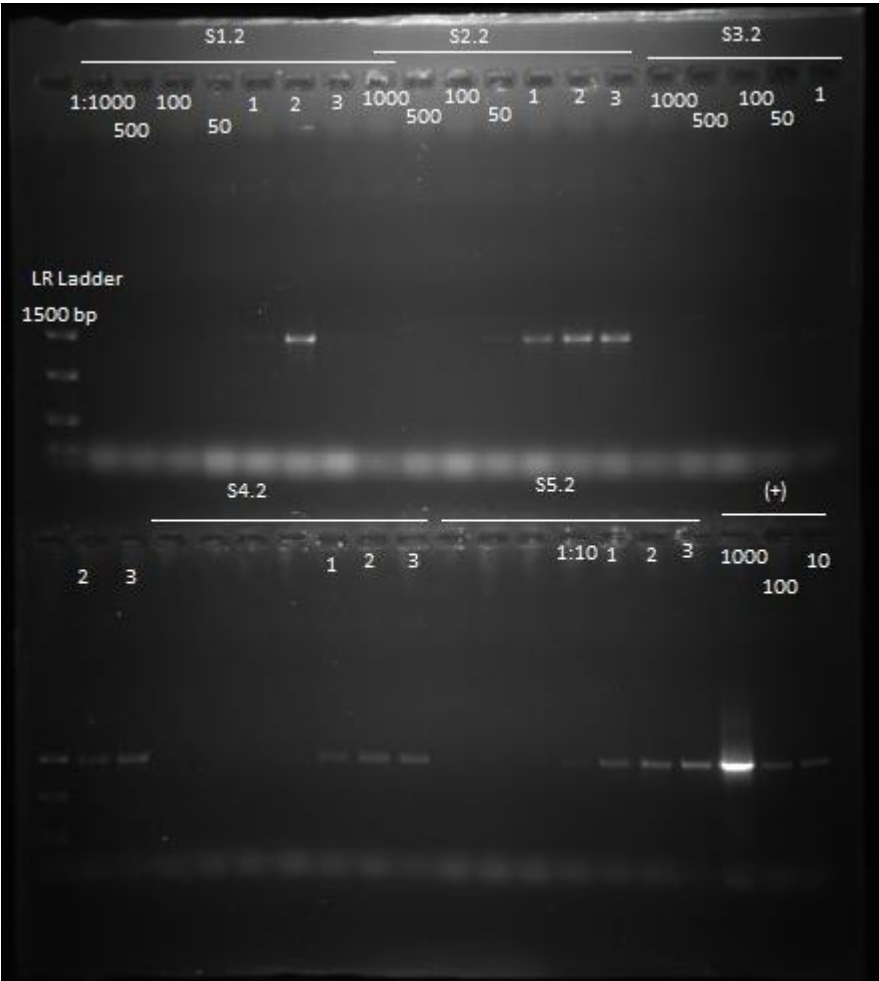


Figure C. 1: December 2015 S1.2, S2.2 and S3.2 *16S* PCR products (1465 bp; in dilution (1:000, 1:500, 1:100, 1:50 and 1 μl, 2μl and 3 μl DNA concentrations) visualised on an agarose gel. (+) Positive control was DNA extracted from *E. coli*.
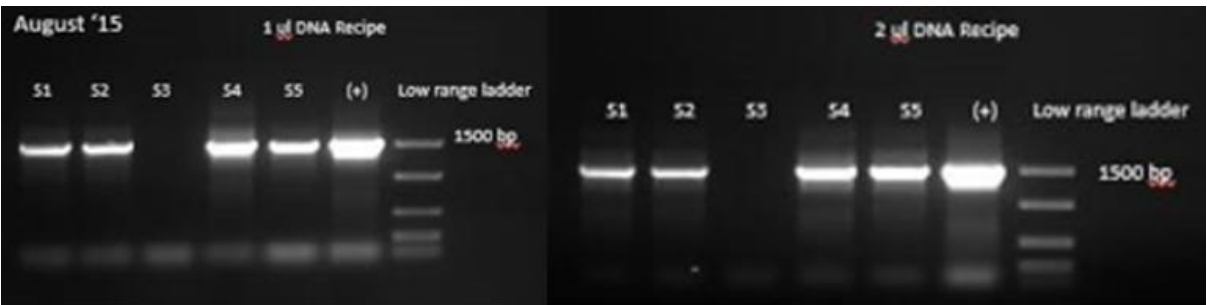


Figure C. 2: August 2015 samples S1-S5 *16S rRNA* PCR products (1465 bp) (1 μl and 2 μl DNA concentrations) visualised on an agarose gel. (+) Positive control was DNA extracted from *E. coli*.
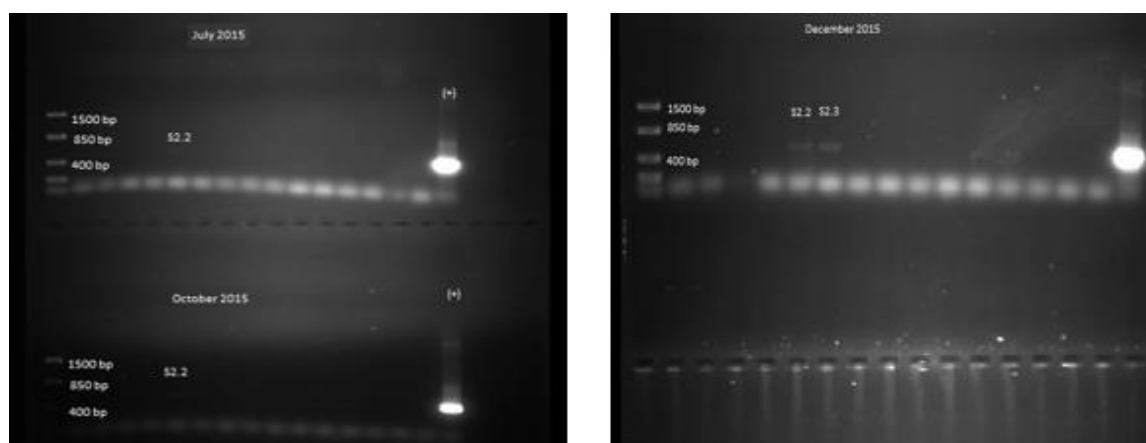
Figure C. 3: Gel images of bacterial *amoA* PCR products (491 bp) using Horz et al. (2000) cycling conditions on July, October, and December 2015 eDNA. (+) Positive control was a plasmid prep of a cloned *amoA* sequence from *Nitrosomonas europea.*
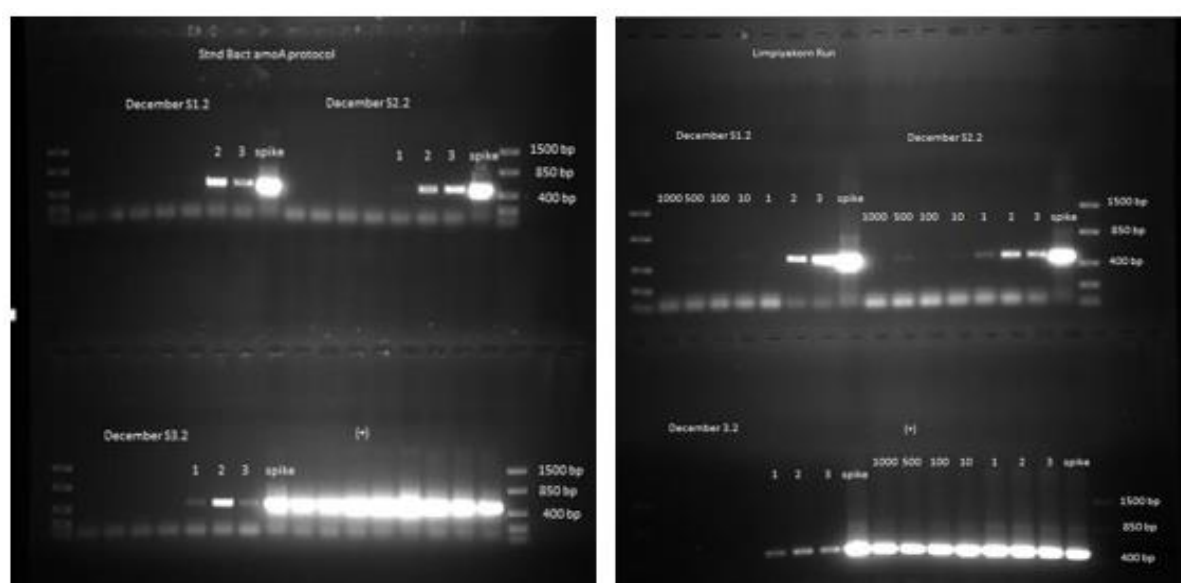


Figure C. 4: Bacterial *amoA* PCR products (490 bp) visualised on an agarose gel to compare two thermal cycling conditions (Horz et al. (2000) labelled "Stnd Bact *amoA* protocol" and Limpyakorn et al. (2011) on eDNA at different concentrations and spiked with positive standard DNA.



Figure C. 5: Bacterial *amoA* PCR products (490 bp) using Limpiyakorn et al. (2011) cycling conditions on July 2015 samples with 1 μl, 2 μl and 3 μl DNA volumes. (+) Positive control was a plasmid prep of a cloned *amoA* sequence from *Nitrosomonas europea.*
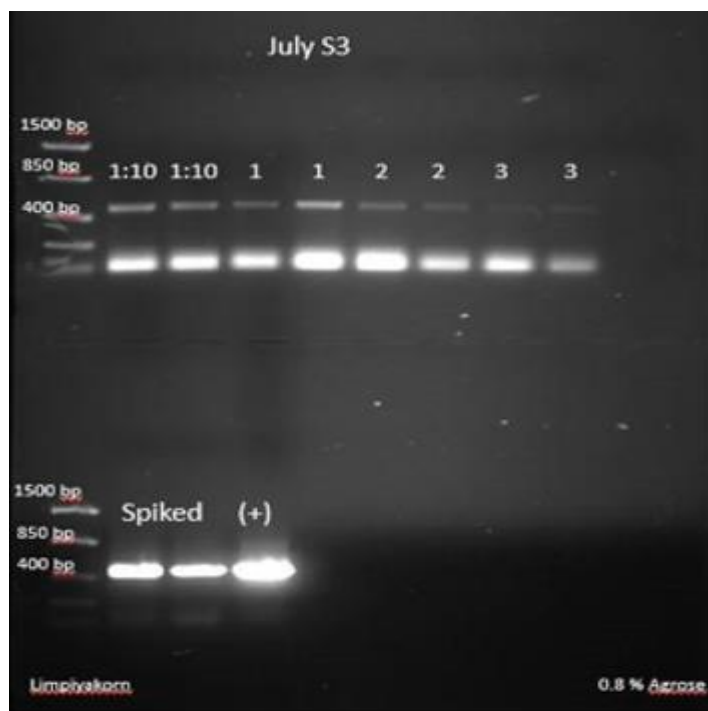
Figure C. 6: Bacterial *amoA* PCR products (490 bp) troubleshooting July S3 DNA Samples using Limpyakorn et al. (2011) cycling conditions. (+) Positive control was a plasmid prep of a cloned *amoA* sequence from *Nitrosomonas europea*.
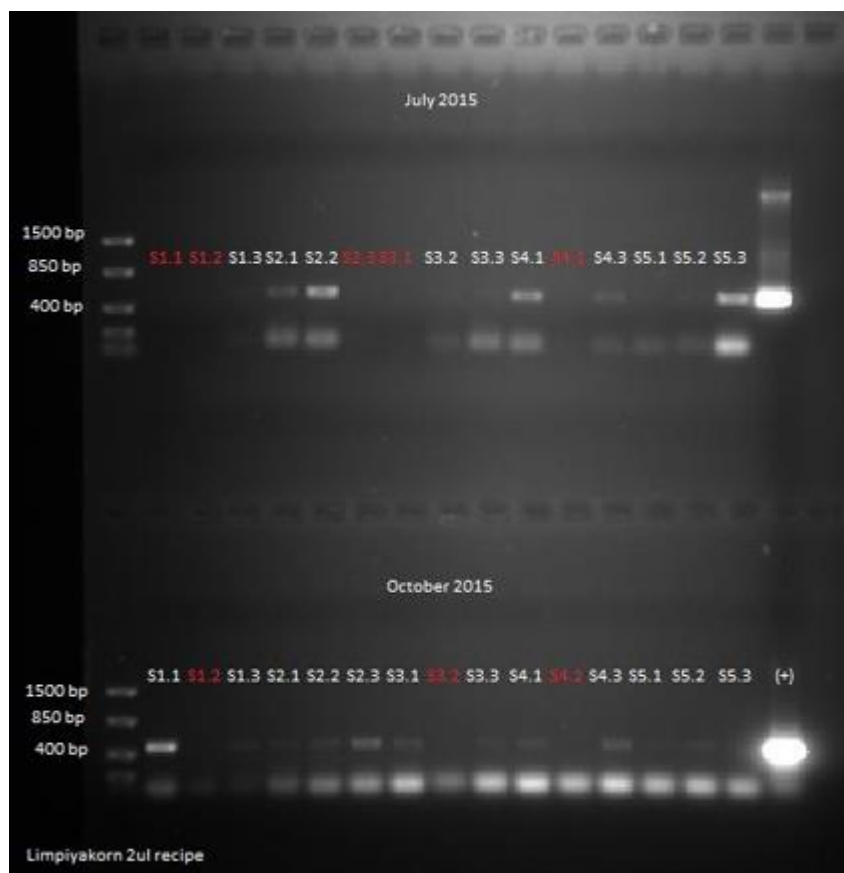


Figure C. 7: Post PCR 2 µl DNA PCR products (490 bp) carried out as per Limpyakorn et al. (2011) on July and October 2015 samples. The red labels indicate no amplification. (+) Positive control was a plasmid prep of a cloned *amoA* sequence from *Nitrosomonas europea*.

Figure C. 8: 2 µl DNA PCR products (490 bp) carried out as per Limpyakorn et al. (2011) on December 2015 samples. The red labels indicate no amplification. (+) Positive control was a plasmid prep of a cloned *amoA* sequence from *Nitrosomonas europea*.
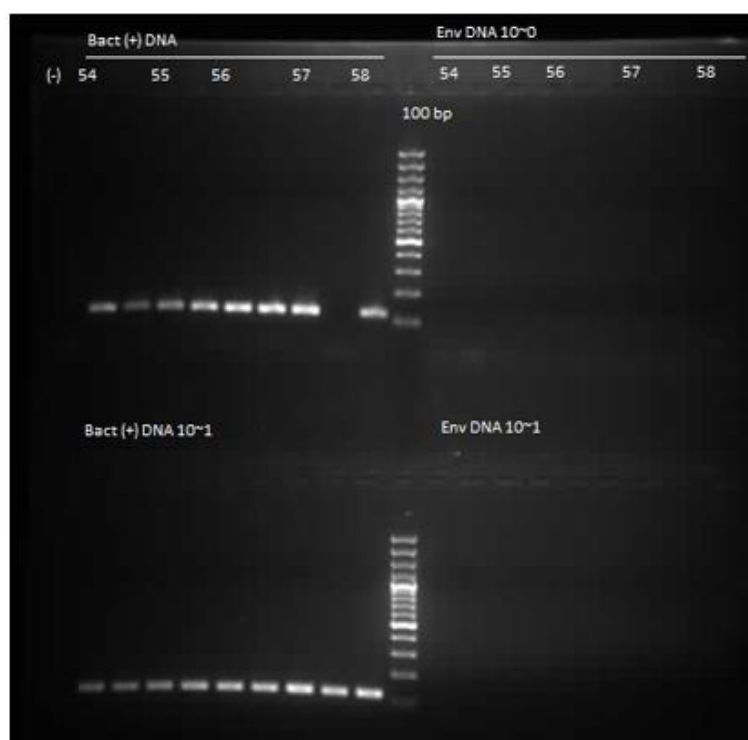


Figure C. 9:: Gradient PCR (at temperatures 54°C- 58°C) bacterial *amoA* products from positive standards and environmental DNA (490 bp) at neat and 1:10 dilutions visualised on an agarose gel. (+) Positive standard was a plasmid prep of a cloned *amoA* sequence from *Nitrosomonas europea*.



Figure C. 10: Gel image after Rotthauwe et al. (1997) bacterial amoA (490bp) PCR cycling conditions of July and August 2015 samples (S1- S5). (+) Positive control was a plasmid prep of a cloned *amoA* sequence from *Nitrosomonas europea*.
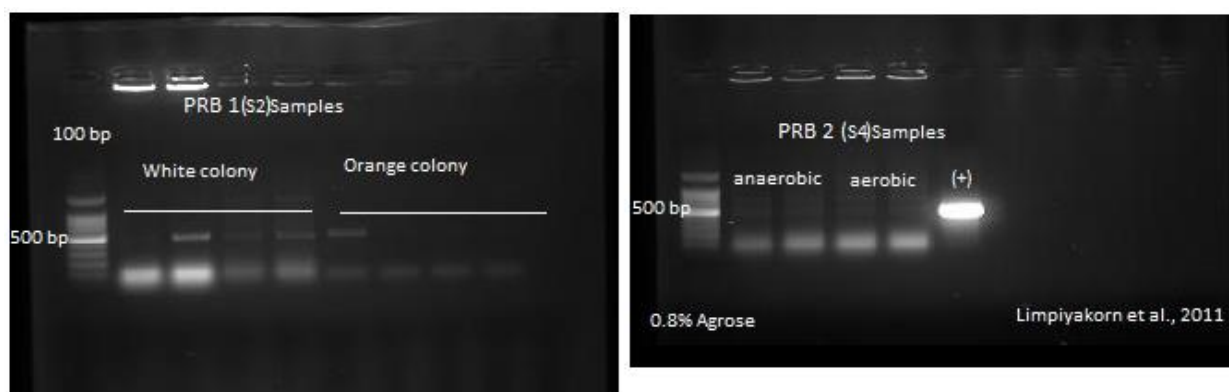
Figure C. 11: Gel image after Bacterial *amoA* PCR (490 bp) performed on PRB 1 and PRB 2 samples. (+) Positive control was a plasmid prep of a cloned *amoA* sequence from *Nitrosomonas europea.*
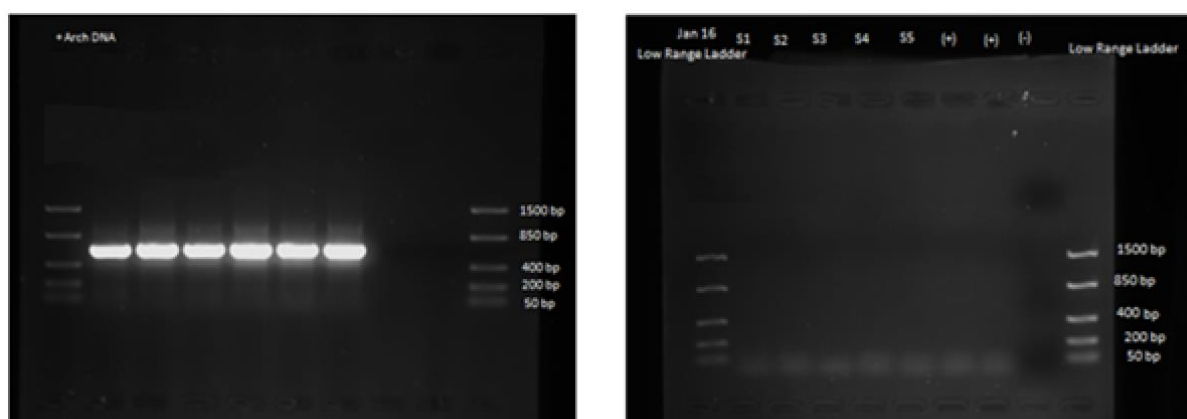


Figure C. 12: Post PCR products (709 bp) check on archaeal *amoA* DNA (left) and envrionmental samples (right). (+) Positive control was a plasmid prep of a cloned *amoA* sequence from *Nitrosoarchaeum limnia*
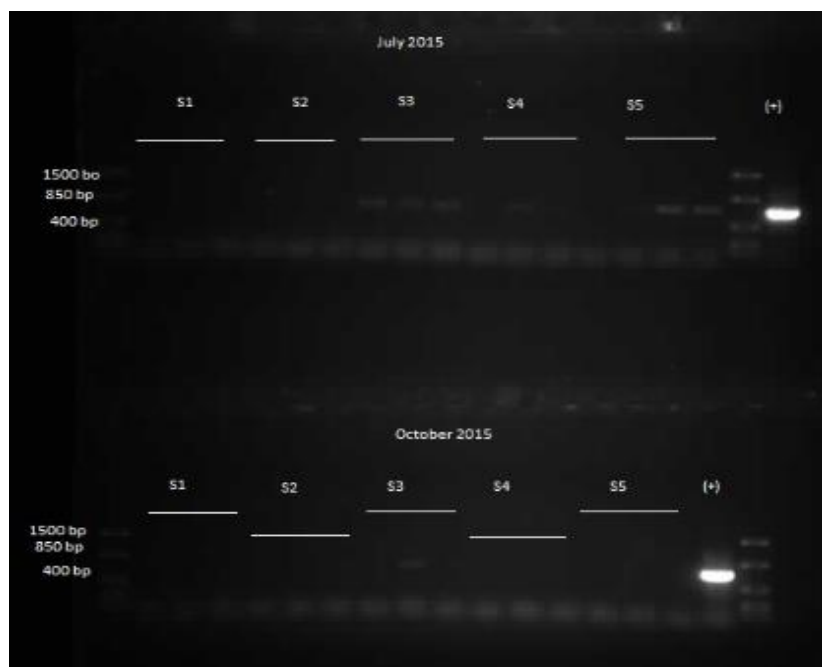


Figure C. 13: Archaeal *amoA* PCR products (709 bp) from samples collected in July and October 2015 visualised on an agarose gel. (+) Positive control was a plasmid prep of a cloned *amoA* sequence from *Nitrosoarchaeum limnia*
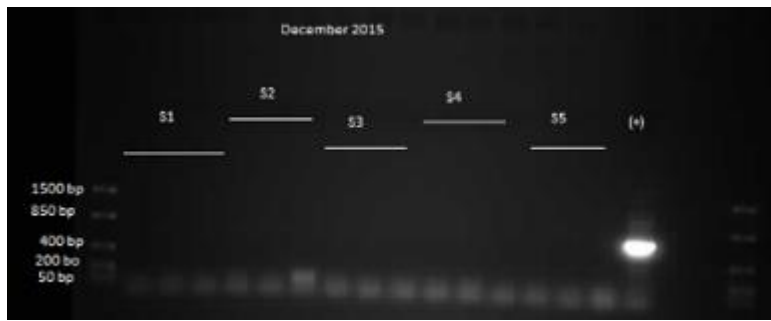
Figure C. 14: Archaeal *amoA* PCR products (709 bp) from samples (S1-S5) collected in December 2015. (+) Positive control was a plasmid prep of a cloned *amoA* sequence from *Nitrosoarchaeum limnia*
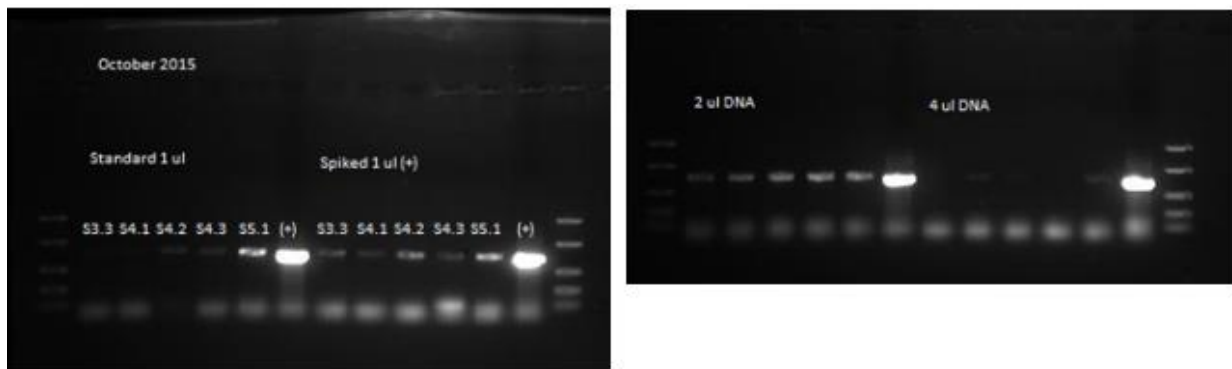


Figure C. 15: Post archaeal *amoA* PCR products (709 bp) using October 2015 samples spiked and with 2 μl and 4 μl eDNA volumes. (+) Positive control was a plasmid prep of a cloned *amoA* sequence from *Nitrosoarchaeum limnia*
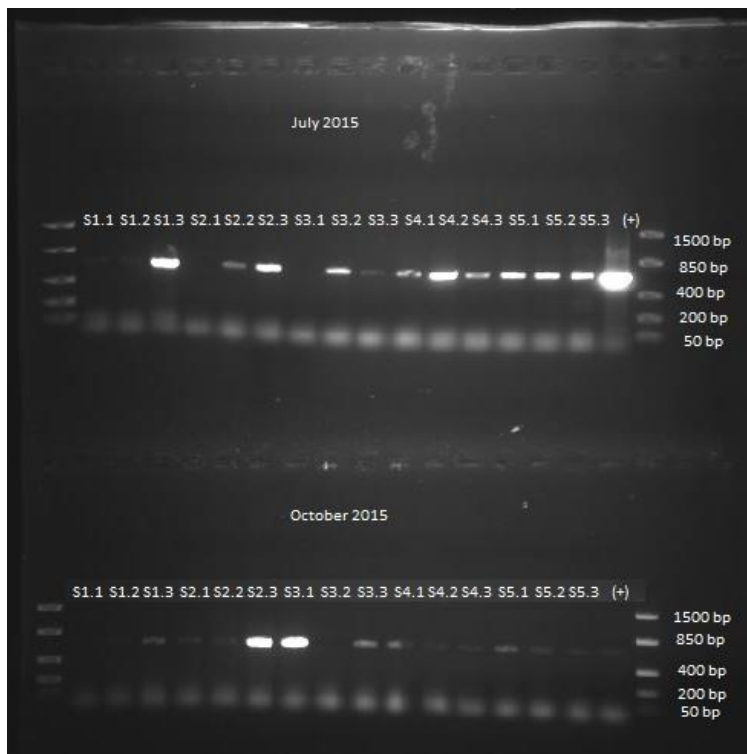


Figure C. 16: Archaeal *amoA* PCR products (709 bp) of July and October 2015 (S1- S5) samples using 2 μl DNA recipe. (+) Positive control was a plasmid prep of a cloned *amoA* sequence from *Nitrosoarchaeum limnia*
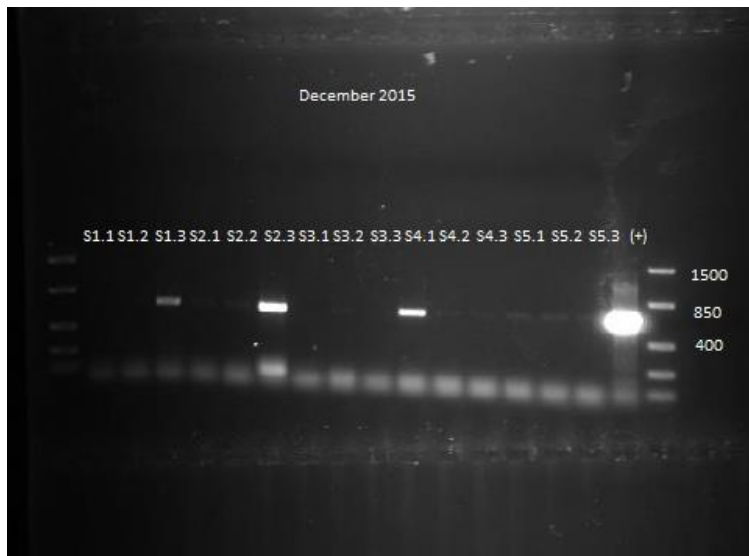
Figure C. 17: Archaeal *amoA* PCR products (709 bp) of December 2015 samples using 2 µl DNA recipe visualised on an agarose gel. (+) Positive control was a plasmid prep of a cloned *amoA* sequence from *Nitrosoarchaeum limnia*
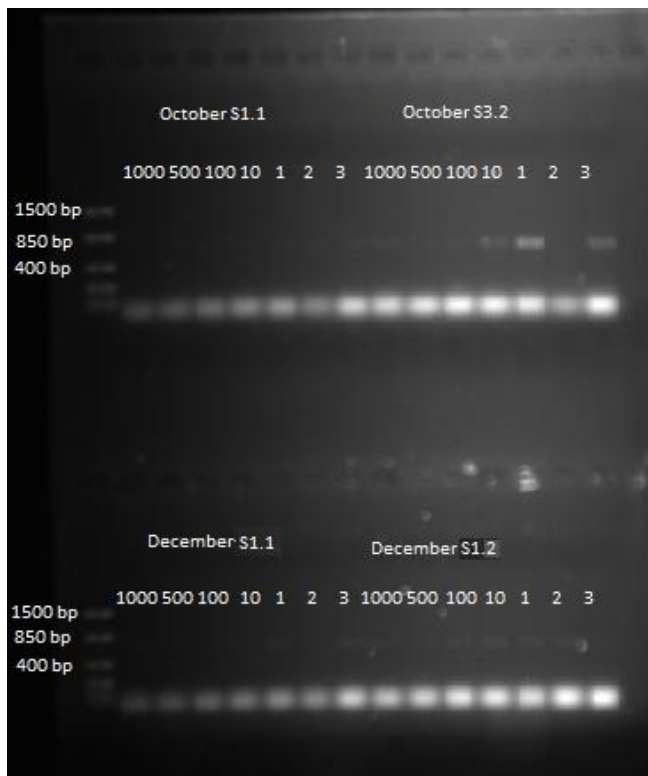


Figure C. 18: Archaeal *amoA* PCR products (709 bp) using October and December 2015 samples at various dilutions and concentration. (+) Positive control was a plasmid prep of a cloned *amoA* sequence from *Nitrosoarchaeum limnia*
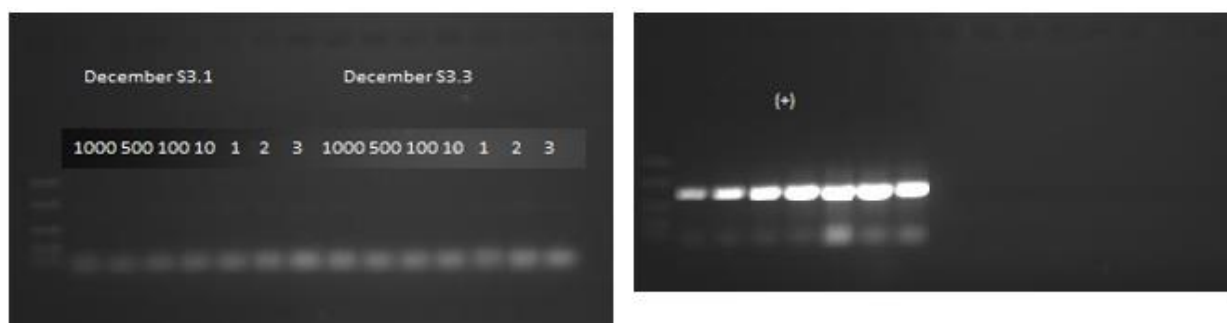
Figure C. 19: Archaeal *amoA* PCR products using December 2015 samples at various dilutions and concentrations. (+) Positive control was a plasmid prep of a cloned *amoA* sequence from *Nitrosoarchaeum limnia*



Figure C. 20: Archaeal *amoA* PCR products (709 bp) using samples with low amplification visualised on an agarose gel. (+) Positive control was a plasmid prep of a cloned *amoA* sequence from *Nitrosoarchaeum limnia*
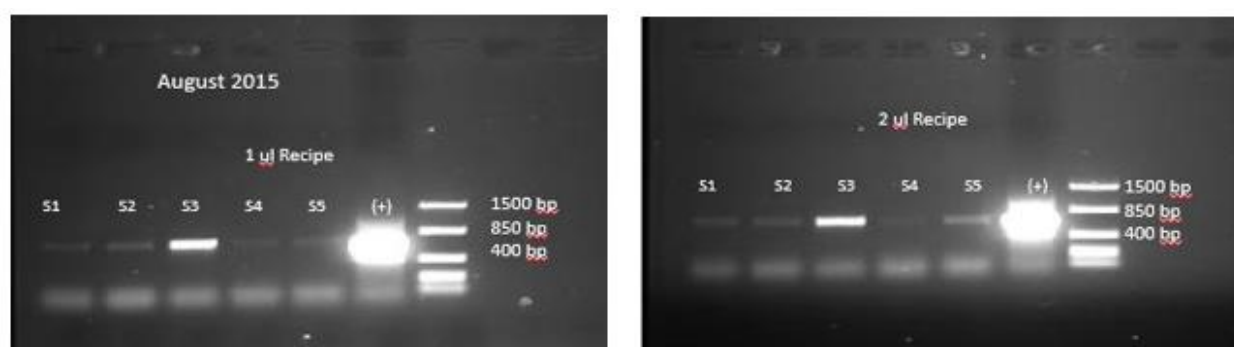


Figure C. 21: Archaeal *amoA* PCR products (709 bp) of August 2015 samples visualised on an agarose gel. (+) Positive control was a plasmid prep of a cloned *amoA* sequence from *Nitrosoarchaeum limnia*
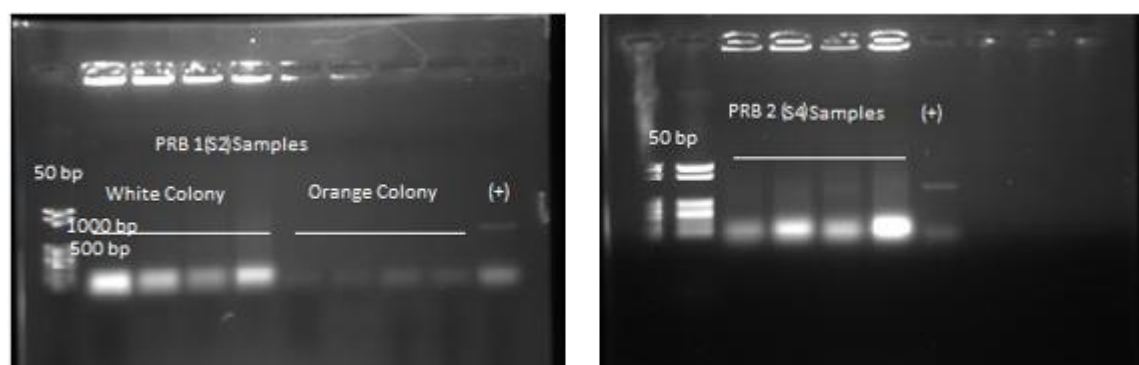


Figure C. 22: Archaeal *amoA* PCR products (709 bp) from PCR carried out on cultures grown on nutrient agar inoculated by water samples from PRB 1 and PRB2 visualised on an agarose gel. (+) Positive control was a plasmid prep of a cloned *amoA* sequence from *Nitrosoarchaeum limnia*
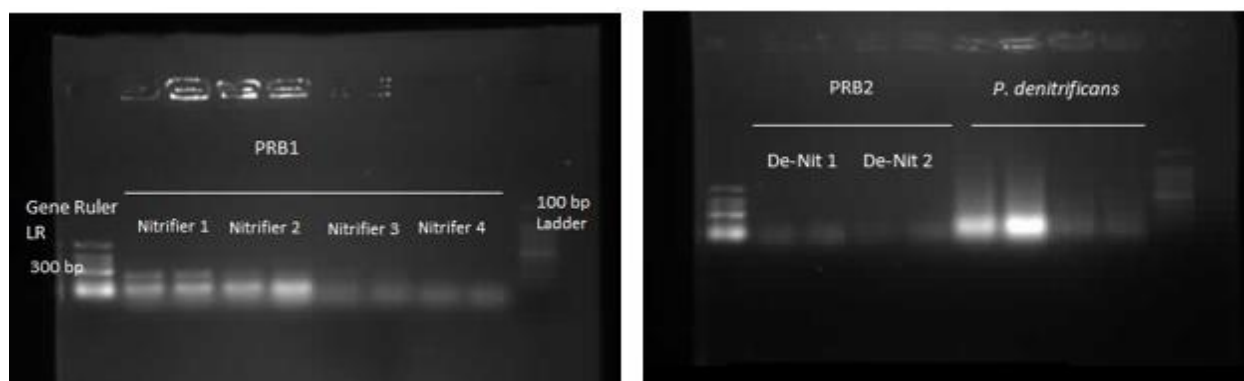
Figure C. 23: *nirK* PCR products (514 bp) from PCR carried out on cultures grown on nutrient agar inoculated by water samples from PRB 1 and PRB2 and on revived cultures of *Pseudomonas denitrificans* visualised on an agarose gel
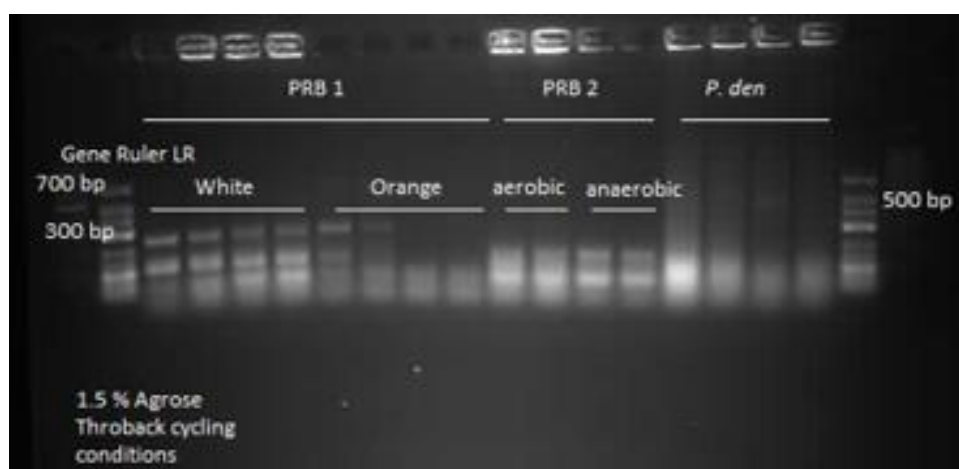


Figure C. 24: *nirK* PCR products (514 bp) from PCR using Throback et al. (2004) cycling conditions carried out on cultures grown on nutrient agar inoculated by water samples from PRB 1 and PRB2 visualised on an agarose gel
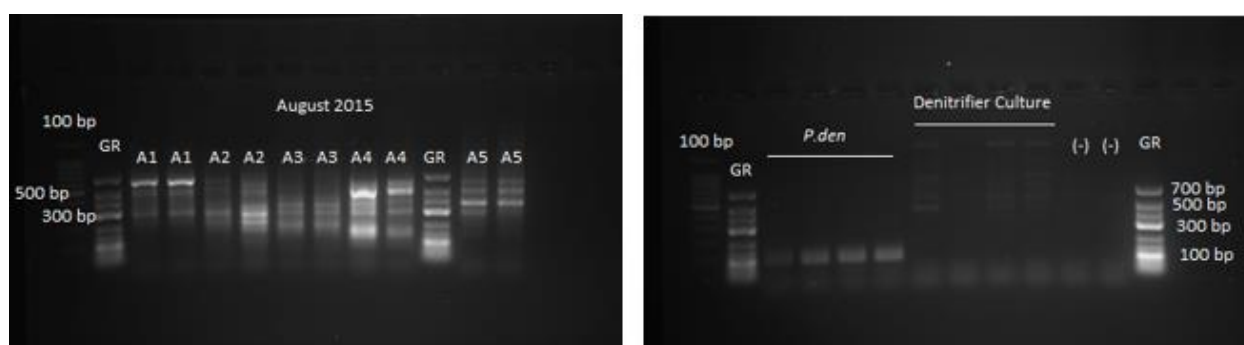


Figure C. 25: *nirK* PCR products (514 bp) from PCR using Throback et al. (2004) cycling conditions carried out on August 2015 eDNA samples and denitrifier cultures grown on nutrient agar inoculated by water samples from PRB 1 and PRB2 visualised on an agarose gel
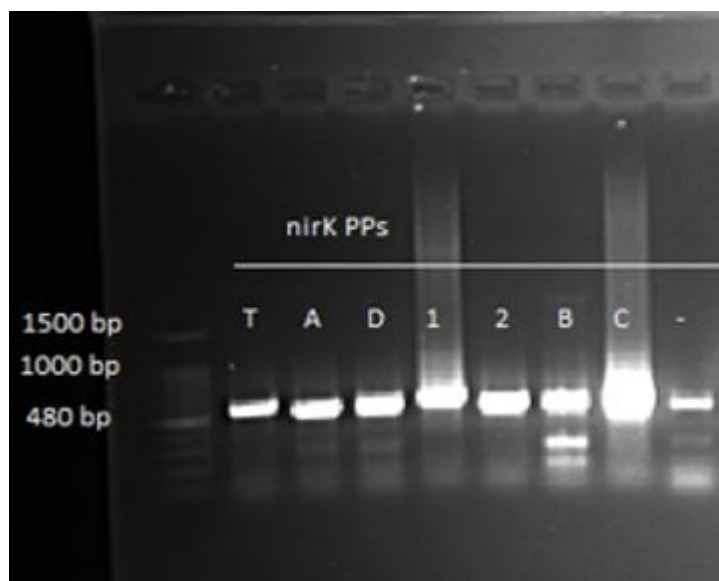
Figure C. 26: *nirK* PCR plasmid prep PCR products visualised on an agarose gel showing strong bands of appropriate size (514 bp)
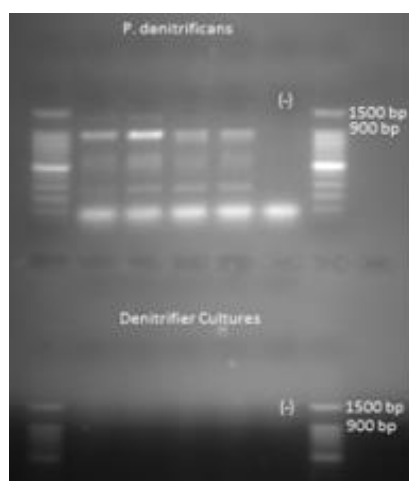


Figure C. 27: *nirS* PCR products (890 bp) from PCR carried out on denitrifier cultures grown on nutrient agar inoculated by water samples from PRB2 and on revived cultures of *Pseudomonas denitrificans* visualised on an agarose gel



Figure C. 28: *nirS* gradient PCR (temperature 51°C to 56°C) products (890 bp) from *Pseudomonas denitrificans* DNA visualised on an agarose gel
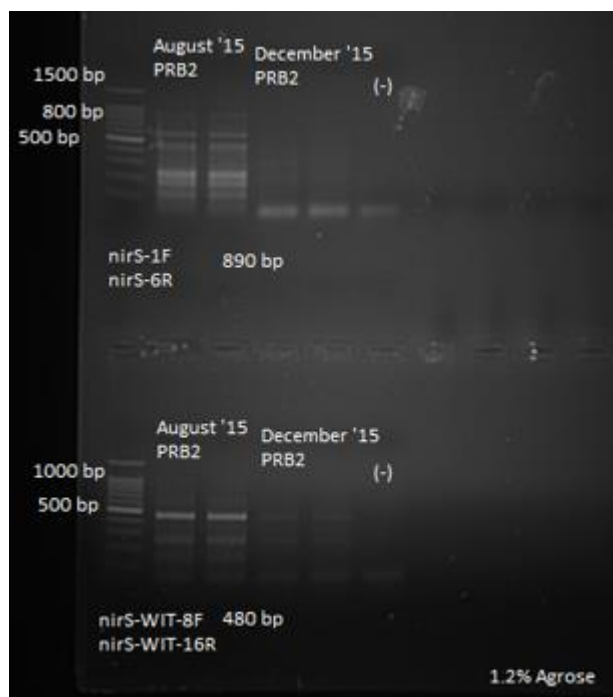
Figure C. 29: *nirS* PCR products using primer sets nirS-1f/-6R (Braker et al., 1998) and nirs-8F/-16R (this study) on eDNA samples from PRB2 collected in August and December 2015
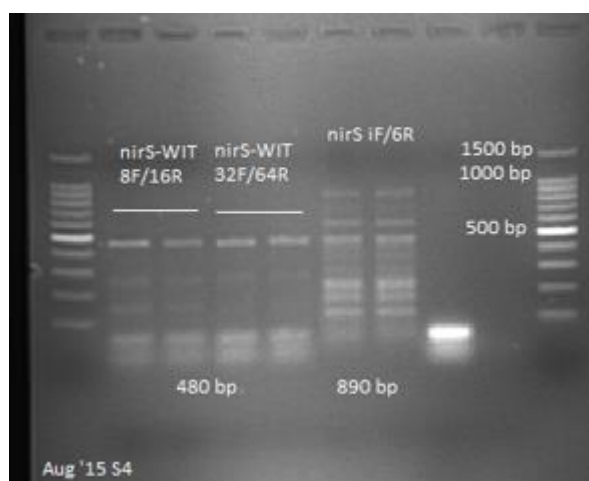


Figure C. 30: nirS PCR products visualised to compare three primer sets (nirS-WIT8F/16R and nirS-WIT32F/64R; 480 bp) and nirS-WIT1F/6R; 890 bp.
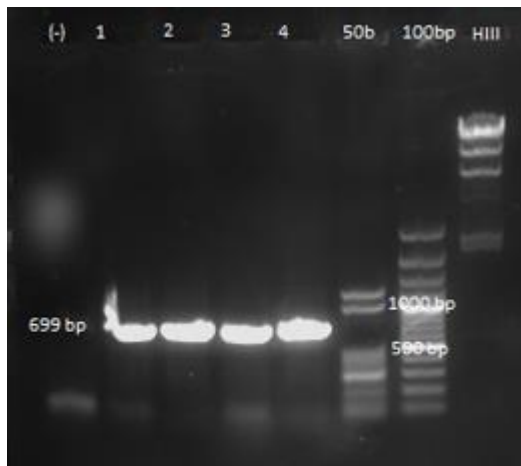
Figure C. 31: Gel image of four post nosZ PCR plasmid preps of a cloned *nosZ* sequence from *Pseudomonas denitrificans* showing product of correct size (699 bp).
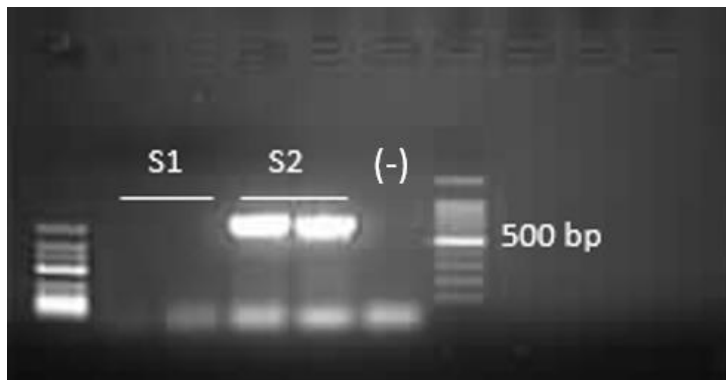


Figure C. 32: *nosZ P*CR products (699 bp) from PCR carried out on July 2016 samples S1 and S2 visualised on an agarose gel
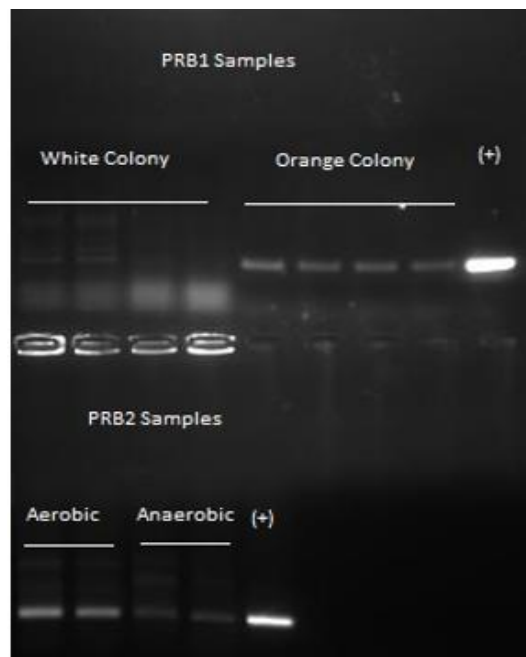


Figure C. 33: *nosZ* PCR products (699 bp) from cultures grown from PRB1 and PRB2 visualised on an agarose gel. (+) Positive control was a plasmid prep of a cloned *nosZ* sequence from *Pseudomonas denitrificans*

# Appendix D: Amplification Plots & Agarose Gel Images from qPCR optimisation
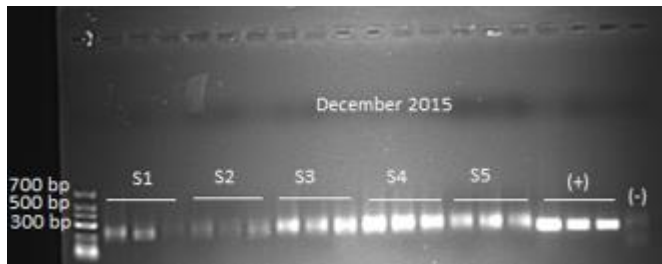


Figure D. 1: *16S rRNA* qPCR products (200 bp) from samples (S1-S5) collected in December 2015 were visualised on an agarose gel (December 2015 samples). Positive control was DNA extracted from *E. coli*.
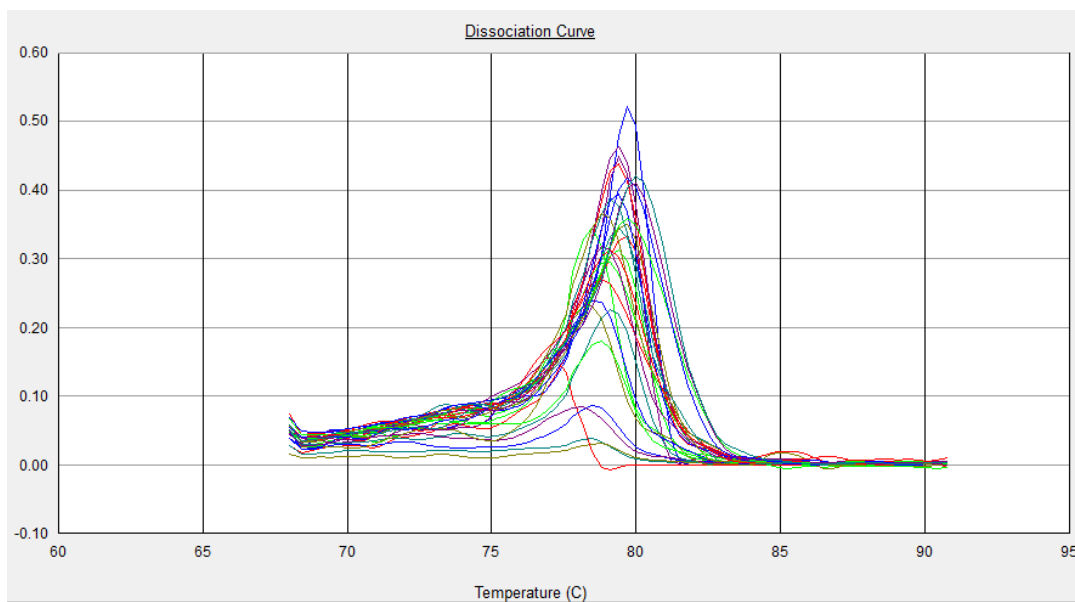


Figure D. 2: Melt curve analysis of 16S rRNA qPCR displaying an average dissociation of 79°C.
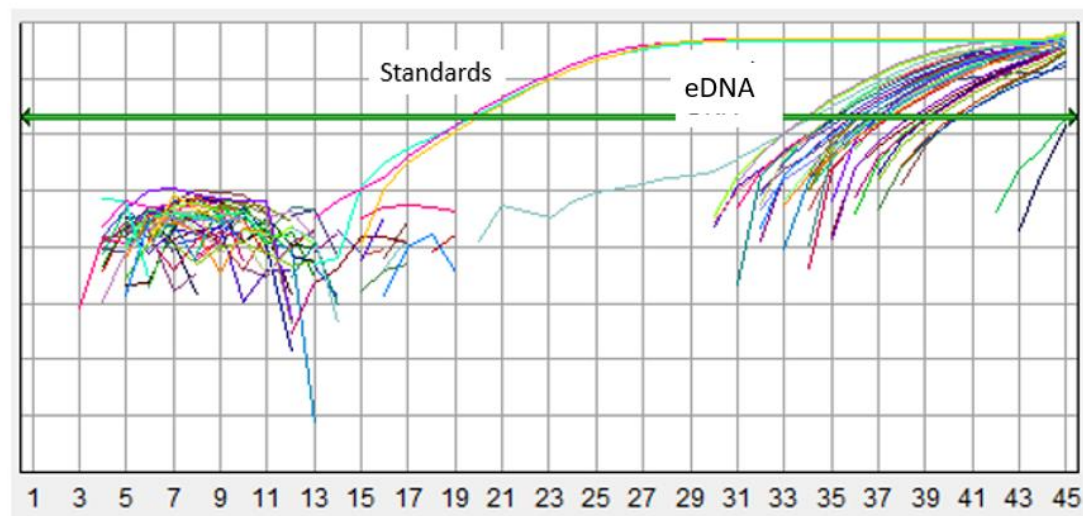


Figure D. 3: Real time amplification plot of bacterial *amoA* gene using July, October, and December 2015 eDNA samples. Positive control was a plasmid prep of a cloned *amoA* sequence from *Nitrosomonas europea*
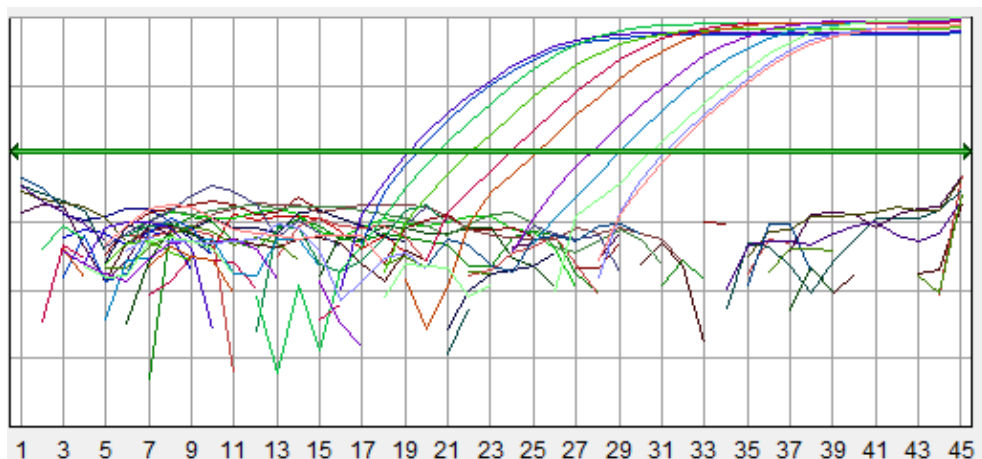
Figure D. 4: Real time amplification plot of bacterial *amoA* using eDNA samples and spiked samples.
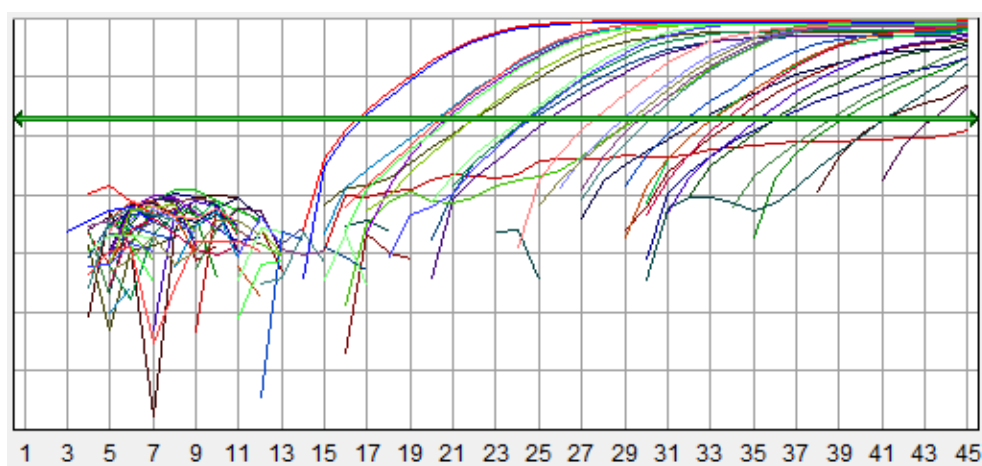


Figure D. 5: Real time amplification plot of bacterial *amoA* using environmental high volume DNA samples and spiked samples
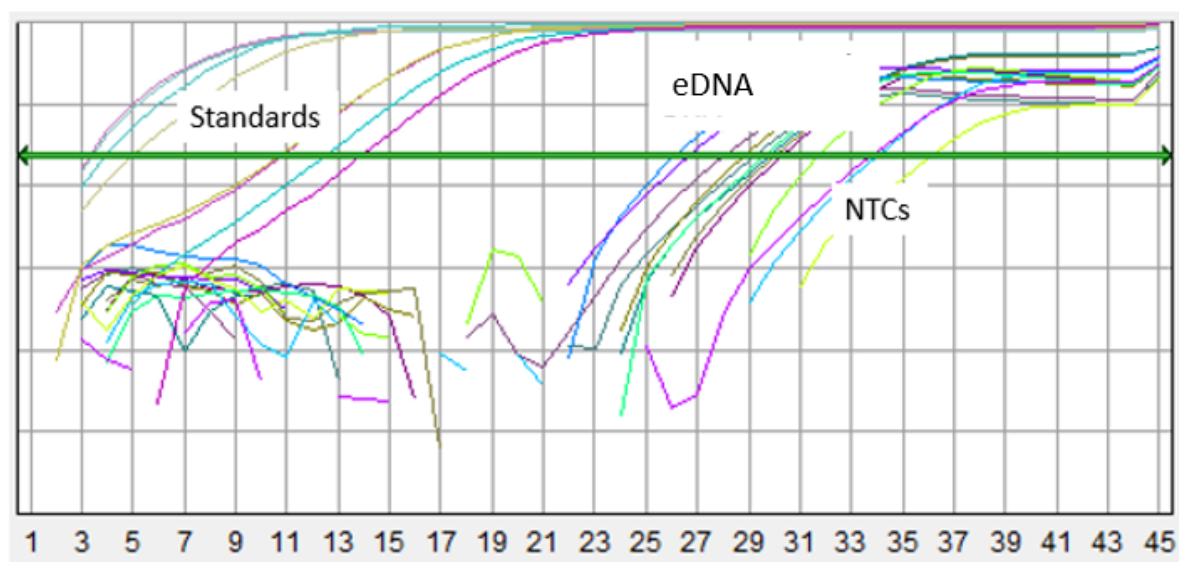


Figure D. 6: Real time amplification plot of bacterial *amoA* using eDNA and Rotthauwe et al. (1997) primers. Positive standards were a dilution series of plasmid prep of a cloned *amoA* sequence from *Nitrosomonas europea*

194
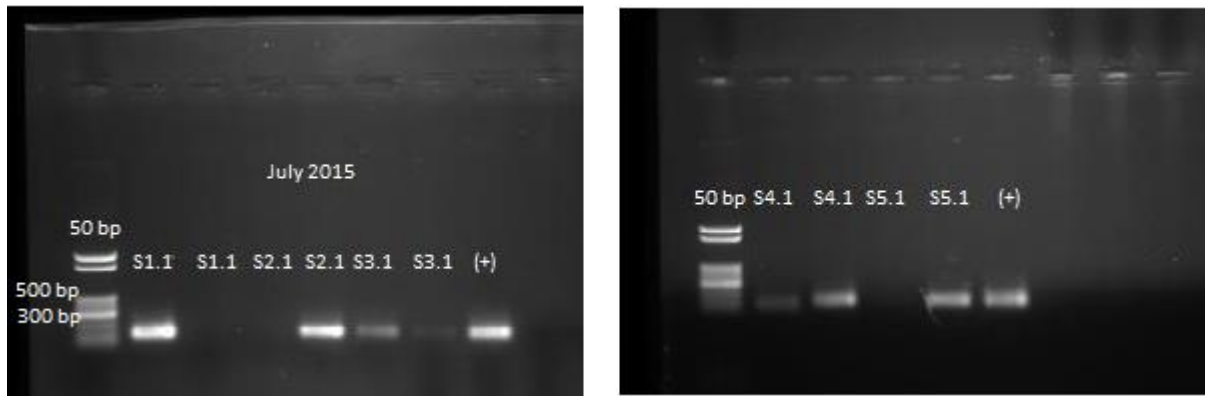
Figure D. 7: Bacterial *amoA* qPCR products (490 bp) were visualised on a gel showing that the bacterial *amoA* gene was not present. (+) Positive control was a plasmid prep of a cloned *amoA* sequence from *Nitrosomonas europea*



Figure D. 8:  Bacterial *amoA* qPCR 50 µl products from August 2015 samples (S1-S5) and positive standards (490 bp) visualised on an agarose gel. Positive standards were a dilution series of a plasmid prep of a cloned *amoA* sequence from *Nitrosomonas europea*
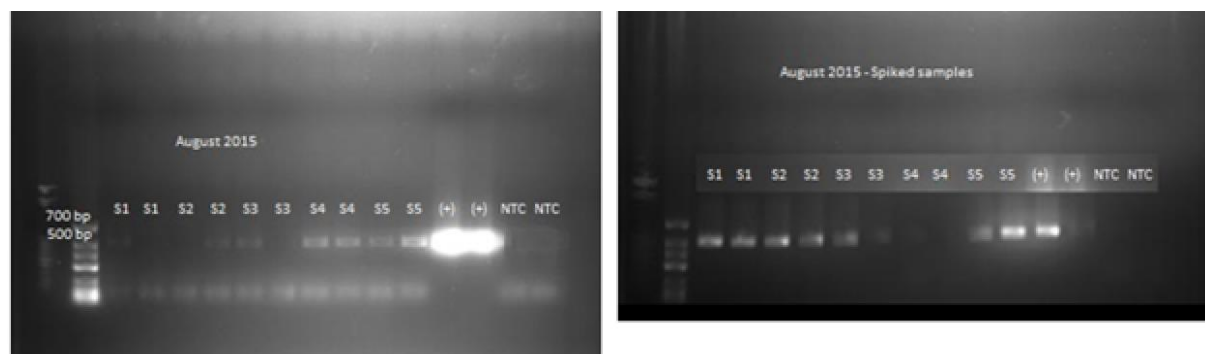


Figure D. 9: Bacterial *amoA* qPCR products (490 bp) of August and August spiked samples were visualised on an agarose gel. (+) Positive standards were a dilution series of a plasmid prep of a cloned *amoA* sequence from *Nitrosomonas europea*

195
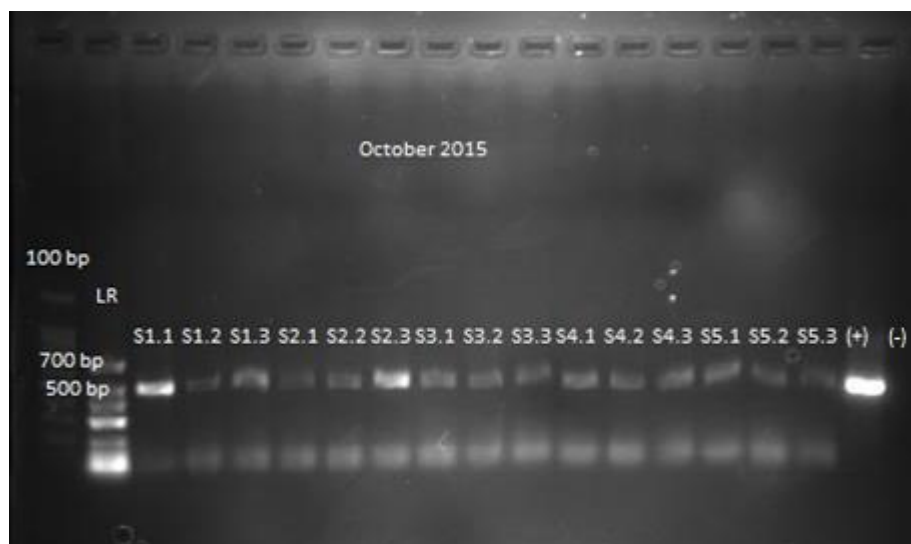
Figure D. 10: Bacterial *amoA* qPCR products (490 bp) of October 2015 samples were visualised on an agarose gel. Positive control was a plasmid prep of a cloned *amoA* sequence from *Nitrosomonas europea*
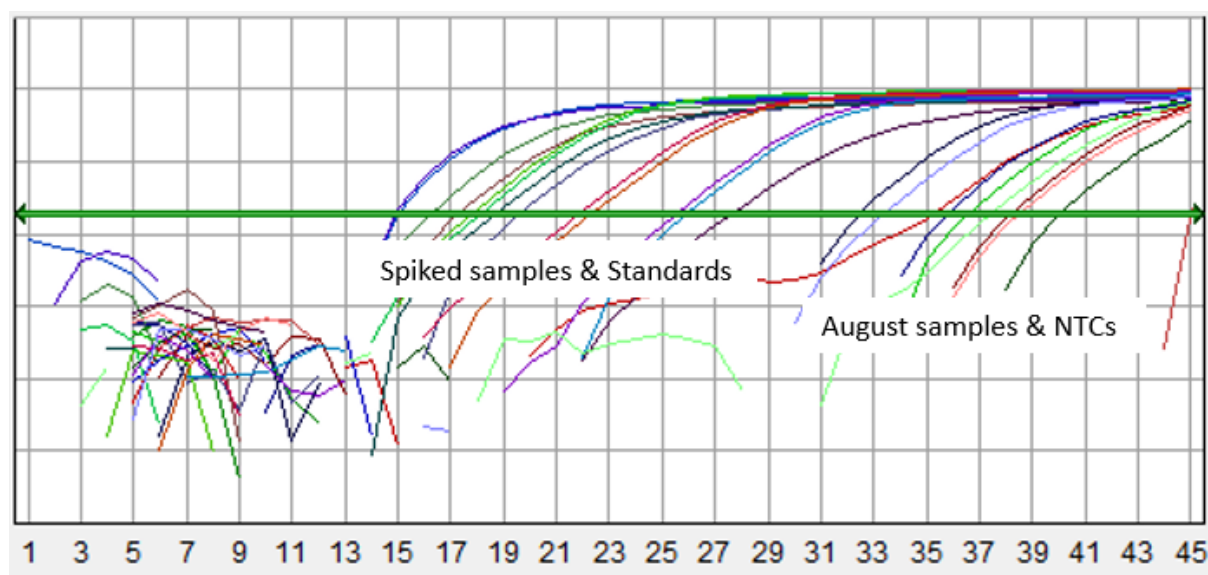


Figure D. 11: Real time amplification plot of August and spiked August 2015 samples
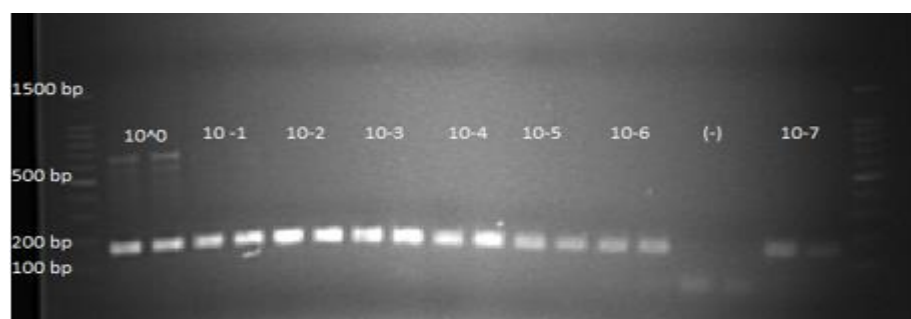


Figure D. 12: The positive standard dilution series was visualised on an agarose gel showing appropriate band size of 165 bp.

196
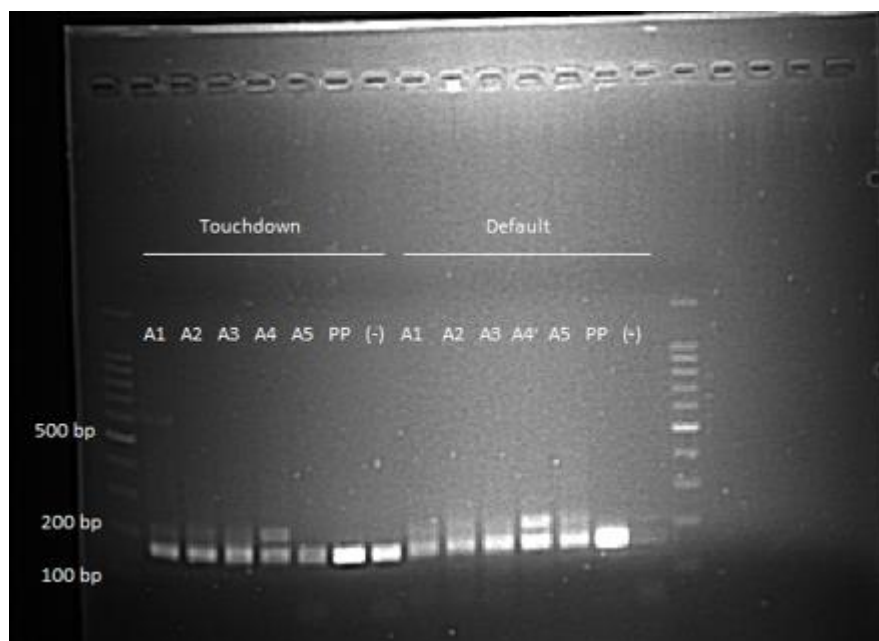
Figure D. 13: The *nirK* post qPCR products (165 bp) visualised on an agarose gel after qPCR to compare touchdown cycling conditions (Henry et al., 2004) and the instrument's default cycling conditions.
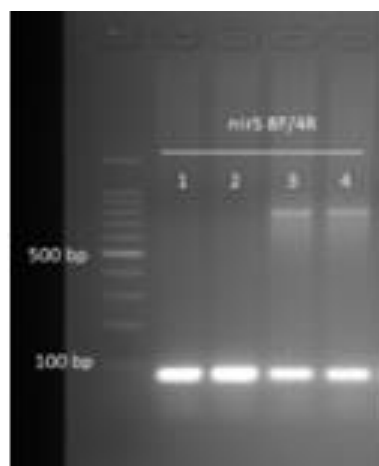


Figure D. 14: *nirS* qPCR products from a plasmid prep of a cloned *amoA* sequence from *Acidovorax carolinensis* visualised on an agarose gel showing appropriate 80 bp products

# Appendix E: *16S* and Functional Gene qPCR Results and Gene Copy Number

Table E. 1: Ct values, Tm values and gene copy numbers of the *16S* gene following qPCR for samples collected in June, September and December 2015 and March 2016. Green shading indicates correct band showing on agarose gel post qPCR. UND: Undetermined

| 16S | Jun-15 | | | Sep-15 | | | Dec-15 | | | Mar-16 | | |
|---|---|---|---|---|---|---|---|---|---|---|---|---|
| | Ct Value | Tm | Gene Copy No. per ul eDNA | Ct Value | Tm | Gene Copy No. per ul eDNA | Ct Value | Tm | Gene Copy No. per ul eDNA | Ct Value | Tm | Gene Copy No. per ul eDNA |
| S1 | 18.44 | 77.4 | 4.64E+03 | 11.6 | 79.2 | 6.08E+05 | 21 | 80 | 7.60E+02 | 12.8 | 80.9 | 2.62E+05 |
| | 18.35 | 77.4 | 4.95E+03 | 11.4 | 79.2 | 6.86E+05 | 21.1 | 79 | 7.18E+02 | 13.1 | 80.6 | 2.09E+05 |
| | 18.41 | 77.6 | 4.75E+03 | 12 | 79.2 | 4.47E+05 | 21.7 | 80 | 4.42E+02 | 11.9 | 80 | 5.05E+05 |
| | 18.88 | 78 | 3.39E+03 | 11.9 | 78.9 | 4.98E+05 | 22.4 | 79 | 2.78E+02 | 11.5 | 80.3 | 6.71E+05 |
| | 19.45 | 76.5 | 2.26E+03 | 12.1 | 78.9 | 4.41E+05 | 24.9 | 79 | 4.76E+01 | 12.6 | 80 | 3.04E+05 |
| | 18.93 | 76.5 | 3.28E+03 | 12.4 | 78.6 | 3.41E+05 | UND | 79 | - | 12.6 | 79.7 | 3.02E+05 |
| PRB1 | UND | 77.6 | - | 14.4 | 79.2 | 8.15E+04 | 27.3 | 77 | 8.54E+00 | 14.6 | 80 | 7.11E+04 |
| | 21.28 | 77.1 | 6.14E+02 | 14.6 | 79.5 | 6.96E+04 | 21.1 | 79 | - | 15.2 | 80 | 4.57E+04 |
| | 21.01 | 77.1 | 7.44E+02 | 14.1 | 79.5 | 9.94E+04 | UND | 79 | | UND | 71.7 | - |
| | 21.35 | 77.6 | 5.84E+02 | 14.6 | 79.5 | 7.01E+04 | 27.7 | 78 | 6.56E+00 | UND | 70.9 | - |
| | 20.76 | 77.4 | 8.89E+02 | 14.2 | 79.5 | 9.53E+04 | UND | 79 | - | 10.1 | 80.6 | 1.72E+06 |
| | 21.11 | 77.1 | 6.93E+02 | UND | 75.3 | | UND | 79 | - | 10.6 | 80.6 | 1.22E+06 |
| S3 | 18.33 | 76.5 | 5.02E+03 | 11.3 | 80.1 | 7.74E+05 | 25.5 | 79 | 3.10E+01 | 19.6 | 80.3 | 2.09E+03 |
| | 17.87 | 78 | 6.97E+03 | 12.9 | 79.8 | 2.49E+05 | 25.6 | 79 | 2.83E+01 | 19.7 | 80.3 | 1.92E+03 |
| | 18.09 | 77.6 | 5.96E+03 | 12.1 | 79.8 | 4.28E+05 | 23.6 | 79 | 1.16E+02 | 15.5 | 80 | 3.91E+04 |
| | 17.67 | 77.4 | 8.04E+03 | 12.4 | 79.8 | 3.41E+05 | 22.9 | 79 | 1.96E+02 | 15.3 | 80.3 | 4.48E+04 |
| | 17.46 | 77.6 | 9.34E+03 | 12.9 | 79.5 | 2.34E+05 | 25.6 | 79 | 2.87E+01 | UND | 75.1 | - |
| | 17.51 | 77.6 | 9.01E+03 | 12.4 | 79.2 | 3.51E+05 | 26.1 | 80 | 2.02E+01 | 13.9 | 81.2 | 1.15E+05 |
| PRB2 | 17.96 | 77.4 | 6.54E+03 | 15.3 | 80.4 | 4.35E+04 | 19.1 | 79 | 2.88E+03 | 18.3 | 80 | 5.28E+03 |
| | 17.68 | 77.6 | 7.98E+03 | 15.9 | 80.1 | 2.84E+04 | 21.6 | 79 | 4.99E+02 | 18.2 | 80 | 5.59E+03 |
| | 17.76 | 77.6 | 7.54E+03 | 15.6 | 80.4 | 3.42E+04 | 19.1 | 79 | 3.01E+03 | 14 | 79.4 | 1.12E+05 |
| | 17.79 | 77.1 | 7.38E+03 | 15.5 | 80.4 | 3.69E+04 | 18.7 | 79 | 3.86E+03 | 13.9 | 79.4 | 1.21E+05 |
| | 17.61 | 77.4 | 8.39E+03 | 15.6 | 80.4 | 3.64E+04 | 21.5 | 79 | 5.14E+02 | 11 | 80.9 | 9.25E+05 |
| | 17.67 | 77.4 | 8.04E+03 | 15.2 | 80.4 | 4.67E+04 | 21.5 | 79 | 5.44E+02 | UND | 70.9 | - |
| S5 | 20.8 | 79.2 | 8.64E+02 | 16.2 | 79.5 | 2.36E+04 | 22.4 | 79 | 2.69E+02 | 10.2 | 83.4 | 1.67E+06 |
| | 20.78 | 79.8 | 8.77E+02 | 15.8 | 79.5 | 3.16E+04 | 22.3 | 80 | 3.03E+02 | 10.1 | 83.7 | 1.74E+06 |
| | 20.84 | 79.8 | 8.40E+02 | UND | 71 | - | 17 | 80 | 1.30E+04 | UND | 70.9 | - |
| | 20.04 | 79.8 | 1.49E+03 | 16.7 | 79.5 | 1.65E+04 | 16.8 | 80 | 1.55E+04 | 10.7 | 83.7 | 1.17E+06 |
| | 20.18 | 79.8 | 1.34E+03 | 16.5 | 79.2 | 1.85E+04 | 17.6 | 80 | 8.76E+03 | 13.8 | 83.4 | 1.26E+05 |
| | 19.74 | 80.1 | 1.84E+03 | 16.5 | 78.9 | 1.84E+04 | 17.9 | 80 | 6.73E+03 | 12.9 | 83.1 | 2.39E+05 |
| NTCs | 30.44 | 76.8 | - | 30.4 | 76.8 | - | 29 | 79 | - | 29 | | - |
| | 30.62 | 76.2 | - | 30.6 | 76.2 | - | 28.9 | 79 | - | 28.9 | | - |
| | UND | 75 | - | UND | 75 | - | 30.8 | 77 | - | 30.8 | | - |

Table E. 2: Ct values, Tm values and gene copy number of the *16S* gene following qPCR for samples collected in June, September and December 2016 and March 2017. Green shading indicates correct band showing on agarose gel post qPCR. UND: Undetermined

| *16S* | Jun-16 | | | Sep-16 | | | Dec-16 | | | Mar-17 | | |
|---|---|---|---|---|---|---|---|---|---|---|---|---|
| | Ct Value | Tm | Gene Copy No. per ul eDNA | Ct Value | Tm | Gene Copy No. per ul eDNA | Ct Value | Tm | Gene Copy No. per ul eDNA | Ct Value | Tm | Gene Copy No. per ul eDNA |
| S1 | 11.76 | 78.4 | 5.42E+05 | 13.1 | 80 | 2.03E+05 | 12.2 | 78 | 3.88E+05 | 15.4 | 81 | 4.17E+04 |
| | 12.5 | 70.7 | 3.20E+05 | 13 | 80 | 2.22E+05 | 12.7 | 79 | 2.70E+05 | 15.6 | 80 | 3.46E+04 |
| | 11.22 | 79.4 | 7.96E+05 | 16.7 | 79.7 | 1.62E+04 | 13.6 | 79 | 1.47E+05 | 26 | 76 | 2.11E+01 |
| | 12.35 | 79.4 | 3.56E+05 | 16.3 | 80 | 2.16E+04 | 13.7 | 79 | 1.39E+05 | 18.5 | 80 | 4.39E+03 |
| | 12.51 | 79.1 | 3.18E+05 | 14 | 79.7 | 1.14E+05 | 13.1 | 80 | 2.07E+05 | 14.5 | 80 | 7.48E+04 |
| | 12.75 | 78.7 | 2.68E+05 | 14 | 79.4 | 1.08E+05 | 13.3 | 80 | 1.76E+05 | 14.5 | 79 | 7.75E+04 |
| PRB1 | 16.89 | 79.4 | 1.40E+04 | 14.6 | 80 | 7.11E+04 | 23.1 | 78 | 1.69E+02 | 17.4 | 80 | 9.81E+03 |
| | 15.03 | 78.7 | 5.27E+04 | 14.7 | 80.4 | 6.91E+04 | 21 | 79 | 7.39E+02 | 16.8 | 80 | 1.48E+04 |
| | 14.89 | 79.4 | 5.83E+04 | 12.3 | 80.4 | 3.80E+05 | 18.1 | 79 | 6.13E+03 | 16.5 | 80 | 1.85E+04 |
| | 15.35 | 78.4 | 4.20E+04 | 12.3 | 80.4 | 3.72E+05 | 18.7 | 78 | 3.97E+03 | 16.1 | 80 | 2.43E+04 |
| | 10.13 | 78.7 | 1.73E+06 | 14.1 | 80.4 | 1.03E+05 | 14.4 | 79 | 8.32E+04 | 17.1 | 79 | 1.22E+04 |
| | 10.73 | 79.1 | 1.13E+06 | 14.3 | 80.7 | 8.81E+04 | 14.9 | 79 | 5.66E+04 | 16.6 | 79 | 1.74E+04 |
| S3 | 16.98 | 79.1 | 1.31E+04 | 16.9 | 80.4 | 1.35E+04 | 21.4 | 80 | 5.76E+02 | 14.1 | 81 | 1.05E+05 |
| | 17.37 | 79.4 | 9.96E+03 | 16.8 | 80.4 | 1.52E+04 | 22.3 | 80 | 2.93E+02 | 13.6 | 81 | 1.47E+05 |
| | 14.85 | 79.4 | 6.00E+04 | 17.1 | 80 | 1.23E+04 | 15.8 | 80 | 3.07E+04 | 17 | 80 | 1.26E+04 |
| | 14.75 | 79.1 | 6.44E+04 | UND | 71 | - | 15.6 | 80 | 3.59E+04 | 16.7 | 80 | 1.66E+04 |
| | 14.72 | 79.7 | 6.58E+04 | 18.3 | 79.7 | 5.06E+03 | 15.6 | 80 | 3.54E+04 | 14.2 | 80 | 9.53E+04 |
| | 14.5 | 79.7 | 7.69E+04 | 18.2 | 79.7 | 5.59E+03 | 16.1 | 80 | 2.39E+04 | 14.3 | 80 | 9.06E+04 |
| PRB2 | 13.53 | 80 | 1.54E+05 | 15.1 | 80.4 | 5.13E+04 | 15.6 | 80 | 3.42E+04 | 16.9 | 79 | 1.39E+04 |
| | 13.37 | 80 | 1.72E+05 | 15.8 | 80.7 | 2.98E+04 | 16.4 | 80 | 1.96E+04 | 16.4 | 80 | 1.96E+04 |
| | 13.5 | 79.7 | 1.57E+05 | 13.4 | 80.7 | 1.68E+05 | UND | 76 | - | 15.8 | 80 | 3.00E+04 |
| | 13.47 | 79.7 | 1.60E+05 | 13.6 | 80.7 | 1.50E+05 | UND | 73 | - | 15.2 | 80 | 4.74E+04 |
| | 11.98 | 80.4 | 4.63E+05 | 12.4 | 79.4 | 3.51E+05 | 14.1 | 80 | 1.01E+05 | 15.1 | 80 | 4.98E+04 |
| | 12.46 | 79.4 | 3.29E+05 | 11.9 | 79.4 | 4.87E+05 | 14.5 | 79 | 7.86E+04 | 15.2 | 79 | 4.57E+04 |
| S5 | 17.77 | 81 | 7.49E+03 | 18.5 | 80.4 | 4.48E+03 | 13.3 | 80 | 1.85E+05 | 16.2 | 80 | 2.26E+04 |
| | 17.43 | 81 | 9.54E+03 | 19.1 | 80 | 2.84E+03 | 12.9 | 80 | 2.34E+05 | 16.8 | 79 | 1.45E+04 |
| | 13.84 | 81 | 1.23E+05 | 16.1 | 79.7 | 2.50E+04 | 13.2 | 80 | 1.96E+05 | 16.9 | 79 | 1.42E+04 |
| | 14.47 | 80.7 | 7.86E+04 | 15.6 | 79.7 | 3.54E+04 | 13 | 80 | 2.29E+05 | 17.5 | 79 | 9.01E+03 |
| | 13.11 | 78.7 | 2.07E+05 | UND | 71.9 | - | 13.8 | 80 | 1.27E+05 | 16.9 | 79 | 1.44E+04 |
| | 12.97 | 78.7 | 2.29E+05 | 18.7 | 80 | 3.78E+03 | 13.8 | 80 | 1.31E+05 | 16.9 | 79 | 1.37E+04 |
| NTCs | 29.62 | 78.7 | - | 29.6 | 78.7 | | 25.7 | 77 | - | 25.7 | | - |
| | 25.15 | 79.1 | - | 25.2 | 79.1 | | 27.7 | 76 | - | 27.7 | | - |
| | 29.39 | 78.1 | - | 29.4 | 78.1 | | 26.6 | 79 | - | 26.6 | | - |

Table E. 3: Ct values, Tm values and gene copy number of the bacterial *amoA* gene following qPCR for samples collected in June, September and December 2015 and March 2016. Green shading indicates correct band showing on agarose gel post qPCR. UND: Undetermined

| Bacterial *amoA* | Jun-15 | | | Sep-15 | | | Dec-15 | | | Mar-16 | | |
|---|---|---|---|---|---|---|---|---|---|---|---|---|
| | Ct Value | Tm | Gene Copy No. per ul eDNA | Ct Value | Tm | Gene Copy No. per ul eDNA | Ct Value | Tm | Gene Copy No. per ul eDNA | Ct Value | Tm | Gene Copy No. per ul eDNA |
| S1 | 32.36 | 70.8 | 4.95E+03 | 29.8 | 84.1 | 2.80E+04 | 28.09 | 71.2 | 8.93E+04 | 34.25 | 71.5 | 1.38E+03 |
| | 33.36 | 70.8 | 2.51E+03 | 29.57 | 84.1 | 3.28E+04 | 29.55 | 71.5 | 3.32E+04 | 33.44 | 71.2 | 2.38E+03 |
| | 34.36 | 70.8 | 1.28E+03 | 29.86 | 84.5 | 2.69E+04 | 23.7 | 81.2 | 1.75E+06 | 39.62 | 71.7 | 3.62E+01 |
| | 35.36 | 70.8 | 6.48E+02 | 29.38 | 84.1 | 3.73E+04 | 24.11 | 81.2 | 1.32E+06 | 34.85 | 70.9 | 9.16E+02 |
| | 36.36 | 70.8 | 3.29E+02 | 30.19 | 83.8 | 2.15E+04 | 30.28 | 71.2 | 2.03E+04 | 37.32 | 70.9 | 1.72E+02 |
| | 37.36 | 70.8 | 1.67E+02 | 30.3 | 83.8 | 2.00E+04 | 30.04 | 71.2 | 2.38E+04 | UND | 82.4 | |
| PRB1 | UND | 70.8 | | 32.03 | 71.4 | 6.19E+03 | 29.41 | 80 | 3.65E+04 | 31.95 | 71.2 | 6.53E+03 |
| | 33.06 | 70.8 | 3.08E+03 | 34.31 | 70.8 | 1.32E+03 | 27.8 | 80.6 | 1.09E+05 | 32.68 | 70.9 | 3.98E+03 |
| | 34.01 | 70.8 | 1.62E+03 | 32.25 | 71.7 | 5.33E+03 | 30.97 | 70.9 | 1.27E+04 | UND | 85.4 | |
| | 34.75 | 70.8 | 9.80E+02 | 32.1 | 71.4 | 5.90E+03 | 31.65 | 70.9 | 8.01E+03 | UND | 85.7 | |
| | 34.11 | 70.8 | 1.51E+03 | 31.67 | 71.4 | 7.90E+03 | 32.24 | 80.3 | 5.37E+03 | 30.75 | 84.1 | 1.47E+04 |
| | UND | 70.8 | | 32.71 | 71.1 | 3.90E+03 | 34.36 | 70.9 | 1.28E+03 | 30.74 | 84.4 | 1.48E+04 |
| S3 | 32.59 | 71.1 | 4.24E+03 | 30.24 | 70.8 | 2.08E+04 | 35.53 | 70.9 | 5.78E+02 | 31.52 | 71.5 | 8.74E+03 |
| | 33.08 | 71.1 | 3.04E+03 | 30.15 | 84.5 | 2.21E+04 | 35.18 | 71.2 | 7.32E+02 | 32.78 | 71.2 | 3.72E+03 |
| | 31.75 | 71.1 | 7.48E+03 | 30.77 | 70.8 | 1.45E+04 | 28.63 | 80.6 | 6.20E+04 | 32.05 | 70.9 | 6.11E+03 |
| | 33.02 | 70.8 | 3.16E+03 | 30.48 | 70.8 | 1.77E+04 | 27.5 | 81.2 | 1.33E+05 | 32.36 | 71.2 | 4.95E+03 |
| | 33.6 | 71.1 | 2.14E+03 | 30.76 | 70.8 | 1.46E+04 | 34.59 | 70.9 | 1.09E+03 | 35.18 | 70.9 | 7.32E+02 |
| | 31.89 | 71.1 | 6.81E+03 | 31.15 | 70.8 | 1.12E+04 | 34.88 | 71.2 | 8.98E+02 | 39.06 | 70.9 | 5.29E+01 |
| PRB2 | 32.21 | 71.4 | 5.48E+03 | 29.87 | 70.8 | 2.67E+04 | 27.65 | 70.9 | 1.20E+05 | 33.38 | 71.2 | 2.48E+03 |
| | 33.01 | 71.7 | 3.19E+03 | 29.89 | 70.8 | 2.64E+04 | 27.31 | 70.9 | 1.52E+05 | 33.08 | 71.5 | 3.04E+03 |
| | 32.25 | 71.1 | 5.33E+03 | 30.24 | 71.1 | 2.08E+04 | 31.36 | 70.9 | 9.75E+03 | 34.01 | 80.9 | 1.62E+03 |
| | 33.08 | 70.8 | 3.04E+03 | 29.53 | 77.7 | 3.37E+04 | 32.27 | 70.9 | 5.26E+03 | 32.48 | 71.2 | 4.56E+03 |
| | 33.64 | 70.8 | 2.08E+03 | 30.92 | 70.8 | 1.31E+04 | 34.36 | 70.9 | 1.28E+03 | 31.7 | 71.7 | 7.74E+03 |
| | 33.6 | 70.8 | 2.14E+03 | 30.09 | 71.1 | 2.30E+04 | 34.11 | 71.2 | 1.51E+03 | 32.05 | 71.5 | 6.11E+03 |
| S5 | 32.4 | 71.1 | 4.82E+03 | 31.73 | 71.7 | 7.58E+03 | 32.04 | 71.2 | 6.15E+03 | 35.06 | 71.2 | 7.94E+02 |
| | 32.67 | 71.1 | 4.01E+03 | 31.56 | 71.7 | 8.51E+03 | 28.24 | 71.5 | 8.07E+04 | 34.61 | 71.5 | 1.08E+03 |
| | 31.9 | 71.1 | 6.76E+03 | 33.15 | 71.1 | 2.90E+03 | 29.34 | 71.2 | 3.83E+04 | 31.38 | 84.4 | 9.61E+03 |
| | 31.84 | 71.4 | 7.04E+03 | 32.09 | 71.7 | 5.94E+03 | 29.77 | 71.2 | 2.86E+04 | 31.4 | 84.4 | 9.48E+03 |
| | 31.87 | 71.1 | 6.90E+03 | 31.7 | 71.4 | 7.74E+03 | 31.37 | 71.5 | 9.68E+03 | 34.2 | 71.5 | 1.42E+03 |
| | 32.89 | 71.4 | 3.46E+03 | 32.15 | 70.8 | 5.71E+03 | 31 | 72.1 | 1.24E+04 | 32.78 | 71.2 | 3.72E+03 |
| NTCs | UND | 70.8 | - | UND | 70.8 | - | 37.98 | 70.9 | - | 37.98 | 70.9 | - |
| | UND | 70.8 | - | UND | 70.8 | - | 39.35 | 70.9 | - | 39.35 | 70.9 | - |
| | UND | 70.8 | - | UND | 70.8 | - | 36.49 | 70.9 | - | 36.49 | 70.9 | - |

Table E. 4: Ct values, Tm values and gene copy number of the bacterial *amoA* gene following qPCR for samples collected in June, September and December 2016 and March 2017. Green shading indicates correct band showing on agarose gel post qPCR. UND: Undetermined

| Bacterial *amoA* | Jun-16 | | | Sep-16 | | | Dec-16 | | | Mar-17 | | |
|---|---|---|---|---|---|---|---|---|---|---|---|---|
| | Ct Value | Tm | Gene Copy No. per ul eDNA | Ct Value | Tm | Gene Copy No. per ul eDNA | Ct Value | Tm | Gene Copy No. per ul eDNA | Ct Value | Tm | Gene Copy No. per ul eDNA |
| S1 | 39.55 | 70.8 | 3.79E+01 | 39.31 | 70.8 | 4.46E+01 | UND | 71.5 | #VALUE! | 28.17 | 71.2 | 8.46E+04 |
| | UND | 70.8 | #VALUE! | 30.54 | 71.1 | 1.70E+04 | 39.49 | 70.9 | 3.95E+01 | 27.27 | 71.2 | 1.56E+05 |
| | 32.51 | 70.8 | 4.47E+03 | 35.02 | 71.1 | 8.16E+02 | 29.9 | 70.9 | 2.62E+04 | 27.21 | 71.2 | 1.62E+05 |
| | 39.36 | 70.8 | 4.31E+01 | 34.7 | 71.1 | 1.01E+03 | 30.01 | 70.9 | 2.43E+04 | 26.11 | 70.9 | 3.42E+05 |
| | 39.29 | 70.8 | 4.52E+01 | 39.22 | 70.8 | 4.74E+01 | 32.24 | 70.9 | 5.37E+03 | 29.13 | 70.9 | 4.42E+04 |
| | 39.27 | 70.8 | 4.58E+01 | 39.25 | 70.8 | 4.65E+01 | 38.32 | 70.9 | 8.73E+01 | 28.19 | 70.9 | 8.35E+04 |
| PRB1 | 39.41 | 86.2 | | 36.19 | 71.1 | 3.69E+02 | UND | - | #VALUE! | 27.73 | 71.2 | 1.14E+05 |
| | 32.53 | 70.8 | 4.41E+03 | 33.04 | 71.4 | 3.12E+03 | 30.79 | 70.9 | 1.43E+04 | 28.24 | 71.5 | 8.07E+04 |
| | 39.27 | 70.8 | 4.58E+01 | 30.78 | 71.4 | 1.44E+04 | 34.16 | 70.9 | 1.46E+03 | 27.56 | 71.5 | 1.28E+05 |
| | 29.47 | 70.8 | 3.51E+04 | 30.69 | 71.4 | 1.53E+04 | 30.25 | 71.2 | 2.07E+04 | 28.04 | 71.5 | 9.24E+04 |
| | 39.41 | 70.8 | 4.17E+01 | 32.46 | 71.7 | 4.63E+03 | UND | - | #VALUE! | 27.64 | 71.2 | 1.21E+05 |
| | UND | 70.8 | | 31.43 | 71.7 | 9.29E+03 | UND | 70.9 | #VALUE! | 27.02 | 71.5 | 1.84E+05 |
| S3 | 39.27 | 70.8 | 4.58E+01 | 26.44 | 71.7 | 2.73E+05 | 33.91 | 70.9 | 1.73E+03 | 29.55 | 71.8 | 3.32E+04 |
| | 39.21 | 70.8 | 4.77E+01 | 26.03 | 72 | 3.61E+05 | 34.7 | 70.9 | 1.01E+03 | 28.63 | 71.8 | 6.20E+04 |
| | 29.27 | 70.8 | 4.02E+04 | 29.46 | 71.4 | 3.53E+04 | 37.01 | 71.2 | 2.12E+02 | 28.41 | 71.2 | 7.19E+04 |
| | 30.29 | 71.4 | 2.01E+04 | 29.06 | 71.1 | 4.63E+04 | 36.78 | 71.2 | 2.48E+02 | 26.62 | 71.5 | 2.42E+05 |
| | 29.75 | 71.4 | 2.90E+04 | 32.46 | 71.1 | 4.63E+03 | 35.81 | 71.2 | 4.78E+02 | 26.77 | 71.2 | 2.18E+05 |
| | 28.2 | 71.1 | 8.29E+04 | 32.58 | 71.1 | 4.26E+03 | 33.33 | 71.2 | 2.57E+03 | 28.27 | 70.9 | 7.91E+04 |
| PRB2 | 29.78 | 71.1 | 2.84E+04 | 26.73 | 71.4 | 2.24E+05 | UND | - | #VALUE! | 28.17 | 71.5 | 8.46E+04 |
| | 30.41 | 71.1 | 1.85E+04 | 25.87 | 71.7 | 4.02E+05 | 36.21 | 71.2 | 3.65E+02 | 28.64 | 71.2 | 6.15E+04 |
| | 31.11 | 70.8 | 1.15E+04 | 29.08 | 71.7 | 4.57E+04 | 36.33 | 71.2 | 3.36E+02 | UND | 70.9 | |
| | 39.14 | 70.8 | 5.01E+01 | 28.23 | 71.7 | 8.12E+04 | 38 | 70.9 | 1.08E+02 | UND | 71.2 | |
| | 39.2 | 70.8 | 4.81E+01 | 31.01 | 71.4 | 1.24E+04 | UND | - | #VALUE! | 24.35 | 81.5 | 1.13E+06 |
| | 39.14 | 70.8 | 5.01E+01 | 30.97 | 71.4 | 1.27E+04 | 24.45 | 70.9 | 1.05E+06 | 24.21 | 81.2 | 1.24E+06 |
| S5 | 31.17 | 71.1 | 1.11E+04 | 32.19 | 71.7 | 5.55E+03 | 34.14 | 70.9 | 1.48E+03 | 23.08 | 71.8 | 2.66E+06 |
| | 30.68 | 71.4 | 1.54E+04 | 32.37 | 71.4 | 4.92E+03 | 36.14 | 71.2 | 3.82E+02 | 23.06 | 71.8 | 2.70E+06 |
| | 31.84 | 71.1 | 7.04E+03 | 31.57 | 71.7 | 8.45E+03 | 34.35 | 71.2 | 1.29E+03 | 27.11 | 71.5 | 1.74E+05 |
| | 31.36 | 71.1 | 9.75E+03 | 31.22 | 71.7 | 1.07E+04 | 33.66 | 71.5 | 2.05E+03 | 27.41 | 71.5 | 1.42E+05 |
| | 39.26 | 71.1 | 4.62E+01 | 31.58 | 71.4 | 8.40E+03 | 21.31 | 71.8 | 8.83E+06 | 28.78 | 71.5 | 5.60E+04 |
| | 31.74 | 71.4 | 7.53E+03 | 31.81 | 71.1 | 7.18E+03 | 36.44 | 71.8 | 3.12E+02 | 28.75 | 71.2 | 5.71E+04 |
| NTCs | UND | 70.8 | - | UND | 70.8 | - | 30.64 | - | 70.9 | 30.64 | - | 70.9 |
| | UND | 83.5 | - | UND | 83.5 | - | UND | - | 70.9 | UND | - | 70.9 |
| | 22.34 | 72.3 | - | 22.34 | 72.3 | - | 38.67 | - | 76.1 | 38.67 | - | 76.1 |

Table E. 5: Ct value, Tm values and gene copy number of the archaeal *amoA* gene following qPCR for samples collected in June, September and December 2015 and March 2016. Green shading indicates correct band showing on agarose gel post qPCR. UND: Undetermined

| Archaeal *amoA* | Jun-15 | | | Sep-15 | | | Dec-15 | | | Mar-16 | | |
|---|---|---|---|---|---|---|---|---|---|---|---|---|
| | Ct Value | Tm | Gene Copy No. per ul eDNA | Ct Value | Tm | Gene Copy No. per ul eDNA | Ct Value | Tm | Gene Copy No. per ul eDNA | Ct Value | Tm | Gene Copy No. per ul eDNA |
| S1 | 30.2 | 72 | 6.42E-09 | 33.06 | 72.5 | 4.52E-09 | 31.75 | 72.7 | 3.92E-09 | 28.07 | 73.9 | 1.69E-09 |
| | 25.7 | 72.2 | 5.58E-09 | 33.25 | 72.5 | 4.52E-09 | 26.47 | 72.7 | 3.92E-09 | 28.08 | 73.6 | 2.08E-09 |
| | 24.46 | 72.8 | 3.66E-09 | 29.8 | 72.8 | 3.66E-09 | 28.27 | 72.7 | 3.92E-09 | 27.94 | 73.6 | 2.08E-09 |
| | 25.93 | 72.5 | 4.52E-09 | 31.5 | 72.5 | 4.52E-09 | 30.55 | 72.7 | 3.92E-09 | 26.83 | 73.4 | 2.40E-09 |
| | 25.88 | 72.5 | 4.52E-09 | 32.21 | 72.5 | 4.52E-09 | 43.36 | 73.1 | 2.96E-09 | 29.09 | 73.1 | 2.96E-09 |
| | 25.26 | 72.5 | 4.52E-09 | 30.81 | 72.2 | 5.58E-09 | 34.72 | 72.7 | 3.92E-09 | 30.17 | 72.7 | 3.92E-09 |
| PRB1 | 34.13 | 72.2 | 5.58E-09 | 30.96 | 72.8 | 3.66E-09 | 37.46 | 72.5 | 4.52E-09 | 25.19 | 73.6 | 2.08E-09 |
| | 30.51 | 72.5 | 4.52E-09 | 29.84 | 72.8 | 3.66E-09 | 34.08 | 73.1 | 2.96E-09 | 24.59 | 74.2 | 1.37E-09 |
| | 31.06 | 72.2 | 5.58E-09 | 29.22 | 73.1 | 2.96E-09 | 30.39 | 72.5 | 4.52E-09 | UND | 71.8 | 7.38E-09 |
| | 31.33 | 72 | 6.42E-09 | 30.25 | 73.1 | 2.96E-09 | 30.21 | 72.5 | 4.52E-09 | UND | 70.7 | 1.60E-08 |
| | 32.7 | 72.2 | 5.58E-09 | 30.15 | 73.1 | 2.96E-09 | 31.72 | 72.5 | 4.52E-09 | 26.71 | 73.9 | 1.69E-09 |
| | UND | 71.7 | 7.92E-09 | 30.46 | 76.8 | 2.20E-10 | 29.69 | 72.1 | 5.98E-09 | 26.66 | 74.2 | 1.37E-09 |
| S3 | 31.74 | 72.2 | 5.58E-09 | 28.61 | 76.5 | 2.72E-10 | 30.42 | 73.1 | 2.96E-09 | 25.73 | 74.2 | 1.37E-09 |
| | 31.19 | 72.5 | 4.52E-09 | 28.35 | 76.5 | 2.72E-10 | 32.12 | 73.4 | 2.40E-09 | 25.32 | 74.2 | 1.37E-09 |
| | 31.1 | 72.8 | 3.66E-09 | 27.33 | 76.5 | 2.72E-10 | 28.32 | 73.4 | 2.40E-09 | 26.03 | 74.6 | 1.03E-09 |
| | 33.07 | 72.8 | 3.66E-09 | 27.41 | 76.5 | 2.72E-10 | 28.19 | 73.4 | 2.40E-09 | 25.76 | 74.2 | 1.37E-09 |
| | 29.53 | 72.8 | 3.66E-09 | 27.81 | 76.3 | 3.13E-10 | 32.24 | 73.4 | 2.40E-09 | 31.53 | 73.9 | 1.69E-09 |
| | 33.22 | 72.8 | 3.66E-09 | 27.34 | 76.3 | 3.13E-10 | 30.63 | 73.1 | 2.96E-09 | 39.95 | 72.7 | 3.92E-09 |
| PRB2 | 33.82 | 72.8 | 3.66E-09 | 24.19 | 73.4 | 2.40E-09 | 30.22 | 73.1 | 2.96E-09 | 26.9 | 74.2 | 1.37E-09 |
| | 34.25 | 72.8 | 3.66E-09 | 24.14 | 73.6 | 2.08E-09 | 33.44 | 73.1 | 2.96E-09 | 26.31 | 74.2 | 1.37E-09 |
| | 30.2 | 72.5 | 4.52E-09 | 24.49 | 73.6 | 2.08E-09 | 20.95 | 73.4 | 2.40E-09 | 25.93 | 74.6 | 1.03E-09 |
| | 30.37 | 72.5 | 4.52E-09 | 24.49 | 73.6 | 2.08E-09 | 21.25 | 73.1 | 2.96E-09 | 26.12 | 74.6 | 1.03E-09 |
| | 29.88 | 72.2 | 5.58E-09 | 24.26 | 74 | 1.57E-09 | 32.18 | 73.1 | 2.96E-09 | 25.65 | 74.6 | 1.03E-09 |
| | 29.3 | 72.5 | 4.52E-09 | 24.4 | 73.6 | 2.08E-09 | 32.2 | 72.5 | 4.52E-09 | 25.89 | 74.6 | 1.03E-09 |
| S5 | 31.82 | 72.8 | 3.66E-09 | 28.78 | 74 | 1.57E-09 | 29.02 | 72.7 | 3.92E-09 | 23.91 | 75.4 | 5.89E-10 |
| | 31.6 | 72.5 | 4.52E-09 | 29.37 | 74.2 | 1.37E-09 | 28.1 | 76.9 | 2.05E-10 | 23.65 | 75.4 | 5.89E-10 |
| | 31.7 | 73.1 | 2.96E-09 | 28.47 | 73.6 | 2.08E-09 | 27.33 | 73.6 | 2.08E-09 | 25.67 | 77.9 | 1.02E-10 |
| | 30.02 | 73.4 | 2.40E-09 | 34.04 | 74.2 | 1.37E-09 | 27.35 | 73.4 | 2.40E-09 | 24.69 | 77.9 | 1.02E-10 |
| | 31.13 | 73.1 | 2.96E-09 | UND | 70.5 | 1.84E-08 | 29.37 | 73.6 | 2.08E-09 | 25.55 | 73.6 | 2.08E-09 |
| | 30.98 | 73.4 | 2.40E-09 | 30.9 | 73.6 | 2.08E-09 | 29.23 | 73.6 | 2.08E-09 | 25.73 | 73.6 | 2.08E-09 |
| NTCs | 32.05 | 72 | - | 32.05 | 72 | - | 30.3 | 73.6 | - | 30.3 | 73.6 | - |
| | 36.45 | 72.8 | - | 36.45 | 72.8 | - | 31.21 | 73.6 | - | 31.21 | 73.6 | - |
| | UND | - | - | UND | - | - | 40.27 | 72.1 | - | 40.27 | 72.1 | - |

Table E. 6: Ct values, Tm values and gene copy number of the archaeal *amoA* gene following qPCR for samples collected in June, September and December 2016 and March 2017. Green shading indicates correct band showing on agarose gel post qPCR. UND: Undetermined

| Archaeal *amoA* | Jun-16 | | | Sep-16 | | | Dec-16 | | | Mar-17 | | |
|---|---|---|---|---|---|---|---|---|---|---|---|---|
| | Ct Value | Tm | Gene Copy No. per ul eDNA | Ct Value | Tm | Gene Copy No. per ul eDNA | Ct Value | Tm | Gene Copy No. per ul eDNA | Ct Value | Tm | Gene Copy No. per ul eDNA |
| S1 | 32.63 | 72.1 | 5.98E-09 | 30.13 | 72.7 | 3.92E-09 | 30.04 | 72.9 | 3.41E-09 | 26.19 | 74.1 | 1.47E-09 |
| | 33.3 | 71.7 | 7.92E-09 | 30.61 | 72.7 | 3.92E-09 | 28.58 | 73.2 | 2.76E-09 | 24.83 | 74.1 | 1.47E-09 |
| | 33.26 | 71.7 | 7.92E-09 | 30.62 | 72.7 | 3.92E-09 | 27.94 | 73.5 | 2.24E-09 | 27.61 | 73.5 | 2.24E-09 |
| | 31.3 | 72.1 | 5.98E-09 | 29.95 | 72.4 | 4.84E-09 | 30.05 | 73.2 | 2.76E-09 | 26.54 | 73.8 | 1.81E-09 |
| | 44.96 | 72.1 | 5.98E-09 | 31.14 | 72.4 | 4.84E-09 | 28.28 | 73.5 | 2.24E-09 | 25.23 | 73.5 | 2.24E-09 |
| | 38.82 | 72.1 | 5.98E-09 | UND | 71.7 | 7.92E-09 | 29.13 | 73.2 | 2.76E-09 | 26.98 | 73.5 | 2.24E-09 |
| PRB1 | UND | 72.4 | 4.84E-09 | 31.5 | 72.7 | 3.92E-09 | 30.12 | 73.5 | 2.24E-09 | 27.23 | 73.5 | 2.24E-09 |
| | 33.1 | 72.1 | 5.98E-09 | 31.41 | 73 | 3.18E-09 | 30.12 | 73.2 | 2.76E-09 | 26.4 | 74.1 | 1.47E-09 |
| | 28.44 | 72.1 | 5.98E-09 | 30 | 73 | 3.18E-09 | 29.39 | 73.5 | 2.24E-09 | 24.58 | 74.1 | 1.47E-09 |
| | 27.92 | 72.1 | 5.98E-09 | 30.29 | 73 | 3.18E-09 | 28.18 | 72.9 | 3.41E-09 | 27.64 | 73.8 | 1.81E-09 |
| | 32.81 | 71.7 | 7.92E-09 | 30.46 | 73 | 3.18E-09 | 27.18 | 73.2 | 2.76E-09 | 27.53 | 74.1 | 1.47E-09 |
| | 32.09 | 71.7 | 7.92E-09 | 30.96 | 73 | 3.18E-09 | 28.93 | 72.4 | 4.84E-09 | 25.85 | 74.4 | 1.19E-09 |
| S3 | 28.46 | 72.1 | 5.98E-09 | 31.15 | 73 | 3.18E-09 | 28.27 | 73.2 | 2.76E-09 | 25.85 | 73.5 | 2.24E-09 |
| | 28.1 | 72.4 | 4.84E-09 | 31.28 | 73 | 3.18E-09 | 29.12 | 72.9 | 3.41E-09 | 25.54 | 78.3 | 7.67E-11 |
| | 30.73 | 72.4 | 4.84E-09 | 30.77 | 73 | 3.18E-09 | 26.7 | 73.5 | 2.24E-09 | 25.14 | 74.1 | 1.47E-09 |
| | 30.26 | 72.4 | 4.84E-09 | 31.12 | 72.7 | 3.92E-09 | 25.27 | 73.5 | 2.24E-09 | 22.55 | 74.1 | 1.47E-09 |
| | 31.28 | 72.4 | 4.84E-09 | 30.69 | 72.4 | 4.84E-09 | 27.57 | 73.5 | 2.24E-09 | 24.25 | 73.5 | 2.24E-09 |
| | 30.58 | 72.7 | 3.92E-09 | 31.48 | 72.4 | 4.84E-09 | 30 | 73.2 | 2.76E-09 | 24.44 | 73.5 | 2.24E-09 |
| PRB2 | 30.21 | 72.4 | 4.84E-09 | 30.24 | 72.7 | 3.92E-09 | 29.52 | 73.5 | 2.24E-09 | 23.61 | 74.1 | 1.47E-09 |
| | 29.59 | 72.7 | 3.92E-09 | 29.64 | 73 | 3.18E-09 | 29.13 | 73.8 | 1.81E-09 | 24.69 | 74.4 | 1.19E-09 |
| | 31.27 | 72.4 | 4.84E-09 | 31.66 | 73 | 3.18E-09 | UND | 72.4 | 4.84E-09 | 25.24 | 74.4 | 1.19E-09 |
| | 32.1 | 72.1 | 5.98E-09 | 31.06 | 73 | 3.18E-09 | UND | 70.6 | 1.72E-08 | 24.61 | 74.4 | 1.19E-09 |
| | 30.76 | 72.1 | 5.98E-09 | 32.27 | 73 | 3.18E-09 | 27.57 | 73.5 | 2.24E-09 | 25.39 | 74.4 | 1.19E-09 |
| | 30.88 | 72.1 | 5.98E-09 | 32.24 | 73 | 3.18E-09 | 27.49 | 73.2 | 2.76E-09 | 25.29 | 74.4 | 1.19E-09 |
| S5 | 33.52 | 72.4 | 4.84E-09 | 29.92 | 73 | 3.18E-09 | 27.29 | 74.1 | 1.47E-09 | 24.82 | 74.4 | 1.19E-09 |
| | 30.61 | 72.7 | 3.92E-09 | 28.81 | 73 | 3.18E-09 | 28.1 | 73.8 | 1.81E-09 | 25.95 | 74.4 | 1.19E-09 |
| | 29.69 | 72.7 | 3.92E-09 | 30.22 | 72.7 | 3.92E-09 | 27.86 | 73.8 | 1.81E-09 | 24.52 | 74.1 | 1.47E-09 |
| | 29.45 | 72.7 | 3.92E-09 | 29.05 | 73 | 3.18E-09 | 22.83 | 74.1 | 1.47E-09 | 24.52 | 74.1 | 1.47E-09 |
| | 31.25 | 72.7 | 3.92E-09 | 30.41 | 72.7 | 3.92E-09 | 25.15 | 74.1 | 1.47E-09 | 24.75 | 74.1 | 1.47E-09 |
| | 31.58 | 72.7 | 3.92E-09 | 30.56 | 72.4 | 4.84E-09 | 25.61 | 74.1 | 1.47E-09 | 24.44 | 73.8 | 1.81E-09 |
| NTCs | 33.5 | 72.4 | - | 33.5 | 72.4 | - | 33.28 | 73.5 | - | 33.28 | 73.5 | - |
| | 35.21 | 72.1 | - | 35.21 | 72.1 | - | UND | - | - | UND | - | - |
| | 33.01 | 71.4 | - | 33.01 | 71.4 | - | UND | - | - | UND | - | - |

Table E. 7: Ct values, Tm values and gene copy number of the *nirK* gene following qPCR for samples collected in June, September and December 2015 and March 2016. Green shading indicates correct band showing on agarose gel post qPCR. UND: Undetermined

| *nirK* | Jun-15 | | | Sep-15 | | | Dec-15 | | | Mar-16 | | |
|---|---|---|---|---|---|---|---|---|---|---|---|---|
| | Ct Value | Tm | Gene Copy No. per ul eDNA | Ct Value | Tm | Gene Copy No. per ul eDNA | Ct Value | Tm | Gene Copy No. per ul eDNA | Ct Value | Tm | Gene Copy No. per ul eDNA |
| S1 | 28.11 | 82.6 | 1.09E+05 | 21.76 | 82.6 | 9.62E+06 | 22.1 | 82.4 | 7.57E+06 | 22.25 | 82.1 | 6.81E+06 |
| | 28.06 | 82.6 | 1.13E+05 | 22.33 | 82.6 | 6.44E+06 | 22.4 | 83 | 6.00E+06 | UND | 70.6 | - |
| | 27.57 | 82.9 | 1.60E+05 | 22.18 | 82.9 | 7.15E+06 | 23.2 | 82.1 | 3.58E+06 | 17.39 | 84 | 2.10E+08 |
| | 27.61 | 82.9 | 1.55E+05 | 22.18 | 82.9 | 7.15E+06 | 17.1 | 83.4 | 2.50E+08 | 17.85 | 84.3 | 1.52E+08 |
| | 28.27 | 82.9 | 9.76E+04 | 22.11 | 83.9 | 7.52E+06 | 17 | 83.7 | 2.86E+08 | 17.57 | 84 | 1.85E+08 |
| | 27.94 | 82.6 | 1.23E+05 | 22.05 | 82.6 | 7.84E+06 | 16.7 | 83.7 | 3.41E+08 | 17.6 | 84.3 | 1.81E+08 |
| PRB1 | 26.53 | 74.7 | 3.33E+05 | 24 | 83.2 | 1.98E+06 | 23.1 | 83.4 | 3.82E+06 | 19.32 | 85.9 | 5.38E+07 |
| | 31.3 | 82.2 | 1.15E+04 | 24.09 | 83.2 | 1.86E+06 | 22.2 | 83 | 7.21E+06 | 19.05 | 85.9 | 6.50E+07 |
| | 26.82 | 72.2 | 2.71E+05 | 24.18 | 83.2 | 1.75E+06 | 22.3 | 83 | 6.81E+06 | UND | 70.6 | - |
| | 27.02 | 81.9 | 2.36E+05 | 24.27 | 83.5 | 1.64E+06 | 22.3 | 81.8 | 6.67E+06 | UND | 70.6 | - |
| | 29.33 | 83.5 | 4.62E+04 | 32.17 | 83.2 | 6.24E+03 | 23 | 81.5 | 3.96E+06 | 16.07 | 83.7 | 5.32E+08 |
| | 25.07 | 72.2 | 9.32E+05 | 30.4 | 74 | 2.17E+04 | 23.3 | 81.8 | 3.27E+06 | 16.26 | 83.7 | 4.65E+08 |
| S3 | 26.05 | 74.7 | 4.67E+05 | 22.69 | 83.2 | 4.99E+06 | 23 | 81.8 | 4.01E+06 | 22.31 | 82.7 | 6.53E+06 |
| | 27.61 | 82.2 | 1.55E+05 | 21.6 | 84.5 | 1.08E+07 | 23.5 | 81.8 | 2.88E+06 | 22.32 | 83 | 6.48E+06 |
| | 29.35 | 74.3 | 4.56E+04 | 22.31 | 83.2 | 6.53E+06 | 23.1 | 82.1 | 3.85E+06 | 19.32 | 85.6 | 5.38E+07 |
| | 28.72 | 85.2 | 7.11E+04 | 22.25 | 82.6 | 6.81E+06 | 22.9 | 82.4 | 4.46E+06 | 19.92 | 85.2 | 3.52E+07 |
| | 28.21 | 82.9 | 1.02E+05 | 28.65 | 74.3 | 7.47E+04 | 23.2 | 82.1 | 3.46E+06 | 17.86 | 83 | 1.51E+08 |
| | 28.85 | 72.8 | 6.49E+04 | 22.35 | 82.6 | 6.35E+06 | 19.9 | 82.7 | 3.60E+07 | UND | 70.6 | - |
| PRB2 | 24.78 | 73.1 | 1.14E+06 | 24.8 | 83.2 | 1.13E+06 | 21.5 | 84.9 | 1.20E+07 | 21.69 | 86.5 | 1.01E+07 |
| | 29.11 | 82.9 | 5.40E+04 | 25.14 | 83.5 | 8.87E+05 | 21.2 | 84.3 | 1.45E+07 | 21.59 | 86.5 | 1.08E+07 |
| | 28.45 | 82.6 | 8.60E+04 | UND | 71.9 | - | 21.9 | 84 | 8.97E+06 | 18.56 | 86.2 | 9.19E+07 |
| | UND | 72.2 | #VALUE! | 25.17 | 83.5 | 8.69E+05 | 21.5 | 84.3 | 1.12E+07 | 18.53 | 86.2 | 9.38E+07 |
| | 27.65 | 82.6 | 1.51E+05 | UND | 71.9 | - | 23.1 | 81.5 | 3.66E+06 | 14.69 | 85.9 | 1.41E+09 |
| | 28.28 | 72.2 | 9.69E+04 | 25.05 | 83.5 | 9.46E+05 | 23.1 | 81.5 | 3.66E+06 | 14.76 | 85.9 | 1.34E+09 |
| S5 | 27.61 | 83.2 | 1.55E+05 | 27.7 | 84.2 | 1.46E+05 | 23.1 | 82.1 | 3.66E+06 | 17.05 | 85.9 | 2.66E+08 |
| | 28.16 | 83.5 | 1.06E+05 | 27.18 | 83.2 | 2.11E+05 | 22.2 | 83.7 | 7.31E+06 | 17.12 | 85.2 | 2.54E+08 |
| | 27.79 | 84.2 | 1.37E+05 | 27.21 | 83.2 | 2.06E+05 | 20.7 | 83 | 2.06E+07 | 15.76 | 85.9 | 6.62E+08 |
| | UND | 71.3 | - | 26.84 | 83.2 | 2.68E+05 | 20.2 | 83 | 2.91E+07 | 15.83 | 85.9 | 6.30E+08 |
| | 27.79 | 84.2 | 1.37E+05 | 27.53 | 82.9 | 1.65E+05 | 21.2 | 83 | 1.43E+07 | 17.01 | 85.6 | 2.74E+08 |
| | 26.15 | 73.4 | 4.35E+05 | 27.09 | 82.6 | 2.24E+05 | 20.9 | 83.7 | 1.79E+07 | 16.83 | 85.2 | 3.11E+08 |
| NTCs | 27.09 | 82.6 | - | 27.09 | 82.6 | - | 23.1 | 81.8 | - | 23.05 | 81.8 | - |
| | 30.45 | 83.9 | - | 30.45 | 83.9 | - | 23.2 | 81.8 | - | 23.15 | 81.8 | - |
| | 29.55 | 81 | - | 29.55 | 81 | - | 23.4 | 81.8 | - | 23.35 | 81.8 | - |

Table E. 8: Ct values, Tm values and gene copy number of the *nirK* gene following qPCR for samples collected in June, September and December 2016 and March 2017. Green shading indicates correct band showing on agarose gel post qPCR. UND: Undetermined

| *nirK* | Jun-16 | | | Sep-16 | | | Dec-16 | | | Mar-17 | | |
|---|---|---|---|---|---|---|---|---|---|---|---|---|
| | Ct Value | Tm | Gene Copy No. per ul eDNA | Ct Value | Tm | Gene Copy No. per ul eDNA | Ct Value | Tm | Gene Copy No. per ul eDNA | Ct Value | Tm | Gene Copy No. per ul eDNA |
| S1 | 25.1 | 81.6 | 9.13E+05 | 25.14 | 85 | 8.87E+05 | 23.2 | 82.1 | 3.58E+06 | 22.12 | 83.1 | 7.46E+06 |
| | 24.39 | 83.6 | 1.51E+06 | 26.27 | 85 | 4.00E+05 | 23 | 82.1 | 4.16E+06 | 22.04 | 83.9 | 7.90E+06 |
| | 33.19 | 82 | 3.04E+03 | UND | 72.8 | - | 24.1 | 82.8 | 1.89E+06 | 24.77 | 83.5 | 1.15E+06 |
| | 34.76 | 83.6 | 1.00E+03 | 29.21 | 83 | 5.03E+04 | 24.3 | 83.1 | 1.60E+06 | 24.37 | 83.9 | 1.53E+06 |
| | UND | 72.8 | - | 26.18 | 84.3 | 4.26E+05 | 22.8 | 82.8 | 4.69E+06 | 21.56 | 84.2 | 1.11E+07 |
| | 34.22 | 82.3 | 1.47E+03 | 26.12 | 83.6 | 4.45E+05 | 23.1 | 82.8 | 3.74E+06 | 21.89 | 83.9 | 8.78E+06 |
| PRB1 | 27.57 | 82.3 | 1.60E+05 | 28 | 82.6 | 1.18E+05 | 19.7 | 82.8 | 4.11E+07 | 24.92 | 84.9 | 1.04E+06 |
| | 27.41 | 82.3 | 1.79E+05 | 27.12 | 82.6 | 2.20E+05 | 20.1 | 82.4 | 3.21E+07 | 25.23 | 84.9 | 8.33E+05 |
| | 26.64 | 82 | 3.08E+05 | 25.19 | 83 | 8.57E+05 | 26.1 | 83.5 | 4.45E+05 | 21.1 | 83.1 | 1.53E+07 |
| | UND | 76.3 | - | 25.39 | 84.6 | 7.44E+05 | 26.5 | 82.8 | 3.43E+05 | 21.02 | 83.1 | 1.62E+07 |
| | 23.78 | 82.3 | 2.32E+06 | 26.39 | 83.3 | 3.68E+05 | 23.8 | 82.4 | 2.32E+06 | 24 | 73.1 | 1.98E+06 |
| | 23.85 | 82 | 2.20E+06 | 26.95 | 83.3 | 2.48E+05 | 24 | 82.4 | 1.95E+06 | 24.29 | 82.8 | 1.62E+06 |
| S3 | 27.55 | 82.3 | 1.62E+05 | 28.49 | 83.9 | 8.36E+04 | 28.2 | 83.5 | 1.03E+05 | 23.33 | 84.9 | 3.18E+06 |
| | 28.5 | 82.3 | 8.30E+04 | 29.23 | 84.6 | 4.96E+04 | 28.6 | 72.7 | 7.90E+04 | 23.74 | 84.6 | 2.38E+06 |
| | 25.36 | 85 | 7.60E+05 | 28.37 | 83.3 | 9.10E+04 | 22.1 | 72.4 | 7.68E+06 | 24.58 | 72.7 | 1.32E+06 |
| | 26.86 | 84.6 | 2.64E+05 | 29.07 | 83 | 5.55E+04 | 22.1 | 73.1 | 7.41E+06 | 24.31 | 74.8 | 1.59E+06 |
| | 26.13 | 85 | 4.42E+05 | 28.35 | 83 | 9.23E+04 | 24.1 | 72.4 | 1.85E+06 | 24.46 | 72.7 | 1.43E+06 |
| | 26.01 | 85 | 4.81E+05 | 28.83 | 82.6 | 6.58E+04 | 26.2 | 83.9 | 4.32E+05 | 24.26 | 84.2 | 1.65E+06 |
| PRB2 | 25.9 | 85 | 5.19E+05 | 27.85 | 83.6 | 1.31E+05 | 22.5 | 83.5 | 5.59E+06 | 25.74 | 85.3 | 5.81E+05 |
| | 27.36 | 84.3 | 1.85E+05 | 27.86 | 83.9 | 1.30E+05 | 23.1 | 83.5 | 3.71E+06 | 24.74 | 84.2 | 1.18E+06 |
| | 27.55 | 82.6 | 1.62E+05 | 27.04 | 85 | 2.32E+05 | UND | 73.7 | - | 23.19 | 83.1 | 3.51E+06 |
| | 27.55 | 82.6 | 1.62E+05 | 26.69 | 83.9 | 2.97E+05 | UND | 70.4 | - | 23.11 | 83.1 | 3.71E+06 |
| | 26.65 | 82.3 | 3.06E+05 | 26.08 | 85 | 4.57E+05 | 24.7 | 82.4 | 1.18E+06 | 23.55 | 84.9 | 2.72E+06 |
| | 26.28 | 84.3 | 3.97E+05 | 26.15 | 85 | 4.35E+05 | 25 | 82.4 | 1.00E+06 | 24.09 | 73.1 | 1.86E+06 |
| S5 | 30.47 | 83 | 2.07E+04 | 30.14 | 84.6 | 2.61E+04 | 23.8 | 83.1 | 2.25E+06 | 24.7 | 84.6 | 1.21E+06 |
| | 30.79 | 83.6 | 1.65E+04 | 30.78 | 85 | 1.66E+04 | 23.4 | 83.5 | 3.05E+06 | 24.47 | 84.6 | 1.42E+06 |
| | 27.23 | 85.3 | 2.03E+05 | 28.5 | 84.6 | 8.30E+04 | 24.7 | 83.5 | 1.18E+06 | 24.27 | 83.1 | 1.64E+06 |
| | 27.7 | 82.6 | 1.46E+05 | 28.59 | 84.3 | 7.79E+04 | 24.6 | 84.2 | 1.33E+06 | 24.67 | 83.1 | 1.24E+06 |
| | 26.42 | 85 | 3.60E+05 | 30.96 | 84.6 | 1.46E+04 | 25.3 | 83.9 | 8.15E+05 | 24.83 | 73.4 | 1.10E+06 |
| | 26.35 | 85 | 3.78E+05 | 30.66 | 83.9 | 1.81E+04 | 25.2 | 84.2 | 8.45E+05 | 24.81 | 83.9 | 1.12E+06 |
| NTCs | 32.84 | 82 | - | 32.84 | 82 | - | 27 | 83.5 | - | 27.03 | 83.5 | - |
| | 35.5 | 72.1 | - | 35.5 | 72.1 | - | 26.6 | 82.8 | - | 26.58 | 82.8 | - |
| | 33.22 | 82 | - | 33.22 | 82 | - | 27.5 | 82.8 | - | 27.48 | 82.8 | - |

Table E. 9: Ct values, Tm values and gene copy number of the *nirS* gene following qPCR for samples collected in June, September and December 2015 and March 2016. Green shading indicates correct band showing on agarose gel post qPCR. UND: Undetermined

| *nirS* | Jun-15 | | | Sep-15 | | | Dec-15 | | | Mar-16 | | |
|---|---|---|---|---|---|---|---|---|---|---|---|---|
| | Ct Value | Tm | Gene Copy No. per ul eDNA | Ct Value | Tm | Gene Copy No. per ul eDNA | Ct Value | Tm | Gene Copy No. per ul eDNA | Ct Value | Tm | Gene Copy No. per ul eDNA |
| S1 | 26 | 78.2 | 1.57E+03 | 18.6 | 80.1 | 2.20E+05 | 24.1 | 79.7 | 5.49E+03 | 24.5 | 79 | 4.17E+03 |
| | 26 | 78.2 | 1.49E+03 | 24.9 | 80.8 | 3.17E+03 | 23.5 | 79.4 | 8.37E+03 | 25.1 | 80 | 2.73E+03 |
| | 26.3 | 78.2 | 1.27E+03 | 19.2 | 79.8 | 1.41E+05 | 23.4 | 79.1 | 8.54E+03 | 22.6 | 79 | 1.49E+04 |
| | 26.3 | 78.2 | 1.27E+03 | 19.3 | 79.5 | 1.40E+05 | 23.3 | 78.8 | 9.08E+03 | 23 | 79 | 1.12E+04 |
| | 26.4 | 78.2 | 1.18E+03 | 19.3 | 79.5 | 1.39E+05 | 25.1 | 80 | 2.84E+03 | 22.1 | 79 | 2.07E+04 |
| | 26.1 | 78.2 | 1.41E+03 | 19.3 | 79.5 | 1.36E+05 | 25.6 | 80 | 2.05E+03 | 21.7 | 79 | 2.64E+04 |
| PRB1 | 31 | 78.2 | 5.29E+01 | 23.2 | 79.5 | 9.84E+03 | 26.9 | 80.4 | 8.45E+02 | 25.2 | 80 | 2.61E+03 |
| | 28.6 | 78.5 | 2.68E+02 | 23.1 | 79.5 | 1.07E+04 | 27 | 80 | 7.95E+02 | 23.8 | 80 | 6.53E+03 |
| | 29.2 | 78.5 | 1.81E+02 | 23.1 | 79.8 | 1.07E+04 | 26 | 80 | 1.54E+03 | UND | 81 | - |
| | 28.7 | 78.5 | 2.46E+02 | 23.2 | 79.5 | 1.01E+04 | 27 | 79.4 | 7.69E+02 | UND | 78 | - |
| | 29.1 | 78.2 | 1.86E+02 | 26.8 | 80.4 | 8.85E+02 | 26 | 79.4 | 1.52E+03 | 21.1 | 80 | 4.11E+04 |
| | 30.5 | 78.2 | 7.60E+01 | 23.2 | 79.8 | 1.01E+04 | 25.8 | 79.4 | 1.79E+03 | 21.3 | 80 | 3.57E+04 |
| S3 | 26.4 | 78.2 | 1.17E+03 | 21.6 | 79.8 | 2.88E+04 | 23.3 | 79.7 | 9.08E+03 | 27.1 | 81 | 7.49E+02 |
| | 26.4 | 78.5 | 1.20E+03 | 22 | 79.5 | 2.17E+04 | 23.2 | 79.4 | 9.64E+03 | 27.2 | 81 | 6.95E+02 |
| | 26.2 | 78.5 | 1.32E+03 | 21.6 | 79.8 | 2.90E+04 | 25.1 | 80.7 | 2.86E+03 | 23.7 | 80 | 7.27E+03 |
| | 26.1 | 78.5 | 1.44E+03 | 22.1 | 79.5 | 2.10E+04 | 23.2 | 80.4 | 9.64E+03 | 24 | 81 | 5.87E+03 |
| | 26.3 | 78.5 | 1.25E+03 | 21.7 | 79.1 | 2.71E+04 | 21.1 | 80.7 | 3.94E+04 | 20.3 | 80 | 7.02E+04 |
| | 26.3 | 78.5 | 1.21E+03 | 22.1 | 79.1 | 2.06E+04 | 21.1 | 80.7 | 4.13E+04 | 20.3 | 80 | 6.83E+04 |
| PRB2 | 27.3 | 79.1 | 6.33E+02 | 25.9 | 79.1 | 1.62E+03 | 23.1 | 80.4 | 1.07E+04 | 27.7 | 80 | 5.01E+02 |
| | 27.6 | 79.1 | 5.28E+02 | 26.2 | 79.1 | 1.32E+03 | 23.4 | 80 | 8.49E+03 | 29 | 80 | 2.02E+02 |
| | 27.3 | 79.1 | 6.46E+02 | 28.1 | 80.8 | 3.75E+02 | 27.2 | 80.4 | 7.00E+02 | 25.4 | 80 | 2.29E+03 |
| | 27.3 | 78.8 | 6.29E+02 | UND | 75 | | 27.3 | 79.7 | 6.25E+02 | 25.6 | 80 | 1.97E+03 |
| | 27.6 | 78.5 | 5.25E+02 | 30.4 | 80.8 | 8.08E+01 | 27.1 | 80 | 7.49E+02 | 22.8 | 81 | 1.30E+04 |
| | 27.4 | 78.5 | 5.84E+02 | 26.3 | 79.8 | 1.25E+03 | UND | 73.6 | - | 23 | 80 | 1.16E+04 |
| S5 | 28.8 | 79.1 | 2.33E+02 | 26.8 | 79.1 | 8.80E+02 | UND | 74.2 | - | 21.4 | 80 | 3.29E+04 |
| | 28.6 | 78.8 | 2.70E+02 | 26.8 | 79.1 | 8.68E+02 | 22.8 | 80.4 | 1.28E+04 | 22.2 | 80 | 1.90E+04 |
| | 29 | 79.1 | 1.97E+02 | 27.4 | 79.1 | 5.84E+02 | 22.8 | 80.7 | 1.27E+04 | 23.1 | 80 | 1.03E+04 |
| | 28.8 | 79.1 | 2.28E+02 | 26.4 | 79.1 | 1.17E+03 | UND | 73.9 | - | 23.4 | 80 | 8.78E+03 |
| | 28.7 | 79.5 | 2.53E+02 | 27.2 | 78.8 | 6.91E+02 | 26.6 | 80.4 | 1.03E+03 | 22 | 79 | 2.20E+04 |
| | 29.7 | 79.1 | 1.27E+02 | 27.2 | 78.5 | 6.68E+02 | 26.3 | 80.7 | 1.23E+03 | 22.1 | 79 | 2.07E+04 |
| NTCs | 30.6 | 74.4 | - | 30.6 | 74.4 | - | UND | - | - | UND | - | - |
| | 31.4 | 78.5 | - | 31.4 | 78.5 | - | 30.7 | 74.2 | - | 30.7 | 74 | - |
| | 29.8 | 73.4 | - | 29.8 | 73.4 | - | 30.62. | 74.2 | - | 30.62. | 74 | - |

Table E. 10: Ct values, Tm values and gene copy number of the *nirS* gene following qPCR for samples collected in June, September and December 2016 and March 2017. Green shading indicates correct band showing on agarose gel post qPCR. UND: Undetermined

| nirS | Jun-16 | | | Sep-16 | | | Dec-16 | | | Mar-17 | | |
|------|--------|-----|--------------------------|--------|-----|--------------------------|--------|-----|--------------------------|--------|-----|--------------------------|
|      | Ct Value | Tm | Gene Copy No. per ul eDNA | Ct Value | Tm | Gene Copy No. per ul eDNA | Ct Value | Tm | Gene Copy No. per ul eDNA | Ct Value | Tm | Gene Copy No. per ul eDNA |
| S1   | 27.1 | 81.4 | 7.14E+02 | 20.4 | 81 | 6.56E+04 | 19.3 | 78.9 | 1.39E+05 | 17.5 | 79 | 4.56E+05 |
|      | 27.5 | 81 | 5.57E+02 | 20.4 | 81 | 6.31E+04 | 20.5 | 79.3 | 6.22E+04 | 19.2 | 80 | 1.41E+05 |
|      | 27 | 81 | 7.90E+02 | 23.6 | 81 | 7.73E+03 | 19.2 | 78.6 | 1.47E+05 | 11 | 79 | 3.59E+07 |
|      | 26.6 | 81.4 | 1.01E+03 | 23.2 | 80.6 | 1.02E+04 | 20.9 | 79.3 | 4.57E+04 | 16 | 79 | 1.23E+06 |
|      | 26.7 | 81 | 9.34E+02 | 21.6 | 80 | 2.86E+04 | 20.3 | 79.6 | 7.16E+04 | 19.5 | 79 | 1.20E+05 |
|      | 26.4 | 81.4 | 1.15E+03 | 22.5 | 80.6 | 1.61E+04 | 16.5 | 78.9 | 8.98E+05 | 20 | 79 | 8.41E+04 |
| PRB1 | 25.2 | 80.3 | 2.62E+03 | 24.8 | 80 | 3.34E+03 | 22.1 | 79.3 | 2.11E+04 | 18.7 | 79 | 2.04E+05 |
|      | 25.3 | 80 | 2.42E+03 | 24.9 | 80.6 | 3.17E+03 | 22.2 | 79.3 | 1.95E+04 | 20.5 | 79 | 5.98E+04 |
|      | 26.8 | 80.6 | 9.03E+02 | 22.2 | 80.3 | 1.94E+04 | 21.4 | 78.9 | 3.33E+04 | 18.7 | 79 | 1.99E+05 |
|      | 26.1 | 80.6 | 1.44E+03 | 22.7 | 80.3 | 1.43E+04 | 21.9 | 78.9 | 2.43E+04 | 20.2 | 79 | 7.61E+04 |
|      | 21.4 | 80 | 3.25E+04 | 23.4 | 80.3 | 8.96E+03 | 18.5 | 78.2 | 2.40E+05 | 19.6 | 79 | 1.13E+05 |
|      | 22.4 | 80 | 1.73E+04 | 23.1 | 80.3 | 1.07E+04 | 18.7 | 76.2 | 1.99E+05 | 21.3 | 80 | 3.57E+04 |
| S3   | 24.6 | 80 | 3.87E+03 | 25.5 | 80.3 | 2.12E+03 | 16.9 | 79.3 | 6.60E+05 | 18.6 | 80 | 2.24E+05 |
|      | 24.9 | 80 | 3.10E+03 | 25.4 | 80.3 | 2.23E+03 | 18.3 | 79.6 | 2.70E+05 | 16.9 | 79 | 6.68E+05 |
|      | 21.7 | 80 | 2.69E+04 | 26.9 | 80.6 | 8.50E+02 | 19.1 | 78.9 | 1.51E+05 | 18.2 | 79 | 2.81E+05 |
|      | 22.2 | 80.3 | 1.95E+04 | 26.1 | 80.3 | 1.44E+03 | 17.2 | 78.6 | 5.58E+05 | 19.4 | 79 | 1.24E+05 |
|      | 21.7 | 80 | 2.65E+04 | 26.8 | 80.6 | 9.09E+02 | 18.5 | 78.6 | 2.30E+05 | 20.2 | 79 | 7.66E+04 |
|      | 21.6 | 80.3 | 2.94E+04 | 26.8 | 80 | 9.03E+02 | 21.2 | 79.3 | 3.81E+04 | 21.3 | 79 | 3.47E+04 |
| PRB2 | 24 | 79.6 | 5.79E+03 | 25.9 | 80 | 1.58E+03 | 17.1 | 80 | 6.13E+05 | 17.3 | 79 | 5.18E+05 |
|      | 23.7 | 79.6 | 6.99E+03 | 28 | 80.6 | 3.96E+02 | 19.1 | 78.9 | 1.60E+05 | 21 | 79 | 4.33E+04 |
|      | 23.8 | 79.3 | 6.53E+03 | 24.2 | 80.6 | 5.00E+03 | 30.7 | 74.5 | 6.69E+01 | 20 | 79 | 8.36E+04 |
|      | 23.7 | 79.3 | 6.89E+03 | 24.2 | 80.3 | 5.13E+03 | 33.9 | 74.1 | 7.62E+00 | 19.9 | 79 | 9.12E+04 |
|      | 21.6 | 78.9 | 2.94E+04 | 22.2 | 81.4 | 1.91E+04 | 15.9 | 77.9 | 1.35E+06 | 21.4 | 80 | 3.22E+04 |
|      | 21.6 | 78.6 | 2.92E+04 | 22.3 | 81.4 | 1.84E+04 | 17.1 | 77.9 | 6.09E+05 | 21.5 | 80 | 3.10E+04 |
| S5   | 28.5 | 79.6 | 2.91E+02 | 29.5 | 81.4 | 1.46E+02 | 13 | 78.9 | 9.46E+06 | 17.3 | 79 | 5.11E+05 |
|      | 28.3 | 79.3 | 3.28E+02 | 29.1 | 81 | 1.93E+02 | 14.8 | 78.9 | 2.79E+06 | 19.1 | 79 | 1.53E+05 |
|      | 25.9 | 79.3 | 1.67E+03 | 26.2 | 81.4 | 1.29E+03 | 16.3 | 79.3 | 1.00E+06 | 18.3 | 79 | 2.67E+05 |
|      | 25.9 | 79.6 | 1.64E+03 | 27.2 | 81.4 | 7.00E+02 | 17.5 | 79.3 | 4.44E+05 | 19.8 | 79 | 9.82E+04 |
|      | 25.1 | 80.3 | 2.83E+03 | 33.4 | 81.4 | 1.06E+01 | 17.4 | 78.9 | 4.88E+05 | 20.2 | 79 | 7.36E+04 |
|      | 25 | 80.3 | 2.96E+03 | 31.6 | 81 | 3.49E+01 | 19.9 | 79.6 | 8.88E+04 | 21.3 | 79 | 3.59E+04 |
| NTCs | 30.6 | 75.1 | - | 30.6 | 75.1 | - | 21.6 | - | 79.9 | 21.6 | - | 79.9 |
|      | 30.9 | 74.8 | - | 30.9 | 74.8 | - | 21 | - | 78.6 | 21 | - | 78.6 |
|      | 30.5 | 74.8 | - | 30.5 | 74.8 | - | 22.3 | - | 77.9 | 22.3 | - | 77.9 |

Table E. 11: Ct values, Tm values and gene copy number of the *nosZ* gene following qPCR for samples collected in June, September and December 2015 and March 2016. Green shading indicates correct band showing on agarose gel post qPCR. UND: Undetermined

| nosZ | Jun-15 Ct Value | Tm | Gene Copy No. per ul eDNA | Sep-15 Ct Value | Tm | Gene Copy No. per ul eDNA | Dec-15 Ct Value | Tm | Gene Copy No. per ul eDNA | Mar-16 Ct Value | Tm | Gene Copy No. per ul eDNA |
|---|---|---|---|---|---|---|---|---|---|---|---|---|
| S1 | 28.71 | 82.2 | 1.01E+03 | 20.14 | 81.9 | 2.16E+05 | 32.4 | 82.5 | 9.97E+01 | 30.7 | 83.1 | 2.89E+02 |
| | 28.67 | 82.2 | 1.03E+03 | 20.04 | 81.9 | 2.30E+05 | 31.4 | 82.5 | 1.84E+02 | 34.07 | 83.1 | 3.50E+01 |
| | UND | 70.4 | - | 20.58 | 81.9 | 1.64E+05 | 33.1 | 82.5 | 6.43E+01 | 25.64 | 83.1 | 6.89E+03 |
| | UND | 71 | - | 20.28 | 81.9 | 1.98E+05 | 33 | 82.5 | 6.68E+01 | 25.13 | 82.8 | 9.48E+03 |
| | 30.11 | 82.6 | 4.19E+02 | 20.34 | 81.4 | 1.91E+05 | 22.5 | 81.5 | 4.99E+04 | 23.57 | 82.5 | 2.52E+04 |
| | 28.48 | 82.2 | 1.16E+03 | 20.76 | 81.1 | 1.47E+05 | 23.4 | 81.5 | 2.73E+04 | 26.62 | 81.8 | 3.73E+03 |
| PRB1 | 29.24 | 82.2 | 7.22E+02 | 24.2 | 82.6 | 1.70E+04 | 31.5 | 82.1 | 1.71E+02 | 24.69 | 83.8 | 1.25E+04 |
| | UND | 70.1 | - | 23.73 | 82.6 | 2.28E+04 | 31.6 | 81.8 | 1.69E+02 | 24.3 | 83.8 | 1.60E+04 |
| | 29.19 | 82.2 | 7.45E+02 | 24.01 | 82.9 | 1.91E+04 | 36.6 | 81.8 | 7.00E+00 | UND | 70.6 | - |
| | 29.21 | 82.2 | 7.36E+02 | 24.72 | 82.6 | 1.23E+04 | 30.7 | 81.8 | 2.82E+02 | UND | 70.6 | - |
| | 28.77 | 82.2 | 9.69E+02 | 23.46 | 82.9 | 2.70E+04 | UND | 81.5 | - | 23.26 | 84.1 | 3.06E+04 |
| | 29.1 | 81.9 | 7.88E+02 | 24.38 | 82.9 | 1.52E+04 | 36.2 | 81.5 | 9.10E+00 | 26.53 | 84.1 | 3.94E+03 |
| S3 | 26.78 | 82.2 | 3.37E+03 | 22.43 | 82.9 | 5.15E+04 | 38.6 | 82.1 | 2.00E+00 | 30.2 | 84.5 | 3.96E+02 |
| | 38.2 | 76.5 | 2.63E+00 | 21.52 | 82.6 | 9.10E+04 | 36.5 | 82.5 | 7.78E+00 | 29.98 | 84.1 | 4.54E+02 |
| | 35.33 | 82.9 | 1.59E+01 | 23.42 | 82.9 | 2.77E+04 | 32.1 | 82.5 | 1.23E+02 | 25.9 | 83.4 | 5.85E+03 |
| | 37 | 75.1 | 5.58E+00 | 22.16 | 82.9 | 6.10E+04 | UND | 75.5 | - | 26.39 | 83.4 | 4.31E+03 |
| | 27.44 | 82.6 | 2.23E+03 | 21.21 | 82.6 | 1.11E+05 | 32.6 | 74.9 | 8.85E+01 | 36.86 | 79.3 | 6.10E+00 |
| | 28.43 | 82.6 | 1.20E+03 | 22.18 | 82.2 | 6.02E+04 | 33.8 | 83.1 | 4.28E+01 | 38.42 | 78.9 | 2.29E+00 |
| PRB2 | 26.28 | 82.6 | 4.61E+03 | 27.12 | 82.6 | 2.73E+03 | 30.8 | 82.1 | 2.67E+02 | 29.5 | 84.1 | 6.13E+02 |
| | 24.61 | 82.2 | 1.31E+04 | 27.69 | 82.6 | 1.91E+03 | 32.8 | 81.5 | 7.86E+01 | 28.9 | 84.1 | 8.93E+02 |
| | 25.25 | 82.6 | 8.80E+03 | 26.37 | 82.6 | 4.36E+03 | UND | 82.1 | - | 24.82 | 83.1 | 1.15E+04 |
| | 24.61 | 82.2 | 1.31E+04 | 26.61 | 82.9 | 3.75E+03 | UND | 82.1 | - | 25.06 | 82.8 | 9.91E+03 |
| | 25.14 | 82.2 | 9.42E+03 | 27.13 | 82.9 | 2.71E+03 | 32.3 | 82.8 | 1.09E+02 | 22.6 | 83.1 | 4.63E+04 |
| | 25.05 | 81.9 | 9.97E+03 | 26.34 | 82.9 | 4.44E+03 | 34.5 | 82.1 | 2.62E+01 | 22.2 | 83.1 | 5.95E+04 |
| S5 | 26.22 | 82.6 | 4.79E+03 | 31.57 | 83.3 | 1.68E+02 | 32.9 | 82.1 | 7.29E+01 | 26.73 | 83.4 | 3.48E+03 |
| | 27.03 | 82.6 | 2.88E+03 | 31.12 | 82.9 | 2.22E+02 | 31.5 | 82.5 | 1.77E+02 | 26.57 | 83.4 | 3.85E+03 |
| | 26.23 | 82.6 | 4.76E+03 | 31.13 | 82.9 | 2.21E+02 | 25.3 | 82.5 | 8.52E+03 | 22.93 | 83.1 | 3.76E+04 |
| | 27.02 | 82.9 | 2.90E+03 | 31.16 | 82.9 | 2.17E+02 | 25.9 | 82.5 | 6.00E+03 | 23.63 | 83.1 | 2.43E+04 |
| | 27.63 | 82.6 | 1.98E+03 | 28.04 | 82.6 | 1.53E+03 | 26.6 | 82.1 | 3.85E+03 | 23 | 82.8 | 3.60E+04 |
| | 26.96 | 82.6 | 3.01E+03 | 30.75 | 82.6 | 2.80E+02 | 26.3 | 82.5 | 4.70E+03 | 23.07 | 82.8 | 3.45E+04 |
| NTCs | 36.65 | 81.4 | - | 36.65 | 81.4 | - | 36.7 | 81.8 | - | 36.65 | 81.8 | - |
| | 37.12 | 81.4 | - | 37.12 | 81.4 | - | 35.3 | 82.1 | - | 35.26 | 82.1 | - |
| | 35.49 | 81.9 | - | 35.49 | 81.9 | - | 35.1 | 31.8 | - | 35.12 | 31.8 | - |

Table E. 12: Ct values, Tm values and gene copy number of the *nosZ* gene following qPCR for samples collected in June, September and December 2016 and March 2017. Green shading indicates correct band showing on agarose gel post qPCR. UND: Undetermined

| *nosZ* | Jun-16 | | | Sep-16 | | | Dec-16 | | | Mar-17 | | |
|---|---|---|---|---|---|---|---|---|---|---|---|---|
| | Ct Value | Tm | Gene Copy No. per ul eDNA | Ct Value | Tm | Gene Copy No. per ul eDNA | Ct Value | Tm | Gene Copy No. per ul eDNA | Ct Value | Tm | Gene Copy No. per ul eDNA |
| S1 | 34.88 | 83.8 | 2.11E+01 | 27.49 | 82.5 | 2.16E+03 | 23.4 | 82.1 | 2.87E+04 | 23.55 | 83.8 | 2.55E+04 |
| | 29.88 | 83.5 | 4.83E+02 | 26.2 | 82.5 | 4.85E+03 | 23.7 | 82.1 | 2.37E+04 | 24.56 | 84.1 | 1.36E+04 |
| | 31.03 | 83.5 | 2.35E+02 | 30.37 | 82.8 | 3.56E+02 | 25.8 | 82.1 | 6.35E+03 | 27.51 | 82.4 | 2.13E+03 |
| | 30.48 | 83.5 | 3.32E+02 | 30.46 | 82.5 | 3.36E+02 | 25.3 | 82.1 | 8.80E+03 | 27.98 | 82.1 | 1.59E+03 |
| | 30.55 | 83.5 | 3.18E+02 | 26.9 | 82.2 | 3.13E+03 | 25.1 | 82.4 | 9.48E+03 | 23.57 | 81.7 | 2.52E+04 |
| | 30.57 | 83.5 | 3.14E+02 | UND | 82.5 | - | 25.4 | 82.4 | 8.21E+03 | 23.15 | 81.4 | 3.28E+04 |
| PRB1 | 31.03 | 81.9 | 2.35E+02 | 28.44 | 82.8 | 1.19E+03 | 33.1 | 80.4 | 6.39E+01 | 27.19 | 83.4 | 2.61E+03 |
| | 32.32 | 81.9 | 1.05E+02 | 27.54 | 83.2 | 2.09E+03 | 32.4 | 82.4 | 9.84E+01 | 27.87 | 83.8 | 1.70E+03 |
| | UND | 76.4 | - | 26.02 | 82.8 | 5.43E+03 | 31.3 | 82.8 | 2.04E+02 | 26.75 | 82.8 | 3.44E+03 |
| | 31.24 | 81.2 | 2.06E+02 | 26.2 | 82.8 | 4.85E+03 | 29.8 | 82.4 | 5.18E+02 | 26.66 | 82.8 | 3.64E+03 |
| | 26.91 | 81.9 | 3.11E+03 | 29.88 | 83.2 | 4.83E+02 | 24.2 | 81.7 | 1.70E+04 | 27.72 | 82.8 | 1.87E+03 |
| | 27.06 | 81.9 | 2.83E+03 | 30.14 | 83.2 | 4.11E+02 | 24.8 | 81.7 | 1.19E+04 | 27.22 | 82.8 | 2.56E+03 |
| S3 | 31.01 | 82.2 | 2.38E+02 | 32.4 | 83.2 | 9.97E+01 | 35.1 | 82.1 | 1.80E+01 | 25.58 | 83.4 | 7.15E+03 |
| | 31.25 | 82.5 | 2.05E+02 | 32.36 | 83.2 | 1.02E+02 | 34.6 | 83.4 | 2.58E+01 | 25.11 | 83.4 | 9.60E+03 |
| | 28.41 | 82.8 | 1.21E+03 | 30.29 | 82.8 | 3.74E+02 | 28.9 | 83.4 | 8.88E+02 | 28.4 | 83.1 | 1.22E+03 |
| | 28.28 | 82.8 | 1.32E+03 | 30.85 | 82.8 | 2.63E+02 | 28.4 | 83.1 | 1.21E+03 | 28.26 | 82.1 | 1.33E+03 |
| | 28.4 | 82.2 | 1.22E+03 | 31.53 | 83.2 | 1.72E+02 | 27.8 | 83.4 | 1.84E+03 | 26.4 | 82.8 | 4.28E+03 |
| | 28.23 | 82.5 | 1.36E+03 | 32.24 | 82.8 | 1.10E+02 | 27.6 | 83.1 | 1.97E+03 | 25.41 | 81.7 | 7.96E+03 |
| PRB2 | 29.34 | 83.2 | 6.78E+02 | 30.48 | 83.2 | 3.32E+02 | 28.4 | 82.8 | 1.21E+03 | 27.26 | 83.4 | 2.50E+03 |
| | 28.2 | 83.2 | 1.39E+03 | 30.74 | 83.2 | 2.82E+02 | 28.7 | 82.4 | 1.04E+03 | 28.06 | 83.1 | 1.51E+03 |
| | 29.83 | 83.2 | 4.99E+02 | 30.78 | 82.8 | 2.75E+02 | UND | 70.7 | - | 26.83 | 83.4 | 3.27E+03 |
| | UND | 78 | - | 30.24 | 82.8 | 3.86E+02 | UND | 73.5 | - | 26.74 | 83.8 | 3.46E+03 |
| | 26.46 | 82.2 | 4.12E+03 | 30.04 | 82.8 | 4.37E+02 | 27.4 | 82.1 | 2.36E+03 | 25.71 | 82.8 | 6.59E+03 |
| | 25.73 | 81.9 | 6.51E+03 | 28.69 | 82.8 | 1.02E+03 | 27.1 | 82.1 | 2.73E+03 | 26.05 | 82.8 | 5.33E+03 |
| S5 | 33.53 | 83.2 | 4.91E+01 | 35.55 | 83.5 | 1.39E+01 | 27 | 82.8 | 2.99E+03 | 28.83 | 83.1 | 9.33E+02 |
| | 34.17 | 83.2 | 3.29E+01 | 35.57 | 84.1 | 1.37E+01 | 26.7 | 82.8 | 3.64E+03 | 28.8 | 83.1 | 9.51E+02 |
| | 30.34 | 82.8 | 3.62E+02 | 34.7 | 83.2 | 2.36E+01 | 27.8 | 83.1 | 1.79E+03 | 28.72 | 82.4 | 1.00E+03 |
| | UND | 71.8 | - | 35.25 | 82.8 | 1.67E+01 | 27.3 | 82.8 | 2.47E+03 | 28.25 | 82.8 | 1.34E+03 |
| | 29.19 | 82.8 | 7.45E+02 | 37 | 84.1 | 5.58E+00 | 28.2 | 82.8 | 1.39E+03 | 28.01 | 82.4 | 1.56E+03 |
| | UND | 79.6 | - | 34.68 | 77.1 | 2.39E+01 | 29.3 | 82.8 | 6.82E+02 | 27.82 | 82.1 | 1.76E+03 |
| NTCs | 34.67 | 80.9 | - | 34.67 | 80.9 | - | 34.5 | - | 81.5 | 34.5 | - | 81.5 |
| | 34.96 | 82.2 | - | 34.96 | 82.2 | - | 30.7 | - | 81.2 | 30.65 | - | 81.2 |
| | 35.37 | 82.2 | - | 35.37 | 82.2 | - | 31.3 | - | 82 | 31.28 | - | 82 |

## More Acknowledgements

This Ph.D. journey was worth it for the many friends I've made along the way and who have enriched my life more than a Ph.D. ever could. From fellow students and lab mates to the porters and technicians who were very generous with their time and support and who helped make the journey a good one. Thanks for the terrible live Oasis songs played at my tiny table Annabel.

Thanks to John for providing the steppingstone into Ph. D life.

Thank you to Clare County Council for graciously providing and supporting the study site.

Thanks to the National Parks & Wildlife Service for their support and my colleagues Beavis and Butt-Head for their help and understanding.

Thanks to my family and friends who supported me, you know who you are. Thank you for minding my dog, Mam. Thanks B&B, L&E for housing my ass for the final furlong.

Thank you, Ryan, for your advice and for the hours you spent proof reading. Mostly though thanks for your kindness, encouragement, and support…. and for keeping me fed.